CHEMISTRY HALL LIBRARY

UNIV. MAR 11 1959 LIBRARY

BULLETIN OF THE CHEMICAL SOCIETY OF JAPAN

Vol. 32 No. 1 January 1959

CONTENTS

General and Physical

T. ISEMURA and T. YAMASHITA: Surface Chemistry of Synthetic Protein Analogues. VII. Polytyrosine and its Related Polypeptides 1

H. TAKAHASHI: Thermal Effects of Some Kaolin Minerals. II. Halloysite. 17

K. SHIMIZU and H. MURATA: Normal Vibrations and Calculated Thermodynamic Properties of Methyltrichlorosilane 46

E. KATO: Phase Transition of Lithium Ferrospinel-Lithium Aluminospinel Solid Solution . 51

H. INOKUCHI and M. NAKAGAKI: The Density of the Polycyclic Aromatic Compounds. . . 65

K. TAKIYAMA: Formation and Aging of Precipitates. X. An Electron Micro-Diffraction Study on Crystal Habit of Barium Sulfate Precipitates. 68

Y. TANIZAKI: Dichroism of Dyes in the Stretched PVA Sheet. II. The Relation between the Optical Density Ratio and the Strech Ratio, and an Attempt to Analyse Relative Directions of Absorption Bands 75

S. TAKAGI, H. CHIHARA and S. SEKI: Vapor Pressure of Molecular Crystals. XIII. Vapor Pressure of α-Glycine Crystal. The Energy of Proton Transfer 84

Analytical and Inorganic

N. MAKI, Y. SHIMURA and R. TSUCHIDA: Polarographic Studies of Metallic Complexes. III. Pentammine Series of Cobalt(III) Complexes 23

I. IWASAKI and T. TARUTANI: Silica in Water. V. Salt Effect on the Colorimetric Determination of Silica in Concentrated Salt Solution. 32

F. AOKI, S. YAJIMA and T. KUROSAWA: Rapid Analysis of Gamma-Emitters Using Gamma-Ray Scintillation Spectrometer. II. Determination of ^{137}Cs in Fission Products . . 42

M. MORI, S. UESHIBA and H. YAMATERA: Photometric Study on the Change of Basic Rhodochromium Ion to Basic Erythrochromium Ion in Aqueous Solution 88

Organic and Biological

K. HATA, K. WATANABE and H. WATANABE: Catalytic Hydrogenation in Vapor Phase with Urushibara Nickel Catalyst. 6

Y. KAWASE: Reactions of Active Methylene Compounds. IV. Synthesis of 2-Hydroxyphenyl Benzyl Ketones and 4-Hydroxy-3-phenylcoumarins. 9

Y. KAWASE: Reactions of Active Methylene Compounds. V. New Synthesis of Hydroxy Substituted 2-Hydroxyphenyl Benzyl Ketones and 4-Hydroxy-3-phenylcoumarins, and Structures of the Latter and Related 2-Imides. 11

S. SAKAKIBARA: Studies on Dehydroalanine Derivatives. I. Synthesis of *N*-Carboxydehydroalanine Anhydride. 13

M. KUROKAWA, K. HOTTA, T. YOSHIMURA, M. MAKITA and I. HARA: Studies on the Cephalin of *Escherichia Coli*. 28

(*Continued on inside cover*)

Published by the Chemical Society of Japan

THE CHEMICAL SOCIETY OF JAPAN

(NIPPON KAGAKUKAI)

Founded in 1948

Successor to the former Chemical Society of Japan founded in 1878 and to the Society of Chemical Industry, Japan founded in 1958.

OFFICERS

Munio KOTAKE, *President*, Osaka University, Osaka
Shin-ichiro FUJISE, *Vice-President*, Tohoku University, Sendai
Taro HAYASHI, *Vice-President*, Ochanomizu Women's University, Tokyo
Tokuichi TSUMAKI, *Vice-President*, Kyushu University, Fukuoka
Kenichi YAMAMOTO, *Vice-President*, Waseda University, Tokyo

BULLETIN OF THE CHEMICAL SOCIETY OF JAPAN

Editor: Yoshiyuki URUSHIBARA, The University of Tokyo, Tokyo
Assistant Editor: Kazuo SAITO, The University of Tokyo, Tokyo
Editorial Board:

Rempei GOTOH	Kei MATSUZAKI	Tadao SHIBA
Hiroshi HAMAGUCHI	Saburo NAGAKURA	Osamu SIMAMURA
Genjiro HAZATO	Hiroshi NOZAKI	Mutsuaki SHINAGAWA
Isao ICHISHIMA	Seizo OKAMURA	Tatsuo TAKESHIMA
Masaji KUBO	Tunetaka SASAKI	Sumio UMEZAWA
Hisao KUROYA	Tetsuro SEIYAMA	

(*Continued from outside cover*)

C. URAKAMI, H. KAMEYAMA and M. OKADA: Antioxygenic Activity of Lecithin and its Hydrolysis Products. II. α- and β-Glycerophosphoric Acids 36

S. NISHIMURA: Raney Nickel and Platinized Raney Nickel with Higher Catalytic Activities. 61

J. HOSHINO: Untersuchungen über die Bildung der Proteinase aus einem *Aspergillus awamori*-Stamm. II. Charakterisierung des Proteinasebildungsvermögens des Mycels im Kultursverlauf durch seinen Stickstoffwechsel. 71

S. UMEZAWA, Y. ITO and S. FUKATSU: Studies on Antibiotics and Related Substances. VII. The Structure of Kanamycin 81

N. TANAKA, I. T. OIWA, T. KUROSAWA and T. NOZOE: The Dissociation Constants of Carboxytropone and Carboxytropolones 92

Applied

T. NODA and Y. SUMIYOSHI: Experiments on Synthetic Mica Crystal Growing. Crystal-Growing with Carbon Granule Resistance Furnace 54

Short Communications

T. IKEDA: Absolute Estination of the Ionic Entropies of Transfer 96

S. FUJISE, M. SUZUKI, Y. WATANABE and S. MATSUEDA: Studies of the Structure of Bergenin 97

V. S. VAIDHYANATHAN: Remarks on the Composition Potential 99

K. HIROTA, K. KUWATA and K. MORIGAKI: Paramagnetic Resonance Absorption in Solution of the Sodium Adducts of Styrene and 1, 1-Diphenylethylene 99

Y. URUSHIBARA and J. INOMATA: 2ξ, 3-(3'-Oxocyclohex-4'-eno)-cholest-4-ene and 2ξ, 3-(3'-Oxocyclohex-4'-eno)-5α-cholestane (Preliminary Note) 101

S. FUJIWARA, M. KATAYAMA and H. SHIMIZU: High Resolution Proton Magnetic Resonance in Fluorobenzene. 101

S. NISHIMURA and K. MORI: Hydrogenolysis and Hydrogenation of Some 2, 3-Unsaturated Alcohols with Platinum Oxide and with Platinized Raney Nickel 103

CHEMISTRY HALL LIBRARY

Surface Chemistry of Synthetic Protein Analogues. VII. Polytyrosine and its Related Polypeptides

By Toshizo ISEMURA and Takuya YAMASHITA

(Received July 22, 1958)

We have previously studied[1-6] the monolayers of synthetic polypeptides with non-electrolytic side chains as well as those with electrolytic side chains at air/water interface. It is well known that tyrosine residue is very specific among other amino acid residues in protein because of the potency of its hydrogen bonding. In the present experiment, poly-L-tyrosine and poly-DL-tyrosine were studied at air/water and oil/water interfaces, in order to investigate the effect of hydrogen bond on the nature of polypeptide monolayer. The monolayer of poly-DL-phenylalanine which lacks only a phenolic OH group per residue was also studied in comparison with polytyrosine. The effect of the phenolic OH group was also investigated by its esterification with benzyl group.

Experimental

Among the samples used in the present investigation, poly-DL-phenylalanine, poly-DL-tyrosine and poly-*o*-benzyl-DL-tyrosine were synthesized by Dr. H. Tani and Dr. H. Yuki of our University, and poly-L-tyrosine by Dr. E. Katchalski and Dr. M. Sela of the Weizmann Institute of Science. The solvents used for each polypeptide are listed in Table I.

Surface pressure and surface potential were measured simultaneously. Surface pressure was measured by Wilhelmy's hanging plate method and surface potential by vibrating air electrode method. The pH of the substrate was adjusted by adding hydrochloric acid or potassium carbonate to any desired pH without buffering. The pH was measured with Beckman's glass electrode or with Toyo pH test paper. Interfacial pressure and interfacial potential were measured by the procedure which was reported previously by Hotta[7-9] of our laboratory, excepting the use of hanging plate instead of detaching ring. At oil/water interface, the interfacial concentration was changed by successive injection method using micrometer syringe. Measurement was carried out five minutes later after every injection. Petroleum ether of boiling point of 90~120°C was used as an oil phase. All the experiments were carried out at room temperature without any temperature regulation. The temperature change never exceeded more than one degree in the course of experiment.

Results and Discussion

Poly-DL-phenylalanine.—We studied at first the film of poly-DL-phenylalanine at air/water and oil/water interfaces as an example of the polypeptide film containing the side chain of benzyl group. In Fig. 1, surface (or interfacial) pressure and surface (or interfacial) moment were plotted per phenylalanyl residue. The surface (or interfacial) moment was calculated from

TABLE I

SOLVENTS USED FOR EACH POLYPEPTIDE

Polypeptide	Solvent	Interface
Poly-DL-phenylalanine	Benzene(9)+Dichloroacetic acid(1)	A/W
	Chloroform	A/W
	Benzene(25)+Dichloroacetic acid(1)	O/W
Poly-L-tyrosine (D. P. 45)	Pyridine(1)+Isopropyl alcohol(1)	A/W, O/W
	Benzene(3)+Dichloroacetic acid(7)	A/W
Poly-DL-tyrosine	Pyridine(1)+Isopropyl alcohol(1)	A/W, O/W
Poly-*o*-benzyl-DL-tyrosine	Benzene(3)+Dichloroacetic acid(2)	A/W, O/W

1) T. Isemura and K. Hamaguchi, This Bulletin, **25**, 40 (1952).
2) T. Isemura and K. Hamaguchi, ibid., **26**, 425 (1953).
3) T. Isemura and K. Hamaguchi, ibid., **27**, 125 (1954).
4) T. Isemura and K. Hamaguchi, ibid., **27**, 339 (1954).
5) K. Hamaguchi and T. Isemura, ibid., **28**, 9 (1955).
6) T. Isemura, K. Hamaguchi and H. Kawasato, ibid., **28**, 185 (1955).
7) T. Isemura, H. Hotta and T. Miwa, ibid., **26**, 360 (1953).
8) H. Hotta, ibid., **26**, 386 (1953).
9) H. Hotta, ibid., **27**, 412 (1954).

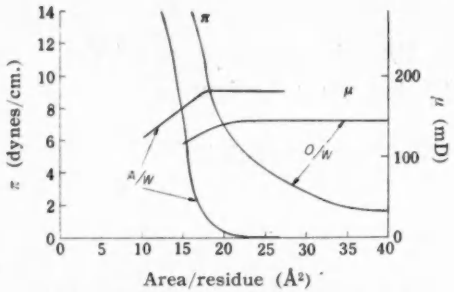

Fig. 1. Surface (or interfacial) pressure (π)-area and surface (or interfacial) moment (μ)-area curves of poly-DL-phenylalanine on distilled water. (A/W interface, 10°C and O/W interface, 13°C).

the observed surface (or interfacial) potential using Helmholtz's formula. $\Delta V = 4\pi n\mu$. The force-area curves of this polypeptide film spread from chloroform solution* and from benzene solution containing a small amount of dichloroacetic acid were exactly identical. A limiting area per residue was found from compressibility-area relation to be 15.8 Å². This area is somewhat larger than that of the typical polypeptide with non-electrolytic paraffine side chains, namely 14.7 Å². Mishuck and Eirich[10] reported that this polypeptide has a small limiting area and attributed this fact to the multilayer formation. On the other hand, Cumper and Alexander[11] found 14.4 Å as the limiting area per residue of this polypeptide from the surface viscosity-area relation. The area found per residue from the force-area relation by them is in rather good agreement with our present result. The surface moment at the area where the film begins to form multilayer is designated by μ_c. μ_c of this polypeptide is 182 mD and is in the same order of magnitude with that of most polypeptide films of non-electrolytic side chains which are spread in β-configuration, whereas Davies[12] reported the surface moment of this polypeptide to be about 100 mD at 30 Å²/residue. At oil/water interface the film is considerably expanded as shown in Fig. 1, because of release of van der Waals force between large side chains such as benzyl groups by oil phase. μ_c was found to be 144 mD and markedly higher than that found by Davies (about 80 mD at 30 Å²).

Poly-L-tyrosine and poly-DL-tyrosine.— The force-area relations of poly-L-tyrosine and poly-DL-tyrosine spread from solutions of respective polypeptide in a mixture of pyridine and isopropyl alcohol (1 : 1) was investigated as a function of pH of the substrate water. The surface pressure-area curves for poly-L-tyrosine and poly-DL-tyrosine are shown in Fig. 2 and Fig. 3, respectively. As shown in these figures on the substrate at pH's less than 9.4 the film considerably condensed. The small area of these polypeptides can not be attributed to partial dissolution of the film as shown in Fig. 4; the presence of salt such as potassium chloride in the substrate water at the concentration of 1.0 mol. per liter scarcely affects the expansion of film. On the other hand, the film is considerably expanded on a substrate at pH's more

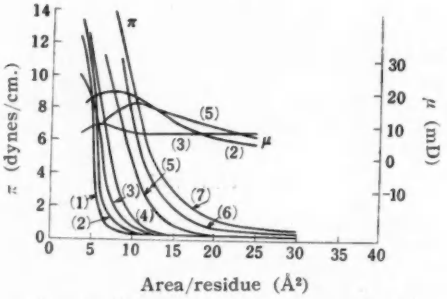

Fig. 2. Surface pressure (π)-area and surface moment (μ)-area curves of poly-L-tyrosine (spread from pyridine-isopropyl alcohol solution). (1) pH 2.0, (2) pH 5.6, (3) pH 7.2, (4) pH 9.4, (5) pH 11.0, (6) pH 11.3 and (7) pH 12.5. (26°C).

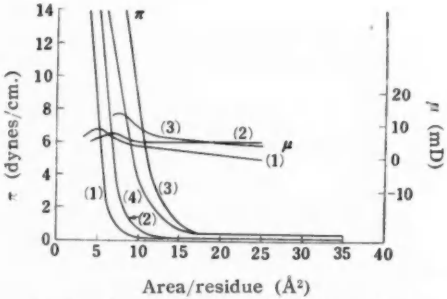

Fig. 3. Surface pressure (π)-area and surface moment (μ)-area curves of poly-DL-tyrosine. (1) pH 5.6, (2) pH 9.2, (3) pH 11.0 and (4) pH 12.5. (24°C).

* Unpublished experiment by Dr. K. Hamaguchi in our laboratory.

10) E. Mishuck and F. R. Eirich, *J. Polymer Sci.*, **16**, 397 (1955).

11) C. W. N. Cumper and A. E. Alexander, *Trans. Faraday Soc.*, **46**, 235 (1950).

12) J. T. Davies, *Biochim. Biophys. Acta*, **11**, 165 (1953).

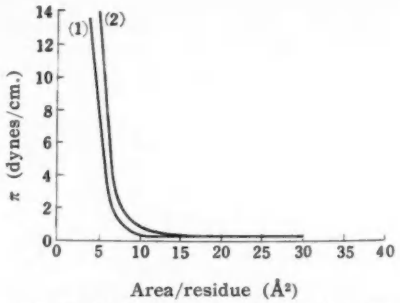

Fig. 4. Effect of the salt on poly-L-tyrosine (spread from pyridine-isopropyl alcohol solution) at pH 5.6. (1) no salt and (2) 1 mol. KCl. (26°C).

than 11.0. However, when the pH of the substrate becomes more than 13, it dissolves rather than expands. In Figs. 2 and 3, the surface moment-area relations of poly-L-tyrosine and poly-DL-tyrosine are also shown, respectively. Surface moment is very small in comparison with that of poly-DL-phenylalanine. The trend of the curve is very different from that of other polymer films. These facts may be caused by the cancellation of dipole by intramolecular hydrogen bond. Several years ago, Masuda and Eda[13] reported the small area per tyrosine residue for poly-DL-tyrosine film. They found a smaller area on acid substrate than on alkaline substrate. This may be caused by partial dissolution of polypeptide because of the smaller degree of polymerization of the polypeptide which they used.

Polytyrosine films spread at air/water interface occupy much less area than the films of other polypeptides such as polyphenylalanine and show much smaller surface moment as mentioned above. These anomalous properties of polytyrosine might come from the hydrogen bonding of phenolic OH group in tyrosine residue. Without this hydroxyl group, polytyrosine may assume exactly a structure of polyphenylalanine. Accordingly, the film would have a limiting area of about 15 Å² per residue. Nevertheless, the limiting area per residue for poly-L-tyrosine was found to be 5.7 Å² and that for poly-DL-tyrosine to be 5.8 Å² both at pH 5.6. These small areas per residue may be attributed to the spreading of these polypeptides in a coiled state, owing to the strong hydrogen bonding of phenolic OH groups. The extremely low value of surface moment supports also this inference. Even on alkaline substrate, the spreading of the film is not complete, although the film expands considerably at pH region between 8.0 and 11.5. As shown in Fig. 5, this finding corresponds to the partial breaking of hydrogen bonds and to the partial dissociation of phenolic OH groups, and to the result of spectrophotometric titration by Katchalski and Sela[14,15]. On the other hand, we obtain the film which seems to assume β-keratin configuration irrespective of the pH of the substrate if we spread it from a solution in dichloroacetic acid which is a strong hydrogen-bond breaking agent. The surface moment of the film thus obtained is about 120~130 mD, as shown in Fig. 6, suggesting the intramolecular cancellation of OH contributions to surface moment

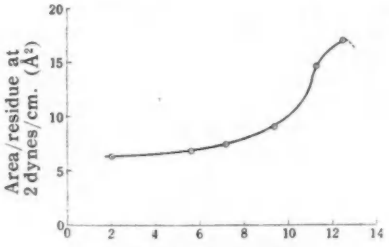

Fig. 5. Effect of pH of the substrate water on the area at 2 dynes/cm. of poly-L-tyrosine (spread from pyridine-isopropyl alcohol solution) at air/water interface.

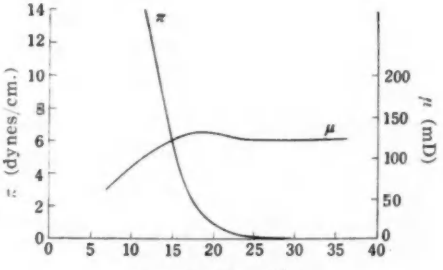

Fig. 6. Surface pressure (π)-area and surface moment (μ)-area curves of poly-L-tyrosine (spread from dichloroacetic acid and benzene solution) on distilled water. (16°C).

13) Y. Masuda and K. Eda, *Science [Japan] (Kagaku)*, **21**, 470 (1951).

14) E. Katchalski and M. Sela, *Bull. Research Council of Israel*, **2**, 315 (1952).

15) E. Katchalski and M. Sela, *J. Am. Chem. Soc.*, **75**, 5284 (1953).

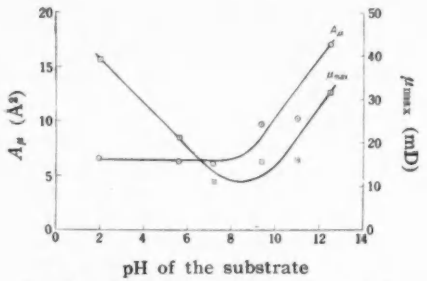

Fig. 7. Monolayers of poly-L-tyrosine (spread from pyridine-isopropyl alcohol solution). Area at maximum surface moment (A_μ)-pH and maximum surface moment (μ_{max})-pH curves.

and tending to the value of surface moment of ordinary polypeptide films. In Fig. 7, the surface moment of polytyrosine increases as the film is compressed and passes a maximum and then decreases, whereas most usual well-spread linear polymer shows a constant surface moment, μ_c until the polymer film is closely packed as the film is compressed and further compression causes the decrease of surface moment. The maximum surface moment, μ_{max} and the area where the maximum moment was found, A_μ, are plotted against pH. μ_{max} increases considerably above pH 8.5. This might be caused by the unfolding and reorientation of polypeptide owing to the breaking of some hydrogen bonds. The reason why μ_{max} increases at the extreme acid substrate is not clear but is presumably due to the formation of oxonium ions[16].

In Figs. 8 and 9, the results obtained at petroleum ether/water interface are shown. The film is considerably expanded.

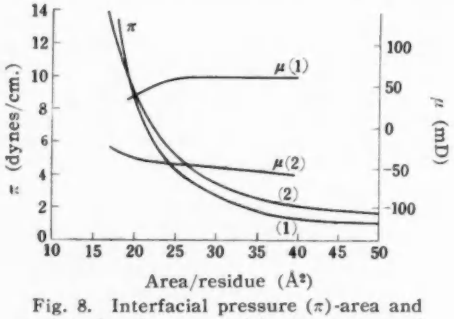

Fig. 8. Interfacial pressure (π)-area and interfacial moment (μ)-area curves of poly-L-tyrosine. (1) pH 2.0, 13°C and (2) 11.0, 15°C.

16) I. Sawai, *Trans. Faraday Soc.*, **31**, 765 (1938).

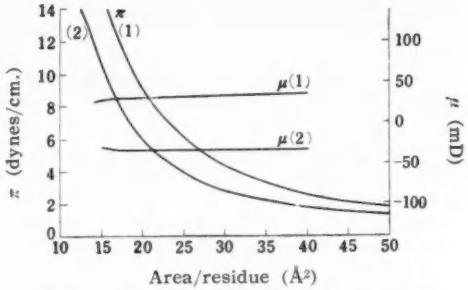

Fig. 9. Interfacial pressure (π)-area and interfacial moment (μ)-area curves of poly-DL-tyrosine. (1) pH 2.0 and (2) pH 11.0. (22°C).

Poly-L-tyrosine film is more expanded at pH 11.0 than at 2.0, whereas poly-DL-tyrosine is more expanded at pH 2.0 than at pH 11.0. The force-area curves are like those of the monolayers of polypeptide with nonpolar side chains such as poly-DL-phenylalanine. At pH 2 all the side chains of *p*-hydroxybenzyl group might be dissolved in the oil phase. Interfacial potential was found to be 60 mD (μ_c) for poly-L-tyrosine and 32 mD at 25 Å²/residue for poly-DL-tyrosine. These values are markedly less than that for poly-DL-phenylalanine (144 mD (μ_c)). This difference might be caused by the contribution of phenolic OH group of tyrosine. Poly-DL-tyrosine is more expanded than poly-L-tyrosine corresponding to the general tendency of expansion of poly-DL-amino acid more than poly-L-amino acid as previously reported[3]. On the other hand, the fact that at air/water interface the film of poly-DL-tyrosine occupies less area than poly-L-tyrosine does at pH 12.5 is due to the general tendency of higher solubility of poly-DL-amino acid than poly-L-amino acid. If the aqueous phase is alkaline, the phenolic OH dissociates and dissolves in the aqueous phase at both air/water and oil/water interfaces. In this case the contribution of dipole is inverse. The negative surface moment was found at oil/water interface, namely −44 mD at 25 Å²/residue for poly-L-tyrosine and −34 mD (μ_c) for poly-DL-tyrosine.

From these results we can conclude that both poly-L-tyrosine and poly-DL-tyrosine spread incompletely at air/water interface and the film is in a partially coiled state because of the hydrogen bonding of phenolic OH group if it is not ionized. However, at oil/water interface by the release of van der Waals force between

side chains due to the intervening of oil, hydrogen bonds are readily broken, and the monolayer which seems to be in β-configuration is obtained. Even at air/water interface, similar monolayer is obtained when we spread the film from a solution in hydrogen bond breaking agent. The obtained force-area curve is very similar to that of poly-DL-phenylalanine. With this monolayer, surface moment of 132 mD (μ_{max}) is found.

Poly-*o*-benzyl-DL-tyrosine. — Force-area and surface (interfacial) moment-area curves of poly-*o*-benzyl-DL-tyrosine at air/water and oil/water interfaces are shown in Fig. 10. Because of lacking of hydrogen bonding agency by esterification of phenolic OH groups, the film is well spread at air/water interface. The area per residue at minimum compressibility is somewhat less than that of poly-DL-phenylalanine and polytyrosine which was spread from the solution containing dichloroacetic acid. The large van der Waals force between side chains seems to cause the condensation of the film. The maximum value of surface moment reached 123 mD. Surface moment increased as the film was compressed, especially when the force-area curve begins to stand steeply at about 20 Å^2 residue. This change is based on the reorientation of large polar side chains. At oil/water interface, poly-*o*-benzyl-DL-tyrosine expanded considerably more than any other polypeptides mentioned above. All large side chains may be in the oil phase, and there is no interaction between the side chain because of the release of van der Waals force between them by intervening of oil. The size and difficulty of packing such large chains may be the cause of the expansion of the film. Interfacial moment was found to be 150 mD

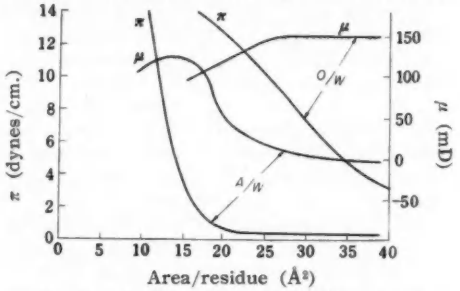

Fig. 10. Surface (or interfacial) pressure (π)-area and surface (or interfacial) moment (μ)-area curves of poly-*o*-benzyl-DL-tyrosine on distilled water. (24°C).

TABLE II

AREAS AND SURFACE AND INTERFACIAL MOMENTS FOR EACH POLYPEPTIDE

	Interface	Aqueous phase	pH	Temp. (°C)	A_π (Å^2/residue)	$A_{\pi=5}$ (Å^2/residue)	μ (mD)	A_μ (Å^2/residue)
Poly-DL-phenyl-alanine	A/W	d.w	5.4	10	15.8	15.6	182(C)	17.8
	O/W	d.w	5.4	13		22.8	144(C)	23.0
Poly-L-tyrosine (Pyridine-Isopropyl alcohol)	A/W	d.w	5.6	26	5.7	5.7	21(M)	6.2
		0.01 N K_2CO_3	11.0	26	10.4	10.0	10(M)	16.0
	O/W	0.01 N HCl	2.0	13		23.7	60(C)	25.0
		0.01 N K_2CO_3	11.0	15		25.0	−44 (at 25 Å^2)	
Poly-L-tyrosine (Dichloroacetic acid-Benzene)	A/W	d.w	3.0	16	15.4	15.6	132(M)	18.8
Poly-DL-tyrosine	A/W	d.w	5.6	24	5.8	5.6	9(M)	4.8
		0.01 N K_2CO_3	11.0	24	11.0	11.0	8(M)	14.0
	O/W	0.01 N HCl	2.0	22		28.0	32 (at 25 Å^2)	15.2
		0.01 N K_2CO_3	11.0	22		22.5	−34(C)	16.0
Poly-*o*-benzyl-DL-tyrosine	A/W	d.w	4.0	24	13.8	13.9	123(M)	14.2
	O/W	d.w	4.2	24		33.7	150(C)	29.2

A_π: Area at minimum compressibility (limiting area), $A_{\pi=5}$: Area at 5 dynes/cm., μ: Surface (or interfacial) moment, (C): Constant value, (M): Maximum value, A_μ: Area at which μ begins suddenly decrease, or area at the maximum value of μ, d.w: Distilled water.

(μ_c) which corresponds namely to the value of poly-DL-phenylalanine.

All the results are summarized in Table II.

Summary

The monolayer properties of synthetic polypeptides which have phenolic OH groups in the side chains such as poly-L-tyrosine and poly-DL-tyrosine were studied to investigate the effect of hydrogen bonding by tyrosyl OH groups. Poly-*o*-benzyl-DL-tyrosine and poly-DL-phenylalanine were also studied for comparison.

At air/water interface, poly-L-tyrosine and poly-DL-tyrosine occupy much smaller area per residue than any other polypeptide films, and have very small surface moment, if they were spread from the solution in pyridine and isopropyl alcohol mixture. These polypeptides might be spread in a strict sense not in an extended monolayer but in a coiled state, suggesting the hydrogen bond between phenolic OH and —CO— or —NH— groups in the main chain. On the alkaline substrate the film expands considerably because of the breaking of hydrogen bonds by the ionization of phenolic OH. At petroleum ether/water interface, the film is also expanded by releasing of van der Waals force. Interfacial moment changes its sign due to whether the aqueous phase is acid or alkaline. It suggests that *p*-hydroxybenzyl groups are in the oil phase at oil/acid solution, whereas they are in the aqueous phase at oil/alkaline solution. Poly-L-tyrosine assumes the configuration very similar to that of poly-DL-phenylalanine, if poly-L-tyrosine is spread from a solution in dichloroacetic acid which is a strong hydrogen bond breaking agent.

Poly-*o*-benzyl-DL-tyrosine gives a monolayer which is somewhat more condensed than poly-DL-phenylalanine at air/water interface, whereas it occupies a larger area per residue than poly-L-tyrosine, poly-DL-tyrosine and poly-DL-phenylalanine at oil/water interface. All these findings are caused by the existence of very large side chains in poly-*o*-benzyl-DL-tyrosine.

The authors express their hearty thanks to Dr. H. Tani and Dr. H. Yuki of the Faculty of Science of Osaka University and Professor E. Katchalski and Dr. M. Sela of the Weizmann Institute of Science in Israel who gave them the valuable samples of synthetic polypeptides. The expense for the experiment was partly defrayed from the grant given by the Ministry of Education, to which the authors' thanks are due.

The Institute of Scientific and Industrial Research, Osaka University, Sakai, Osaka
and
The Institute for Protein Research Osaka University, Tosabori Nishi-ku, Osaka

Catalytic Hydrogenation in Vapor Phase with Urushibara Nickel Catalyst

By Kazuo HATA, Ken-ichi WATANABE and Hamao WATANABE

(Received July 31, 1958)

It has been reported[1] that catalytic hydrogenation in vapor phase with Urushibara nickel catalyst (U-Ni in abbreviation) was carried out for the first time and the experimental results were fairly good. In consequence, it has been proved that U-Ni as a catalyst for hydrogenation is able to be used effectively in vapor phase as well as in liquid phase[2]. It is not as troublesome to use U-Ni as to use other catalysts such as Sabatier's reduced nickel catalyst.

From the previous investigations, we got a suggestion of preparing U-Ni from

1) K. Hata, K. Watanabe and S. Sato, This Bulletin, **30**, 431 (1957).

2) Y. Urushibara and S. Nishimura, ibid., **27**, 480 (1954); Y. Urushibara, S. Nishimura and H. Uehara, ibid., **28**, 446 (1955); K. Hata et al., *J. Chem. Soc. Japan, Pure Chem. Sec.* (*Nippon Kagaku Zasshi*), **77**, 1405 (1956).

nickel chloride solution and aluminum metal in place of zinc dust. In this paper, we introduce a new study using U-Ni which is made from nickel chloride and aluminum metal. It was found that U-Ni thus made was a more excellent hydrogenation catalyst in vapor phase than any other one because of its activity and convenience in practical use.

At first aluminum powder was used for the precipitating agent, and the precipitated nickel was treated with alkali. The catalyst thus obtained was found to be useful for the reduction of some organic substances. However, aluminum powder did not seem to be entirely suitable for the preparation of the catalyst, although the preparation could be carried out more easily by the addition of some detergent. Then grained aluminum (45 meshes) was chosen instead of aluminum powder. Nickel was precipitated from nickel chloride solution on the surface of aluminum grains, and the precipitated nickel was treated with acetic acid containing inorganic salt such as sodium chloride, whereby the precipitated nickel did not separate from the aluminum grains*. U-Ni catalyst thus prepared, which is called U-Ni-AA** in abbreviation, was proved to be a very convenient catalyst for vapor phase hydrogenation because the grains of aluminum remained undissolved after they were treated with acetic acid, and served as carrier.

A similar catalyst prepared by digesting the precipitated nickel with alkali is called U-Ni-BA**, which is also useful for hydrogenation. U-Ni-BA for the liquid phase hydrogenation must be prepared with grained aluminum[3], but for the vapor phase hydrogenation, it was proved that U-Ni-BA prepared from nickel chloride and commercially available aluminum powder was effective enough. The conditions of preparation of these U-Ni catalysts are shown in Table I.

The results of hydrogenation with these catalysts are summarized in Table II. Nitrobenzene was reduced to aniline, phenol to cyclohexanol. Both styrene and acetophenone were hydrogenated with U-Ni-BA to ethylbenzene (Exp. No. 3 and 4); when U-Ni-AA was used, they were reduced further to ethylcyclohexane (Exp. No. 9 and 10). It is very remarkable that benzene was reduced to cyclohexane[4] with U-Ni-AA, but not with U-Ni-BA (prepared with aluminum powder). Benzonitrile was largely reduced to toluene and ammonia[5], and the result of this cleavage reaction was different from that of previous experiments[1] using U-Ni-A (prepared from nickel chloride and zinc dust).

From these results, it is evident that the aromatic ring is able to be reduced by the use of this new type catalyst U-Ni-AA, while not by U-Ni-A*** or U-Ni-B***. In addition, it is interesting to note that U-Ni-AA can also be used in the hydrogenation in liquid phase under the condition of room temperature and ordinary pressure of hydrogen. For example, nitrobenzene was reduced to aniline in 70% yield in ethanol. Thus U-Ni-AA is shown to be effective for hydrogenation both in vapor and liquid phase as well as reduced nickel catalyst. It may be expected that U-Ni prepared from aluminum will be widely applied in the field of catalytic chemistry.

Experimental

U-Ni-AA.—To 60 g. of grained aluminum (45 meshes), a small amount of water is added. In another vessel, 80 cc. of nickel solution containing 32 g. of $NiCl_2 \cdot 6H_2O$ is heated to 50~60°C, and added to the aluminum with stirring. An exchange reaction occurs and nickel deposits on the surface of the aluminum. The reaction is controlled by cooling with cold water or by heating with hot water. The precipitated nickel is washed with cold water. Then 40% acetic acid solution (385 cc., 70°C) containing 89 g. of sodium chloride is added to the nickel. After 3~7 minutes, the acid solution is decanted, and the residue washed with ca. 2 l. of warm water (50~60°C) and then with methanol. The catalyst thus obtained contains 8 g. of nickel.

U-Ni-BA (for vapor phase hydrogenation).—Ten g. of aluminum powder (200 meshes) is suspended in a small amount of water, and heated on a boiling water bath. Then 10 cc. of warm nickel chloride solution containing 4 g. of $NiCl_2 \cdot 6H_2O$ (ca. 90°C) is added to the aluminum. After a violent exchange reaction ceases, all

* The procedure of preparing the catalyst and of the hydrogenation was quite different unless the salt was used, and the catalyst thus prepared was not suitable for hydrogenation.

** In abbreviation, the last A means aluminum as precipitating agent, and the first A and B mean acid and base as the digesting solution for the precipitated nickel.

3) K. Hata, S. Taira and I. Motoyama, This Bulletin, **31**, 776 (1958).

4) P. Sabatier and J. B. Senderens, *Compt. rend.*, **132**, 210 (1901).

5) P. Sabatier and J. B. Senderens, ibid., **140**, 482 (1905); K. Hata, *Sci. Papers Inst. Phys. Chem. Research (Tokyo)*, **23**, 224 (1944); M. Tanaka, K. Watanabe and K. Hata, *J. Chem. Soc. Japan, Pure Chem. Sec.* (*Nippon Kagaku Zasshi*), **76**, 1392 (1955).

*** Only phenol was reduced to cyclohexanol in 20~30% yield with U-Ni-A or U-Ni-B (unpublished).

TABLE I
PREPARATION OF CATALYSTS

Catalyst	$NiCl_2 \cdot 6H_2O$ (g.)	Al (g.)	Al (mesh)	Digesting solution	NaCl (g.)	Carrier
U-Ni-AA	32	60	45	40% CH_3CO_2H (385 cc.)	89*	—
U-Ni-BA	4	10	200	20% NaOH (200 cc.)	—	Pumice stone
U-Ni-BA	12	15	45	20% NaOH (350 cc.)	—	" Hyflosupercel "

* The quantity to saturate the acid solution.

TABLE II
VAPOR PHASE CATALYTIC HYDROGENATION WITH U-Ni CATALYSTS

Exp. No.	Catalyst	Compounds	Weight of sample (g.)	Nickel (g.)	Temp. (°C)	Time (hr.)	Flow velocity of sample (g./min.)	Products and Yields (%)	
1	U-Ni-BA	Nitrobenzene	8	1	240[1]	5	0.038	Aniline[2]	(58)
2	U-Ni-BA	Phenol	10	4	185[1]	6	0.034	Cyclohexanol	(79)
3	U-Ni-BA	Styrene	4.3	1	195[1]	4	0.029	Ethylbenzene	(91)
4	U-Ni-BA[3]	Acetophenone	5	3	200	1 3/4	0.114	Ethylbenzene	(52)
5	U-Ni-AA	Nitrobenzene	5	8	230	2	0.094	Aniline[2]	(65)
6	U-Ni-AA	Phenol	5	8	180	3 1/2	0.111	Cyclohexanol	(66)
7	U-Ni-AA	Benzonitrile	5	8	250	2	0.075	Toluene	(76)
8	U-Ni-AA	Benzene	5	8	176	2 1/3	0.046	Cyclohexane[4]	(83)
9	U-Ni-AA	Styrene	5	8	150	2	0.073	Ethylcyclohexane[5]	(94)
10	U-Ni-AA	Acetophenone	5	8	190	2	0.069	Ethylcyclohexane[6]	(71)

1) The temperature of the oil bath.
2) Besides aniline, high molecular amines were obtained as by-products.
3) Grained aluminum (45 meshes) was used, and " Hyflosupercel " was used as carrier.
4) B. p. 80~81.2°C, $n_D^{20}=1.4270$ (lit. 1.4266).
5) B. p. 127~128°C, $n_D^{20}=1.4347$ (lit. 1.4324).
6) B. p. 128~131.8°C, $n_D^{20}=1.4332$ (lit. 1.4324).

the contents are heated to dryness, and 200 cc. of 20% sodium hydroxide solution is added gradually. Since a vigorous exothermic reaction takes place, the contents are stirred well and cooled with running water, and the aluminum is completely dissolved in a short time. Treatment of the nickel precipitate is accomplished by heating for about five minutes. The supernatant solution is decanted, and the residue washed with warm water (50~60°C) until the washing becomes neutral to litmus, and then with methanol thoroughly. The catalyst thus obtained contains about 1 g. of nickel.

Method of hydrogenation.—In the earlier period of these experiments, a special U-tube apparatus was used for hydrogenation reactions, and the reaction tube was heated in an oil bath, as previously reported[1]. In Table II, the experiments, Nos. 1—3, were carried out by the above method.

The U-tube method being somewhat troublesome, the usual hydrogenation method, e. g. with Sabatier's hydrogenation apparatus, has been adopted for convenience. Further experiments, Nos. 4—10, were carried out by such a method in a hard glass reaction tube, 1.8 cm. in diameter and 90 cm. in length, heated in an electric furnace. In experiment No. 4, " Hyflosupercel " (purified kieselguhr) was used as a carrier.

The catalyst was put into the reaction tube, and heated up to an appropriate reaction temperature, while methanol, which was used for washing the catalyst, was expelled by heating. The vaporized sample, together with a large excess of hydrogen, was introduced into the reaction tube. The reaction products flowing out of the tube were collected into the receiver through a condenser, and were isolated by means of fractional distillation. Then each product was identified by preparing an appropriate derivative respectively, except in the case of cyclohexane and ethylcyclohexane.

Summary

Catalytic hydrogenation in vapor phase with new types of Urushibara nickel catalyst was carried out.

1) New types of U-Ni were prepared from nickel chloride and aluminum. U-Ni-BA and U-Ni-AA were respectively obtained by treating the precipitated nickel with alkali or acetic acid.

2) These catalysts are quite easy to prepare and were proved to be useful for hydrogenation. Above all, U-Ni-AA is the most convenient for vapor phase hydrogenation, since it was found to be highly active and the aluminum served as carrier. It was also used in hydrogenation in liquid phase.

The authors express their gratitude to the Ministry of Education for the financial support of this research.

Department of Chemistry
Faculty of Science
Tokyo Metropolitan University
Setagaya-ku, Tokyo

Reactions of Active Methylene Compounds. IV. Synthesis of 2-Hydroxyphenyl Benzyl Ketones and 4-Hydroxy-3-phenylcoumarins (Continued)

By Yoshiyuki KAWASE

(Received August 4, 1958)

In the previous paper[1], 2-hydroxyphenyl benzyl ketones (III) and 4-hydroxy-3-phenylcoumarins (V) were prepared from 2-methoxybenzoyl-phenylacetonitriles (I) and ethyl 2-methoxybenzoyl-phenylacetates (II). Afterwards, it was known that Chatterjea and Roy[2] had reported a preparation of III (R, R′=H) and V (R, R′=H) from I (R, R′=H) by the action of hydrobromic acid in acetic acid.

The present paper describes a preparation of an analogous series of compounds (Ia, IIa, IIIa, IVa, b, b′ and Va, a′, b) by the same procedure described in the previous paper.

By the action of anhydrous aluminum chloride (2 moles) in nitrobenzene, 4-hydroxy-3-phenylcoumarin-2-imides (IVa, b) were obtained from nitriles Ia, b, methoxy groups of which all, except one in the *o*-position of the carbonyl group, were unaffected. 4-Hydroxy-3-phenylcoumarins (Va, b) were obtained from the imides IVa, b by acid hydrolysis, and Va was also obtained from IIa by means of aluminum chloride in nitrobenzene. By the use of an increased amount (4.5 moles) of aluminum chloride, small amounts of IVb′ and Va′ were obtained from Ib and IIa respectively, 4′-methoxy groups of which were demethylated. Attempted preparations of imide IVa′ from Ia, of coumarins Vb, b′ from IIb, and of IVa by ester condensation of methyl salicylate with *p*-methoxyphenylacetonitrile were unsuccessful.

1) Y. Kawase, This Bulletin, **31**, 390, 440 (1958).
2) J. N. Chatterjea and S. K. Roy, *J. Indian Chem. Soc.*, **34**, 155 (1957) [*Chem. Abst.*, **52**, 1987 (1958)]; cf. J. N. Chatterjea and S. K. Roy, *J. Indian Chem. Soc.*, **34**, 98 (1957) [*Chem. Abst.*, **51**, 16445 (1957)].

Experimental[3]

2-Methoxybenzoyl-4-methoxyphenylacetonitrile (Ia).—To a solution of methyl 2-methoxybenzoate (5.5 g.) and 4-methoxyphenylacetonitrile (4.5 g.) in anhydrous benzene (100 cc.), sodium hydride (1.5 g., 2 moles) was added and the mixture was heated for 4 hr. on an oil-bath (95～100°), most of the benzene being distilled off in the meantime. The well-cooled mixture was treated with water and extracted with ether. The alkaline aqueous solution was acidified and the solid product separated was collected, washed with aqueous sodium bicarbonate, and recrystallized from ethanol in colorless prisms, m.p. 109～110.5°; yield 6 g. or 70%.

Anal. Found: C, 72.37; H, 5.27; N, 5.05. Calcd. for $C_{17}H_{15}O_3N$: C, 72.58; H, 5.37; N, 4.98%.

Ethyl 2-Methoxybenzoyl-4-methoxyphenylacetate (IIa).—A solution of nitrile Ia (2.2 g.) in anhydrous ethanol (50 cc.) containing one mole of water (0.14 cc.) was saturated with hydrogen chloride with cooling. After three days at room temperature, water was added and ethanol was removed in vacuo. The gummy product separated was taken up in ether, washed with aqueous sodium hydroxide, and distilled to give colorless viscous oil, b. p. 180～200°/0.004mm. (bath-temperature); yield 1.6 g. or 62%.

Anal. Found: C, 69.23; H, 5.90. Calcd. for $C_{19}H_{20}O_5$: C, 69.50; H, 6.14%.

2-Hydroxyphenyl 4-Methoxybenzyl Ketone (IIIa).—(*a*) *From nitrile Ia.*—A solution of Ia (0.5 g.) in acetic acid (10 cc.) containing concentrated hydrochloric acid (5 cc.) was heated on a

3) Melting and boiling points are uncorrected.

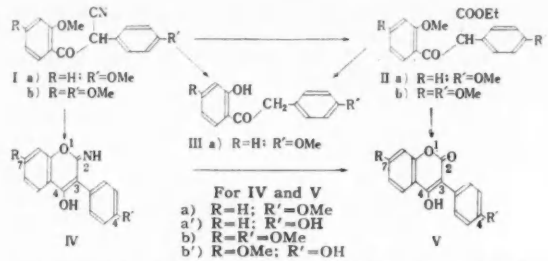

steam-bath for 15 hr. The cooled solution was made alkaline with aqueous sodium hydroxide and extracted with ether. The residue obtained from the ether solution was distilled to give colorless oil, b. p. 160~180°/0.003 mm. (bath-temperature); yield 0.2g. 2,4-Dinitrophenylhydrazone, m. p. 198~199° (from ethanol).

Anal. of 2, 4-dinitrophenylhydrazone. Found: C, 59.66; H, 4.11; N, 13.28. Calcd. for $C_{21}H_{18}O_6N_4$: C, 59.71: H, 4.30; N, 13.27%.

(*b*) *From ester IIa.*—By the same procedure described for (a), 0.2 g. of IIIa was obtained from 0.5 g. of IIa; b. p. 160~180°/0.003 mm. (bath-temperature). 2, 4-Dinitrophenylhydrazone, m. p. 197~198°, was identical with the sample from (a).

4-Hydroxy-4'-methoxy-3-phenylcoumarin-2-imide (IVa).—A mixture of Ia (0.5 g.) and anhydrous aluminum chloride (0.5 g., 2.1 moles) in nitrobenzene (5 cc.) was heated on a steam-bath for 1 hr. The cooled solution was treated with water, and nitrobenzene was removed by steam-distillation. The semi-solid product separated from the residue was taken up in ethyl acetate, and extracted with dilute hydrochloric acid. The acid aqueous solution was made alkaline with aqueous sodium bicarbonate, and the precipitates obtained were crystallized from ethanol in colorless microcrystals, m. p. 214.5~215.5°; yield 0.1 g.

Anal. Found: C, 71.75; H, 5.34; N, 5.16. Calcd. for $C_{16}H_{13}O_3N$: C, 71.90; H, 4.90; N, 5.24%.

4-Hydroxy-4'-methoxy-3-phenylcoumarin (Va).—(*a*) *From imide IVa.*—A solution of IVa (ca. 0.05 g.) in 2 cc. of dilute hydrochloric acid (1 : 1) was heated on a steam-bath for 2 hr. The separated crystals were collected and recrystallized from dilute ethanol in colorless microcrystals, m.p. 228~229°; identical with the sample from (b).

(*b*) *From ester IIa.*—A mixture of IIa (0.5 g.) and aluminum chloride (0.5 g., 2.4 moles) in nitrobenzene (5 cc.) was heated for 1 hr. The cooled solution was treated with dilute hydrochloric acid, and nitrobenzene was removed by steam-distillation. The semi-solid product separated from the residue was taken up in ethyl acetate and extracted with aqueous sodium carbonate. The product obtained by acidifying the alkaline solution was recrystallized from dilute ethanol; m. p. 230~231°, yield 0.1 g.

Anal. Found: C, 71.63; H, 4.54. Calcd. for $C_{16}H_{12}O_4$: C, 71.63; H, 4.15%.

4, 4'-Dihydroxy-3-phenylcoumarin (Va').—A mixture of IIa (0.5 g.) and aluminum chloride (0.8 g., 4 moles) in nitrobenzene was worked up as before, and nitrobenzene was removed by steam-distillation. The residual aqueous mixture was filtered while hot, and the crystalline product formed from the filtrate on cooling was recrystallized from dilute ethanol; m. p. 254~255°, yield ca. 0.05 g. It was identical with the sample which will be described in the next paper.

The semi-solid precipitates obtained in the above mentioned filtration were dissolved in ethyl acetate, and treated as before to give Va (ca. 0.05 g.), m. p. 226~227° (from ethyl acetate); identical with the sample described before.

4-Hydroxy-4', 7-dimethoxy-3-phenylcoumarin-2-imide (IVb).—By the same procedure as described before, 0.1 g. of the compound was obtained from 0.5 g. of Ib and 0.5 g. (2.5 moles) of aluminum chloride; m. p. 214~215° (from ethanol).

Anal. Found: C, 68.59; H, 5.33; N, 5.55. Calcd. for $C_{17}H_{15}O_4N$: C, 68.67; H, 5.08; N, 4.71%.

4-Hydroxy-4', 7-dimethoxy-3-phenylcoumarin (Vb).—By hydrolysis of imide IVb with hydrochloric acid, Vb was obtained in colorless needles, m. p. 213~214° (from dilute ethanol). Reported m. p. is 219~220°[4].

Anal. Found: C, 68.10; H, 5.24. Calcd. for $C_{17}H_{14}O_5$: C, 68.45; H, 4.73%.

4, 4'-Dihydroxy-7-methoxy-3-phenylcoumarin-2-imide (IVb').—By the same procedure as described before, a small amount of the compound was obtained from 0.8 g. of Ib and 1.5 g. (4.5 moles) of aluminum chloride; m. p. 287~288° (from ethanol), soluble in acid and in cold aqueous sodium hydroxide.

Anal. Found: C, 67.33; H, 4.66; N, 4.79. Calcd. for $C_{16}H_{13}O_4N$: C, 67.83; H, 4.59; N, 4.94%.

From the ethanolic mother liquor of recrystallization, 0.1 g. of IVb was obtained.

The author wishes to express his hearty thanks to Professor K. Fukui for his helpful advice and encouragement, and to the members of the Agricultural Department of Kyoto University for microanalyses.

Faculty of Literature and Science
Toyama University, Toyama

4) J. Boyd and A. Robertson, *J. Chem. Soc.*, **1948**, 174.

*Reactions of Active Methylene Compounds. V. New Synthesis of Hydroxy Substituted 2-Hydroxyphenyl Benzyl Ketones and 4-Hydroxy-3-phenylcoumarins, and Structures of the Latter and Related 2-Imides**

By Yoshiyuki KAWASE

(Received August 4, 1958)

The present paper describes the action of anhydrous pyridine hydrochloride on methoxy substituted ethyl 2-methoxybenzoyl-phenylacetates (II) and 2-methoxybenzoyl-phenylacetonitriles (I) to give hydroxy substituted 2-hydroxyphenyl benzyl ketones (III) and 4-hydroxy-3-phenylcoumarins (V) respectively, and the structures of the latter and the intermediate, 2-imides IV of V are discussed through their infrared spectra.

Anhydrous pyridine hydrochloride is often used for demethylation of methyl ether of phenols[1]; for instances, similar to the present work, 2-methoxybenzal-phenylacetonitriles were transformed into 3-phenylcoumarins[2] and 4-hydroxy-2′-methoxy-3-phenylcoumarins into coumarino (3′, 4′: 3, 2) coumarones[3].

The action of this reagent on nitriles Ia~d[4] under reflux caused demethylation of all the methoxy groups and subsequent cyclization to give the intermediate imides IV, which were readily converted into hydroxy substituted 4-hydroxy-3-phenylcoumarins (Va~d) by acid hydrolysis. Methoxy substituted IV and V had been obtained[5] by the action of aluminum chloride on I and II respectively, methoxy groups of which in the *p*-position of carbonyl group were unaffected. On the other hand, the action of pyridine hydrochloride on esters IIa~d[4] caused at first cleavage of ester group, decarboxylation, and then demethylation of all the methoxy groups to give hydroxy substituted 2-hydroxyphenyl benzyl ketones (IIIa~d). Methoxy substituted III had been obtained[4] by the action of hydrochloric acid on I and II, methoxy groups of which expect one in the *o*-position of the carbonyl group were unaffected.

It is reported that absorptions by carbonyl groups of 4-hydroxycoumarins[6,7] are in a shorter region, and that of chromones[7,8] are in a longer region, than 6 μ.

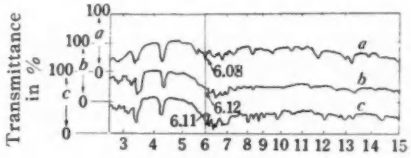

Fig. 1. Infrared spectra of VIII (a), VIa (b) and VIe (c).

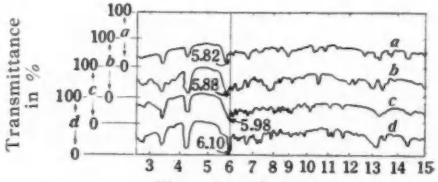

Fig. 2. Infrared spectra of IX (a), X (b), VIIa (c) and XIa(d).

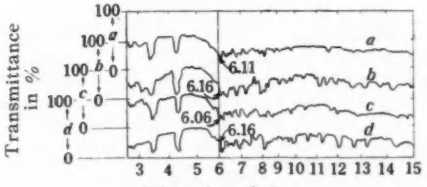

Fig. 3. Infrared spectra of VIIb (a), XIb (b), VIIe (c) and XIc (d).

* Preliminary report: Y. Kawase, *Experientia*, **14**, Nov. (1958).

1) V. Prey, *Ber.*, **74B**, 1219 (1941); **75B**, 350 (1942).
2) Ng. Ph. Bun-Hoï et al., *J. Chem. Soc.*, **1951**, 2307; *J. Org. Chem.*, **21**, 1022 (1956).
3) T. R. Govindachari et al., *J. Chem. Soc.*, **1957**, 548.
4) Y. Kawase, This Bulletin, **31**, 390 (1958); **32**, 9 (1959).
5) Y. Kawase, ibid., **31**, 440 (1958); **32**, 9 (1959).
6) T. R. Govindachari et al., *J. Chem. Soc.*, **1956**, 629; F. M. Dean et al., ibid., **1957**, 3497.
7) a) C. H. Stammer et al., *J. Am. Chem. Soc.*, **80**, 137, 140 (1958); b) A. Fujino and M. Yamaguchi, *J. Japan. Chem.* (*Kagaku no Ryoiki*), *Extra Voll.* **28**, 124, 126 (1958).
8) H. L. Hergert and E. F. Kurth, *J. Am. Chem. Soc.*, **75**, 1622 (1953); B. L. Shaw and T. H. Simpson, *J. Chem. Soc.*, **1955**, 655; G. E. Inglett, *J. Org. Chem.*, **23**, 93 (1958).

The infrared spectra of IVa, e and Va, b, e were measured in Nujol and compared* with those of related 3-phenylcoumarin-2-imide (VIII), 3-phenylcoumarin (IX), 4-hydroxycoumarin (X) and isoflavones (XIa~c). (see Figs. 1—3). (Preparation of IVa, e and Va, e was reported in the previous paper[5]). It seems that 4-hydroxycoumarin structures of IV and V will rather be replaced by chromone structures, namely 2-amino- (VI) and 2-hydroxy-isoflavones (isoflavonols) (VII) respectively, from the whole shapes of their infrared spectra, and from the absorptions by their carbonyl groups in a longer region than 6 μ.

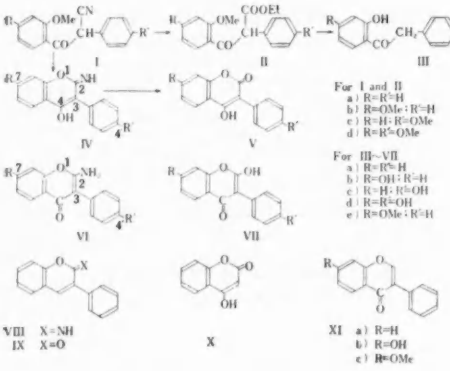

Experimental[9]

2-Hydroxyphenyl Benzyl Ketone (IIIa).—A mixture of ester IIa (0.3 g.) and anhydrous pyridine hydrochloride (1.5 g.) was refluxed for 20 min. on an oil-bath (ca. 220°). The cooled mixture was treated with dilute hydrochloric acid and heated for several minutes on a steam-bath. After being cooled, the solid product separated was collected and recrystallized from ethanol; m. p. 57~58°, identical with the authentic sample[9]; yield 0.1 g. The three following ketones were prepared in the same way.

2, 4-Dihydroxyphenyl Benzyl Ketone (IIIb).—From 0.3 g. of IIb, 0.1 g. of IIIb was obtained, m. p. 110~113° (from water), identical with the authentic sample[10].

2-Hydroxyphenyl 4-Hydroxybenzyl Ketone (IIIc).—From 0.3 g. of IIc, 0.1 g. of IIIc was obtained, m. p. 106~107° (from oqueous ethanol, and dried at 80°).

Anal. Found: C, 73.58; H, 5.30. Calcd. for $C_{14}H_{12}O_3$: C, 73.67; H, 5.30%.

2, 4-Dihydroxyphenyl 4-Hydroxybenzyl Ketone (IIId).—From 0.3 g. of IId, 0.1 g. of IIId was obtained, m. p. 183~184° (from dilute ethanol, and dried at 120°). Reported m. p. is 191~192°[11].

Anal. Found: C, 68.78; H, 5.20. Calcd. for $C_{14}H_{12}O_4$: C, 68.84; H, 4.95%.

2-Hydroxyisoflavone (Isoflavonol) (VIIa).—A mixture of nitrile Ia (0.3 g.) and anhydrous pyridine hydrochloride (1.5 g.) was refluxed for 20 min. on an oil-bath. The cooled mixture was treated with dilute hydrochloric acid and heated on a steam-bath for 1 hr. After being cooled, the deposits were collected and crystallized from ethanol; m. p. 228~229°, yield 0.15 g.; identical with the authentic sample[5]. The following compounds were prepared in the same way.

2, 7-Dihydroxyisoflavone (VIIb).—From 0.3 g. of Ib, 0.15 g. of VIIb was obtained; m. p. 277~278° (from ethanol). Reported m. p. is 284~285°[12] or 285°[13].

Anal. Found: C, 70.68; H, 4.06. Calcd. for $C_{15}H_{10}O_4$: C, 70.86; H, 3.96%.

2-Amino-4'-hydroxyisoflavone (VIc) and 2, 4'-Dihydroxyisoflavone (VIIc) —In the case of Ic, intermediate imide VIc was isolated together with VIIc by the same procedure as described before. Ic (0.3 g.) was treated with pyridine hydrochloride and with dilute hydrochloric acid, and the precipitates thus formed were crystallized from ethanol to give VIc in colorless microcrystals, m. p. ca. 330° (decomp.); yield 0.1 g.

Anal. Found: C, 71.15; H, 4.50; N, 5.42. Calcd. for $C_{15}H_{11}O_3N$: C, 71.14; H, 4.37; N. 5.53%.

From the ethanolic mother liquor of crystallization, VIIc (0.1 g.) was obtained; m. p. 255~256° (from dilute ethanol, and dried at 150°).

Anal. Found: C, 70.64; H, 3.98. Calcd. for $C_{15}H_{10}O_4$: C, 70.86; H, 3.96%.

VIIc was also obtained from imide VIc by hydrolysis with dilute hydrochloric acid for a longer time; m. p. 252~254°.

2, 4', 7-Trihydroxyisoflavone (VIId).—From Id (0.5 g.) and pyridine hydrochloride (2.5 g.), 0.2 g. of VIId was obtained; m. p. ca. 340° (decomp.) (from methanol, and dried at 150°).

Anal. Found: C, 66.63; H, 3.84. Calcd. for $C_{15}H_{10}O_5$: C, 66.67; H, 3.73%.

The author wishes to express his hearty thanks to Professor K. Fukui for his helpful advice and encouragement, to Professor K. Matsui of Kanazawa University for the sample of 4-hydroxycoumarin, to Mr. M. Yamaguchi of Osaka City University for infrared spectroscopy, and to the members of the Agricultural Department of Kyoto University for microanalyses.

Faculty of Literature and Science
Toyama University, Toyama

* λ_{max} (C=O) of coumarin and umbelliferone are 5.80 and 5.95 μ respectively (A. Fujino and M. Yamaguchi, loc. cit.), and that of 2,7-dihydroxychromone is 6.0 μ (C. H. Stammer et al., loc. cit.).

9) Melting points are uncorrected.

10) E. Chapman and H. Stephen, *J. Chem. Soc.*, **123**, 404 (1923).

11) E. Walz, *Ann.*, **489**, 118 (1931).

12) J. Boyd and A. Robertson, *J. Chem. Soc.*, **1948**, 174.

13) C. Menzter and P. Vercier, *Monatsh.*, **88**, 264 (1957) [*Chem. Abst.*, **51**, 14705 (1957)].

Studies on Dehydroalanine Derivatives. I. Synthesis of N-Carboxy-dehydroalanine Anhydride

By Shumpei SAKAKIBARA

(Received August 5, 1958)

It is supposed that thermal or alkaline decomposition of serine, cysteine and peptides containing those amino acids proceed via dehydroalanine[1], and that dehydroalanine must play an important role as a transient intermediate in the course of enzymatic transformations of those substances[2]. If the synthesis of dehydroalanine were possible, this substance would be hydrolysed immediately into pyruvic acid and ammonia because of the presence of very unstable enamine structure in the molecule[3]. On the other hand, *N*-acyl derivatives of dehydroalanine are comparatively stable toward water, and actually some derivatives have been synthesized previously[4-6]. *N*-acetyl[4], *N*-carboethoxy, *N*-carbobenzoxy and *N*-formyl dehydroalanine[5] have been reported to be polymerized into *N*-acyl derivatives of poly-α-amino acrylic acid through a vinyl type polymerization. However, all efforts to prepare the poly-α-amino acrylic acid from these polymer derivatives remain unsuccessful because of the difficulty of the acid or alkaline hydrolysis of these polymers.

Each of the double bonds of suitable dehydroalanine derivatives is supposed to be reactive toward some reagents such as active hydrogen, hydrogen cyanide, hydrogen sulfide, indole and so on, and poly-dehydroalanine[7], if its synthesis is possible, may be converted into poly-alanine, poly-asparagine, poly-cysteine and poly-tryptophane theoretically by the action of such reagents as described above. In this series of papers, the synthetic studies on poly-dehydroalanine and on poly-α-amino acrylic acid will be described chiefly and the reactivities of the obtained polymers will be discussed.

For the starting material of poly-dehydroalanine and of poly-α-amino acrylic acid, *N*-carboxy dehydroalanine anhydride (II) was prepared from *N*-carbobenzoxy dehydroalanine (I) and phosphorous pentachloride in dry ether. The substance I was first synthesized by Frankel and Reichmann[5] through the procedure resembling that for *N*-acetyl dehydroalanine by Bergmann and Grafe[4].

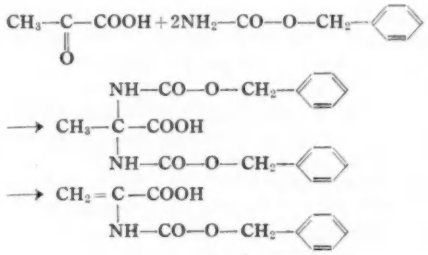

I

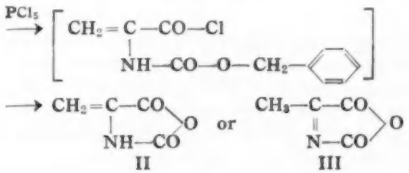

II III

The reagent, phosphorous pentachloride, and its reacted residuals scarcely affected the double bond of the substance II (or III) in the course of the reaction, but the reaction product crystallized very easily. After recrystallization from ethyl acetate and petroleum ether, colorless prisms with melting point of 111~113° (decomp.) were obtained. This substance sublimed at 80° or higher temperature (0.1 mmHg) accompanied by partial polymerization.

If the structure III is more stable than

1) M. Bergmann and A. Miekeley, *Ann.*, **458**, 40 (1927); M. Bergmann and D. Delis, ibid., **458**, 76 (1927); B. H. Nicolet, *J. Biol. Chem.*, **95**, 389 (1932); B. H. Nicolet and L. A. Shinn, ibid., **140**, 685 (1941).

2) C. V. Smythe, ibid., **142**, 387 (1942); E. Chargaff and D. B. Sprinson, ibid., **148**, 249 (1943); C. Fromageot, *Bull. soc. chim.*, **13**, 202 (1946).

3) H. Scheibler and U. Scheibler, *Ber.*, **87**, 379 (1954).

4) R. Adams, J. L. Johnson and B. Englund, *J. Am. Chem. Soc.*, **72**, 5080 (1950).

5) M. Frankel and M. E. Reichmann. *J. Chem. Soc.*, **1952**, 289.

6) T. Wieland, G. Ohnacker and W. Ziegler, *Ber.*, **90**, 194 (1957).

7) This name represents the polypeptide of dehydroalanine in distinction from the vinyl-type polymer of dehydroalanine which is named as poly-α-amino acrylic acid in this series of papers.

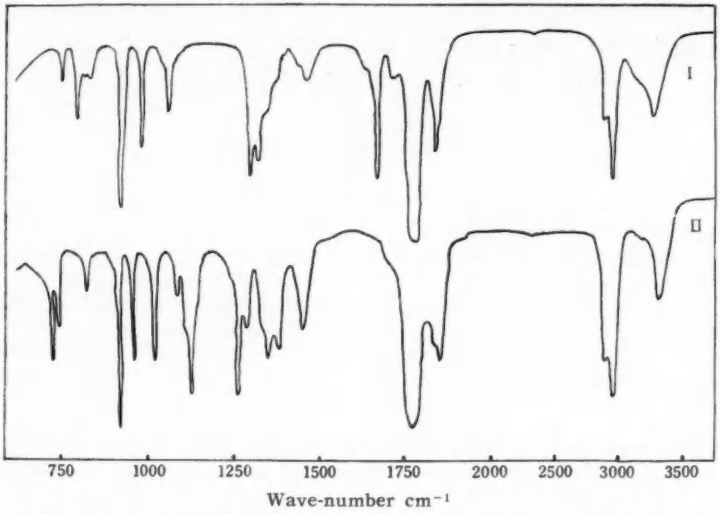

Fig. 1. Infrared spectra recorded on an Adam-Hilger H-80 infrared spectrophotometer: I, *N*-carboxy dehydroalanine anhydride; II, *N*-carboxy DL-alanine anhydride. Nujol suspension.

II, the position of the double bond in the molecule may shift from C=C to C=N in the course of the reaction. The infrared spectrum (Fig. 1) of the product, however, showed absorption bands which were all identical with those supposed for the structure II; that is, the absorption bands at 3050~3300 cm^{-1} indicated the presence of —NH— groups in the molecule, and the absorption bands at 1750~1900 cm^{-1} corresponding to carbonyl groups in a five-membered ring were identified completely as those of *N*-carboxy DL-alanine anhydride. The sharp band at 1675 cm^{-1}, which was not observed in the same region of the spectrum of *N*-carboxy DL-alanine anhydride, may be due to the presence of a double bond directly attached to the five-membered ring in the structure II. The absence of δN–H(amide II) band in both the spectra must be explained by the fact that both NH groups exist in five-membered rings of the respective *N*-carboxy anhydride.

In addition, the structure II was confirmed by the reactions with aniline and with benzylmercaptane. In the case of the former, pyruvic acid anilide IV was obtained in a yield of about 60%, and the structure IV was confirmed by the formation of the 2,4-dinitrophenyl hydrazone. In the case of the latter, *S*-benzyl cysteine formed was identified with an authentic sample by paper-chromatography. These results all supported the structure II for the product.

One of the characteristics of the substance II was its relative stability toward water and amines in comparison with ordinary *N*-carboxy anhydrides. For example, the substance II, which had been prepared about half a year ago and stored in a usual desiccator over phosphorous pentoxide without any precautions, indicated almost the same melting point as that of the original one in spite of the fact that almost all of drying agents have already become tarry. Moreover, the

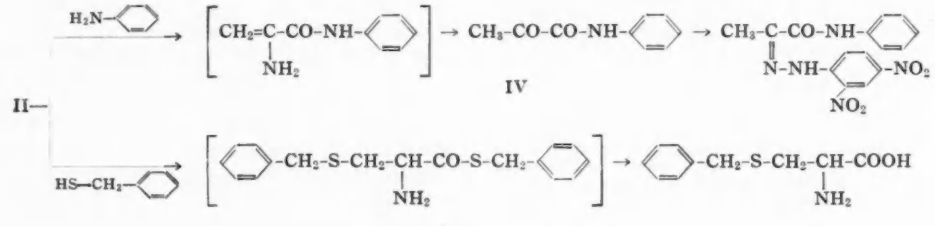

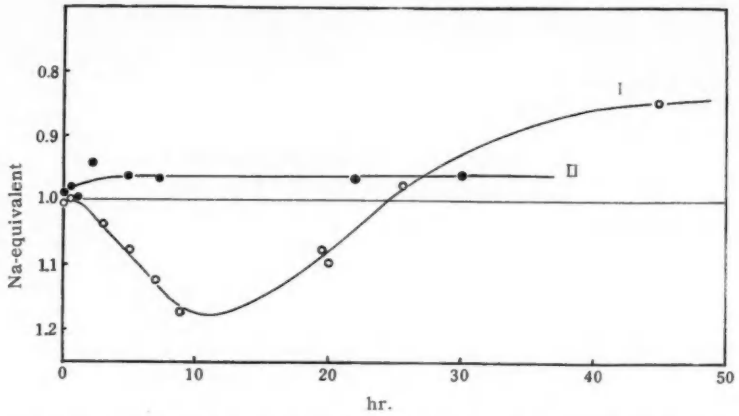

Fig. 2. Time—Na-equivalent curves of *N*-carboxy anhydrides at 30°±0.1° in dioxane containing an equal mole of water: I, *N*-carboxy dehydroalanine anhydride: II, *N*-carboxy DL-alanine anhydride.

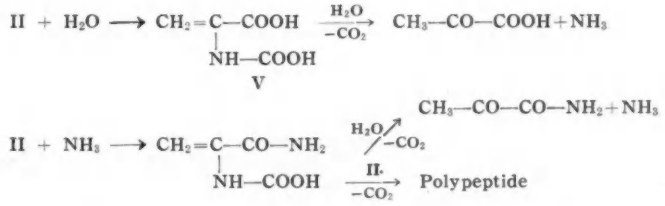

substance II immersed in water seemed to be rather stable below 30° and decomposed gradually under evolution of carbon dioxide at 35° or higher temperature.

For clarifying the hydrolytic reaction of the *N*-carboxy anhydride II, it was dissolved in dioxane containing an equal mole of water (against II) and the solution was allowed to react in a bath at 30°±0.1°. Then, the solution was titrated with sodium methoxide at times according to the procedure of Berger et al.[8] and equivalent values obtained

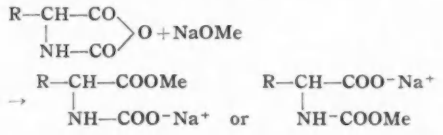

(the residual amount of the *N*-carboxy anhydride plus acidic material formed, such as pyruvic acid) were plotted against time (curve I on Fig. 2). This curve I was compared with that of *N*-carboxy-DL-alanine anhydride (curve II) under the same condition. In this comparison, it was very interesting to find that the curve I fell down at first, then, recovered gradually and began to rise only after 30 hours, notwithstanding the fact that no practical change of titration values was observed within 30 hours in the case of the *N*-carboxy-DL-alanine anhydride. The reason for the increase in the titration values for the substance II beyond the original line should be explained by the formation of carbamic acid V by hydrolysis. Furthermore, this carbamic acid V would possibly be more stable than those from other ordinary *N*-carboxy amino acid anhydrides at room temperature, since the carbamic acid contains the conjugated double bond in the molecule. If the assumption is reasonable, the considerable stability of the *N*-carboxy anhydride II above mentioned should be explained by the retardation of the chain reactions for polypeptide-forming polymerization. On the other hand, *N*-carboxy-DL-alanine anhydride may be hydrolyzed gradually into carbamic acid of DL-alanine, which is decarboxylated immediately into DL-alanine; then, it will be possible to consider that the titration values

8) A. Berger, M. Sela and E. Katchalski, *Anal. Chem.*, 25, 1554 (1953).

of the solution should not change practically, since alanine formed is titrated by sodium methoxide in the same manner as *N*-carboxy anhydride under this condition. The upward tendency of the latter part of the titration curve I may also be explained by the gradual formation of the pyruvic acid amide or by the gradual polymerization which was initiated by the formed ammonia.

This material II will be expected to undergo the poly-peptide-forming polymerization and the vinyl type polymerization independently. The details of both cases will be published in later communications.

Experimental

N-Carbobenzoxy dehydroalanine (I).—It was prepared from α,α-dicarbobenzoxyamido propionic acid[9] (m.p. 138.5°) according to the procedure of Frankel and Reichmann[5]. The yield of the low product with m.p. 107° was about 76~83%. After successive recrystallizations from toluene containing a small amount of hydroquinone, colorless plates with m.p. 112~113° (decomp. at 160°) were obtained. Frankel[5] reported m. p. 105° (decomp.) and Wieland[6] m. p. 119° (decomp.).

Anal. Found: C, 59.65; H, 4.50; N, 6.33; No. of double bond, 0.982[10]. Calcd. for $C_{11}H_{11}O_4N$: C, 59.72; H, 5.01; N, 6.33; No. of double bond, 1.00.

N-Carboxy dehydroalanine anhydride (II).—A solution of 10 g. of I in 50 ml. of dry ether was cooled to 0° in an ice water bath and 10.5 g. of powdered phosphorous pentachloride was added in one portion. Then, the suspension was shaken vigorously with intermittent cooling in the bath for about 50 min. The supernatant was decanted quickly into a distillation flask and was concentrated to syrup under reduced pressure at 25~30°. During the course of the treatment, the residual syrup crystallized gradually. After about 30 min., 50 ml. of petroleum ether was added to the residual crystalline mass and the mixture was cooled in an ice water bath for about one hr. Then, the crystalline mass was filtered off and washed with some petroleum ether. The crude crystals were recrystallized from ethyl acetate-petroleum ether after treatment with some active charcoal. The yield of the light yellow prisms with m.p. 105~108° (decomp.) was 3.5 g. (70%). After recrystallization from the same solvents, the colorless prisms of 3.1 g. with m.p. 111° (decomp.) were obtained. After sublimation at 80~90° (0.1 mmHg), this substance melted and decomposed at 111~113°.

Anal. Found: C, 42.56; H, 2.60; N, 12.13. Calcd. for $C_4H_3O_3N$: C, 42.49; H, 2.67; N, 12.39%.

Reaction of II with aniline.—*Formation of pyruvic acid anilide (IV).*—A solution of 1.13 g. of II in 20 ml. of ethyl acetate was cooled to −10° and 5 g. of aniline was added into the solution, then the mixture was allowed to react overnight in a refrigerator at 0~4°. A small amount of yellow precipitate formed was filtered off and the mother liquor was washed successively with 0.5 N hydrochloric acid, water, 0.5% sodium bicarbonate solution and water, dried over anhydrous sodium sulfate and concentrated to dryness under reduced pressure. The residual syrup was transferred into a sublimation vessel with some ethyl acetate. The main product IV was then separated by sublimation at 100° (0.1 mmHg) from yellow by-products. The colorless needles with m.p. 103~105° were obtained in the yield of 1.0 g. (60%); Nef[11] reported m.p. 104°.

Anal. Found: N, 8.65. Calcd. for $C_9H_9O_2N$: N, 8.60%.

2, 4-Dinitrophenyl hydrazone of IV.—To a solution of 50 mg. of IV in 5 ml. of ethanol was added a solution of 100 mg. of 2, 4-dinitrophenyl hydrazine in 5 ml. of 2 N hydrochloric acid, and the mixture was heated for a short time in a boiling water bath and cooled. The voluminous yellow crystals which formed were filtered off, washed with dil. hydrochloric acid and water, and dried. The yield of the yellow crystals was about quantitative and they melted at 245~247° after recrystallizasion from glacial acetic acid.

Anal. Found: C, 52.48; H, 3.82; N, 21.2. Calcd. for $C_{15}H_{13}O_5N_5$: C, 52.49; H, 3.82; N, 20.4%.

Reaction of II with benzyl mercaptane.—A solution of 100 mg. of II and 500 mg. of benzyl mercaptane in 5 ml. of dry acetone was allowed to react overnight at room temperature. The mixture was concentrated to dryness and the residuals were hydrolyzed for one hr. with 6 N hydrochloric acid. The hydrolysate was extracted with ether and the aqueous layer was concentrated to dryness. The residuals were extracted with absolute ethanol and the extract was concentrated. From the residuals, *S*-benzyl cysteine was detected by paper-chromatography, which was identified by comparison with an authentic sample.

Reaction of II with water.—The substance II (350 mg.) was dissolved in 15.00 ml. of freshly distilled dry dioxane containing 56 mg. of water. The solution was divided into 14 test tubes so that each tube contains 1.00 ml. of the solution, and the tubes were sealed. Then, they were allowed to react in a bath at 30°±0.1° simultaneously. Each of the portions was opened successively at times and dry nitrogen was introduced for about one min. into the solution, which was then titrated with a methanol-benzene solution (ca. 0.3 N) of sodium methoxide using thymol blue as an indicator according to the procedure of Berger, et al.[9]. The sodium methoxide solution was standardized every 5 hr.

9) E. Martell and R. M. Herbst, *J. Org. Chem.*, **6**. 878 (1941).

10) This value was determined by back-titration of the bromine using sodium thiosulfate after a sufficient amount of bromine in glacial acetic acid was added to the sample.

11) J. U. Nef, *Ann.*, **270**, 299 (1892).

with purified benzoic acid. After about 8 hr. the reacting solution began to become turbid, and after about 20 hr. yellow precipitates began to form. (Curve I on Fig. 2)

Reaction of *N*-carboxy-DL-alanine anhydride with water.—*N*-Carboxy -DL-alanine anhydride[12] (m.p. 45°) (356 mg.) was subjected to the reaction under the same condition described above. After about 30 hr. the reacting solution remained clear (Curve II on Fig. 2). A suspension of 18.3 mg. of DL-alanine in 1 ml. of dimethyl formamide was titrated with a methanol-benzene solution (0.306 N) of sodium methoxide with an indicator of thymol blue, and 0655 ml. (0.975 equivalent for DL-alanine) of the solution was required for neutralization.

Summary

N-Carboxy dehydroalanine anhydride was first synthesized from carbobenzoxy dehydroalanine. The structure of the *N*-carboxy anhydride was confirmed by the analysis of its infrared spectrum and by the investigation of its chemical behavior. The hydrolytic reaction of the *N*-carboxy anhydride was compared with that of *N*-carboxy DL-alanine anhydride, and it was supposed that dehydroalanine carbamic acid might exist stably in dioxane at ordinary temperature.

The author wishes to express his thanks to Professor Shiro Akabori and Professor Shunsuke Murahashi for their guidance and encouragement throughout the course of this study, and to Mr. Yukio Okuda for his kind assistance in a part of the experiment.

Department of Chemistry
Faculty of Science
Osaka University, Kita-ku, Osaka
and
Institute for Protein Research
Osaka University
Nishi-ku, Osaka

12) J. L. Bailey, *J. Chem. Soc.*, **1950**, 3461.

Thermal Effects of Some Kaolin Minerals. II. Halloysite

By Hiroshi TAKAHASHI

(Received March 18, 1958)

In the preceding part of this series, studies were made on the structural changes of kaolinite and kaolin mineral of fireclay type with heat-treatment in the relatively low temperature region with respect to the degree of the crystallinity[1].

In the early stage of heat-treatment, the progress of the crystallinity is remarkable. It is mainly due to the loss of the adsorbed water. In the next stage, there occurs the lowering of crystallinity due to the break of the kaolin structure resulting from the loss of the lattice water. In the following stage, the rearrangement of ions for the mullite nucleation becomes remarkable, though the X-ray diagram indicates that this state is an amorphous structure.

Halloysite is composed of the same structural units as those of kaolinite, but the stacking of almino-silicate layers is in almost entirely disorder and generally contains the inter-layer water between unit layers. The crystallinity of halloysite, except a certain type of halloysite[2,5], is lower than that of kaolinite. And, it was also found by Brindley and Robinson that the theory of the reflection for a random layer lattice is applicable to the structure of halloysite[3]. The change in the structure of halloysite owing to the loss of the inter-layer water, was studied in details by Brindley and Goodyear[4].

In this paper, the structural changes of halloysite with heat-treatment in the relatively low temperature region, are presented, through X-ray diffraction method, differential thermal analysis and the density measurement from the point of view of the degree of crystallinity of kaolin minerals and are compared with those of kaolinite.

1) H. Takahashi, This Bulletin, **31**, 1031 (1958).

2) G. Honjo and K. Mihama, *Acta Cryst.*, **5**, 511 (1954).
3) G. W. Brindley and K. Robinson, *Min. Mag.*, **28**, 393 (1948).
4) G. W. Brindley and J. Goodyear, ibid., **28**, 407 (1948).
5) H. Takahashi, This Bulletin, **31**, 275 (1958).

Experimental

Twelve samples of halloysite with the various degrees of crystallinity were used in this study. From the point of view of the degree of crystallinity in halloysite, the following four samples are generally representative for the structural changes through heat-treatment. Four samples mentioned above are as follows: Halloysite from Spruce Pine, N. C., U. S. A.; Halloysite from Bedford, Ind., U. S. A.; Halloysite from Tintic, Utah, U. S. A. and Shichinoe-clay from Shichinoe, Aomori, Japan.

These samples, except for Shichinoe-clay, are the API Standard Clay Minerals. Of all kinds of halloysite used in this study, Shichinoe-clay has the lowest degree of crystallinity. The structural characteristics of these samples have been discussed in the previous paper[5], and those of Shichinoe-clay was also discussed by Sudo[6]. The method of preparation of the experimental specimens and the experimental conditions of all measurements are the same as those in kaolinite and Kibushi-clay.

Results and Discussion

X-ray Diffraction Studies.—Fig. 1 shows the X-ray diffractometer traces of heat-treated specimens of Tintic halloysite. As shown in these traces, the reflections which correspond to hydrated halloysite disappear owing to the loss of the inter-layer water when heat-treated, and it changes into a dehydrated halloysite. With the rise of the treated temperature, the intensity of all reflections increases and (001) reflection becomes sharp to 400°C. In the 545°C heat-treated specimen, the reflections which are apparent in the original sample are not observable, but only a wedge-like background. In the 700°C heat-treated specimen, only a very diffuse and indistinct band is observable. In Tintic halloysite, it is considered that the crystallinity progresses up to 400°C. This is because the residual inter-layer water which exists sporadically between the kaolin layers is lost with the rise of treated temperature, which causes the arrangement of kaolin unit layers to be ordered. Past 400°C, the structure of halloysite begins to disintegrate due to the gradual disappearance of the lattice water. Then the lattice water completely vanishes. Therefore, its crystallinity drops. The X-ray diagram shows also that the rate of change in the heat-treated specimens of other halloysites is similar to that of Tintic halloysite. The only difference is that the loss of lattice water occurs at a lower temperature according to the order of crystallinity of the original sample. The temperature which eliminates the lattice water is the highest in Spruce Pine halloysite and lowest in Shichinoe-clay. This is quite natural in the light of the thermal data.

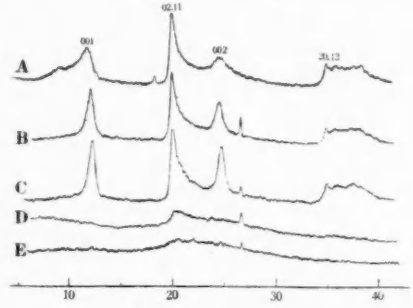

Fig. 1. X-ray diffractometer traces of heat-treated specimens of Tintic halloysite.
A, original halloysite
B, treated at 200°C
C, treated at 400°C
D, treated at 545°C
E, treated at 700°C

It is known by Brindley that halloysite has a pseudo-hexagonal form in symmetry and has a two-dimensional like structure[3]. To the two-dimensional structure, Warren's theory is applicable[7]. This theory has been applied to various kinds of substance[8], particularly to amorphous carbon in the process of graphitization[9]. The structure of halloysite is more complex than that of amorphous carbon in in the chemical composition and the crystal structure. So, it is very dangerous to apply this theory entirely to halloysite. However, the values obtained by the application of this theory should have some relation with the real values to some extent. For this reason, the crystallite dimensions were obtained from the broadening of (001) and (02, 11) reflection lines. There are two elements determining the broadening of the reflection line. One is the crystallite size, and the other is the lattice distortion. Accordingly, to obtain the real crystallite size from the line broadening, the factor of the lattice distortion must be eliminated[10]. However, the

6) T. Sudo, *Clay Min. Bull.*, **2**, 96 (1954).

7) B. E. Warren, *Phys. Rev.*, **59**, 693 (1941).
8) E. Aruja, *Nature*, **154**, 53 (1944).
9) J. Biscoe and B. E. Warren, *J. App. Phys.*, **13**, 364 (1942). H. Akamatu et al., This Bulltin, **29**, 574 (1956).
10) C. R. Houska and B. E. Warren, *J. App. Phys.*, **25**, 1503 (1954).

increase of the line breadth correlates the fact that the lattice distortion becomes remarkable and that the crystallite size becomes reduced. These two facts mean a lowering in the crystallinity. Therefore, the crystallite sizes thus obtained indicate the relative degree of crystallinity rather than the real crystallite sizes. Consequently, the crystallite sizes are not the real crystallite sizes, but the values are proportional to the real crystallite sizes. However, the real crystallite sizes of halloysite are not much different from the values thus obtained, which are probably, approximate values. This fact was also described in the separate paper[11]. The crystallite dimension along the direction of the *c*-axis (L_c) was measured by the Bragg's equation[12] and the crystallite dimension parallel to the layer plane (L_a) was measured by Warren's equation[7].

$$L_c = \frac{0.9\,\lambda}{\beta_c \cos\theta} \quad \text{(Bragg's equation)}$$

$$L_a = \frac{1.84\,\lambda}{\beta_a \cos\theta} \quad \text{(Warren's equation)}$$

λ: wave length (Cu K_α: 1.5418 Å)
θ: diffraction angle (degree)
β: half value of breadth (radian)

In these measurements, quartz was used for a correction substance for the instrumental broadening of the reflection line.

Kaolin minerals generally change in their shapes and physico-chemical properties according to the structural characteristics. Kaolin minerals have two kinds of crystallinity; that is, one is the internal crystallinity and the other is the crystallinity in the stacking of layers[5]. Therefore, these two kinds of crystallinity must be considered. So, the ratio of the intensity of (001) reflection to that of (02,11) band is measured. This term seems to indicate somewhat the order of the crystallinity of halloysite samples. The original samples of halloysite, except for Spruce Pine halloysite, are partially hydrated halloysite. In Fig. 2 is shown the schematic drawing of the X-ray diagram of the partially hydrated halloysite. In Fig. 2, the intensity ratio was obtained by the following equation[4].

$$\text{Intensity ratio} = \frac{I_{(001)} + \dfrac{I_{H(001)}}{4}}{I_{(02,11)}}$$

11) H. Takahashi, "Proc. Sixth Natl. Coference on Clay and Clay Minerals", Natl. Acad. Sci.-Natl. Res. Council, U.S.A. (in Press).
12) W. L. Bragg, "The Crystalline State", Vol. I, p. 189 (1933).

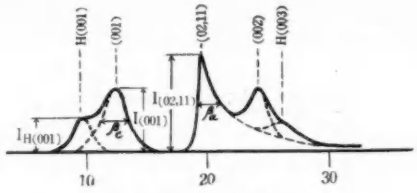

Fig. 2. Schematic drawing of the X-ray diagram of the partially hydrated halloysite.

Fig. 3 shows the change of the spacings of (001) and (02,11) reflections, the crystallite dimensions and the intensity ratios with heat-treatment. Figs. 3-A, -B, -C and -D show the data for four samples of halloysite.

On the crystallite dimensions, L_c-dimension increases with the rise of the treated temperature; when the regularity along the direction of *c*-axis disappears, L_c-dimension sharply decreases. L_a-dimension, in the partially hydrated halloysite, reaches a maximum value, it then decreases slowly, and then sharply decreases, In Spruce Pine halloysite, L_a-dimension curve has no maximum point perhaps owing to the original sample being dehydrated halloysite. The increase of L_c-dimension with heat-treatment, is caused by the progress of regularity along the direction of *c*-axis because of the loss of the inter-layer water, while the decrease in L_a-dimension is due to the fracturing of kaolin layers.

As for the change of the intensity ratio, the value increases and reaches a maximum point with the rise of treated temperature, and then sharply decreases. The value of the intensity ratio is larger as the crystallinity is higher. This means that the higher the crystallinity of halloysite is, the higher is the regularity along the direction of *c*-axis. From the value of the intensity ratio, it is understood that Spruce Pine halloysite has very high crystallinity. The maximum value in the change of the intensity ratio is considered to indicate the degree of crystallinity of halloysite. In the hydrated halloysite with very low crystallinity, found in Japan, the results are reverse to those so far described, as far as the intensity ratio is concerned. This is for the reason that there is a remarkable disorderliness in the kaolin layers[6].

As for the changes in spacing, the spacing of (001) reflection slowly reduces

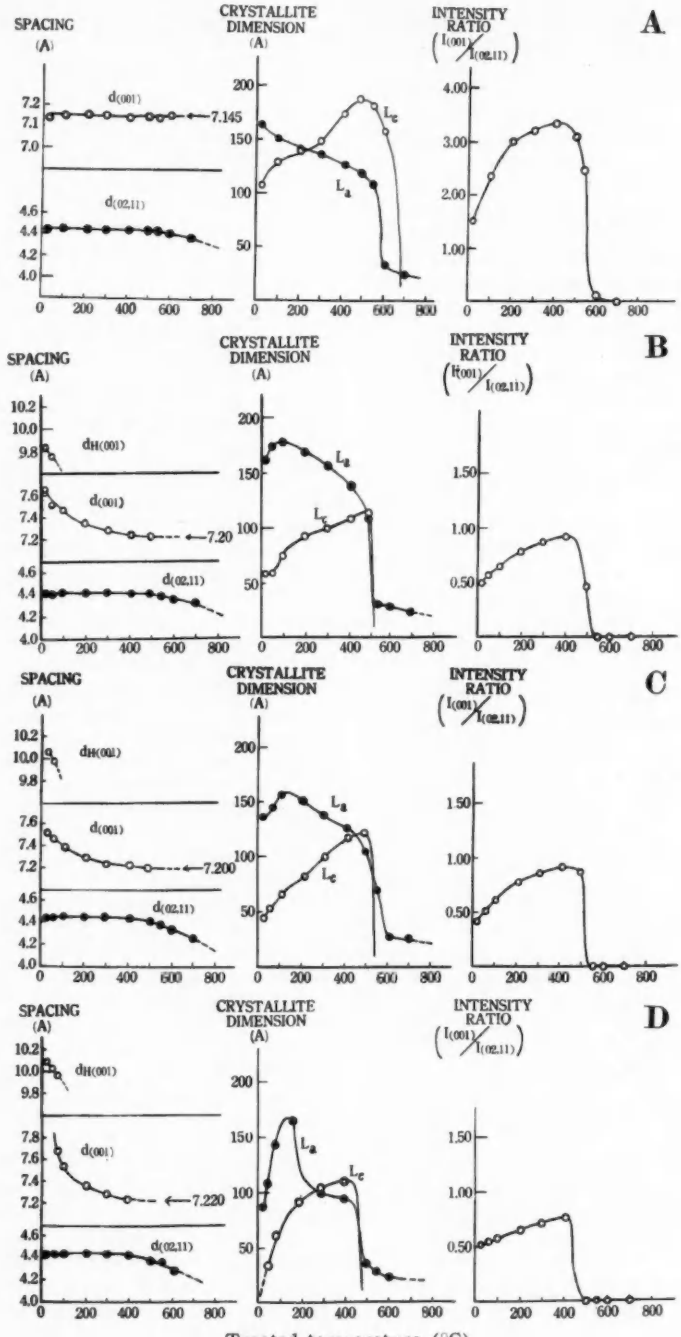

Fig. 3. Curves showing the changes of the spacing of (001) and (02, 11) reflections, the crystallite dimensions and the intensity ratios with the heat-treated temperature.

A, Spruce Pine halloysite
B, Bedford halloysite
C, Tintic halloysite
D, Shichinoe halloysite

with the loss of the inter-layer water until it reaches a nearly constant value. This maintained value seems to indicate the order of the crystallinity in halloysite. The spacing of (02,11) band decreases sharply with the loss of lattice water. This corresponds to the disintegration of the kaolin structure.

Differential Thermal Analysis.—The differential thermal analysis curves of some specimens with heat-treatment are shown in Fig. 4, and Table I shows the thermal data obtained from these curves.

In the heat-treated specimens of halloysite except for Spruce Pine halloysite, the endothermic reaction (E_{N1}) associated with the loss of the inter-layer or adsorbed water is observable even in the 400°C heat-treated specimen of halloysite. This might be due to the fact that after the heat-treatment it adsorbs water vapor so rapidly from the atmospheric air. This phenomenon corresponds to the crystallinity of the original sample in the low stage.

In the endothermic reaction (E_{N2}) caused by the loss of the lattice water in Spruce Pine halloysite, the peak height and area of this reaction reduce in the 545°C heat-treated specimen. And in the 700°C heat-treated specimen, this reaction is unobservable. In the 545°C heat-treated specimen of Shichinoe-clay, this reaction disappears. This means that the structure

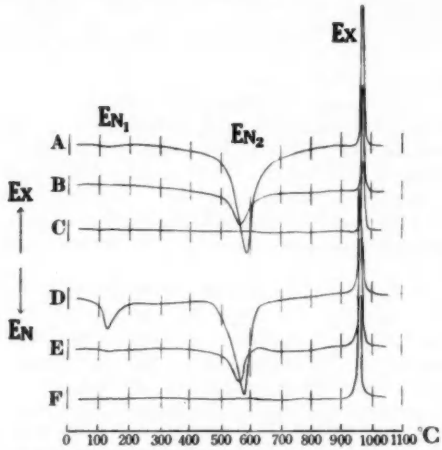

Fig. 4. Differential thermal analysis curves of heat-treated specimens of Spruce Pine and Tintic halloysite.
A, original Spruce Pine halloysite
B, treated at 545°C
C, treated at 700°C
D, original Tintic halloysite
E, treated at 545°C
F, treated at 700°C

TABLE I
THERMAL DATA OF HEAT-TREATED SPECIMENS OF HALLOYSITE
(ALL TEMPERATURES ARE DEGREES CENTIGRADE)

Specimen	Treated-temp.	E_{N1}		E_{N2}		E_x		
		Temp. at peak	Height of peak	Temp. at peak	Height of peak	Temp. at peak	Height of peak	Breadth of peak
Halloysite	original	125°	1	583°	17	973°	45	4.0°
(Spruce Pine, N. C.)	200°	—	—	581	17	971	46	3.4
	400	—	—	573	15	969	48	2.2
	545	—	—	555	5	968	51	3.4
	700	—	—	—	—	967	52	3.6
Halloysite	original	125	2	574	16	970	34	4.5
(Bedford, Ind.)	200	120	1	574	16	969	32	4.2
	400	120	1	574	14	967	32	4.7
	545	—	—	563	6	966	30	4.8
	700	—	—	—	—	964	38	5.1
Halloysite	original	130	4	571	12	969	16	9.4
(Tintic, Utah)	200	115	2	570	15	963	24	4.3
	400	115	1	565	13	965	34	4.2
	545	—	—	558	4	964	30	4.9
	700	—	—	—	—	959	46	5.2
Halloysite	original	129	6	550	12	885	7	23.4
(Shichinoe, Aomori)	200	115	2	546	13	885	8	23.4
	400	125	1	543	9	886	9	25.6
	545	—	—	—	—	883	12	26.6
	700	—	—	—	—	881	12	27.0

of Shichinoe-clay disintegrates at a lower temperature as compared with that of Spruce Pine halloysite. This fact corresponds to the fact that the original sample of Shichinoe-clay has the lowest degree of crystallinity of all the halloysite samples used in this study.

In the exothermic reaction (E_x) associated with the mullite nucleation, the features of this reaction are the same as those of kaolinite. That is, the peak temperature tends to lower, though very slightly, and the peak height gradually increases with the rise of treated temperature.

In the 700°C heat-treated specimen, the peak height is large as compared with that of the original sample. This fact seems to indicate that in the metakaolin state, the rearrangement of ions takes place for the mullite nucleation though this state is amorphous from the X-ray diagram. Therefore, the heat-treatment accelerates the rearrangement of ions for the mullite nucleation. As a result, the peak height of the exothermic reaction increases. The peak breadth of this reaction reduces with the rise of the heat-treatment, and attains a minimum value, and then slightly increases again.

Density.—In Fig. 5 are shown the changes of the density of halloysite specimens with heat-treatment. Measurements were made on dried specimens.

The rate of change in the density are very similar to those of kaolinite and Kibushi-clay described in the preceding part of this study. The density increases at first with the rise of treated temperature, and reaches a maximum point; then it falls suddenly and maintains the minimum value. Past the minimum point in the density curve which corresponds to the disappearance of the lattice water, the density increases sharply and straight. The curve is steeper as the crystallinity of the original sample is higher. The same phenomena were also observable in kaolinite and Kibushi-clay.

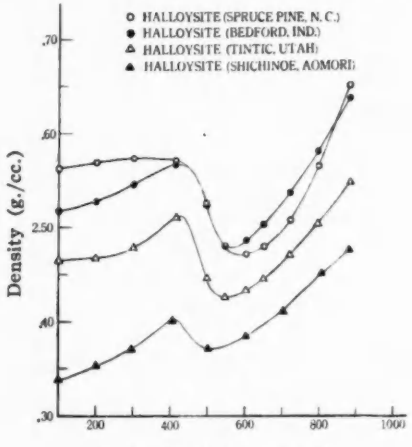

Fig. 5. Curves showing the changes of the density of the halloysite specimens with heat-treated temperature.

When the inclinations in the density curves of kaolinite and ordinary halloysite are compared, that of kaolinite is larger than that of the other.

Therefore, past the minimum point on the density curve, it is considered that the inclination of the density curve of kaolin mineral is corrected to the degree of crystallinity of the kaolin mineral, particularly to the internal degree of crystallinity. This indicates that the rearrangement of ions occurs in the metakaolin state, despite of the fact that the structure is amorphous by the X-ray diagram, and that the stronger the structure of the original sample is, the faster and more perfect is the rearrangement of ions. The mullite nucleation is more remarkable as the crystallinity of the original kaolin mineral is higher.

Mechanism of Structural Change of Halloysite with Heat-treatment.—In the heat-treatment process of halloysite, there are three steps of the structural change with respect to the degree of crystallinity. In the first process, crystallites in one neighborhood aggregate as the inter-layer water vanishes gradually, and so the apparent crystallite size and the value of the density increase and its crystallinity therefore progresses. This tendency is remarkable particularly along the direction of c-axis. In the second process, the hydroxyl ions oriented with the metal ions are cut out and dehydrated, and then kaolin changes into metakaolin. The density decreases suddenly in this stage. As the result, the crystallinity owing to the disintegration of the structure of halloysite. Past this stage, the structure of halloysite becomes amorphous. However, the value of the density of all kinds of halloysite sharply increases with the rise of treated temperature similar to that in kaolinite. The higher the crystallinity is, the larger is the proportion of the increase of the density in all kaolin minerals. This fact shows that even in this amorphous state,

the rearrangement of ions for the mullite nucleation occurs. The higher the original crystallinity is, the more perfect is the rearrangement.

Summery

The structural change of halloysite with heat-treatment in the relatively low temperature region has been studied, and was compared with those of kaolinite and Kibushi-clay. There are three processes, same as in the case of kaolinite. The first process is accompanied by the loss of the inter-layer and adsorbed water, and thə second process by the loss of the lattice water. In the third process, which is an amorphous state corresponding to the metakaolin state, the rearrangement of ions takes place for the mullite nucleation. The rate of the structural change depends on the degree of crystallinity of the original kaolin mineral.

The author wishes to express his hearty thanks to Professor H. Akamatu for his continuous advice and encouragement.

Department of Chemistry
Faculty of Science, the
University of Tokyo
Hongo, Tokyo

Polarographic Studies of Metallic Complexes. III.[1] *Pentammine Series of Cobalt(III) Complexes*[2]

By Nobufumi MAKI, Yoichi SHIMURA and Ryutaro TSUCHIDA

(Received June 9, 1958)

The relation between the structure of metallic complexes and their half-wave potentials has been studied to some extent[3-12]. For instance, Hall et al.[9] studied several kinds of platinum(IV) complex and found the following facts. Platinum (IV) complexes of halogenopentammine type were reduced irreversibly to platinum (II) complexes in one step and the half-wave potentials were at more positive values for halogenopentammineplatinum (IV) complexes than for hexammineplatinum(IV) ion, $[Pt(NH_3)_6]^{4+}$. The shift, however, was to a more negative value for hydroxypentammineplatinum(IV) complex. Namely the polarographic stability of the pentammineplatinum(IV) complexes, $[Pt(NH_3)_5X]$, increases in the following order of ligand X;

$$Br^- < Cl^- < NH_3 < OH^-$$

They also found that tris(ethylenediamine)-platinum(IV) complex ion was reduced irreversibly to $[Pt\,en_3]^{2+}$, through $[Pt\,en_3]^{3+}$, in two steps at a little more negative potential than the corresponding reduction of hexammineplatinum(IV) ion.

Brigando[11] reported that, on the basis of polarographic measurements and absorption spectra, the following complexes were ranked in order of increasing stability;

$[Co(NH_3)_4(NH_2CH_3)_2]Cl_3$

$[Co(NH_3)_6]Cl_3$, $[Co\,en_3]Cl_3$

$[Co(NH_2CH_2CH_2NHCH_2CH_2NH_2)_2]Cl_3$

The half-wave potentials for these complexes at the dropping mercury electrode in 0.6 F sodium perchlorate were respectively as follows; −0.215 V., −0.297 V., −0.392 V., and −0.420 V. (vs. S. C. E.).

For the same purpose, the present paper deals with the polarography of pentam minecobalt(III) complex ions, $[Co(NH_3)_5X]^{(3-n)+}$.

1) Part II of this series: N. Maki, Y. Shimura and R. Tsuchida, This Bulletin, **31**, 413 (1958).
2) Partly presented at the Eleventh Annual Meeting of the Chemical Society of Japan, Tokyo, April 6, 1958.
3) T. Uemura, K. Morinaga, H. Takesawa and H. Kobayashi, presented at the Symposium on Co-ordination Compounds, Tokyo, Nov. 13, 1951.
4) J. B. Willis, J. A. Friend and D. P. Mellor, *J. Am. Chem. Soc.*, **67**, 1680 (1945).
5) H. F. Holtzclaw, Jr., ibid., **73**, 1821 (1951).
6) H. F. Holtzclaw, Jr. and D. P. Sheetz, ibid., **75**, 3053 (1953).
7) J. Brigando, *Compt. rend.*, **236**, 708 (1953).
8) H. F. Holtzclaw, Jr., *J. Phys. Chem.*, **59**, 300 (1955).
9) J. R. Hall and R. A. Plowman, *Australian J. Chem.*, **8**, 158 (1955).
10) J. R. Hall and R. A. Plowman, ibid., **9**, 143 (1956).
11) J. Brigando, *Bull. soc. chim. France*, **1957**, 221.
12) N. Maki, Y. Shimura and R. Tsuchida, This Bulletin, **30**, 909 (1957).

TABLE I

HALF-WAVE POTENTIALS OF PENTAMMINE SERIES OF COBALT(III) COMPLEXES

Complex compound	Supporting electrolyte; 0.1 F KCl		Supporting electrolyte; 0.5 F K_2SO_4	
	$E_{1/2}$ of 1st wave [Co(III)→Co(II)]	$E_{1/2}$ of 2nd wave [Co(II)→Co(0)]	$E_{1/2}$ of 1st wave [Co(III)→Co(II)]	$E_{1/2}$ of 2nd wave [Co(II)→Co(0)]
$[Co(NH_3)_5I]Cl_2$[13]	+	-1.24_5	+	—
$[Co(NH_3)_5Br]Br_2$[14]	+	-1.24_5	+	—
$[Co(NH_3)_5Cl]Cl_2$[15]	+	−1.24	+	—
$[Co(NH_3)_5NO_3](NO_3)_2$[16]	+	-1.25_5	-0.05_5	−1.28
$[Co(NH_3)_5N_3]Cl_2$[17]	+	−1.23	-0.12_5	-1.28_5**
$[Co(NH_3)_5SO_4]ClO_4$[18]	-0.10_5	-1.23_5	-0.24_5	-1.27_5
$[Co(NH_3)_5NO_2](ClO_4)_2$[19]	−0·12	*	−0.26	-1.28_5
$[Co(NH_3)_5S_2O_3]Cl$[20]	−0.13	-0.96_5	about −0.12	*
$[Co(NH_3)_5C_2O_4]Br\cdot 1.5\,H_2O$[21]	−0.21	-1.23_5	−0.33	−1.29
$[Co(NH_3)_5OCOCH_3](ClO_4)_2$[22]	-0.22_5	−1.24	−0.37	−1.27
$[Co(NH_3)_6](NO_3)_3$	-0.23_5	-1.25_5	−0.43	−1.28
$[Co(NH_3)_5CO_3]NO_3$[23]	-0.38_2	−1.25	−0.50	*
$[Co(NH_3)_5HCO_3](NO_3)_2$[24]	—	—	-0.50_2	−1.28
$[Co(NH_3)_5OH_2]_2(SO_4)_3\cdot 3H_2O$[25]	−0.38	-1.24_5	−0.47	-1.27_5
$[Co(NH_3)_5OH]SO_4\cdot 1.5\,H_2O$[26]	−0.39	-1.25_5	-0.47_5	-1.27_5
$[Co(NH_3)_5CrO_4]Cl$[27]	+	*	+	*
$[Co(NH_3)_5NCS]SO_4\cdot 2\,H_2O$[28]	+	*	+	*

* Maximum wave.

** The data obtained in the presence of 0.0016% Tween-80.

1) The concentration of the complex; 0.001 gram complex ion per liter.

2) Potential unit; V. vs. S. C. E.

3) Temperature, 25°C.

Experimental

The experimental setup and technique are the same as in the previous work and have been described in the earlier communications[1,12]. The capillary had an m-value of 1.356 mg./sec. and a drop time of 5.82~6.23 sec./drop in 0.1 F potassium chloride or 0.5 F potassium sulfate at a potential of 0.0 V. against the saturated calomel electrode with the mercury head of 96 cm. All the measurements were made at 25±0.1°C, the temperature being maintained by a water thermostat. The reversibilities of the electrode reaction were examined by determining the slope of $\log i/(i_d-i)$ vs. potential. Slopes of the log plots indicated irreversible reaction throughout.

The complex compounds studied were prepared by the method described in previous literature[13-27]. (The references are given in Table I.) Each solution for the electrolysis was made freshly from the dry crystalline cobalt(III) complexes before use and polarographic measurements were made as soon as possible after the removal of oxygen dissolved in solution. No maximum suppressor was used except in the case of azidopentamminecobalt(III) ion. Regarding the complexes of pentammine type, the presence of the maximum suppressor causes the lowering of the diffusion current and the shift of the half-wave potential to negative direction. The supporting electrolytes used were 0.5 F potassium sulfate and 0.1 F potassium chloride.

Results and Discussion

In Table I are shown the half-wave potentials of the cobalt(III) complexes of pentammine series. All the compounds are irreversibly reduced in two steps at the dropping mercury electrode with two exceptions. One of the exceptions is the complexes which contain the ligand reducible by itself, such as chromate ion. The other is the complexes which aquate easily in solution.

From Table I it is seen that the first wave exhibits various half-wave potential

13) R. G. Yalman, *J. Am. Chem. Soc.*, **77**, 3219 (1955).
14) H. H. Willard and D. Hall, ibid., **44**, 2220 (1922).
15) W. A. Hynes, L. K. Yanowsky and M. Schiller, ibid., **60**, 3253 (1938).
16) A. Benrath and A. Miens, *Z. anorg. allgem. Chem.*, **177**, 289 (1929).
17) M. Linhard and H. Flygare, *Z. anorg. Chem.*, **262**, 340 (1950).
18) F. Ephraim and W. Flügel, *Helv. Chim. Acta*, **7**, 738 (1924).
19) M. Linhard, H. Siebert and M. Weigel, *Z. anorg. allgem. Chem.*, **278**, 287 (1955).
20) P. R. Rây, *Quart. J. Indian Chem. Soc.*, **4**, 71 (1927).
21) J. C. Duff, *J. Chem. Soc.*, **1923**, 566, 573: S. M. Jörgensen, *Z. anorg. Chem.*, **11**, 425 (1896).
22) M. Linhard and B. Rau, *Z. anorg. allgem. Chem.* **271**, 121 (1953).
23) A. B. Lamb and K. J. Mysels, *J. Am. Chem. Soc.*, **67**, 468 (1945).
24) A. Werner, *Ber.*, **40**, 4098 (1907).
25) S. M. Jörgensen, *Z. anorg. Chem.*, **17**, 461 (1898).
26) A. Werner, *Ber.*, **40**, 4104 (1907).
27) S. H. C. Briggs. *J. Chem. Soc.*, **1919**, 70.
28) A. Werner and A. Müller, *Z. anorg. Chem.*, **22**, 102 (1900).

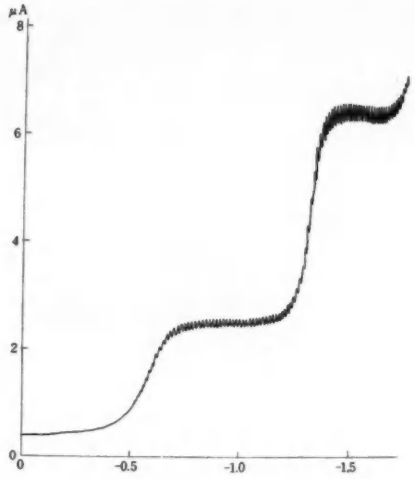

Fig. 1. The polarogram of $[Co(NH_3)_5CO_3]^+$ at the concentration of 0.001 F in the solution of 0.5 F K_2SO_4.
The first wave: $E_{1/2}=-0.50$ V., $i_d=1.52$ μA.
The second wave: $E_{1/2}=-1.28$ V., $i_d=3.04$ μA.

values from compound to compound, while the potentials of the second reduction are always in close proximity to that of hexaquocobalt(III) ion. (−1.428 V. vs. S. C. E. in 0.5 F potassium sulfate solution[4]). Fig. 1 shows the typical polarogram of the pentamminecobalt(III) complexes.

The height of the second wave was very close to twice that of the first wave. The heights of either waves were linearly related with the concentration of the complex ion in the range of $1\times10^{-2}\sim5\times10^{-4}$ F. Accordingly the first wave, corresponding to a one-electron transfer, represents the reduction of cobalt(III) to cobalt(II), and the second, corresponding to a two-electron, represents the reduction of cobalt(II) to metallic state.

As regards the process of the reduction of pentamminecobalt(III) complexes in dilute solution, Willis et al.[1] proposed the following mechanism;

$$[Co(NH_3)_5X]^{n+} + e^- \longrightarrow [Co(NH_3)_5X]^{(n-1)+}$$

$$[Co(NH_3)_5X]^{(n-1)+} + 6H_2O \xrightarrow{\text{rapidly}} [Co(OH_2)_6]^{2+} + 5NH_3 + X^{-n+3}$$

$$[Co(OH_2)_6]^{2+} + 2e^- \longrightarrow Co + 6H_2O$$

From the reduction scheme, it may be seen that the first step in the polarographic reduction of the pentamminecobalt(III) complexes corresponds to the disruption of the complexes, so its half-wave potential of the first wave may be regarded as a measure of the stability against the polarographic reduction.

The polarographic stability of the pentammine series of cobalt(III) complexes increases in the following order of the ligands;

$$I^-, Br^-, Cl^-, CrO_4^{2-}, NCS^- < NO_3^- < SO_4^{2-} < NO_2^- < S_2O_3^{2-} < C_2O_4^{2-} < CH_3COO^- < NH_3 < CO_3^{2-} < OH_2 < OH^-$$

(Supporting electrolyte; 0.1 F potassium chloride).

This order of the stability varied scarcely by the kind of the supporting electrolyte. The reverse of the order is seen between carbonate and water molecule when 0.5 F potassium sulfate was used as a supporting electrolyte.

$$I^-, Br^-, Cl^-, CrO_4^{2-}, NCS^- < NO_3^- < N_3^- < SO_4^{2-} < NO_2^- < C_2O_4^{2-} < CH_3COO^- < NH_3 < OH_2 < OH^- < CO_3^{2-}, HCO_3^-$$

(Supporting electrolyte; 0.5 F potassium sulfate).

No relation between the above order of the polarographic stability and that of the spectrochemical series[29] could be found.

Polarographic Behavior of Individual Complexes.—Some cobalt(III) complexes of pentammine series gave a "prewave" which precedes the actual second

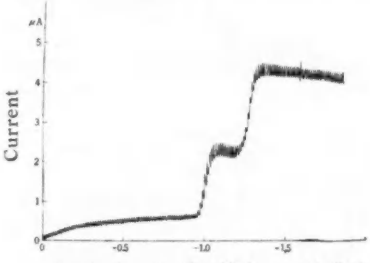

Fig. 2. The polarogram of $[Co(NH_3)_5Br]^{2+}$ at the concentration of 0.001 F in the solution of 0.1 F KCl.
The diffusion current of the second wave: 3.62 μA.
A prewave occurs at around −1.0 V.

29) Y. Shimura and R. Tsuchida, This Bulletin, **29**, 311 (1956).

wave. Brdička[30] explained the prewave as being due to the pentaquomonohydroxocobalt(II) ion formed by hydrolysis, the ion being in slow equilibrium with the hexaquocobalt(II) ion. Fig. 2 shows Brdička's prewave obtained in the reduction of bromopentamminecobalt(III) ion. Similar prewaves were found in the following ions;

$[Co(NH_3)_5I]^{2+}$, $[Co(NH_3)_5Br]^{2+}$

$[Co(NH_3)_5Cl]^{2+}$, $[Co(NH_3)_5SO_4]^{+}$

$[Co(NH_3)_5NO_2]^{2+}$, $[Co(NH_3)_5OH]^{2+}$

$[Co(NH_3)_5OH_2]^{3+}$, $[Co(NH_3)_5OCOCH_3]^{2+}$

On the other hand in the following ions the prewave was completely absent;

$[Co(NH_3)_5S_2O_3]^{+}$, $[Co(NH_3)_5SO_3]^{+}$

$[Co(NH_3)_5HCO_3]^{2+}$, $[Co(NH_3)_5CO_3]^{+}$

$[Co(NH_3)_5C_2O_4]^{+}$

The ion, $[Co(NH_3)_5NO_3]^{2+}$ shows a prewave in 0.1 F potassium chloride, but does not in 0.5 F potassium sulfate.

Thiosulfato- or sulfono-pentamminecobalt(III) ion[31] gave the first wave which had too small a slope at the reduction potential to determine its half-wave potential exactly. This is considered to be due to the aquation of the ion. In 1 F sodium sulfite a well-defined wave of the ion, $[Co(NH_3)_5SO_3]^{+}$ was obtained, because the presence of an overwhelming amount of sulfite ions causes an interruption of the aquation of the complex to some extent (Fig. 3).

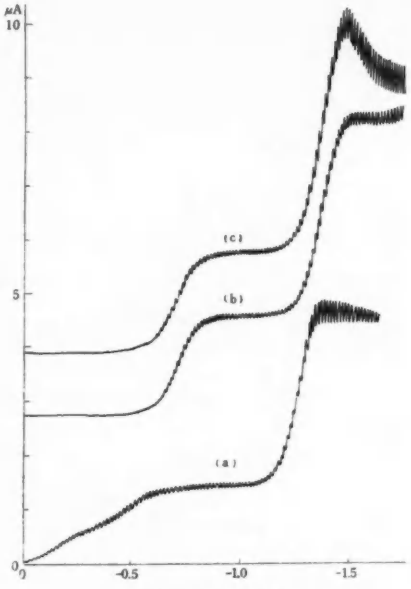

Fig. 3. The polarograms of $[Co(NH_3)_5SO_3]^{+}$ obtained at the concentration of 0.001 F in the solution of 0.5 F K_2SO_4 and of 1 F Na_2SO_3.
a) Supporting electrolyte: 0.5 F K_2SO_4
b) Supporting electrolyte: 1 F Na_2SO_3, in the presence of 0.0016% Tween-80.
c) Supporting electrolyte: 1 F Na_2SO_3, in the absence of the maximum suppressor.

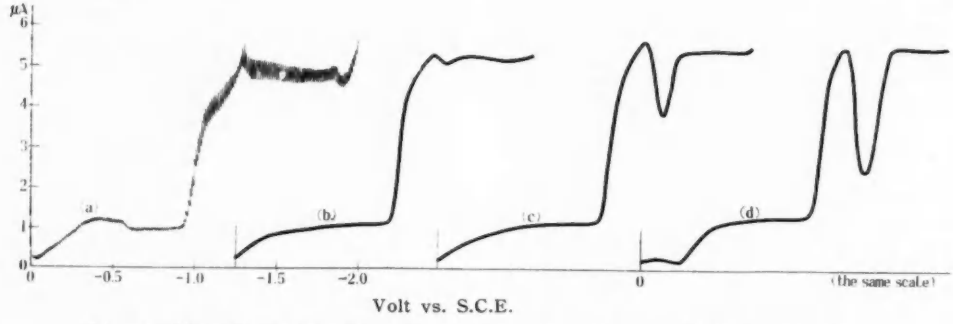

Fig. 4. The effects of maximum suppressor on the current-voltage curves of $[Co(NH_3)_5NCS]^{2+}$ at the concentration of 0.001 F in the solution of 0.5 F K_2SO_4.
a) The polarogram obtained in the absence of maximum suppressor.
b) Current-voltage curve taken in the presence of 0.0032% Tween-80.
c) In the presence of 0.0065% Tween-80.
d) In the presence of 0.0097% Tween-80.

30) R. Brdička, *Collection Czechoslov. Chem. Communs.*, 5. 113 (1933).

31) The "sulfono group" is SO_3^{2-} radical bound to the central metal ion by the sulfur atom.

The reduction potential of the second step of thiosulfato-pentamminecobalt(III) ion, $[Co(NH_3)_5S_2O_3]^+$, is -0.965 V. vs. S.C.E. in 0.1 F potassium chloride. This value is quite different from that of the other pentamminecobalt(III) complexes. This fact means that through the reduction of the thiosulfatopentamminecobalt (III) ion, a cobalt(II) complex ion was formed, which was reducible more easily than hexaquocobalt(II) ion. The cobalt (II) complex is probably thiosulfatopentaquocobalt(II) ion or a similar one.

The first wave of isothiocyanatocobalt (III) ion has a small maximum wave which can easily be suppressed in the presence of 0.0032% Tween-80.* The effect of the maximum suppressor on the wave form of the ion, $[Co(NH_3)_5NCS]^{2+}$, are shown in Fig. 4. Chromatopentamminecobalt(III) ion shows many complicated waves. This may be an overlap of the waves of the cobalt(III) complexes and of chromate ion (Fig. 5).

In a neutral solution the first wave of aquopentamminecobalt(III) complex ion has always a smaller slope at the half-wave potential than the other pentamminecobalt(III) complexes (Fig. 6). On the other hand, in 1 F perchloric acid, a well-defined wave which had a sharp slope was obtained. One of the reasons for this is considered to be the shift of the equilibrium between the aquopentamminecobalt (III) ion and the hydroxopentamminecobalt(III) ion.

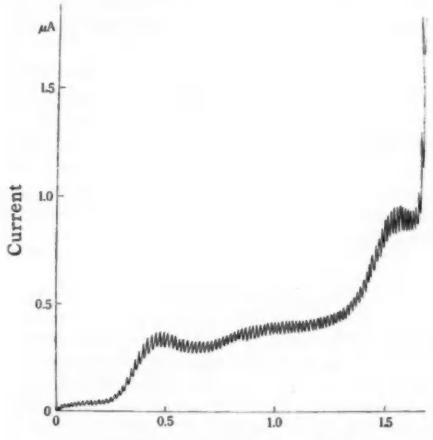

Fig. 5. The polarogram of $[Co(NH_3)_5CrO_4]^+$ obtained at the concentration of 0.001 F in the solution of 0.5 F K_2SO_4.

* Polyoxyethylene sorbitan mono-oleate.

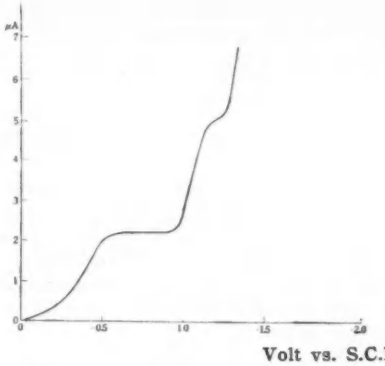

Fig. 6. Current-voltage curve of $[Co(NH_3)_5OH_2]^{3+}$ at the concentration of 0.001 F in the solution of 0.1 F KCl.

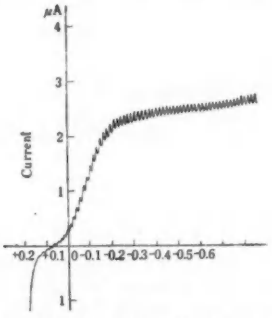

Fig. 7. The polarogram of $[Co(NH_3)_5OH_2]^{3+}$ obtained at 0.001 F in 1 F $HClO_4$. $E_{1/2}$ and i_d, respectively, -0.045 V. and 2.25 μA.

$$[Co(NH_3)_5OH_2]^{3+} \rightleftarrows [Co(NH_3)_5OH]^{2+} + H^+$$

In perchloric acid the above equilibrium is markedly shifted to the left hand. Consequently the well-defined wave of the aquopentamminecobalt(III) ion could be obtained (Fig. 7).

Summary

1. Most of the cobalt(III) complex ions of pentammine series, $[Co(NH_3)_5X]^{(3-n)+}$, are reduced irreversibly in two steps at the dropping mercury electrode. The first diffusion current corresponds to the reduction, cobalt(III) → cobalt(II) and the second to the reduction, cobalt(II) → cobalt (0). The diffusion current and concentration were linearly related.

2. The polarographic stability of cobalt (III) complexes of the pentammine series increases in the following order of the ligands;

I^-, Br^-, Cl^-, CrO_4^{2-}, $NCS^- < NO_3^- < N_3^- < SO_4^{2-} < NO_2^- < C_2O_4^{2-} < CH_3COO^- < NH_3 < OH_2 < OH^- < CO_3^{2-}$, HCO_3^-

(Supporting electrolyte; 0.5 F potassium sulfate).

The reverse of the order was found between carbonate and water molecule when 0.1 F potassium chloride was used as a supporting electrolyte. This order did not agree with that of the spectrochemical series of the pentamminecobalt(III) complexes.

3. In dilute perchloric acid the well-defined wave was obtained for aquopentamminecobalt(III) ion, $[Co(NH_3)_5OH_2]^{3+}$, while the ion gave a modified wave in the first reduction step in neutral supporting electrolyte, potassium chloride or potassium sulfate.

The authors wish to thank Dr. J. Fujita for his kindness in giving them some of the complex compounds used in this study.

Department of Chemistry
Faculty of Science
Osaka University
Kita-ku, Osaka

Studies on the Cephalin of Escherichia Coli

By Masaharu KUROKAWA, Kyoko HOTTA, Tomoko YOSHIMURA, Mitsuo MAKITA and Ichiro HARA*

(Received June 16, 1958)

To investigate the lipids of gramnegative bacilli two procedures are available. One of these is concerned with the lipids extracted directly from bacilli[1] and the other is carried out on the lipids of lipopolysaccharide protein complxes isolated from bacteria. The lipopolysaccharide-protein complexes of gramnegative bacilli are designated as O-antigen[2]. According to Westphal and Lüderitz[3], lipopolysaccharide-protein complexes are divided into several components as represented in Fig. 1.

Fig. 1
Lipopolysaccharide-lipid-protein complex (Vollantigen)

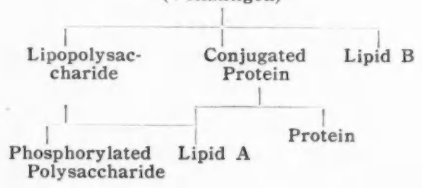

There were two kinds of lipid in the complex; one of these, designated as lipid B, was separated readily in contrast to the other lipid A, which could be extracted only by treatment with chloroform-ethanol mixture containing hydrochloric acid. The latter was also designated as the bound lipids by Čmelik. Lipid B was regarded as cephalin and like phospholipid, nonantigenic.

This report accounts for the chemical nature of the lipid B(possibly containing some lipid A), which was isolated to investigate the antigenic properties, especially of hapten or testantigen to anti-E. coli rabbit sera. Serological and biological properties of this lipid fraction will be reported later.

Experimental

Preparation of crude toxic substance.—A culture of *E. coli* 0—23 was autolyzed at 37°C for 48 hr. by addition of chloroform. Zinc complex of crude toxic substance was precipitated from the culture by adding 50% solution of zinc chloride in proportion of 20 ml./l. of the culture. The zinc complex was separated by centrifuge, treated with 40% disodium phosphate solution, and centrifuged to remove zinc phosphate. The supernatant was dialyzed against distilled water. The dialyzate was treated with its twothirds

* Present Address, Department of Chemistry, Faculty of Liberal Arts, Chiba University, Konakadai-cho, chiba.

1) S. Čmelik, *Z. physiol. Chem.*, **293**, 222 (1953); ibid., **296**, 67 (1954); ibid., **302**, 20 (1955).
2) H. Zinsser and J. T. Parker, *J. Exper. Med.*, **37**, 275 (1923).
3) O. Westphal and O. Lüderitz, *Angew. Chem.*, **66**, 407 (1954).

volume of saturated ammonium sulfate solution to precipitate crude toxic substance. The precipitate of crude toxic substance was dialyzed toxic and then lyophilized. Total yield of crude substance was 1 g. per 10 l. culture.

In the paperelectrophoretic pattern (Fig. 2), three peaks were shown by protein staining[4] and two peaks by lipid staining[5], but no further purification was carried out.

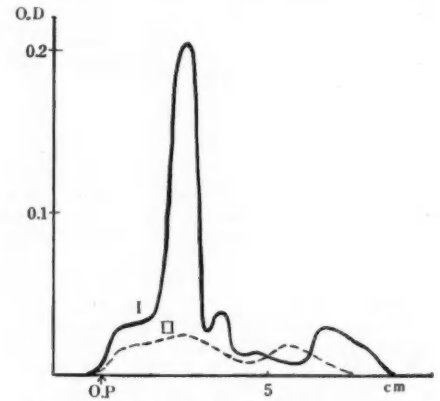

Fig. 2. The paperelectrophoretic pattern. I—Protein, II—Lipid, 0.2 mA/cm; 17 hr's electrophoresis. Veronal buffer pH 8.6, μ 0.05. Filterpaper Tōyō-roshi No. 51

Chemical analysis.—Phosphorus was assayed by King's method[6]. One to two mg. of lipids was digested with 1.2 ml. of perchloric acid, and then colorimetrically determined with 1.0 ml. of 5% ammonium molybdate solution and 0.5 ml. of 1-amino-2-naphthol-4-sulfonic acid solution (0.25 g. of 1-amino-2-naphthol-4-sulfonic acid in 125 ml. of water containing 15 g. of sodium bisulfite and 3 g. of sodium sulfite). Total nitrogen was assayed by the micro Kjeldahl procedure. After hydrolyzing the lipids according to the procedure described in the next section, the main chemical constituents were analyzed respectively. Cholin was assayed by Entenman's method[7]. To the hydrolyzate containing 100 mg. of cholin was added the ammonium reineckate solution (2 g. of ammonium reineckate in 100 ml. of 1.2 N hydrochloric acid). The precipitated cholin reineckate was dissolved in acetone and colorimetrically determined at 500~570 mμ. Serine and ethanolamine were assayed by Axelrod-Reichenthal's method[8]. To the hydrolyzate containing 100 μg of serine and 50 μg ethanolamine was added 0.1 ml. of dinitrofluorobenzene (DNFB) reagent (0.1 ml. of DNFB in 2ml. of absolute ethanol). The dinitrophenyl ethanolamine (DNP-EA) was extracted with chloroform, dinitrophenyl serine (DNP-S) remaining in aqueous solution. DNP-EA and DNP-S were colorimetrically determined at 420 mμ. Total glycerophosphoric acid was determined by Burmaster's method[9]. To the hydrolyzate containing 10~50 μg. of phosphorus were added 1 ml. of 4% sodium sulfite solution, 1 ml. of 10 N sulfuric acid, 1 ml. of 7% sodium molybdate solution and 1 ml. of stannous chloride solution (40 g. of stannous chloride was dissolved in 100 ml. hydrochloric acid and 1 ml. of this solution was diluted with 200 ml. of distilled water). According to this procedure, the inorganic-phosphate phosphorus (Inorg.-P) was colorimetrically determined at 540 mμ. To the hydrolyzate containing 10~50 μg of phosphorus were added 1 ml. of 10 N sulfuric acid and 1 ml. of 0.05 M periodic acid. This solution was immersed in boiling water for 1 hr. and to this were added 1 ml. of 4% sodium bisulfite solution, 0.5 ml. of 10 N sulfuric acid, 1 ml. of 7% sodium molybdate solution and 1 ml. of the diluted stannous chloride solution after cooling. By this procedure the glycerophosphoric acid phosphorus (GPA-P) plus the inorganic phosphate phosphorus were determined. (GPA-P+Inorg-P)−Inorg-P= GPA-P. Sugar was determined with anthrone reagent[10]. Neutralization values of fatty acids were also determined.

Intact lipids and their constituents in the hydrolyzates were qualitatively determined by paper chromatography on Toyo-roshi No. 51 paper with a mixture of n-butanol, ethylene glycol and water (4:1:3); phosphorus was identified by spraying Hanes-Isherwood's reagent[11] and amino compounds were by spraying 0.2% ninhydrin in n-butanol. In paper chromatography, the ascending method was used at 35°C, for 6 hr.

Fractionation and Hydrolysis.—From lyophilized crude toxic substance (10.1 g.), lipids were extracted with a mixture of chloroform and methanol (9:1 v/v) in a hot-water bath for 72 hr. Extractions were repeated 3 times with new solvents in the same way. Extracted lipids were fractionated according to the following scheme (Fig. 3).

Nitrogen-containing impurities removed from F—I with 0.25 M magnesium chloride solution by McKibbin's method[12]. Six fractions were obtained from F—II (Table I).

F—VII and F—VIII were hydrolyzed as follows respectively: 50 mg. of lipids was refluxed with 30 ml. of saturated barium hydroxide solution for 5 hr., and then 3.25 ml. of concentrated hydrochloric acid was added. Hydrolysis was continued for 75 min. After cooling, the extraction of fatty acids was carried out thrice with each 15 ml. of chloroform. To the aqueous layer was added 18 ml. of 2 N sulfuric acid to precipitate

4) E. L. Durrum, *J. Am. Chem. Soc.*, **72**, 2943 (1950).
5) B. Swahn, *Scand. J. Clin. Lab. Invest.*, **4**, 98 (1952).
6) E. J. King, *Biochem. J.* **26**, 292 (1932).
7) C. Entenman et al., *J. Biol. Chem.*, **155**, 13 (1944).
8) J. Axelrod and J. Reichenthal, ibid., **204**, 903 (1953).
9) C. F. Burmaster, ibid., **164**, 233 (1946).
10) F. A. Loewus, *Anal. Chem.*, **24**, 219 (1952).
11) C. S. Hanes and F. A. Isherwood, *Nature*, **164**, 1107 (1949).
12) J. M. McKibbin and W. E. Taylor, *J. Biol. Chem.*, **178**, 17 (1949).

Fig. 3

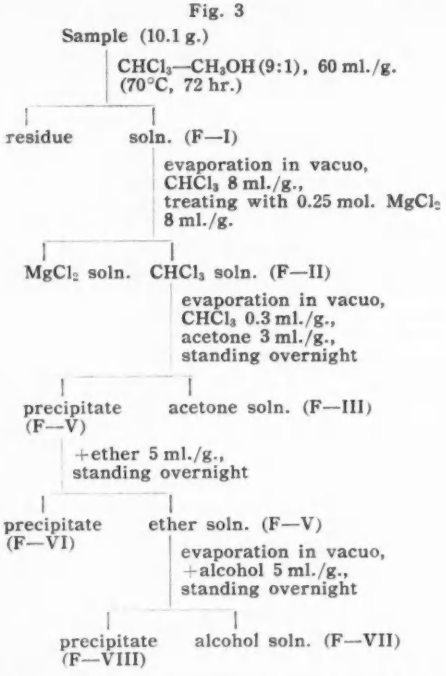
Sample (10.1 g.)
$CHCl_3$—CH_3OH (9:1), 60 ml./g. (70°C, 72 hr.)
residue
soln. (F—I)
evaporation in vacuo, $CHCl_3$ 8 ml./g., treating with 0.25 mol. $MgCl_2$ 8 ml./g.
$MgCl_2$ soln.
$CHCl_3$ soln. (F—II)
evaporation in vacuo, $CHCl_3$ 0.3 ml./g., acetone 3 ml./g., standing overnight
precipitate (F—V)
acetone soln. (F—III)
+ether 5 ml./g., standing overnight
precipitate (F—VI)
ether soln. (F—V)
evaporation in vacuo, +alcohol 5 ml./g., standing overnight
precipitate (F—VIII)
alcohol soln. (F—VII)

barium sulfate. To remove the residual hydrochloric acid, vacuum distillations were repeated. Both aqueous solutions free from hydrochloric acid, were analyzed according to the procedures described above (Table II).

There was no choline in F—VII, F—VIII, and F—I hydrolyzates. It could not be seen that lecithin and sphingomyelin were contained in these fractions. The results agreed with those of many researches on the bacterial lipids. From

TABLE I

ANALYTICAL DATA AND YIELDS OF THE FRACTIONS

	Yield*	N(%)	P(%)	N/P
F—I	100	7.3	1.01	2.28	0.98
F—II	81.3	6.0	0.84	2.20	0.85
F—III	44.2	3.2	0.02	0.09	0.45
F—IV	32.0	2.4	1.54	2.85	1.20
F—V	27.9	2.0	1.45	3.11	1.03
F—VI	4.2	0.3	1.29	0.00	—
F—VII	12.5	0.9	1.52	3.50	0.96
F—VIII	14.6	1.1	1.12	3.46	0.72

* For F—I for crude toxin.

Table II it was concluded that F-VII and F—VIII were so-called cephalin fractions. The principal nitrogen-containing constituents of F—VII and F—VIII were ethanolamine and serine respectively. Glycerophosphoric-acid contents in these fractions were 17.7% and 14.6% respectively, but these amounts were less than the calculated amounts (24% for F—VII and 22% for F—VIII), if F—VII and F—VIII consisted of only phosphatidyl ethanolamine and phosphatidyl serine respectively. There was also some inorganic phosphorus in these hydrolyzates, but its origin was obscure. Neutralization values of fatty acids of F—VII and F—VIII were 194 and 239 respectively, but detailed researches on the natures of fatty acids were not satisfactorily completed.

R_f values of paper chromatography of intact lipids and their hydrolyzates indicated similarly that F—VII consisted mainly of phosphatidyl ethanolamine and that F—VIII was a mixture of phosphatidyl ethanolamine and phosphatidyl serine. There were neither free amino acids nor related compounds in F—VII and F—VIII according to the spots of paper chromatography.

TABLE II

ANALYTICAL DATA OF THE HYDROLYZATES

	F—VII (33040 μg)		F—VIII (36800 μg)		Note
	μg	%	μg	%	
Intact Lipid N	664	1.52	412	1.12	
Intact Lipid P	1170	3.54	1275	3.46	
$CHCl_3$ solution	19100	57.9	23000	62.5	
$CHCl_3$ N and P	none	—	none	—	
Aqueous solution	13900	42.1	13800	37.5	
N	630	95.0	372	90.3	% to total N
Choline-N	none	—	none	—	
Serine-N	72	10.8	224	54.4	% to total N
Serine	480	1.5	1680	4.6	% to total lipid
Ethanolamine-N	522	78.6	164	39.8	% to total N
Ethanolamine	2310	7.0		2.0	% to total lipid
P	1140	97.5	1240	97.3	% to total P
Inorganic P	66	5.6	168	13.5	% to water sol. P
G.P.A.—P	1053	92.6	964	77.7	% to water sol. P
G.P.A.	5850	17.7	5360	14.6	% to total lipid
Sugar	2265	6.9	1008	2.7	% to total lipid
Neutralization Value	194		239		Fatty acids

TABLE III

R_f VALUES OF FRACTIONS AND THEIR HYDROLYZATE

	Intact Lipid		Hydrolyzates	
	P-Staining	Ninhydrin	P-Staining	Ninhydrin
F—IV	0.60 0.82	0.59 0.81		
F—VII	0.80	0.79	0.03	0.13 0.39
F—VIII	0.60 0.80	0.60 0.80	0.03	0.02 0.14, 0.38
Cephalin	0.60 0.80	0.60 0.79		
Ethanolamine				0.38
Serine				0.15
G.P.A.*			0.03	

*Glycerophosphoric acid

Discussion

It could be supposed from the value N/P (0.96) that F—VII contained only monoaminophosphoglyceride. The calculated amounts of phosphatidyl ethanolamine and phosphatidyl serine, based upon Table II, were 88% and 12% respectively. Glycerophosphoric acid amounts calculated from the above estimation were 23.7%, being 6% more than the observed values.

From the value N/P (0.76) it was considered that F-III might contain not only monoaminophosphoglyceride, but also phosphatidic acids. The calculated amounts of phosphatidyl ethanolamine and phosphatidyl serine were 28% and 33% respectivly. The calculated glycerophosphoric acid amount was 18.0%, being 4% more than the observed. The discrepancies of phosphor values in both cases were compensated for by inorganic phosphorus amounts, but the origins of the latter were not ascertained.

Sugars were also contained 6.9% in F—VII and 2.7% in F—VIII. There was no cerebroside because the chloroform-soluble portions of these two hydrolyzates contained no sphingosine-nitrogen. But it was considered that these are probably some sugar containing lipids, such as phosphatidylinosito-dimannoside in *Mycobacterium tuberculosis* reported by Lederer[13].

Summary

The lipids were extracted from the crude toxic substances, isolated from *Escherichia coli* by Hosoya's method[14]. These lipids which were 7.2% of the crude toxic substances by weight, were fractionated by solvents. One of these fractions, that was soluble in diethyl ether and ethanol, contained 7.0% ethanolamine and 1.5% serine, and the other that was soluble in diethyl ether, but insoluble in ethanol contained 2.0% ethanolamine and 4.6% serine. There was no choline in any fraction. Average neutralization values of fatty acids in these two fractions were 194 and 239 respectively.

The authors wish to express their deepest appreciation to Professor Susumu Mitsuhashi, M. D., Gumma University Medical School, for much useful guidance and helpful discussion.

The Kitasato Institute for Infectious Diseases, Minato-ku, Tokyo

13) E. Vilkas and E. Lederer, *Bull. soc. chim. biol.*, **38**, 111 (1956).
14) S. Hosoya and S. Miyata, *C. R. Soc. Biol.*, **99**, 773 (1928); S. Hosoya, et al., *Jikken Igaku*, **28**, 420 (1944).

Silica in Water. V. Salt Effect on the Colorimetric Determination of Silica in Concentrated Salt Solution*

By Iwaji IWASAKI and Toshikazu TARUTANI

(Received June 13, 1958)

In a concentrated salt solution, the amount of silica obtained by colorimetric methods (silicomolybdate and molybdenum blue method) is lower than that obtained in the absence of salt**. This phenomenon is called the salt effect or the salt error, and the ratio of the true silica content to the value obtained in the presence of salt is called the salt factor, since it gives a measure of the salt effect. Some salt factors were reported for the colorimetric determination of silica in sea water[1-5], and the salt effect was also investigated for the colorimetric determination of small amounts of silica in alkali[6]. The properties of silicomolybdic acid in a concentrated salt solution have not been studied systematically. The following experiments were carried out to make clear the properties of salt effect and to find the method for correcting the salt effect.

Silicomolybdate Method

Reagents and apparatus. — *Silica solution.*— Portions 0.500 g. of anhydrous silica were fused with 4 g. of sodium carbonate, the melt was dissolved in distilled water, and diluted to 1000 cc. Solutions of a suitable concentration of silica were prepared by diluting this stock solution.

Ammonium molybdate solution.—10%.

Sulfuric acid.—Various normalities.

Salts.—All chemicals were of analytical reagent grade or C. P. purity.

Apparatus.—Hitachi EPU-2 spectrophotometer, 10 mm. cell.

Variations of absorption spectrum of molybdate with acidity and salts.—In the measurement of absorbance of silicomolybdic acid by using a spectrophotometer or a photoelectric colorimeter, distilled water or a solution prepared by adding acid and ammonium molybdate solution to distilled water (or salt solution) is used as the reference. When the latter is used, it must be considered that the absorption spectrum of molybdate in the solution varies with acidity. The absorption spectra of molybdate in the solutions prepared by adding 2 cc. of sulfuric acid of various normalities and 2 cc. of 10% ammonium molybdate solution to 50 cc. of distilled water were measured against distilled water. The results are shown in Fig. 1. The absorption spectra of

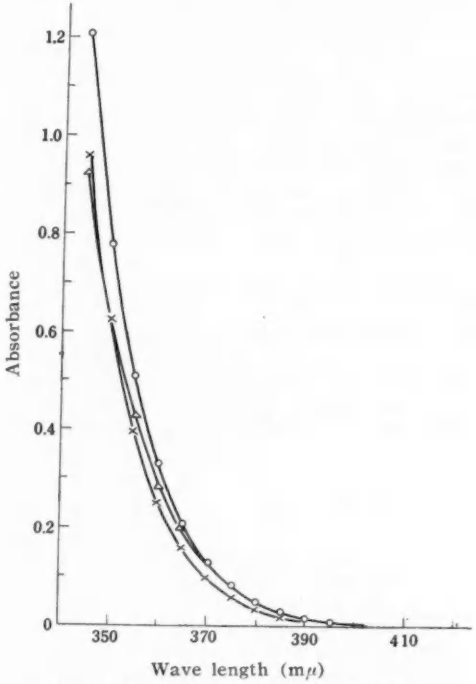

Fig. 1. Variation of absorption spectrum of molybdate with acid concentration.
× 0.037 N
○ 0.11 N (0.074 N, 0.15 N)
△ 0.22 N

* For previous paper in this series see T. Tarutani, *J. Chem. Soc. Japan, Pure Chem. Sec.* (*Nippon Kagaku Zasshi*), **77**, 1815 (1956).

** The latter gives the true content of silica.

1) D. T. W. Chow and R. J. Robinson, *Anal. Chem.*, **25**, 646 (1953).
2) R. J. Robinson and H. J. Poor, *Ind. Eng. Chem., Anal. Ed.*, **8**, 455 (1936).
3) A. Saeki, *J. Oceanog. Soc. Japan*, **6**, 39 (1950).
4) I. Iwasaki, T. Tarutani, T. Katsura and H. Shimojima, *Japan Analyst* (*Bunseki Kagaku*), **2**, 210 (1953).
5) J. B. Mullin and J. Riley, *Anal. Chim. Acta*, **12**, 162 (1955).
6) O. A. Kenyon and H. A. Bewick, *Anal. Chem.*, **25**, 145 (1953).

molybdate in 0.074 N or 0.15 N sulfuric acid is almost the same as that in 0.11 N. However, in 0.037, 0.11, and 0.22 N sulfuric acid, the spectra are different from one another.

In the concentrated salt solution, the absorption spectrum of molybdate varies with the kind of salt and the concentration of salts, even when quantities of reagents added to the solution are constant. The absorption spectra of molybdate in distilled water, 1 M sodium chloride solution, and 0.5 M sodium sulfate solution, were measured against distilled water (Fig. 2). These solutions contained the same quantity of ammonium molybdate, and the concentration of sulfuric acid was 0.11 N. It can be seen that the absorption spectrum of molybdate varies with the concentration of salts and the kind of salt.

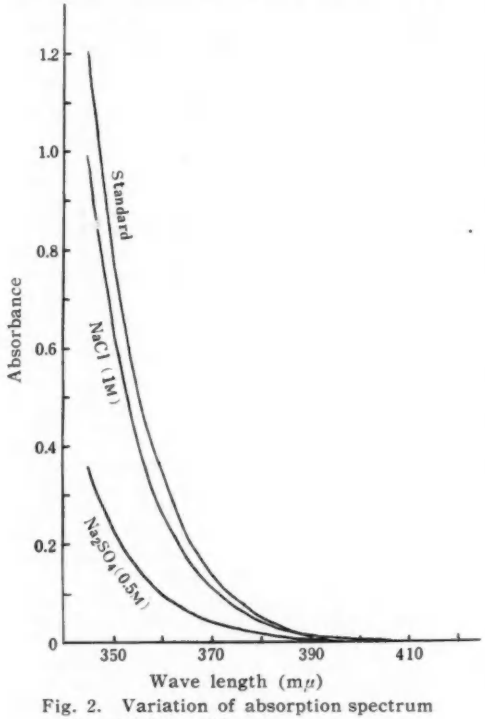

Fig. 2. Variation of absorption spectrum of molybdate with salts.

From the results shown in Figs. 1 and 2, the following conclusions may be drawn. When the solution prepared by adding definite quantities of reagents to distilled water is used for zero standard and the absorbance of silicomolybdic acid in the sample solution containing very small amounts of salt is determined, ultraviolet light can be used.

In the colorimetric determination of silica in the concentrated salt solution, when a wave length above 400 mμ is used, the solution prepared by adding definite quantities of reagents to distilled water can be used as zero standard, but when ultraviolet light is used, the solution of the same concentration of salt as the sample solution has to be used after addition of definite quantities of reagents, because the absorption spectrum of molybdate varies with the concentration of salts.

Time required for the maximum color development of silicomolybdic acid and the stability of color.—The time required for the maximum color development of silicomolybdic acid and the stability of color varies with acidity, temperature, kind of salt, concentration of salts, and quantity of molybdate. The effect of acidity, temperature, and quantity of molybdate on the time required for the maximum color development of silicomolybdic acid were already reported[7]. In a concentrated salt solution, the stability of color is smaller than that in the solution of a negligibly small salt concentration. An example is shown in Fig. 3. These experiments were carried out at 15°C. In Fig. 3, the time necessary for maximum

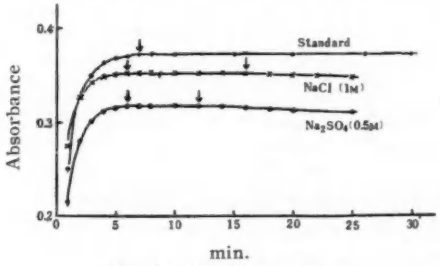

Fig. 3. Stability of color.

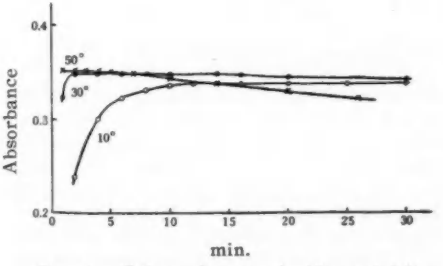

Fig. 4. Color change of silicomolybdic acid with temperature.

7) T. Tarutani, *J. Chem. Soc. Japan, Pure Chem. Sec.* (*Nippon Kagaku Zasshi*), **77**, 743 (1956).

color development are shown by the left arrow, and the time when the color intensity begins to decrease is shown by the right arrow. The color change of silicomolybdic acid with temperature are shown in Fig. 4. These experiments were carried out by the following procedure. Fifty cc. of the sample solution containing 10 p.p.m. of silica was taken, and 2 cc. of 3 N sulfuric acid and 2 cc. of 10% ammonium molybdate solution were added, and the absorbance of silicomolybdic acid was measured against distilled water at 400 mμ. From the results shown in Figs. 3 and 4, in the determination of absorbance of silicomolybdic acid, the time required for the maximum color development must be measured to obtain an accurate result.

Salt effect.—In this section, the experiments were carried out by the following procedure. The absorbance of silicomolybdic acid in the solution prepared by adding 2 cc. of 3 N sulfuric acid and 2 cc. of 10% ammonium molybdate solution to 50 cc. of the salt solution was measured against a blank containing the same amounts of salt, molybdate and acid.

Table I summarizes the previous data on the salt factor of sea water. The value reported by Iwasaki and Tarutani is differs from others. These data are supposed to suggest that the salt effect may vary with the wave length used.

TABLE I

SALT FACTOR OF SEA WATER

Author	Apparatus used	Wave length used	Salt factor
Robinson, Chow[1]	Spectro-photometer	430 mμ	1.23
Robinson, Poor[2]	Pulfrich photometer	430 mμ (filter)	1.16
Saeki[3]	Ukena tube	—	1.25
Iwasaki, Tarutani[4]	Duboscq colorimeter	—	1.09
Mullin, Riley[5]	Spectro-photometer	812 mμ (Mo-blue)	1.1

Therefore, the salt effects were measured at various wave lengths (Fig. 5). The concentration of silica in the salt solution was 10 p. p. m. The ordinate in Fig. 5 is the ratio of the absorbance of salt solution to the absorbance of standard silica solution. As will be seen in Fig. 5, the salt effect varies with wave length used and the salt effect at a longer wave length is greater than that at shorter wave length. And also the salt effect varies with the kind of salt, for example, the effect of sulfate is greater than that of chloride. In the salt solution having large salt effect e. g. ammonium sulfate solution, the variation of salt effect with wave length is large, but in the salt solution having smaller salt effect, e. g., sodium chloride solution, this variation is small.

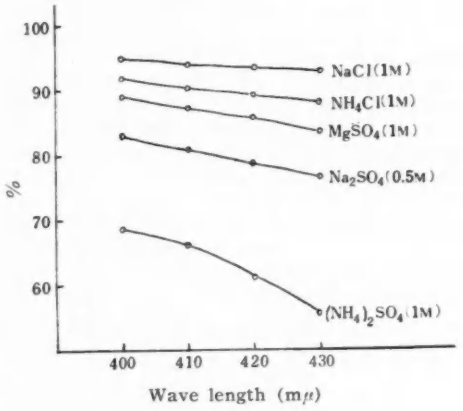

Fig. 5. Salt effect.

The absorbance was measured for a number of concentrations of sodium sulfate solution containing 10 p. p. m. of silica (Fig. 6). The straight line was obtained and it is shown that the salt effect is proportional to the salt concentration.

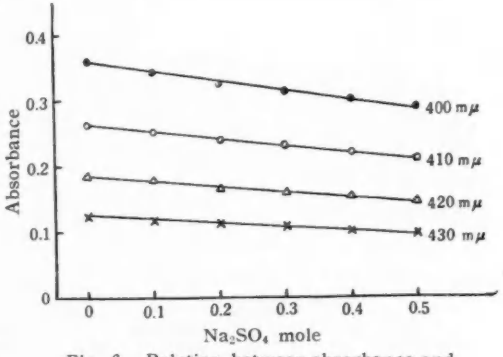

Fig. 6. Relation between absorbance and Na_2SO_4 concentration.

The absorbance was measured for different concentrations of silica in distilled water and in 0.5 M sodium sulfate solution (Fig. 7). Wave length of 400 mμ was used. A straight line was obtained. The absorbance of silicomolybdic acid in the salt solution obeys Beer's law. The ratio of the slopes of the two straight lines obtained for distilled water and salt solution gives the value of salt factor.

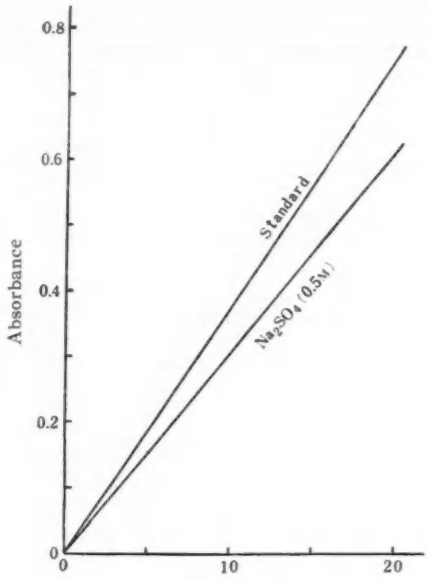

Fig. 7. Calibration curve.

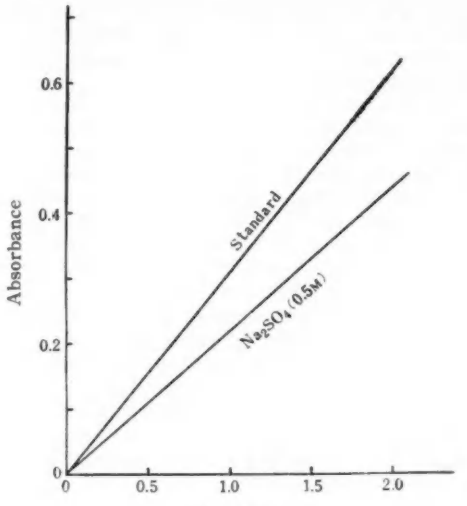

Fig. 8. Calibration curve.

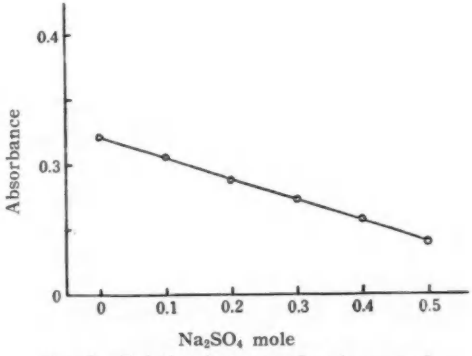

Fig. 9. Relation between absorbance and Na_2SO_4 concentration.

Molybdenum Blue Method

Reagents.—*Sulfuric acid.*—3 N.
Ammonium molybdate solution.—10%.
Reducing agent.—Twenty grams of sodium bisulfite, 2 g. of anhydrous sodium sulfite, and 0.5 g. of 1-amino-2-naphthol-4-sulfonic acid were dissolved in 200 cc. of distilled water, and stored in an amber-colored glass bottle.

Experiments.—Fifty cc. of a sample solution was taken, and 2 cc. of 3 N sulfuric acid and 2 cc. of 10% ammonium molybdate solution were added. After the color of yellow silicomolybdic acid reaches maximum, 5 cc. of reducing agent was added. After the color of molybdenum blue reaches maximum, the absorbance was measured against a blank containing the same amount of reagents at 820 mμ. Fine crystals sometimes separated out from the solution, when the concentration of salts were very high and temperature was low.

The absorbance was measured for different concentrations of silica in distilled water and in 0.5 M sodium sulfate solution, and the results obtained are shown in Fig. 8. Straight lines were obtained—i. e. the absorbance of molybdenum blue complex in the salt solution obeys Beer's law as in silicomolybdate method, and the ratio of the slopes of two straight lines gives the salt factor.

The variation of salt effect with wave length was not measured, but in this method, the salt effect will vary with wave length as in the silicomolybdate method. The absorbance was measured for a number of concentrations of solution containing 1 p.p.m. of silica (Fig. 9). A straight line was obtained. The salt effect is proportional to the salt concentration.

Conclusion

1) Wave length, kind of salt, and concentration of salts are important factors which affect the salt effect in both silicomolybdate method and molybdenum blue method.

2) In the silicomolybdate method, the salt effect is great at a longer wave length. Also, it varies with the kind of salt. The effect of sulfate is greater than that of chloride.

3) The absorbance of both silicomolybdic acid and molybdenum blue complex

in a salt solution obeys Beer's law, when the concentration of salt and reagents are maintained constant, and a definite wave length is used.

4) In the salt solutions containing definite quantities of silica, the absorbance decreases linearly with salt concentration under the conditions described above.

5) From the properties of salt effect mentioned above, it is possible to explain the reasons that several different salt factors were reported for sea water by different authors.

6) In order to obtain the true silica content in the concentrated salt solutions by the colorimetric method, one of the following procedures may be used.

(a) A sample solution is diluted with distilled water to the extent that the salt effect can be neglected, and then absorbance is measured.

(b) The calibration curve is made by using the same concentration of salt as that of the sample solution.

(c) The calibration curve is made by using the standard silica solution, and it is used for the determination of silica in a concentrated salt solution. The concentration (A) of silica in the sample solution is determined and the concentration (B) of silica in the sample solution diluted twice with distilled water is measured. The true silica content (S) can be obtained by the following formula.

$$S = A + 2(2B - A)$$

The cost of this research was defrayed from the Scientific Research Encouragement Grant from the Ministry of Education, to which the authors wish to express their thanks.

Laboratory of Analytical Chemistry and Geochemistry
Tokyo Institute of Technology
Meguro-ku, Tokyo

Antioxygenic Activity of Lecithin and its Hydrolysis Products. II. α- and β-Glycerophosphoric Acids*

By Chieko URAKAMI, Haru KAMEYAMA and Mitsuko OKADA

(Received May 30, 1958)

Since the last paper on the subject[1] was published, we have observed considerable variations in the activities of α- and β-glycerophosphoric acid with different batches of crude oleic acid obtained from beef tallow. Thus it became necessary to find some means of overcoming this difficulty. In the method of purification by low temperature crystallization, it was found difficult to remove acetone completely and we suspected that some impurities soluble in acetone might have been carried over to the final product to give these varied results. This difficulty was overcome, however, by crystallizing oleic acid as urea complex. The samples of the substrate purified in this way gave rather consistent results.

Further evidences were obtained as to the formation of oil-soluble products from both α- and β-glycerophosphoric acid during autoxidation, as suggested in the previous paper, by applying chromatographic techniques and measuring the ultraviolet absorption of the fractions obtained.

Experimental

Materials.—*Oleic acid.*—Crude oleic acid from beef tallow was supplied by the laboratory of Nihon Yushi Co., Ltd. Olive oil was treated according to the procedure described by Knight, et al.[2] to obtain crude oleic acid. These crude products were purified by the following two methods: *Method A*; The samples were purified by low temperature crystallization from acetone, as described in the previous paper. *Method B*;

* The preceding paper (This Bulletin **29**, 921 (1956).) will be designated as Part I of the series under this new title.

1) Chieko Urakami, Y. Kakutani and H. Okura, This Bulletin, **29**, 921 (1956).

2) H. B. Knight, E. F. Jordan, Jr., E. T. Roe and D. Swern, "Biochemical Preparation," Vol. 2, John Wiley & Sons, Inc., New York (1952). pp. 100.

The samples of oleic acid obtained in the above manner were treated with urea according to the procedure described by Swern and Parker[3]. The constants of these samples are summarized in Table I.

TABLE I

CONSTANTS OF SAMPLES OF OLEIC ACID

Source	Code No.	b. p.	n_D^{20}	Iodine No.	Acid No.
Beef tallow					
Method A	O-1	200~201/2	1.4596	90.2	197.9
〃	O-2	189~192/2	1.4589	91.8	198.3
Olive oil					
Method B	O-3	214/5	1.4600	90.0	198.2
Lit. or calcd. values		210/5	1.4585 1.4599	89.9	198.6

Methyl oleate.—Esterification of oleic acid was carried out by following the procedure described by Knight et al.[2] The samples of the ester prepared from the oleic acid which was purified by Method A and those prepared from the oleic acid which was purified by Method B are classed in the respective group in Table II.

TABLE II

CONSTANTS OF SAMPLES OF METHYL OLEATE

Source	Code No.	b. p.	n_D^{20}	Iodine No.	Acid No.
Beef tallow					
Method A	M-1	173~174/2	1.4520	84.5	194.2
〃	M-2	205/12	1.4352	88.6	196.1
Method B	M-3	160~164/3	1.4515	81.8	195.2
Olive oil					
Method B	M-4	166~169/1.8	1.4526	86.1	188.3
Lit. or calcd. values		172~173/2	1.4526 1.4522	85.7	189.2

α-Glycerophosphoric acid.—An ethanolic solution of the free acid was prepared from the sodium salt (procured from Daito Seiyaku Co., Ltd.) in the same manner as described in the previous paper[1]. This sample was found to contain about 21% β-glycerophosphoric acid and was used in the experiments with oleic acid. A sample containing 14% β-isomer was prepared by isomerization in an acid medium[4] and used in the runs with methyl oleate.

β-Glycerophosphoric acid.—An ethanolic solution was prepared from its sodium salt (obtained from Yashima Yakuhin Co., Ltd.) as described above. The sample was found to be 100% pure. The concentrations of the ethanolic solutions were determined by Burmaster's method[5].

Autoxidation.—The procedure employed was essentially the same as that described previously, except that the bath temperature was maintained at 45°C for the runs with methyl ester, instead of 50°C used for runs with the acid. The concentration of the glycerophosphoric acids in the substrate was 0.1%.

Peroxide determinations. — The method described in the previous paper was followed, except that the use of nitrogen gas was omitted. As shown in Table III, the values obtained by titration under nitrogen did not significantly differ from those obtained without bubbling nitrogen through the sample solution, as long as one to two drops of a 0.05% solution of hydroquinone in isopropanol had been added to each aliquot taken.

TABLE III

PEROXIDE VALUES OBTAINED BY TITRATION UNDER NITROGEN AND IN AIR

	Sample wt. g.	P. V. mM/100 g.
Under nitrogen	0.1824	2.54
	0.2107	2.53
In air	0.2180	2.52
	0.1926	2.58

Recovery test.—The recovery of the water-soluble glycerophosphoric acids from the substrates during autoxidation was examined in the same manner as described previously. The results are shown in Figs. 1 and 2 and Table IV.

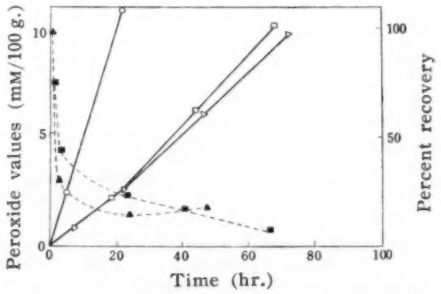

Fig. 1. Peroxide values and percent recovery against time.
○ Oleic acid, O-1, alone. △ Peroxide values for the same sample of oleic acid containing 0.1% α-glycerophosphoric acid (79% purity). □ Peroxide values for the same sample of oleic acid containing 0.1% β-glycerophosphoric acid. ▲ Percent recovery of the α-glycerophosphoric acid. ■ Percent recovery of the β-glycerophosphoric acid.

Chromatography. — Since the method described by Huennekens and his associates[6] affords separation of oleid acid from phosphorus containing substances of biological interest, we utilized the method in removing the substrate from the substance which seemed to be formed from the glycerophosphoric acids added initially. The

3) D. Swern and W. B. Parker, *J. Am. Oil Chemists' Soc.*, **29**, 614 (1955).
4) E. Chargaff, *J. Biol. Chem.*, **144**, 455 (1942).
5) C. F. Burmaster, ibid., **164**, 233 (1946).
6) F. M. Huennekens, D. J. Hanahan and M. Uziel, ibid., **206**, 443 (1954).

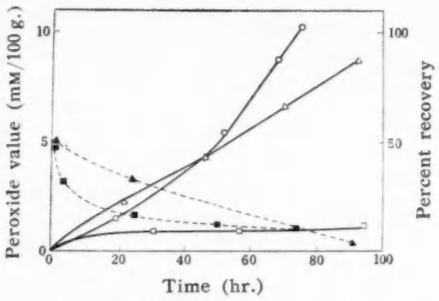

Fig. 2. Peroxide values and percent recovery against time
○ Methyl oleate, M-1, alone. △ Peroxide values for the same sample of methyl oleate containing 0.1% α-glycerophosphoric acid (86% purity). □ Peroxide values for the same sample of methyl oleate containing 0.1% β-glycerophosphoric acid. ▲ Percent recovery of the α-glycerophosphoric acid. ■ Percent recovery of the β-glycerophosphoric acid.

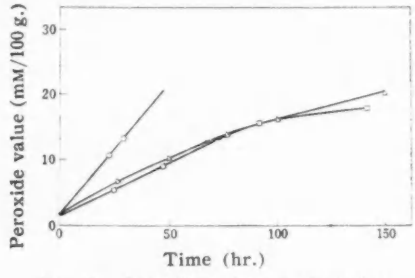

Fig. 3. Peroxide values against time
○ Oleic acid, O-2, alone. △ The same sample of oleic acid containing 0.1% α-glycerophosphoric acid (79% purity).
□ The same sample of oleic acid containing 0.1% β-glycerophosphoric acid.

TABLE IV
RECOVERY OF GLYCEROPHOSPHORIC ACIDS FROM SUBSTRATES

Time hr.	P. V. mM/100g.	Sample wt. g.	Recovery in water, mg. α	β	Total
0	0	0.1345[a]	10.03	4.11	14.15 (36.1)
87.5	1.18	0.1487[a]	0.104	0.045	0.149 (0.38)
139	15.07	1.3200[b]	0.0036 (1.5)		
182	23.85	1.7680[c]		0.0064 (2.0)	

a) Methyl oleate obtained from beef tallow containing 7% α-isomer. The ratio of the recovered α:β before and after oxidation remained the same, 70:30. b) Methyl oleate obtained from olive oil containing 0.1% α-isomer. c) Oleic acid from olive oil containing 0.1% β-isomer. The figures in the parentheses represent percent recovery.

last two samples shown in Table IV were subjected to chromatography, after removing any unreacted glycerophosphoric acids by repeated washing with water.

By a trial run with paper, using about 200 mg. each of the samples and a mixture of 1-propanol and water (8:1) as a developing solvent (at 21°C for 15.5 hr.), it was found that a significantly large amount of phosphorus was present in the upper half (toward the solvent front) of the chromatogram. This was somewhat more concentrated in the section 3/4 from the original point of application. Therefore, the upper half of the chromatogram was extracted successively three times with a 50 cc. portion of diethyl ether, twice with 25 cc. of ethanol and finally with 10cc. of a 0.1 N solution of sodium hydroxide. Each extract was tested for the presence of phosphorus and it was found to be present only in the alkaline extract. Therfore, the same sample was subjected to column chromatography in the same manner, using cellulose powder (Toyo-Roshi No. 50), except that a larger amount of diethyl ether was used in place of extracting with ethanol. A blank run was made in exactly the same way. The ultraviolet absorption curves obtained with the ether extract are shown in Fig. 9 and those of the alkaline extracts in Fig. 10 (corrected for the absorption of the blank).

Measurements of ultraviolet absorption.— A Beckman DU-spectrophotometer was used. For the purpose of comparison of the sample obtained from the incorporation of the α- and that from the incorporation of the β-isomer, the extinction coefficients were calculated on the basis of mg. %* of phosphorus since their molecular weights are unknown.

Results

In the present study with oleic acid obtained from two different batches of beef tallow and purified by Method A, both glycerophosphoric acids were found to be active in a comparable strength (see Figs. 1 and 3) but marked differences in activity were observed in the methyl ester prepared from the corresponding sample of oleic acid. In one sample the β-isomer was found to be strongly active, while the α-isomer almost inactive in the early stages of autoxidation as shown in Fig. 2. The activity shown in the later stages is considered to be due to the presence of some 14% β-isomer since the curve obtained by another run with the α-isomer containing 21% β-isomer runs closely parallel to the one shown here, except with an increased activity in the later stages. In

* This expression is used for a matter of convenience instead of the conventional expression, for the products have neither been isolated in pure form nor characterized. However, the estimated values for their molecular extinctions at certain characteristic wave lengths are given in the discussion section.

another sample of the substrate, on the other hand, both acids were found to be active in comparable strength as shown in Fig. 3, although some difference was observed in the later stages. These results are not only in disagreement with our previous finding but also are peculiar in that the activity of the same substance differs in oleic acid and in the methyl ester prepared from the corresponding sample of oleic acid. (Fig. 1 and 2).

The results of the recovery of the glycerophosphoric acids in the aqueous phase during the autoxidation (see Fig. 1 and 2) show, however, that a marked decrease in recovery occurs in the first several hours regardless of whether or not the activity is observed, although a somewhat gradual decrease is shown with the α-isomer during the period in which its activity is depressed. Therefore, it is considered that some minor impurities which could not be removed by low-temperature crystallization from acetone may have interfered so as to give the varied results observed, rather than the difference in the configurations of the glycerophosphoric acids as we suggested in the previous paper.

In the methyl oleate prepared from beef tallow and purified by Method B, both acids were found to be active in an equal strength, (Fig. 4). Comparable results were obtained in oleic acid and its methyl ester prepared from olive oil and purified by the same method, (Figs. 5 and 6). In the latter case, the α-isomer was found to be consistently somewhat more active than the β-isomer. When samples of the substrate obtained from olive oil purified by Method A were used (not presented here), on the other hand, a marked difference in activity was observed, the α-isomer being more strongly active than the β-isomer. It should be pointed out, however, that the β-isomer in methyl oleate did not show activity up to a peroxide value of 10 mM/100 g. but a strong activity in the later stages, Fig. 6. This might have been the case with the β-isomer in the previous report where the experiment was carried out up to this level of peroxide value.

From these results, it is probably certain that α- and β-glycerophosphoric acid are active antioxidants of a comparable strength at a concentration of 0.1%. It is also evident from these results that the purification by low-temperature crystallization from acetone is unsuitable for the study of this nature. Accordingly, those results obtained by using substrates which have been purified by merely repeating distillation of saponified products of fats should be subjected to re-examination.

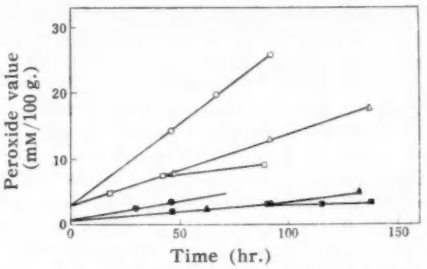

Fig. 4. Peroxide values against time.
○ Methyl oleate, M-2, alone. △ Methyl oleate, M-2, containing 0.1% α-glycerophosphoric acid (86% purity). □ Methyl oleate, M-2, containing 0.1% β-glycerophosphoric acid. ● Methyl oleate, M-3, alone. ▲ Methyl oleate, M-3, and 0.1% α-glycerophosphoric acid (86% purity). ■ Methyl oleate, M-3, containing (0,1%) β-glycerophosphoric acid.

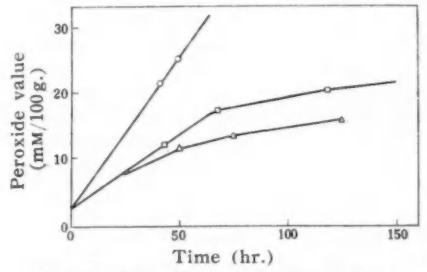

Fig. 5. Peroxide values against time.
○ Oleic acid, O-3, alone. △ The same sample of oleic acid containing 0.1% α-glycerophosphoric acid (79% purity). □ The same sample of oleic acid containing 0.1% β-glycerophosphoric acid.

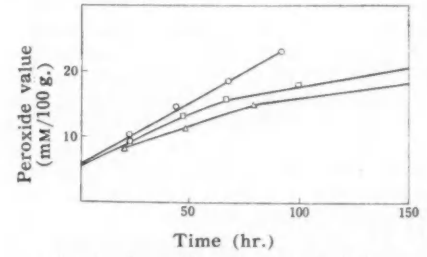

Fig. 6. Peroxide values against time.
○ Methyl oleate, M-4, alone. △ The same sample of methyl oleate containing 0.1% α-glycerophosphoric acid (86% purity). □ The same sample of methyl oleate containing 0.1% β-glycerophosphoric acid.

The absorption spectra observed in the region longer than 300 mμ in Fig. 7 are due to the presence of the α-isomer at a concentration of 7% since the *E* values calculated for the sample of glycerophosphoric acid employed (see Fig. 8) are much greater than those of the substrate before and after autoxidation (see Fig. 9). Therefore, the absorption spectrum observed after 87.5 hours' autoxidation indicates the presence of a substance other than the glycerophosphoric acid itself, probably a substance formed from it during the autoxidation.

With a low concentration of either α- or β-glycerophosphoric acid as actually used (0.1%) for testing their antioxygenic activities, it would be in possible to observe such an absorption in the ultraviolet region before autoxidation but it should be possible after autoxidation, only, however with the sample to which the α-isomer has been incorporated. This is shown in Fig. 9 A where the curve indicated by the solid line represents the absorption due to the presence of an intensely absorbing substance since the substrate isolated from it by the chromatographic means shows a lower intensity of absorption (dotted line). This sort of observation would not be possible with the

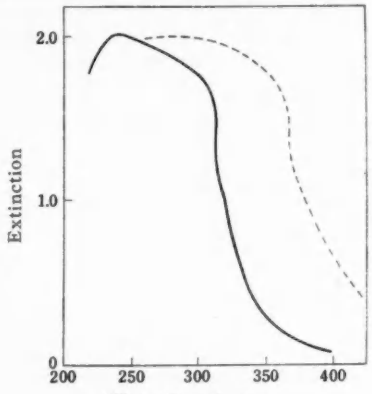

Fig. 7. Absorption curves of 1% ether solutions of methyl oleate containing 7% α-glycerophosphoric acid.
—— At zero time (in ether). ------ At the end of 87.5 hours of autoxidation (in ether).

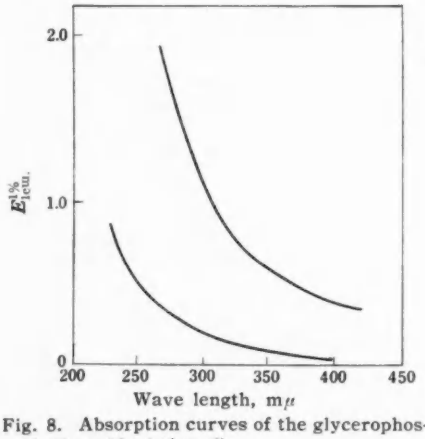

Fig. 8. Absorption curves of the glycerophosphoric acids (ethanol).
The upper curve, α-glycerophosphoric acid.
The lower curve, β-glycerophosphoric acid.

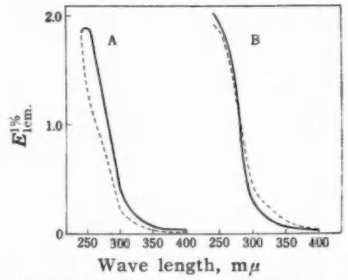

Fig. 9. Absorption curves of the ether solutions of: A, solid line, methyl oleate containing 0.1% α-glycerophosphoric acid (sample b, Table IV); dotted line, the ester isolated by the column chromatography. B, solid line, oleic acid containing 0.1% β-glycerophosphoric acid (sample c, Table IV); dotted line, oleic acid isolated by the column chromatography.

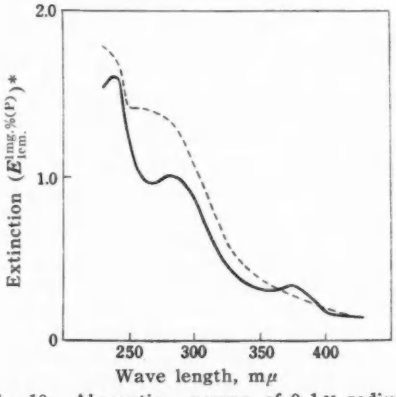

Fig. 10. Absorption curves of 0.1 N sodium hydroxide solutions of the phosphorus containing substances isolated by the column chromatography: dotted line, from the α-glycerophosphoric acid added sample (sample b, Table IV); solid line, from the β-glycerophosphoric acid added sample (sample c, Table IV).

β-isomer since the absorption of its ethanolic solution is much less intense than that of the α-isomer (see Fig. 8), and this found to be the case as shown in Fig. 9B where the absorption curve of the isolated substrate coincides with that of the substrate to which the β-isomer has been added.

Fig. 10 shows the absorption spectra of the phosphorus-containing substances found to be present in the alkaline extracts of the column chromatograms. They differ from those of the glycerophosphoric acids (see Fig. 8). The unknown substance which appears to be formed from β-glycerophosphoric acid shows $E_{1cm}^{1mg\%(P)}$ 1.6 at 240 mμ and 1.0 at 380 mμ and 0.96 at 270 mμ, an inflection. The substance believed to be formed from the α-isomer does not show a sharp maximum but an inflection at 250 mμ with $E_{1cm}^{1mg\%(P)}$ 1.42. This substance is probably a mixture of at least two compounds, one formed from the α- and the other from the β-isomer since the sample incorporated contained some 14% β-isomer and no isomerization is apparent as indicated in Table IV.

Discussion

Although varied reactivities of α- and β-glycerophosphoric acid were observed in different samples of the substrate, both must be active antioxidants since the consistent results could be obtained when highly purified oleic acid and methyl oleate were used. This may reasonably be supported by the isolation of the unknown substances with high intensity of absorption in the ultraviolet region from the substrates to which both α- and β-glycerophosphoric acid have been incorporated.

The antioxygenic activity of the glycerophosphoric acids may, however, be secondary in nature; that is, the unknown substances formed during autoxidation may be responsible for the activity observed, rather than the glycerophosphoric acids themselves. It is unlikely that the involvement of the glycerophosphoric acid molecule is analogous to that of hydroquinone where the molecule itself is ultimately oxidized to quinone after terminating free radical chain reactions by reacting with peroxy radicals[7]. Strong indications for this are that recovery of the glycerophosphoric acids drops sharply in the early stages of autoxidation and that the unknown substances with high intensity of absorption in the ultraviolet region can be isolated from samples which are still exhibiting antioxygenic activity, Table IV and Figs. 7 and 10.

Assuming the molecular weight of the unknown substances to be about 436, (which is the sum of the molecular weight of oleic acid and that of the glycerophosphoric acid minus a mole of water and is considered to be the lowest limit of those oxidized products retaining the original carbon chain length) their molecular extinctions are calculated to be about 42,000 at 270 mμ, at the inflection of the solid line (Fig. 10), and 70,000 at 240 mμ (the maximum). These values are probably higher than those calculated from absorption measured in non-polar solvents but they, nevertheless, indicate that the K-bands are involved. The absorption curve with λ_{max} at 240 and 380 and $\lambda_{infl.}$ at 270 resembles, in its general trend, those reported for oxidized products of ethyl oleate[8] and for the olefinic keto-acids[9]. Therefore, it appears that the glycerophosphoric acids have reacted with some highly conjugated form of compounds produced from the substrate molecule by a free-radical attack during autoxidation.

These results do not reveal, however, whether the phosphoryl group of the glycerophosphoric acid molecule is involved in such a reaction. Because compounds with the same absorption characteristics can possibly be formed, too, if a coordination takes place between a radical of a highly conjugated form (produced from the substrate molecule) and a radical of the glycerophosphoric acid involving the glycerol moiety, or between the former and inorganic phosphoric acid released from the glycerophosphoric acid, as a result of a free radical attack on the glycerol moiety, has been observed to take place in aqueous solutions by irradiation of ionizing radiations[10]. The latter case is least feasible, however, in the system under consideration. Some evidence for this can be provided by the results obtained here. If it had occurred, the absorption band indicated by the solid line in Fig. 9 A or the absorption spectrum observed after 87.5 hours of autoxidation (see Fig. 7) would not have been detected since the E value

7) J. L. Bolland and P. Ten Haave, *Trans. Faraday Soc.*, **43**, 2011 (1947).

8) R. T. Holman, W. O. Lundberg, W. M. Lauer and G. O. Burr, *J. Am. Chem. Soc.*, **67**, 1285 (1945).

9) G. King, *J. Chem. Soc.*, **1951**, 1980.

10) G. Scholes, W. Taylor and J. Weiss, ibid., **1957**, 235.

of orthophosphoric acid in ethanol at λ_{max} 250 mμ is 0.024(measured in our laboratory) and its extinction even at a concentration of 7% is less than 0.167, which is smaller than the E value of β-glycerophosphoric acid, 0.18 at 265 mμ. The β-isomer does not show absorption of the product in the presence of the substrate, (Fig. 9B). The question as to the former case will be treated in a later paper. A highly probable case is, however, participation of the phosphoryl group since phosphoric acid or its alkaline acid salts are known to add readily to ethylene oxide[11] or react with hydroperoxides obtained from lard[12].

Confirmation of the structures of the unknown substances containing phosphorus and exhibiting the high intensity of absorption in the ultraviolet region is of great importance in providing information as to requirements of molecular structures of phosphorus containing compounds of this nature for antioxygenic activity. It also appears to be important from the standpoint of elucidating free radical chain reaction mechanism which is yet obscure and of current interest to a number of workers[8,9,13-15]. The method employed in the present work for the isolation of the unknown substances may find its usefulness in the study of structures of products formed in early stages, if not primary products of a free-radical attack, of autoxidation of ethylenic compounds.

Summary

It has been demonstrated that the method of purification of the substrate by low temperature crystallization is not suitable for the study of antioxidant activity of the glycerophosphoric acids and that further purification by crystallization as the urea complex gives consistent results. In such a highly purified substrate, both acids have been found to be active in a comparable strength.

The study of ultraviolet absorption of the phosphorus-containing substances isolated by the column chromatography has shown that the glycerophosphoric acid molecule acquires a highly conjugated system during autoxidation. Discussions have been presented as to possibilities incurred in the formation of such highly conjugated compounds.

Faculty of the Science of Living
Osaka City University
Nishi-ku, Osaka

11) F. R. Atherton, H. T. Openshaw and A. R. Todd, ibid **1945**, 382.
12) F. Q. Quackenbush and O. S. Privett, *J. Am. Oil Chemists' Soc.*, **31**, 225 (1954).
13) R. W. Brauer and L. T. Steadman, *J. Am. Chem. Soc.*, **66**, 563 (1944).
14) L. Bateman and J. L. Bolland, *The British Rubber Producers' Association Publication*, No. 126 (1950); L. Bateman and A. L. Morris, ibid., No. 173 (1952); L. Bateman, G. Gee, A. L. Morris and W. F. Watson, ibid., No. 155 (1951).
15) D. Swern, H. B. Knight and J. E. Coleman, *J. Am. Oil Chemists' Soc.*, **28**, 498 (1951); **32**, 79, 221 (1955).

*Rapid Analysis of Gamma-Emitters Using Gamma-Ray Scintillation Spectrometer. II. Determination of ^{137}Cs in Fission Products**

By Fumio AOKI, Seishi YAJIMA** and Toshio KUROSAWA

(Received June 20, 1958)

The rapid and accurate determination of ^{137}Cs in fission products is very important for instance, in the determination of the "fine structure" of the fission yield curve, or in the treatment of the fuel elements and radioactive wastes.

Beta-ray assay, which has been generally used, involves many tedious procedures and requires skill[1], because the object must be isolated prior to the activity measurement. The chemical yield through the procedures is not always highly reliable.

A gamma-ray scintillation spectrometer has been favorably used owing to the speediness of its procedure and

* Read at 11th Annual Meeting of the Chemical Society of Japan.
** Present address. Japan Atomic Energy Research Institute, Tokai, Ibaragi-Prefecture.

1) F. Brown, *J. Inorg. Nuclear Chem.*, **1**, 248 (1955).

reliability. But when the sample contains many gamma-emitters, it is, in general, difficult or impossible to determine the individual activity accurately without separation, because of the possible superposition of the spectra of the gamma-rays.

Peirson[2] analysed the fission products from uranium 235 without chemical separations using a two-crystal gamma-ray scintillation spectrometer, which does not give rise to the Compton continua but shows only the photopeaks in the recorded spectrum. Even if such an excellent instrument is available, chemical separations will still be necessary in such cases as:

i) When the gamma-energy of a nuclide in question can not be resolved from superposing spectra of other nuclides.

ii) When the gamma-intensity of the nuclide is weak and overwhelmed by those of others.

Woodhead et al.[3] determined the activity of ^{137}Cs in fission products. They separated ^{137}Cs solely by anion exchange resin using carriers, and measured its gamma-intensity with a gamma-ray scintillation spectrometer. If it were not necessary to separate ^{137}Cs solely, the procedures would become more simple.

The authors have worked out a method for the rapid determination of ^{137}Cs in fission products combining the partial separation of nuclides with anion exchange resin followed by gamma-ray spectrometry.

Method. — *Extraction of Uranium.* — The bulk of the uranium is extracted from the solution of the irradiated fuel elements with a mixture of tributyl phosphate (T. B. P.) and diethyl ether. (1:1), together with most of neptunium formed. The residual neptunium is removed by the resin treatment shown below (Table I). In this process the loss of ^{137}Cs is in the order of 10^{-5}, which is negligible in its determination.

Anion Exchange.—In treating the fission product solution, free from uranium, by a mixed bed of carbonate- and oxalate-form anion exchange resin (see section III), alkali metals go completely through the column together with some of alkali earths, while almost all of the other ions are retained in the column[4].

The leakage of alkali earths is reduced by the addition of strontium ions. Tables

TABLE I
RETENTION OF MAIN ELEMENTS (%)

pH of the soln.	Retention of				
	I	Ru	Rare earths. Y	Transition metals	Np
6	93	96	100	100	100
8	96	96	100	100	100
10	98	98	100	100	100

TABLE II
LEAKAGE OF Ba AND Sr (%)

Addition of Sr^{2+} mg/20 ml	Leakage of	
	Ba	Sr
0	89	80
5	53	65
10	46	10
20	36	0
30	30	0
40	42	0
60	42	0

I and II show the retention and leakage of some elements.

Measurement.—The fission product solution after the resin treatment will contain ^{140}Ba-^{140}La and ^{137}Cs-^{137m}Ba, when it is short-aged, and ^{137}Cs-^{137m}Ba only, when it is long-aged. (^{133m}Cs and ^{135m}Cs are also formed in fission, but their lives are extremely short. ^{135}Cs, the daughter of ^{135m}Cs, emits no gamma-ray and its life is very long. They are all left out of consideration.)

The activity of ^{137}Cs is represented by the peak height of 0.661 MeV gamma of ^{137m}Ba in equilibrium with ^{137}Cs, the parent. Some of ^{137m}Ba is retained in the resin column, but the parent and daughter soon (about 30 min. after the resin treatment) reach a state of equilibrium. Because of the short half life of ^{137m}Ba (2.6 min.) compared with that of ^{137}Cs (30 y.), the difference between the activities of ^{137m}Ba in equilibrium before and after the resin treatment is negligible.

^{140}La, originally present in the sample, is also removed by the resin treatment, but it grows form ^{140}Ba in the effluent and reaches a state of equilibrium within a week.

When the effluent is measured by a scintillation spectrometer for long-aged samples, the 0.661 MeV peak height gives the activity of ^{137}Cs without correction, because no other nuclides are present. But when the sample is short-aged, the peak is superposed by the Compton pulses of ^{140}Ba-^{140}La gammas, which must be subtracted from the observed peak

2) D. H. Peirson, *Brit. J. Appl. Phys.*, **6**, 444 (1955).
3) J. L. Woodhead et al., *Analyst*, **81**, 570 (1956).
4) S. Yajima et al., not yet published.

height[5]. The correction factor depends on the crystal dimensions and geometry. In our case pure ^{140}Ba-^{140}La source (in equilibrium) gives Compton pulses of 59% of the 0.82 MeV peak height at the photopeak of ^{137m}Ba gamma.

Experimental

Chemical Procedures.—Two kinds of sample were prepared, one for the long-aged and the other for the short-aged, which are:

a) F. P. (about 0.4 μC) + uranyl nitrate (several mg.) + pure ^{137}Cs solution (x ml).

b) Sample a) (F. P. and pure ^{137}Cs activities suffered a little change) + ^{140}Ba-^{140}La (about 0.2μC)*.

The cooling time of the fission products, which had been supplied by United State Atomic Energy Commitee, was about 3 years. The quantity of the ^{137}Cs (x) was taken as 0, 0.1, 0.3, 0.5, 0.75, 1.0, 1.25, 1.5, 1.75 and 2.0. One ml. of the pure ^{137}Cs solution corresponded to about 0.01 μC and 0.05 μC in sample a and b, respectively. Other elements of fission products than ^{140}Ba-^{140}La are almost completely retained in the resin column; hence they were left out of consideration. After the samples were dissolved in 50 ml of 5 N nitric acid, uranium was extracted with a mixture of T. B. P. and diethyl ether (1 : 1).

The same quantities of two forms of anion exchange resin (Dowex 1—X7.5, 50—100 mesh, treated by 5% oxalic acid solution and by 10% ammonium carbonate solution) were mixed in a beaker. After carbon dioxide gas was thoroughly removed, a column of about 6 mm. in diameter and 100 mm. in length was set up out of the mixture.

Each fission product sample in nitric acid solution free from uranium was taken in a beaker. After evaporating off most of the nitric acid, the residue was dissolved in 20 ml. of 3 N hydrochloric acid solution and again evaporated to dryness. This process was taken so that the resin column could retain almost all ^{106}Ru, which had been proved empirically. Each of the short-aged samples was dissolved in 20 ml. of 0.5% ammonium chloride solution which contains 30 mg. of strontium ion. The pH value was adjusted to 9 with aqueous ammonia solution. The solution was allowed to run through the resin column followed by a passage of 30 ml. of 1% aqueous ammonia solution. Each effluent was concentrated to 2 ml. and transferred to a polyethylene tube in order to measure the gamma-intensity in the same condition.

Measurements.—The same scintillation spectrometer as that used in the previous study[6] was used. One week after the resin treatment, the samples in polyethylene tubes were placed in the well of the sodium iodide (activated with thallous ions) crystal and the activity was measured. Typical gamma-ray spectra of the samples are shown in Figs. 1 and 2.

The effluents of the long-aged samples contained no other radioactive nuclides than ^{137}Cs-^{137m}Ba,

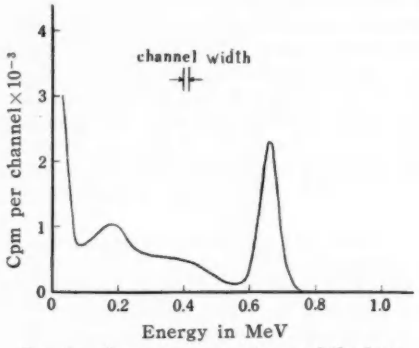

Fig. 1. Gamma-ray spectrum of the long-aged sample treated by the resin column.

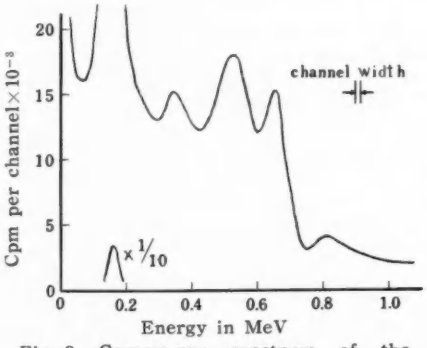

Fig. 2. Gamma-ray spectrum of the short-aged sample treated by the resin column.

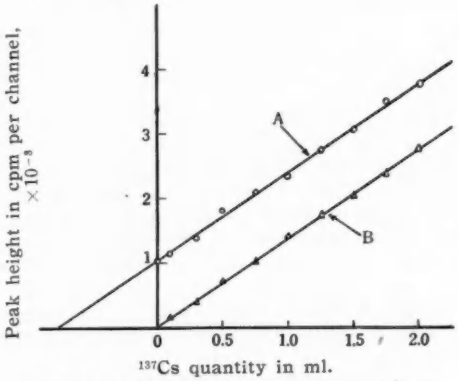

Fig. 3. 0.66 MeV peak heights vs. added ^{137}Cs quantities of the long-aged samples.

5) R. E. Connally M. Leboeuf, *Anal. Chem.*, **25**, 1075 (1953).

* In practice this case was first investigated, but because of the unexpected results, as shown in Fig. 4, the sample a) was next studied. The changes of the activities were due to the shortage of the F. P. and pure ^{137}Cs solution.

6) F. Aoki et al., This Bulletin, **30**, 583 (1957).

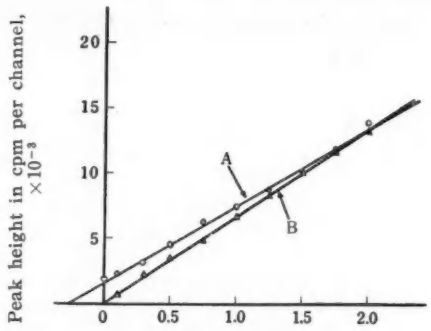

Fig. 4. 0.66 MeV peak heights vs. added ^{137}Cs quantities of the short-aged samples.

but those of the short-aged contained ^{137}Cs-^{137m}Ba and ^{140}Ba-^{140}La, which were identified by the gamma-energies.

The real peak heights of the 0.66 MeV gamma were plotted against the quantities of the added ^{137}Cs solutions (Figs. 3 and 4).

The straight lines, 'A' and 'B' show the 0.66 MeV peak height of the samples and that of pure ^{137}Cs solution added to the fission products, respectively; both have good linearities. In Fig. 3, both lines are parallel, but in Fig. 4 the slope of the straight line 'B' is a little greater than that of 'A'. This fact shows that the peak height, in spite of the correction for the Compton pulses of ^{140}Ba-^{140}La gammas, does not represent the ^{137}Cs quantity, but always gives too low a value. This phenomenon has not yet been sufficiently investigated, but one possible explanation is that some of the 0.66 MeV gamma pulses are summed up with photoelectric or Compton pulses of ^{140}Ba-^{140}La gammas to form higer pulses. However, the length between the origin of the coordinate and the intersection of the straight line 'A' and the abscissa gives the quantity of ^{137}Cs originally present in the fission products, which does not depend on the presence of ^{140}Ba-^{140}La. When the straight line 'A' is determined by the method of least squares, the most probable value of the quantity in question is obtained.

The results are shown in Table III, where N is the 0.66 MeV peak height in counts per minute per channel and x the volume of ^{137}Cs solution in milli litres. The analysed ^{137}Cs quantity corresponds to the absolute value of x at $N=O$, and is given in the same unit as that of the added ^{137}Cs solution whose activity is temporarily shown in milli litres.

TABLE III
ANALYSIS OF ^{137}Cs IN THE FISSION PRODUCTS

Sample	Straight line	^{137}Cs quantity (ml)
Long-aged	$N=1037.44-1370.83x$	0.757
Short-aged	$N=1553.51-5963.95x$	0.260

In this experiment the quantities of ^{137}Cs originally present in the fission products were unkown, so the errors of the measured quantities can not be shown. The maximum deviations of the peak heights from the straight lines determined by the method of least squere are 6% and 10% in the case of the long-aged and the short-aged, respectively.

Summary

A method for the rapid determination of ^{137}Cs in fission products has been studied. Simple and reliable analysis is possible by combining oxalate- and carbonate-form anion exchange resin and a gamma-ray scintillation spectrometer as follows.

Take several samples of equal quantity from a given fission products solution. Add various known quantities of pure ^{137}Cs to them respectively. Extract the bulk of uranium with T. B. P. in diethyl ether. Treat them through a mixed bed of carbonate- and oxalate-form anion exchange resin. Measure each aliquot using a gamma-ray scintillation spectrometer. Plot the real peak height of the 0.66 MeV gamma vs. the added ^{137}Cs quantity, and determine the straight line by the method of least square. Find the intersection of the straight line and the abscissa.

The quantity in question is given by the length of the abscissa between the intersection and the origin.

The authors wish to thank Dr. S. Uchida and Mr. K. Hashimoto for encouraging the prosecution of this work.

Government Chemical Industrial Research Institute
Shibuya-ku, Tokyo

Normal Vibrations and Calculated Thermodynamic Properties of Methyltrichlorosilane

By Kazuhiro SHIMIZU and Hiromu MURATA

(Received June 27, 1958)

Methylchlorosilane is the simplest of those methylchlorosilanes which are both industrially important and theoretically interesting. The infrared and the Raman spectrum of this compound have been reported by several investigators[1-5]. But the normal vibrational frequencies have been calculated and assigned only by a method in which a methyl group is regarded as one particle. Therefore, the vibrational frequencies accompanied by the motion of hydrogen atoms have been excluded from the calculations, and the coupling between the skeletal vibrations and the characteristic modes of the methyl group has been ignored. To make all the normal modes clear, it is necessary that the vibrations of hydrogen atoms are taken into account. In this paper, the fundamental frequencies are calculated and assigned, their normal modes are determined, and the thermodynamic properties are calculated.

Normal Coordinate Treatment. — In methyltrichlorosilane, there are two symmetrical groups, CH_3 and $SiCl_3$. Because of the interaction between the CH_3 and the $SiCl_3$ group, the internal rotation is restricted, and it is more correct in the present consideration to treat the relative movement of CH_3 and $SiCl_3$ as torsional oscillation rather than as free internal rotation. This molecule belongs to the point group C_{3v} whether the groups have staggered or eclipsed forms. According to the group theory, it is clearly shown that this molecule has twelve fundamental frequencies of which five belong to species a_1, one to species a_2, and six to species e. All vibrations except the a_2 torsional mode are both infrared and Raman active. If this molecule has the torsional angle about the Si—C axis, it belongs to the point group C_3. The species a_1 and a_2 of the point group C_{3v} correspond to the species a of the point group C_3. Previous work by Collins and Nielsen[6] shows a normal coordinate treatment of the staggered configuration of methyltrifluorosilane having a structure similar to methyltrichlorosilane. But, in this investigation, at first, we undertake to make an attempt to carry out a normal coordinate treatment with an arbitrary torsional angle, and, next, to calculate the normal vibrational frequencies of the point group C_{3v} molecule for which the torsional angle θ is 0° in the eclipsed from, and 180° in the staggered form. We do not calculate the a_2 mode which is both infrared and Raman inactive. A normal coordinate treatment was carried out using the Wilson *FG* matrix method[7]. The *F* matrix elements were formed from the force constants in a Urey-Bradley force field[8].

The various bond distances, the interbond angles, and the distances between nonbonded atoms used to determine the internal coordinates are shown in Fig. 1. From the internal coordinates the following orthonormal symmetry coordinates were found; for the a vibrations,

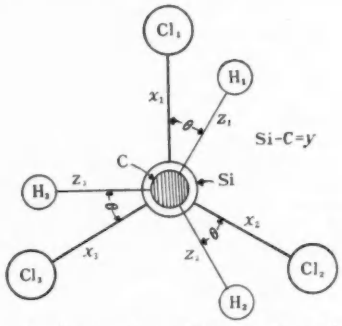

Fig. 1. Internal coordinates of methyltrichlorosilane.

1) J. Goubeau, H. Siebert and M. Winterwerb, *Z. anorg. Chem.*, **259**, 239 (1949).
2) T. Shimanouchi, I. Tsuchiya and Y. Mikawa, *J. Chem. Phys.*, **18**, 1306 (1950).
3) L. Burnelle and J. Duchesene, ibid., **20**, 1324 (1952).
4) H. Murata, *J. Chem. Soc. Japan, Pure Chem. Sec.*, (*Nippon Kagaku Zasshi*), **73**, 465 (1952).
5) A. L. Smith, *J. Chem. Phys.*, **23**, 1997 (1953).
6) R. L. Collins and J. R. Nielsen, ibid., **23**, 351 (1955).
7) E. B. Wilson, Jr., ibid., **7**, 1047 (1939); **9**, 76 (1941).
8) T. Shimanouchi, ibid., **17**, 245, 734, 848 (1949).

$$R_1=\Delta(z_1+z_2+z_3)/\sqrt{3}$$
$$R_2=\Delta(z_1y+z_2y+z_3y-z_1z_2-z_1z_3-z_2z_3)/\sqrt{6}$$
$$R_3=\Delta y$$
$$R_4=\Delta(x_1+x_2+x_3)/\sqrt{3}$$
$$R_5=\Delta(x_1y+x_2y+x_3y-x_1x_2-x_1x_3-x_2x_3)/\sqrt{6}$$

and for the e vibrations

$$R_{6a}=\Delta(2z_1-z_2-z_3)/\sqrt{6}$$
$$R_{7a}=\Delta(2z_2z_3-z_1z_3-z_1z_2)/\sqrt{6}$$
$$R_{8a}=\Delta(2z_1y-z_2y-z_3y)/\sqrt{6}$$
$$R_{9a}=\Delta(2x_1-x_2-x_3)/\sqrt{6}$$
$$R_{10a}=\Delta(2x_1y-x_2y-x_3y)/\sqrt{6}$$
$$R_{11a}=\Delta(2x_2x_3-x_1x_3-x_1x_2)/\sqrt{6}$$

The numbering of these coordinates corresponds to the numbering of the fundamentals in Table II.

From the coefficients of the symmetry coordinates and the potential constants of a Urey-Bradley force field, one gets the following F matix elements:
for the a vibrations,

$$F_{11}=K_z+4s^2_{zz}F_{zz}+s^2_{zy}F_{yz}+t^2_{zy}F'_{yz}$$
$$F_{12}=[(t_{yz}s_{zy}F_{yz}+t_{zy}s_{yz}F'_{yz})y-2t_{zz}s_{zz}(F_{zz}+F'_{zz})z]/\sqrt{2}$$
$$F_{13}=\sqrt{3}\,(s_{yz}s_{zy}F_{yz}-t_{yz}t_{zy}F'_{yz})$$
$$F_{22}=(H_{yz}+t_{yz}t_{zy}F_{yz}-s_{yz}s_{zy}F'_{yz})yz/2+(H_{zz}+t^2_{zz}F_{zz}-s^2_{zz}F'_{zz})z^2/2+3\sqrt{2}\,\kappa'/4$$
$$F_{23}=\sqrt{6}\,(t_{zy}s_{yz}F_{yz}+t_{yz}s_{zy}F'_{yz})z/2$$
$$F_{33}=K_y+3(s^2_{yx}F_{xy}+t^2_{yx}F'_{xy})+3(s^2_{yz}F_{yz}+t^2_{yz}F'_{yz})$$
$$F_{34}=\sqrt{3}\,(s_{xy}s_{yx}F_{xy}-t_{xy}t_{yx}F'_{xy})$$
$$F_{35}=\sqrt{6}\,(t_{xy}s_{yx}F_{xy}+t_{yx}s_{xy}F'_{xy})x/2$$
$$F_{44}=K_x+4s^2_{xx}F_{xx}+s^2_{xy}F_{xy}+t^2_{xy}F'_{xy}$$
$$F_{45}=[(t_{yx}s_{xy}F_{xy}+t_{xy}s_{yx}F'_{xy})y-2t_{xx}s_{xx}(F_{xx}+F'_{xx})x]/\sqrt{2}$$
$$F_{55}=(H_{xx}+t^2_{xx}F_{xx}-s_{xx}F'_{xx})x^2/2+(H_{xy}+t_{xy}t_{yx}F_{xy}-s_{xy}s_{yx}F'_{xy})xy/2+3\sqrt{2}\,\kappa/4$$
$$F_{14}=F_{15}=F_{24}=F_{25}=0$$

for the e vibrations

$$F_{66}=K_z+s^2_{zz}F_{zz}+3t^2_{zz}F'_{zz}+s^2_{zy}F_{yz}+t^2_{zy}F'_{yz}$$
$$F_{67}=-t_{zz}s_{zz}(F_{zz}+F'_{zz})z$$
$$F_{68}=(t_{yz}s_{zy}F_{yz}+t_{zy}s_{yz}F'_{yz})y$$
$$F_{77}=(H_{zz}+t^2_{zz}F_{zz}-s^2_{zz}F'_{zz})z^2+\sqrt{2}\,\kappa'/4$$
$$F_{78}=-\kappa'/\sqrt{2}$$
$$F_{88}=(H_{yz}+t_{yz}t_{zy}F_{yz}-s_{yz}s_{zy}F'_{yz})yz+\sqrt{2}\,\kappa'/4$$
$$F_{99}=K_x+s^2_{xx}F_{xx}+3t^2_{xx}F'_{xx}+s^2_{xy}F_{xy}+t^2_{xy}F'_{xy}$$
$$F_{910}=(t_{yx}s_{xy}F_{xy}+t_{xy}s_{yx}F'_{xy})y$$
$$F_{911}=-t_{xx}s_{xx}(F_{xx}+F'_{xx})x$$
$$F_{1010}=(H_{xy}+t_{yx}t_{xy}F_{xy}-s_{xy}s_{yx}F'_{xy})xy+\sqrt{2}\,\kappa/4$$
$$F_{1011}=-\kappa/\sqrt{2}$$
$$F_{1111}=(H_{xx}+t^2_{xx}F_{xx}-s^2_{xx}F'_{xx})x^2+\sqrt{2}\,\kappa/4$$

and

$$F_{69}=F_{610}=F_{611}=F_{79}=F_{710}=F_{711}=F_{89}=F_{810}=F_{811}=0$$

where the following abbreviations are adopted:

$s_{zz}=4z/3q_{zz}$	$t_{zz}=2\sqrt{2}\,z/3q_{zz}$
$s_{zy}=(3z+y)/3q_{yz}$	$t_{zy}=2\sqrt{2}\,y/3q_{yz}$
$s_{yz}=(3y+z)/3q_{yz}$	$t_{yz}=2\sqrt{2}\,z/3q_{yz}$
$s_{yx}=(3y+x)/3q_{xy}$	$t_{yx}=2\sqrt{2}\,x/3q_{xy}$
$s_{xy}=(3x+y)/3q_{xy}$	$t_{xy}=2\sqrt{2}\,y/3q_{xy}$
$s_{xx}=4x/3q_{xx}$	$t_{xx}=2\sqrt{2}\,x/3q_{xx}$

and the symbols used for the equilibrium values of the interatomic distances are x=Si—Cl, y=Si—C, z=C—H, q_{xx}=Cl···Cl, q_{xy}=C···Cl, q_{yz}=Si···H and q_{zz}=H···H.

The G matrix elements are obtained by use of the table of Decius[9]. In terms of the abbreviations ρ_x, ρ_y and ρ_z for the reciprocals of the Si—Cl, Si—C and C—H bond lengths, respectively, and μ_x, μ_y, μ_c and μ_h for the reciprocals of the atomic masses of the Cl, Si, C and H, the following G matrix elements are found, assuming all angles to be tetrahedral:
for the a vibrations,

$$G_{11}=\mu_h+\mu_c/3$$
$$G_{12}=4\rho_z\mu_c/3$$
$$G_{13}=-\mu_c/\sqrt{3}$$
$$G_{22}=2(\mu_h+8\mu_c/3)\rho^2_z$$
$$G_{23}=-4\rho_z\mu_c/\sqrt{3}$$
$$G_{33}=\mu_y+\mu_c$$
$$G_{34}=-\mu_y/\sqrt{3}$$
$$G_{35}=-4\rho_x\mu_y/\sqrt{3}$$
$$G_{44}=\mu_x+\mu_y/3$$
$$G_{45}=4\rho_x\mu_y/3$$
$$G_{55}=2(\mu_x+8\mu_y/3)\rho^2_x$$
$$G_{14}=G_{15}=G_{24}=G_{25}=0,$$

for the e vibrations,

$$G_{66}=\mu_h+4\mu_c/3$$

9) J. C. Decius, ibid., **16**, 1025 (1948).

$$G_{67}=4\sqrt{2}\,\rho_z\mu_c/3$$
$$G_{68}=-\sqrt{2}\,(3\rho_y+\rho_z)\,\mu_c/3$$
$$G_{610}=\sqrt{2}\,\rho_y\mu_c\cos\theta$$
$$G_{77}=(8\mu_c/3+5\mu_h/2)\,\rho^2{}_z$$
$$G_{78}=-2(3\rho_y+\rho_z)\,\rho_z\mu_c/3+\rho^2{}_z\mu_h/2$$
$$G_{710}=2\rho_y\rho_z\mu_c\cos\theta$$
$$G_{88}=3\rho^2{}_y\mu_y/2+(3\rho_y+\rho_z)^2\mu_c/6+\rho^2{}_z\mu_h$$
$$G_{89}=\sqrt{2}\,\rho_y\mu_y\cos\theta$$
$$G_{810}=-[(3\rho_y+\rho_z)\mu_y+(3\rho_y+\rho_z)\mu_c]\,\rho_y\cos\theta/2$$
$$G_{811}=2\rho_x\rho_y\mu_y\cos\theta$$
$$G_{99}=\mu_x+4\mu_y/3$$
$$G_{910}=-\sqrt{2}\,(3\rho_y+\rho_z)\mu_y/3$$
$$G_{911}=4\sqrt{2}\,\rho_x\mu_y/3$$
$$G_{1010}=\rho^2{}_x\mu_x+(3\rho_y+\rho_x)^3\mu_y/6+3\rho^3{}_y\mu_c/2$$
$$G_{1011}=\rho^2{}_x\mu_x/2-2(3\rho_y+\rho_x)\,\rho_x\mu_y/3$$
$$G_{1111}=(5\mu_x/2+8\mu_y/3)\,\rho^2{}_x$$
$$G_{69}=G_{611}=G_{79}=G_{711}=0$$

Since the repulsive force constants between non-bonded atoms are ignored, the F matrix elements of an eclipsed configuration are equal to those of a staggered one. Also, as shown in the G matrix elements, the different point between an eclipsed and a staggered configuration is only the change of the signs of G_{610}, G_{710}, G_{89}, G_{810} and G_{811} elements. However, the calculated values of GF for both the configurations are equivalent.

The C—H stretching vibrations were split off by the method of Wilson. The molecular constants and the potential constants used are listed in Table I. As an aid in determining some of the potential constants, K_x, K_y, K_z, H_{xx}, H_{xy}, H_{zz}, F_{xx}, F_{xy}, F_{zz} and κ, the results from previous investigations of methane[8] and the skeletal vibrations of this molecule[2] were used. But for K_y, a slightly lower value was adopted. We gave -0.05 md/A to the value of κ', taking into consideration the corresponding constants found for methane, monochloromethane, monofluoromethane and methyl alchohol. The values of H_{yz} and F_{yz} were selected so as to give the good agreement with the observed fundamentals. The values of F' are assumed to be $-0.1\,F$.

TABLE I
MOLECULAR AND POTENTIAL CONSTANTS OF METHYLTRICHLOROSILANE

Bond distance and angle	Potential constants (md/A) Type	
x=Si—Cl	K_x(Si—Cl)	2.59
=2.021 A	K_y(Si—C)	2.72
y=Si—C	K_z(C—H)	4.63
=1.876 A	H_{xx}(Cl—Si—Cl)	0.059
z=C—H	H_{xy}(Cl—Si—C)	0.035
=1.093 A	H_{yz}(Si—C—H)	0.20
all angles	H_{zz}(H—C—H)	0.40
=tetrahedral	F_{xx}(Cl···Cl)	0.29
	F_{xy}(Cl···C)	0.162
	F_{yz}(Si···H)	0.13
	F_{zz}(H···H)	0.10
	κ($CSiCl_3$)	0.17 A^2
	κ'($SiCH_3$)	-0.05 A^2

Normal Frequencies.—A normal coordinate treatment of the skeletal vibrations which assumed the methyl group to be one particle was carried out by Goubeau et al.[1] and Shimanouchi et al.[2]. The calculated frequencies of all the normal vibrations are in good agreement with the observed, if the assignment of these frequencies is made adequately as shown in Table II. In it, the results of previous investigations are listed together for comparison.

The L matrices, whose components give the modes of vibrations and the potential energy distribution for each normal vibration were calculated. They are shown in Tables III and IV. Since the ν_1 and ν_6 are considered to have almost pure C—H streching frequencies, their L mairices and potential energy distributions are omitted.

Judging from the values of the contribution of each symmetry coordinate to the normal coordinates Q_{10} and Q_{11} in Table III and the distribution of potential energy in the symmetry coordinates for the normal frequencies ν_{10} and ν_{11} in Table IV, it is reasonable to designate the frequencies 229 cm^{-1} and 164 cm^{-1} respectively as "$SiCl_3$ rocking" and "$SiCl_3$ non-symmetric deformation". Thus, the classification given in Table II is reasonable.

As shown in Tables III and IV, the skeletal vibrations and the vibrations accompanied by the motion of hydrogen atoms are separated to a considerable extent. Therefore, the calculated values of the skeletal vibrations are expected to be in good agreement with their corresponding observed values.

Internal Rotation.—The torsional vibration belongs to the species a_2 and is both infrared and Raman inactive. The frequency can be calculated if the height of the potential barrier hindering the internal rotation is known. However, the

TABLE II

RAMAN AND INFRARED DATA, PROBABLE VALUES OF THE OBSERVED FUNDAMENTALS, CALCULATED WAVE NUMBERS, AND ASSIGNMENTS FOR METHYLTRICHLOROSILANE

Type	Mode of vibration	G.S.W.[a]	S.T.M.[b]	B.D.[c]	M.[d]	S.[e]	calc.	obs.
a_1	ν_1(CH_3 sym. str.)	—	—	2915	—	2923	2928	2923
	ν_2(CH_3 sym. def.)	—	—	1271	—	1271	1274	1271
	ν_3(Si—C str.)	758	761	764	760	764	760	764
	ν_4(Si—Cl sym. str.)	450	450	457	450	458	449	458
	ν_5($SiCl_3$ sym. def.)	228	229	—	230	229	228	229
e	ν_6(CH_3 nonsym. str.)	—	—	2977	—	2990	2980	2990
	ν_7(CH_3 nonsym. def.)	—	—	1416	—	1417	1431	1417
	ν_8(CH_3 rocking)	—	—	807	—	804	843	804
	ν_9(Si—Cl nonsym. str.)	569	576	578	575	577	597	577
	ν_{10}($SiCl_3$ rocking)	351	229	—	230	164	227	229
	ν_{11}($SiCl_3$ nonsym. def.)	162	164	—	165	229	165	164

a Goubeau, Siebert and Winterwerb, reference 1;
b Shimanouchi, Tsuchiya and Mikawa, reference 2;
c Burnelle and Duchesene, reference 3;
d Murata, reference 4;
e Smith, reference 5.

TABLE III

L MATRICES OF THE NORMAL VIBRATIONS OF METHYLTRICHLOROSILANE

a_1 vibrations,

	Q_2	Q_3	Q_4	Q_5
R_2(CH_3 sym. def.)	1.41	0.17	0.03	0.01
R_3(Si—C str.)	−0.16	0.30	0.04	0.01
R_4(Si—Cl sym. str.)	0.01	−0.09	0.18	−0.01
R_5($SiCl_3$ sym. def.)	0.01	−0.14	0.07	0.19

e vibrations,

	Q_7	Q_8	Q_9	Q_{10}	Q_{11}
R_7(CH_3 nonsym. def.)	1.47	−0.27	−0.03	0.01	0.00
R_8(CH_3 rocking)	0.36	0.88	0.12	−0.02	−0.01
R_9(Si—Cl nonsym. str.)	−0.01	−0.06	0.27	0.02	0.00
R_{10}($SiCl_3$ rocking)	−0.03	0.11	−0.12	0.16	0.10
R_{11}($SiCl_3$ nonsym. def.)	0.00	−0.04	0.12	−0.09	0.13

TABLE IV

POTENTIAL ENERGY DISTRIBUTION $F_{ii}L_{ia}^2/\lambda_a$ FOR THE NORMAL VIBRATIONS OF METHYLTRICHLOROSILANE

a_1 vibrations,

	ν_2	ν_3	ν_4	ν_5
R_2(CH_3 sym. def.)	0.96	0.03	0.00	0.00
R_3(Si—C str.)	0.08	0.89	0.04	0.01
R_4(Si—Cl sym. str.)	0.00	0.07	0.94	0.01
R_5($SiCl_3$ sym. def.)	0.00	0.04	0.03	0.96

e vibrations,

	ν_7	ν_8	ν_9	ν_{10}	ν_{11}
R_7(CH_3 nonsym. def.)	0.92	0.08	0.00	0.01	0.00
R_8(CH_3 rocking)	0.06	0.90	0.03	0.01	0.00
R_9(Si—Cl nonsym. str.)	0.00	0.02	0.98	0.04	0.00
R_{10}($SiCl_3$ rocking)	0.00	0.01	0.04	0.55	0.40
R_{11}($SiCl_3$ nonsym. def.)	0.00	0.00	0.05	0.23	0.79

question as to the potential hill has not been definitely settled. Here, the potential barrier of monomethylsilane, methyltrichlorosilane and methyltrifluorosilane are compared with the values of ethane, 1,1,1-trichloroethane and 1,1,1-trifluoroethane, respectively. The heights of ethane[10], 1,1,1-trichloroethane[11] and 1,1,1-trifluoroethane[12] are respectively 2.875±0.125 kcal/mole, 2.97 kcal/mole and 3.25±0.40 kcal/mole. That is to say, the value of 1,1,1-trichloroethane is found between the value of ethane and of 1,1,1-trifluoroethane. On the other hand, the value of monomethylsilane[13] and of methyltrifluorosilane[14] are respectively 1.314±0.229 kcal/mole and 1.20 ±0.16 kcal/mole. Thus it seems that the height of the potential barrier of methyltrichlorosilane is 1.30±0.25 kcal/mole.

TABLE V

HEAT CAPACITY, ENTROPY, FREE ENERGY, AND HEAT CONTENT OF METHYLTRICHLOROSILANE FOR THE IDEAL GASEOUS STATE AT 1 ATOMS PRESSURE (cal. deg.$^{-1}$ mol.$^{-1}$)

T°K		$\frac{(H^0-E^0_0)}{T}$	$-\frac{(F^0-E^0_0)}{T}$	S^0	C^0_p
	torsional:	0.58	0.26	0.84	1.39
100	other:	9.71	51.47	61.18	13.28
	total:	10.29	51.73	62.02	14.67
		1.32	1.23	2.55	1.89
273.15		15.03	63.61	78.64	22.27
		16.35	64.84	81.19	24.16
		1.36	1.35	2.71	1.90
298.15		15.66	64.96	80.62	22.98
		17.02	66.31	83.33	24.88
		1.37	1.35	2.72	1.90
300		15.70	65.05	80.75	23.15
		17.07	66.40	83.47	25.05
		1.51	1.77	3.28	1.94
400		17.94	69.89	87.83	26.11
		19.45	71.66	91.11	28.05
		1.60	2.12	3.72	1.96
500		19.82	74.10	93.92	28.41
		21.42	76.22	97.64	30.37
		1.66	2.42	4.08	1.97
600		21.40	77.85	99.25	30.19
		23.06	80.27	103.33	32.16
		1.70	2.67	4.37	1.97
700		22.76	81.32	104.08	31.66
		24.46	83.99	108.45	33.63
		1.74	2.90	4.64	1.97
800		23.95	84.37	108.32	32.85
		25.69	87.27	112.96	34.82
		1.76	3.11	4.87	1.98
900		25.00	87.25	112.25	33.88
		26.76	90.36	117.12	35.86
		1.78	3.29	5.07	1.98
1000		25.93	89.93	115.86	34.76
		27.71	93.22	120.93	36.74

In the present investigation, the usual $V=V_0\ (1-\cos 3\theta)/2$ is adopted as the form of the potential barrier. In this formula, V_0 is the height of the potential barrier and θ is the torsional angle. The torsional frequency can now be obtained from V_0. The calculated value $147\pm15\ \mathrm{cm}^{-1}$ is believed to be not far from the real torsional frequency.

Thermodynamic Properties.—The probable values of the wave numbers of the normal frequencies given in Table II were used to calculate values of the heat content, free energy, entropy and heat capacity for the ideal gaseous state at 1 atoms pressure (rigid rotator, harmonic oscillator approximation). The bond distances and the interbond angles given in Table I were used to calculate the product of the principal moments of inertia, using the Hirschfelder formula[15]. The value obtained was $I_aI_bI_b=1.48102\times10^{-112}\ \mathrm{gm^3\,cm^6}$. The molecular weight used was 149.496 and the symmetry number was 3. In Table V, the contributions of the torsional frequency and the others (translational, rotational and vibrational except torsinal) are listed separately to facilitate revision of the table, if and when a better way is found to calculate the contribution for the former.

The authors wish to thank Professor Y. Morino and Dr. T. Shimanouchi of the University of Tokyo and Dr. H. Shingu of Kyoto University for making many valuable discussions.

Osaka Municipal Technical Research Institute, Kita-ku, Osaka

10) K. S. Pitzer, *Disc. Faraday Soc.*, **10**, 66 (1951).
11) K. S. Pitzer and J. L. Hollenberg, *J. Am. Chem. Soc.*, **75**, 2219 (1953).
12) H. W Thompson and R. B. Temple, *J. Chem. Soc.* **1948**, 1428.
13) D. R. Lide and D. K. Coles, *Phys. Rev.*, **80**, 911 (1950).
14) J. Sheridand and W. Gordy, *J. Chem. Phys.*, **19**, 965 (1951).
15) J. O. Hirschfelder, ibid., **8**, 431 (1940).

*Phase Transition of Lithium Ferrospinel-Lithium Aluminospinel Solid Solution**

By Eizo KATO**

(Received July 8, 1958)

The phase transition of lithium ferrospinel was studied by means of thermal, electric[1] and X-ray measurements[2]. Lithium aluminospinel is a compound in which ferric ion in LFS changes into aluminum ion. Kordes[3], Verwey[4], Braun[5] and Yamaguchi[6] found that the crystal structure of LAS is the same as that of LFS, but its physico-chemical properties are not evident. No information pertaining to a phase transition of LFS–LAS solid solution has ever been presented in the literature. In the present paper, some physico-chemical changes attributed to exchange ferric ion for aluminum ion in LFS–LAS solid solution are systematically investigated by means of X-ray diffraction and differential thermal analysis, besides, formation of LFS–LAS solid solution is discussed.

Experimental

Specimens***.—Hydroxides coprecipitated from mixed aqueous solutions of ferric and aluminum nitrate were mixed with lithium oxalate in acetone, then dried, pressed and calcined in an electric furnace at 1200°C for three days. Specimens in a low temperature form (an ordered phase) were obtained by annealing in the same furnace from ca. 1200°C to the room temperature for a day, while specimens in a high temperature form (a disordered phase) were quenched by immersion into water from ca. 1300°C in 1~2 seconds.

Apparatus and Procedures. — Thermal analyses were carried out up to 1000°C at a heating rate of 10°/min. by the apparatus reported already[7]. The measurements above 1000°C were performed at a rate of 3°/min. by an apparatus with a sample holder of sillimanite. X-ray powder photographs were taken with Co $K\alpha$ radiation by a back-reflection technique, and lattice constants

TABLE I

CHEMICAL COMPOSITIONS, LATTICE CONSTANTS AND ENDOTHERMIC TEMPERATURES OF SOLID SOLUTIONS

Specimen	Composition, Fe/Al	Lattice constant (Å)			Endothermic temperature (°C)
		Ordered phase	Disordered phase	Δ (%)	
A	0/5	7.909	7.911	0.03	ca. 1200
B	1/4	7.999	8.010	0.14	ca. 1130
C	1.5/3.5	8.005 8.206	8.053_6	—	ca. 1090 ca. 880
P	2/3	8.004 8.206	8.095_8	—	875~880
R	2.5/2.5	8.004 8.206	8.143	—	880
Q	3/2	8.177_3	8.183_8	0.08	916
D	3.5/1.5	8.00 8.210	8.212	0.03	887
E	4/1	8.257	8.263	0.08	826
F*	5/0	8.329_6	8.332_6	0.04	765

* given from the previous report[1]

* Lithium ferrospinel and lithium aluminospinel are abbreviated to LFS and LAS, respectively, in the following.

** Present adress, Idemitsu Kōsan Co. Ltd., Chuō-ku, Tokyo.

1) E. Kato, This Bulletin, **31**, 113 (1958).
2) E. Kato, ibid., in press.
3) E. Kordes, *Z. Krist.*, **91**, 193 (1935).
4) E. J. W. Verwey and E. L. Heilmann, *J. Chem. Phys.*, **15**, 174 (1947).
5) P. B. Braun, *Nature*, **170**, 1123 (1952).
6) G. Yamaguchi, This Bulletin, **26**, 206 (1953).

*** By Kordes[3] lithium fluoride was used as a mineralizer in order to prepare homogeneous specimens. It was proved by X-rays that fluoride was scarcely reacted with ferric oxide, so that this synthesis was not employed.

7) E. Kato, This Bulletin, **31**, 108 (1958).

were accurately determined by an extrapolation method against $1/2(\cos^2\theta/\sin\theta+\cos^2\theta/\theta)$

Results and Discussion

Order-Disorder Transition of Solid Solution.—From spacings and reflection intensities measured by X-ray diffraction, the crystal structures of the low temperature and the high temperature form of LFS–LAS solid solution were found to be an ordered lattice, O^6—$P4_33$, and a disordered lattice, O_h^7—$Fd3m$, respectively. Both lattices are identified by arrangements of cations at octahedral interstices, and have the same structures with those in LFS or LAS alone. The values of the lattice constant as a function of the chemical composition for the ordered and the disordered phase of the solid solution are shown in Table I and Fig. 1. The relation of the lattice constants vs. the composition for disordered phases was calculated by a method of least squares.

$$y=7.912_5+0.4907x-0.0699x^2$$

where x is the mole fraction of LFS in the solid solution, and y thelattice constant of disordered phase.

On the other hand, experimental results for the ordered phase were too few to find an equation similar to the above one. Lattice expansions (Δ) at the transition from the ordered phase to the disordered one is small as is listed in Table I, and these values are in 0.03~0.14% regardless of the composition. If the magnitude of the expansion is estimated at 0.05%, the observed values of lattice constant of the ordered phase will agree with those calculated by the above equation.

Physico-chemical changes of the solid solution in occurrence of the transition were observed by differential thermal analysis. The endothermic reaction due to the transition was already seen in the measurement of LFS, and thermal changes similar to LFS or LAS were found in all specimens of ordered phase of the solid solution*. Though the transition temperature of LFS or LAS** is known, no paper was reported for those of the solid solutions. The exact value of the transition temperature had better be measured by a dilatometry with a considerable slower heating rate. The dilatometry was, however, not carried out, because of difficulty to prepare aluminum-rich specimens by sintering. In place of the relation of the transition temperature vs. the chemical composition, that of the endothermic temperature vs. the composition in a series of specimens was measured and is shown

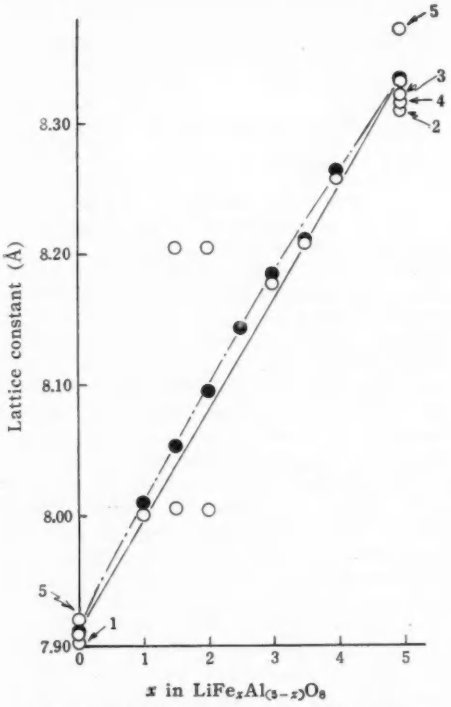

Fig. 1. Relation between the lattice constant and the chemical composition in the solid solutions.
○: ordered phase, present author
●: disordered phase, present author
1: disordered phase, E. Kordes[8]
2: disordered phase, A. Hoffman[9]
3: disordered phase, F. Barblan et al.[10]
4: disordered phase, R. Collongues and G. Chaudron[11]
5: disordered phase, E. Kordes and E. Röttig[12]

* Thermal analysis of LAS was studied by the present author for the first time. The endothermic reaction due to a ferromagnetism, which was found in LFS, was not observed in the case of the solid solution.

** By Braun[5] the transtion takes place at the temperature below 1350°C.

8) H. Forestier and M. Vetter, *Compt. rend.*, **209**, 164 (1939).
9) A. Hoffmann, *Naturwiss.*, **26**, 431 (1938).
10) F. Barblan, E. Brandenberger and P. Niggli, *Helv. Chim. Acta*, **27**, 88 (1944).
11) R. Collongues and G. Chaudron, *Compt. rend.*, **231**, 143 (1950).
12) E. Kordes and E. Rötting, *Z. anorg. allgem. Chem.*, **264**, 34 (1951).

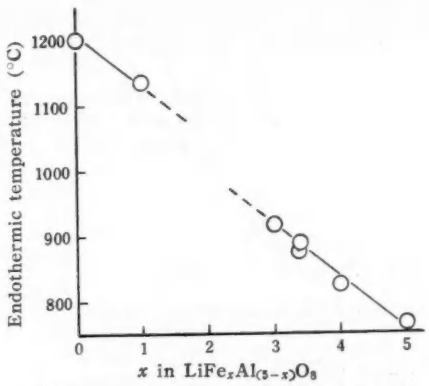

Fig. 2. Relation between the endothermic temperature and the chemical composition in the solid solutions.

in Table I and Fig. 2. The endothermic temperature of LFS is lower than that of any composition of the solid solution, and the more the aluminum content, the higher this temperature. An analogous relation is seen in that of ferromagnetic Curie point vs. chemical composition in nickel-magnesium, cupric-nickel and zinc-nickel ferrospinel solid solution[8]. It is very remarkable that no continuous change of the endothermic temperature against the composition is found in any kinds of specimens of the solid solution but in those of the compositions rich in ferric ion or aluminum ion. This is supposed to be caused by some differences in crystal structure between iron-rich and aluminum-rich compositions. The true transition temperatures, which are provided to be lower than the endothermic temperatures by 10~30° from the result of LFS, will also be given in the similar manner as above-mentioned.

It is concluded that the transition of LFS-LAS solid solution is the order-disorder transition of the same type as that of LFS or LAS from the results on the crystal structure and the endothermic reaction.

Formation of Homogeneous Solid Solution. —In the disordered phase, homogeneous solid solutions were formed at any compositions. In the ordered phase, however, the solid solutions were homogenized in the specimens of iron-rich composition (D and E in Table I) or of aluminum-rich (B). There might be two phases separated in the specimens of intermediate compositions (C, P and R). The compositions of the separated phases were estimated by the measurements of lattice constants and the use of the above equation, and it was determined that in one of these two phases it is of 20 mole per cent LFS, and in the other 68 mole per cent. In thermal analysis, the only endothermic temperature was measured in the case of specimens B, D and E, while two endothermic temperatures corresponded to two phases were revealed in the case of C, P and R. X-ray diffraction results were in conformity with thermal analysis'. The formation of a homogeneous solid solution in the ordered phase of Q, though it was annealed on the same condition as others, is assumed due to a difference in a disordering velocity* from that of the others. Whether the homogeneous solid solution can be formed in the ordered phase at a higher temperature or in the disordered phase quenched at a lower temperature, no knowledge is offered from the present work.

Homogeneous solid solutions were not formed in the region of 20~68 mole per cent LFS, where the discrepancy in the relation of the transition temperature vs. the chemical composition was also observed. The conditions necessary to form a homogeneous solid solution are usually those mentioned below[13]; (1) both phases have the same crystal structure, (2) the values of lattice constants resemble each other, (3) the chemical properties are also similar, (4) the ionic radii of constructing ions are the similar size. Typical examples are revealed in the ferrospinel mentioned above, lead phosphate-lead arsenate and lead phosphate-lead vanadate solid solution[14]. Systematic studies on relations of solid solutions of solid solution with order-disorder transition have hitherto been reported very rarely. The ordered phase of LFS and that of LAS have the same crystal structure and the difference between their lattice constants is small. It is also the case in the disordered phase. These is a considerable agreement between an ionic radius of ferric ion (0.67 Å) and that of aluminum ion (0.55 Å). Though having the conditions necessary to be homogenized, LFS-LAS solid solutions cannot

* From the condition of annealing, the transition velocity of each composition was found to be very rapid as that of LFS.

13) R. Kiriyama and S. Seki, "Crystal Chemistry (Kesshō no Kagaku)", Part II, Sōgensha, Osaka, 1950, p. 135.

14) M. Amadori, *Gazz. chim. Ital.*, **49**, 38 (1919).

be formed over all ratios. Such phenomena might be caused by an averaged structure, i. e., a cation arrangement at the octahedral or the tetrahedral interstices in the crystal. Detailed experiments along this line will be discussed in the following paper.

The author wishes to express his sincere thanks to Mr. Kazuo Sasaki of Osaka City University for his discussion.

Institute of Polytechnics
Osaka City University
Kita-ku, Osaka

*Experiments on Synthetic Mica Crystal Growing. Crystal Growing with Carbon Granule Resistance Furnace**

By Tokiti NODA and Yoshihiro SUMIYOSHI

(Received July 2, 1958)

In experiments on the growing of synthetic fluor-phlogopite, it is necessary first to melt the mixture of raw materials of fluor-phlogopite composition to a clear liquid by heating it at about 1450°C and then to maintain the resultant melt for many hours at temperatures within a range of several tens of degrees around its crystallizing temperature of about 1350°C. For the growing of large crystals, the melt should be cooled very slowly.

The rate of cooling necessary for the growing of large crystals may be acquired in two ways.

1) For small melts, by precise control of the temperature of the melt; 2) by using a large enough quantity of melt to obtain the necessary rate through natural cooling or by less precise control of temperature. A large mass of melt will provide sufficient space for growing large crystals.

The first way may be carried out by applying the technique originally designed by Stöber[1], Bridgman[2] and Kyropoulos[3] for growing large single crystals, techniques which have been used in the manufacture of optical crystals. The results of experiments done along this line will be reported later; experiments on growing synthetic mica crystals in large melts are described in the present paper.

* Summary of papers published in *J. Chem. Soc. Japan, Ind. Chem. Sec.*, (*Kogyo Kagaku Zasshi*), **59**, 352, 1323 (1956); and *J. Ceram. Assoc. Japan.* (*Yogyo Kyokai Shi*), **64**, 95 (1956).

1) F. Stöber, *Z. Krist.*, **61**, 299 (1925).

2) P. W. Bridgman, *Proc. Am. Acad. Arts. Sciences*, **60**, 303 (1925).

3) S. Kyropoulos, *Z. anorg. Chem.*, **154**, 308 (1926); *Z. Phys.*, **63**, 849 (1930).

Experimental

Apparatus.—Among various types, platinum resistance, silicon carbide resistance, carbon resistance and gas-fired furnaces may meet the requirements for the temperature range for synthetic mica crystal growing. In small-scale experiments, the first two types of furnace were used. In large-scale experiments, however, carbon granule resistance furnaces, designed especially for this purpose, were used. Because, the platinum resistance furnace being excluded for its prohibitive expense, a silicon carbide resistance furnace was unexpectedly found to serve only a short time, as heating resistors were attacked by fluorine-containing vapor evolved from the melt.

The first requisite was to design and construct a carbon granule resistance furnace having all the characteristics needed to meet the requirements of temperature control necessary for synthetic mica crystal growing, because this type of furnace is usually considered inadequate for precise temperature control and the furnace is apt to have a reducing atmosphere.

As a preliminary step in designing the furnace, characteristic data, such as electric power input per unit surface area of heating zone, specific resistance of carbon granule heating element, and power input per unit volume of carbon granule heating element, were investigated by a critical examination of several commercial furnaces of the carbon granule resistance type.

A furnace of 2 kg. melting capacity of this type was constructed, employing these characteristic data as a design basis, and used for medium scale experiments on synthetic mica crystal growing. Then based on a close examination of both calculated and observed characteristic data of this furnace, a furnace of carbon granule resistance type having a 30 kg. melting capacity was constructed for large-scale experiments on synthetic mica crystal growing. The furnace

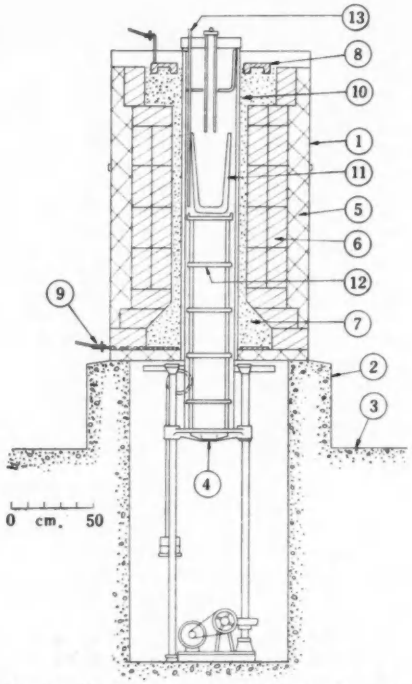

Fig. 1. Carbon granule resistance furnace.

1: Steel case 2: Concrete foundation 3: Floor 4: Motor-driven lift 5: Heat insulator 6: Refractories 7: Carbon granule resistance 8: Upper electrode 9: Lower electrode 10: Core tube 11: Clay crucible 12: Buffer plate 13: Thermocouple protection tube

Inner dia. of core tube 30 cm., Outer dia. of core tube 34 cm., Width of heating element 6 cm., Height of heating element L 110 cm., Sectional area of heating element A 154 cm^2, L/A 0.15_9 cm^{-1}, Volume of heating element V 82.9 l,

Specific resistance of carbon granule resistor
ρ 1.44 Ω cm. (room temp.)
0.50_6 Ω cm. (at 1675 °C),

Total resistance of heat element R
0.21_6 Ω (room temp.) 0.07_9 Ω (at 1675 °C),

Surface area of heating zone A_i 104 dm^2,

Power input per unit surface area of heating zone EI/A_i
0.09_6 kW./dm^2 (room temp.)
0.38_4 kW./dm^2 (1675 °C),

Total input EI
10 kW. (room temp.) 40 kW. (1675 °C),

Power input per unit volume of heating element EI/V
0.12_0 kW/l (room temp.) 0.46_2 (1675 °C),

Current I 215 amp. (room temp.)
720 amp. (1675 °C),

Terminal voltage E 46.5 V. (room temp.)
55.8 V. (1675 °C),

was remodeled several times in the process of the research and a sectional sketch of the furnace in its final form is given in Fig. 1, with its characteristic data.

The power input (P) for heating the furnace up to a certain temperature and the power input (P') for keeping the furnace at that temperature are related to temperature (θ), the effective surface area of heating zone (a), and the time (t) required for heating the furnace up to the temperature by the following equations[4]:

$$P = ca^{0.9}\theta^{1.55}t^{-0.5} \quad (1)$$

$$P' = c'a^{0.9}\theta^{1.55} \quad (2)$$

For this furnace, the values of c and c' were found to be 76 and 7.5 respectively. The power input for keeping the furnace at 1350°C was about 20 kW, the heat loss at the furnace side wall being about 65% of total input, and at the top and the bottom of the furnace, about 35%.

The furnace was harnessed with two voltage regulators in sequence, i.e. a motor-driven induction regulator, controlled by an electronic controller, was used with a saturable reactor combined with a magnetic amplifier and a D.C. voltage stabilizer. With this device, the temperature of the furnace could be controlled within ±2~3°C in the temperature range of 1300° and 1400°C by regulating the terminal voltage within ±0.05%.

A motor-driven lift was attached under the furnace, so that a crucible placed on the lift could be raised to a predetermined height in the furnace.

Raw Materials.—Raw materials, such as quartzite, alumina, magnesia, talc and potassium silicofluoride, were of commercial grade except the poassium carbonate which was of chemical grade. These materials were analysed and were found to have sufficient purity for the present purpose. All gradients of these raw materials were taken into account in calculating the mixing ratio of the raw materials for the preparation of batch mixtures.

Because the loss of fluorine due to decomposition of fluoride in the batch during heating is accelerated by the presence of water vapor[5], the mixture of calculated amounts of silica, magnesia, talc, alumina and potassium carbonate was first calcined at about 1000°C to expel water and carbon dioxide contained in the mixture and then the calculated amout of potassium silicofluroride was added.

Batches of POM 2 composition were used in most of the experiments of the present series because it was found, from results of experiments on the determination of crystallizing

4) T. Hayashi, *J. Electrochem. Soc. Japan*, (*Denki Kagaku*), **15**, 55 (1947).

5) a. V. Middel, PB 32546 (1947); b. R. A. Hatch and R. A. Humphrey, *Office of Naval Research* (1950), The Synthetic Mica Program 2; c. A. Van Valkenburg and R. G. Pike, *J. Res. Natl. Bur. Stand.*, **48**, 360 (1952); d. W. Eitel, R. A. Hatch and M. V. Denny, *J. Amer. Ceram. Soc.*, **36**, 341 (1953).

temperature of fluor-phlogopite[6] and also from results of a large number of crystal growing experiments[7], that this composition was one of the most favorable compositions for crystal growing. Two examples of batch mixtures are given in Table I.

TABLE I

	POM 2 composition %		Batch mixture I %	Batch mixture II %
SiO_2	40.58	Alumina	11.72	11.30
Al_2O_3	11.60	Talc	60.29	48.07
MgO	27.32	Magnesia	5.88	10.51
K_2O	10.79	Potassium silicofluoride	18.38	18.77
F	9.71	Potassium carbonate	3.73	2.35
		Quartzite		7.61

Experimental Procedure.—The evaporation of fluorine in the batch is highest in the course of reaction during heating above 1000°C and is comparably low in the molten state. Therefore, it was planned to melt the batch as quickly as possible to minimize the evaporation of fluorine.

At first it was our plan to follow the melting procedure in this way, viz: the crucible containing the batch is placed in a low position within the furnace (c.f. Fig. 1), heated up to about 1000°C, and then moved to a higher temperature region which had already been heated to 1400°C. After completion of the melting, the crucible is raised or lowered to ensure the required temperature difference between the top and the bottom of the crucible and then cooled slowly by controlling the power input of the furnace. The heating and cooling curve of the experiment carried out in this way is shown in Fig. 2.

This procedure was abandoned because of operational difficulties, such as failure to get the crucible, buffer plates, thermocouple protecting tube and other furnace furnitures on the lift to raise smoothly, and the increase of undesired updraft of cold air during and after the raising operation. Most of the experiments were carried out in the following way. An unfilled crucible is first placed in the furnace; then the furnace is heated by passing electric current through the resistance element. After the temperature has reached about 1400°C, the crucible is charged several times with the batch until it is filled with the melt. Upon completing the charge, the crucible is covered with a lid, the temperature of the crucible is maintained above 1400°C for 5~6 hours to obtain the clear melt, and then cooled slowly by controlling the power input of the furnace.

Because well-sintered high-aluminous clay crucibles used in the earlier stages of this series of experiments were found to be less resistant to thermal shock, calcined but unsintered high-aluminous clay crucibles were used in later stages of the series. They were first heated in the furnace up to 1650°C to sinter. After the sintering, the temperature of the furnace was lowered to about 1400°C, the crucible was charged with the batch material and after completion of the melting, the melt was cooled slowly, as described above. The heating and cooling curve of a typical experiment of this series is given Fig. 3.

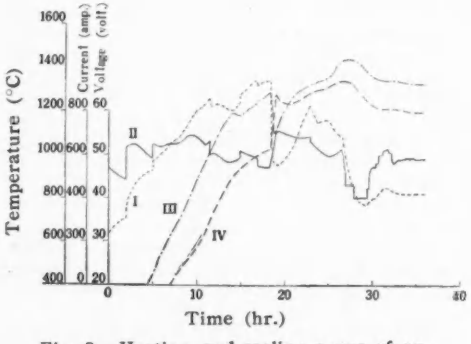

Fig. 2. Heating and cooling curve of experiment No. 1.
I: electric current
II: terminal voltage
III: temperature at the top of the crucible
IV: temperature at the bottom of the crucible

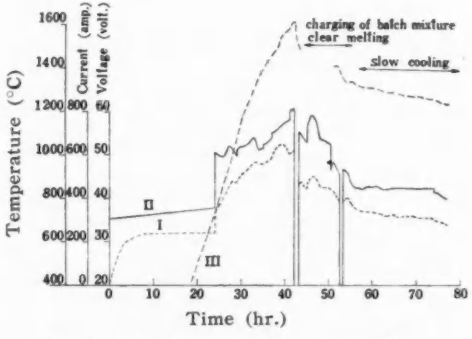

Fig. 3. Heating and cooling curve of experiment No. 13.
I: electric current
II: terminal voltage
III: temperature at the bottom of the crucible

Crucible Material.—Graphite and high-aluminous clay crucibles were used in the experiments because graphite was known not to be wetted and corroded by the melt, and a well-sintered alumina or high-aluminous clay body

6) T. Noda and S. Sugiyama, *J. Chem. Soc. Japan, Ind. Chem. Sec.*, (*Kogyo Kagaku Zasshi*), **46**, 1082 (1943); cf. T. Noda, *J. Amer. Ceram. Soc.*, **38**, 147 (1955).

7) T. Noda, *Industrial Physical Chemistry* (*Kogyo Butsuri Kagaku*), No. 1, 108 (1948); cf. T. Noda, This Bulletin, **23**, 40 (1950).

was found to resist the corrosion[8].

Graphite crucibles used were cylindrical in shape, 25 cm. in outer diameter, 50 cm. in height and 46 cm. in depth. The crucible was placed in a sagger made of fire clay, with grog powder packed in the interstitial space between the crucible and the sagger, thus preventing the oxidation of graphite. Buffer plates and cylinders made of fire clay were placed on and under the sagger in the furnace in order to decrease unfavorable convection current in the furnace.

Mica aggregates which crystallized in graphite crucibles were gray, minute carbon particles deposited in interstitial glass between mica crystals discoloring them. Crystals grown in graphite crucibles were generally small, and even when they grew large, they were mostly of mosaic nature.

It seems that one of the causes of small crystal formation is that the wall of graphite crucible is not wetted with the melt and consequently the wall does not initiate the nucleation of mica, so that the melt tends to become supercooled and forms a large number of nuclei when it starts to crystallize at a supercooled temperature.

In one experiment with graphite crucible, the molten state was maintained down to a temperature of about 150°C below the crystallizing temperature and small mica crystals rapidly formed around a steel wire when it was quickly dipped into the melt, while glass adhered to a wire quickly dipped into a melt in a high-aluminous clay crucible.

These observations suggest that the melt in graphite crucible was in a supercooled state or was in a state of easy crystallization with slight stimulus. Another suspected cause for small crystal formation was that a change in chemical composition of the melt was accelerated by the reducing atmosphere, but the change was not verified by chemical analysis. Also, the presence of minute carbon particles might stimulate the nucleation, although no positive assertion can be made.

High-aluminous clay crucibles used in the experiments were of alumina and silica, about 50% each. Crucibles sintered at about 1600°C or below were heavily corroded by the melt, so that the thickness of crucible wall decreased to about one-half of its original thickness, changing the chemical composition of the melt markedly and often leaking the melt completely.

Crucibles sintered at about 1650°C were found to withstand corrosion of the melt. The wall of clay crucibles initiated the nucleation of mica crystals, so that in the earlier stage of crystallization, large numbers of small crystals were formed in the vicinity of the wall. However, in the course of slow cooling, some of these crystals or crystal nuclei which were spontaneously formed in the melt grew to large single crystals of good quality. Mica aggregates crystallized in clay crucibles were slightly colored brown owing to iron contamination coming from crucible material. These aggregates contained a slightly larger amount of glass than those crystallized in the graphite crucible, but contained no carbon.

Result

Temperature Gradient in Melt and Oriented Growing of Crystals.—The formation of large crystals grown horizontally in the surface layer of melt was often observed when the temperature difference between the top and the bottom of the crucible was small during the crystallization period. Crystals grown in this way are shown in Fig. 4a. The crystal in the lower part of the figure measured 7 cm. by 12 cm. and was slightly curved. The evaporation of potassium and fluorine from the surface of the melt must have caused the crystallizing temperature of the surface layer of the melt to become higher and the early-formed crystals in this layer may have been in contact with the melt and may have had a longer time to grow than crystals formed later in the bulk of the melt. This may be the reason for small crystals growing at random in the bulk of the melt in spite of the formation of large crystals in the surface layer. Crystals grew upwards from the bottom of the crucible when the bottom temperature was sufficiently lower than the top temperature to cause the crystal nuclei to form originally at the bottom of the crucible. Edges of basal planes of vertically grown crystals can be seen on the surface of the crystalline mass shown in Fig. 4b. Rapid cooling causes new crystal nuclei to form in a slightly displaced direction from the orientation of

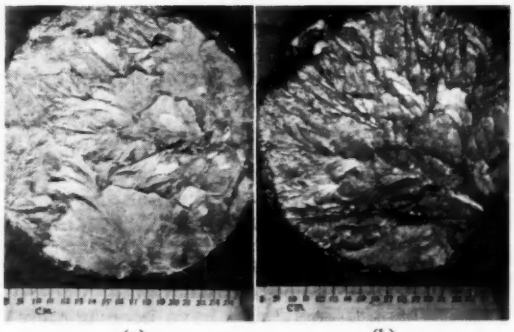

(a) (b)

Fig. 4. Top view of crystallized mass

8) T. Noda and M. Konno, *J. Ceram. Assoc. Japan, (Yogyo Kyokai Shi)*, **57**, 25 (1949); T. Noda and K. Mori, ibid., **57**, 104 (1949); T. Noda and T. Ikenoue, ibid., **57**, 163 (1949).

TABLE II
TEMPERATURE GRADIENT AND ORIENTED CRYSTAL GROWING

Experiment	Height of melt cm.	Temperature difference °C	Temperature gradient °C/cm.	Oriented growing
5	30	10	0.3	none
6	30	40～150	1.3～5	slight
8	30	115	3.8	slight
9	30	150	5	noticeable

the original crystals. This type of formation results in curved crystals of mosaic nature and under the most unfavorable conditions in dendritic crystals which are manifested by the branched edges of basal plane, as seen in Fig. 4b.

For the purpose of obtaining the relationship between the temperature gradient in the melt and the oriented growing of crystals, the temperature difference between the top and the bottom of the crucible and the qualitative degree of oriented crystal growing are given in Table II.

Although temperature readings with thermocouples placed at the top and bottom level of the crucible may not always indicate true temperatures of the melt at the same levels, the temperature gradient calculated by dividing the temperature difference by the depth of melt may, for practical purposes, be used for deduction of the experimental result. It can be seen from data of Table II that no oriented growth of crystals was observed when the temperature gradient was 1～2°C /cm. and that the temperature gradient of 4～5°C/cm. may be needed for oriented growth.

Rate of Growth and Quality of Crystal. —In one experiment in which the temperature at the bottom was higher than that at the top, a steel wire was frequently dipped into the charge contained in a graphite crucible to see the start of crystallization. When the temperature was 1230°C at the top and 1375°C at the bottom, the charge was in the molten state; when the temperature was 1205°C at the top and 1335°C at the bottom, a part of the charge began to solidify, the main part being a viscous melt; the crystallization was completed when the temperature was 1185°C at the top and 1325°C at the bottom. Because of the inverted temperature gradient, the convection may have occurred in the melt to equalize the temperature difference, so the real temperature of the upper layer of the melt may have been higher than the measured value. However, a considerable temperature gradient may still have been held, because crystals grew vertically downward from the upper layer. The crystallizing temperature of the melt was estimated to be about 1350°C, while in the above case the actual crystallization began between 1325°C and 1205°C.

This means that a great supercooling took place. It seems that a rapid rate of cooling may favor the occurrence of supercooling. Therefore the melt does not always begin to crystallize when the temperature of the melt is cooled to that corresponding to its crystallizing temperature, and the rate of cooling of the melt, calculated by dividing temperature-drop in the slow cooling period by the duration of slow cooling, does not necessarily correspond to the true rate of cooling during the crystallization. However, in the course of slow cooling, a slow-down of the cooling rate due to the generation of the heat of crystallization* was generally observed, and it can be assumed that the period of the slow-down of the cooling rate corresponds to the duration of crystallization. Therefore the rate of crystal growth of basal plane can be calculated by dividing the size of the largest crystal found in the solidified mass by the duration of crystallization, assuming that the crystal had grown throughout the duration of crystallization, although the solidified mass in the crucible was usually composed of a large number of crystals of various sizes. The rate of crystal growth thus calculated and the quality of crystals produced are given in Table III.

In experiment No. 13, using a well-sintered high-aluminous clay crucible, several clear single crystals measuring about 5 cm. by 5 cm. could be split from the solidified mass, although the yield of crystals of this size was very small. Two of these crystals are shown in Fig. 5. In this experiment, the rate of cooling was 2～5°C/hr.. The quality of these crystals is designated in Table III as "excellent". Crystals which are not perfect

* 74±3 cal./g., N. Daimon, T. Horibe, K. Mukumoto and T. Noda, *J. Chem. Soc. Japan, Ind. Chem. Sec.*, (*Kogyo Kagaku Zasshi*), **55**, 762 (1952).

TABLE III

RATE OF CRYSTAL GROWTH AND QUALITY OF CRYSTAL

Exp. No.	Crucible used	Crystallization time hr.	Cooling rate °C/hr.	Largest crystal cm.	Crystal growth rate mm./min.	Quality of crystal
5	Graphite	21	2～ 5	10	0.08	good
6	〃	17	3～20	13	0.13	poor
8	〃	2	rapid cooling	5	0.42	very poor
9	〃	2	15～20	3	0.25	poor
13	High aluminous clay	13	2～ 5	5	0.06	excellent

TABLE IV

CHEMICAL COMPOSITION OF BATCHES AND PRODUCTS

Exp. No.		MgO %	SiO_2 %	SiO_2 %mod*	SiO_2 Δ%**	Al_2O_3 %	Al_2O_3 %mod*	Al_2O_3 Δ%**	K_2O %	K_2O %mod*	K_2O Δ%**	F %	F %mod*	F Δ%**
11	batch	27.64	42.92			12.16			11.43			9.93		
	product	27.03	43.74	44.74	+1.84	13.61	13.92	+1.76	10.42	10.65	−0.78	9.33	9.54	−0.39
12	batch	26.84	41.07			12.58			11.26			9.46		
	product	26.75	43.79	43.92	+2.85	14.98	15.02	+2.50	9.71	9.74	−1.52	8.09	8.11	−1.35
13	batch	27.35	39.19			15.43			11.07			9.50		
	product	24.14	43.02	48.74	+9.55	17.21	19.57	+4.41	10.65	11.96	+0.90	8.11	9.19	−0.31

* %mod = (% in product) × (MgO % in batch) / (MgO % in product)

** Δ% = (%mod) − (% in batch)

single ones, but are of mosaic nature are designated as "poor" in quality. When they were split from the solidified mass, these crystals separated into many small ones. Crystals grown at a rate higher than 0.1 mm./min. were always imperfect mosaic crystals. It can be deduced then that in order to grow good single crystals which can be split from the solidified mass, the rate of growth should be less than one-tenth of a millimeter per minute.

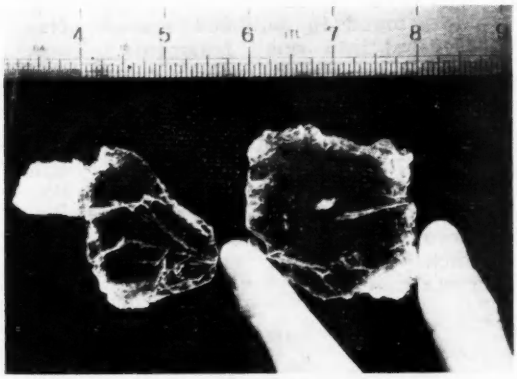

Fig. 5. Single crystals of fluor-phlogopite.

Change in Chemical Composition of Charge during Process.—Chemical compositions of batch mixtures and solidified products of three experiments are given in Table IV.

We used in experiment No. 11, a slightly-sintered high-aluminous clay crucible for melting for a relatively short period, in experiment No. 12, a slightly-sintered high-aluminous clay crucible for a long period and, in experiment No. 13, a well-sintered high aluminous clay crucible for a long period. Changes in individual components of the charge during the melting were calculated on the assumption that the content of magnesia was kept constant because no magnesia came from the crucible and the evaporation of magnesium fluoride was negligible.

In experiment No. 11 where the short period melting and the rapid cooling were used, small crystals resulted without remarkable change in the chemical composition of the melt. In experiment No. 12, the clay crucible was heavily corroded. This resulted in a considerable increase in content of alumina and silica. The loss of fluorine and potassium due to the evaporation was also remarkable. The great shift of the chemical composition and especially a remarkable deficit of fluorine in the melt, may be to blame for the formation of small crystals. The well-sintered clay crucible used in experiment No. 13 strongly resisted the corrosion of melt. The slow-cooling procedure was carried out as planned and the solidified mass contained many large crystals, as described above. The chemical composition

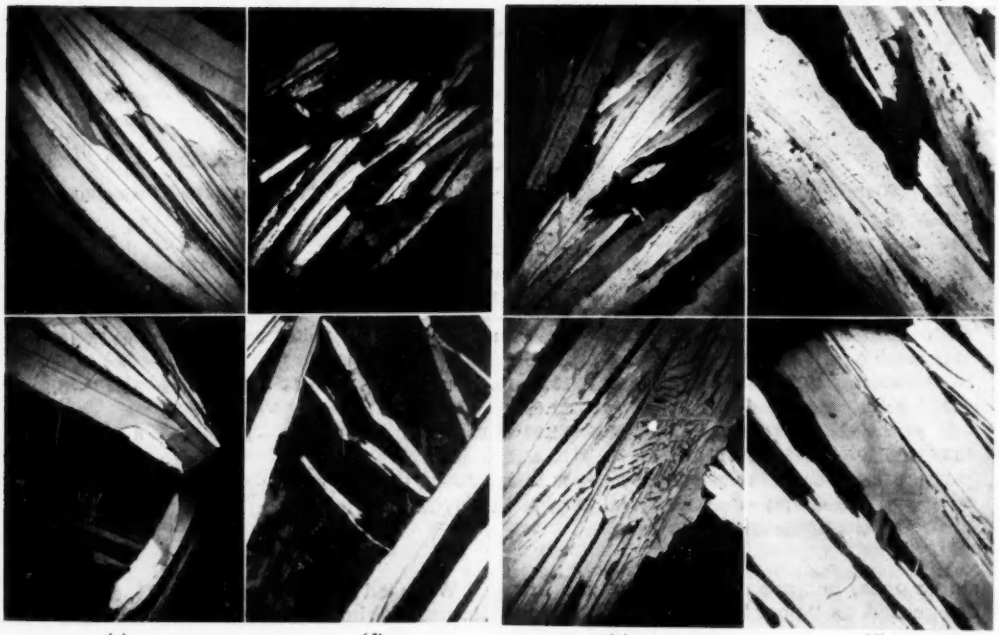

(a) (×8 cross nicol) (b) (×8 cross nicol)
(c) (×8 cross nicol) (d) (×30 cross nicol)

Fig. 6. Microphotograph of fluor-phlogopite (1).

(a) (×8 cross nicol) (b) (×8 cross nicol)
(c) (×8 cross nicol) (d) (×8 cross nicol)

Fig. 7. Microphotograph of fluor-phlogopite (2).

of the product of experiment No. 13, given in Table IV, shows a remarkable increase of silica and alumina content, a slight increase of potassium and a slight decrease of fluorine. Because the excessive potassium of the batch usually concentrates in the glassy part of solidified mass, the analysed sample may have contained a slightly larger amount of glass than average. However, it seems to be essential that in order to obtain good large crystals, the fluorine and potassium content of the melt must not be deficient.

Microscopic Observation.—Curved crystals were often found in solidified masses. Some crystals bent 90° or more. A slightly curved crystal is shown in Fig. 6a. The curved crystals may have been bent by crystals growing from other directions. The curved crystals retain their form after they have been split from the mass. Sometimes the growing pressure of the other crystals was so great that the bent crystal was deformed to become a mosaic crystal, as shown in Fig. 6c. In Fig. 6b there is another example of imperfect curved crystals. Small crystals grown in interstices between large crystals perpendicular to the basal plane of large crystals were bent and ruptured by the pressure of contraction action on the basal planes of large crystals while the temperature was cooling (Fig. 6d).

As was previously described, large basal plates found in solidified masses often separated into small fragments. These plates were almost entirely composed of small crystals grown in the same direction or slightly inclined toward each other or were imperfect skeleton crystals, as shown in Fig. 7a, b, and c. All these crystals were formed by rapid cooling. With slow cooling, we obtained perfect crystals grown parallel to each other (Fig. 7d), which when split made clear single crystals.

Summary

Synthetic mica crystal growing experiments were carried out with a graphite crucible and a well-sintered high-aluminous clay crucible in a carbon granule resistance furnace of 30 kg. melting capacity, specially designed for this purpose. In experiments with a graphite crucible, the

melt often became supercooled and crystallized rapidly, to result in small crystals once crystallization started at the supercooled temperature. With a clay crucible, several experiments failed because of cracks in the crucible or because of corrosion of the crucible by the melt. Only with a well-sintered high-aluminous clay crucible and under the condition of small loss of fluorine and potassium in the melt were perfect large single crystals measuring about 5 cm. by 5 cm. formed even at a mean cooling rate of 2~5°C/hr. in the range of 1360°C to 1300°C. The yield of large single crystals was very small, doubtless because only the few crystals which had formed earlier had enough time and space to be in contact with the melt and thus to grow to large size. If the growing crystals come into contact or collide with other growing crystals, the crystals are either prevented from growing further or become strained or bent. Consequently, for crystals to grow to a large size, they must be in contact with the melt for a long time without being disturbed by other crystals. This can be done when crystals grow in the same direction. It was found that the temperature gradient of 4~5°C/cm. was necessary for crystals to grow in one direction.

Among many factors affecting the growth of crystals, the rate of cooling should be controlled to secure the rate of crystal growth at less than 0.06 mm./min. in order to grow perfect and flawless single crystals of mica.

Needless to say, a sufficient volume of melt is necessary to grow large crystals, i.e. a large quantity of melt gives more opportunity for large crystals to grow. Crystals measuring 5 cm. by 5 cm. were never obtained before the 30 kg. melting experiments were carried out.

This research was carried out during the period from 1946 to 1954 by the cooperation of Messrs. K. Tamura, S. Kanatsu, I. Tate, M. Horiguchi, K. Inagaki, E. Kato, D. Ishii and K. Hata with the aid of the Scientific Research and Development Fund of the Ministry of Education, the Asahi Science Promotion Fund and a special aid by the Electocommunication Laboratory, the Japan Telegram and Telephone Corporation.

Department of Applied Chemistry
Faculty of Engineering
Nagoya University
Chikusa-ku, Nagoya

Raney Nickel and Platinized Rany Nickel with Higher Catalytic Activities

By Shigeo NISHIMURA

(Received July 8, 1958)

Preparation of Raney Nickel Catalysts.—In a previous paper[1], it was reported that a Raney nickel catalyst with a higher activity can be obtained by adding aqueous sodium hydroxide in portions to the suspension of a Raney alloy in water. To obtain a catalyst of high activity the usual methods of developing the Raney alloy, e.g. the method of Adkins and Billica[2], seemed unfavorable for the following reasons.

a) The reaction of the Raney alloy with sodium hydroxide in an aqueous solution is strongly exothermic and it is very difficult to put the alloy into the solution within a short time. Therefore, a catalyst developed uniformly can not be obtained, because the portion of the alloy added at the beginning is treated with the most concentrated sodium hydroxide for the longest time and that added last with the most dilute sodium hydroxide for the shortest time.

The lack of uniformity can not be neglected in such a catalyst as W-7 of Adkins and Billica[2], which is prepared with a

1) S. Nishimura and Y. Urushibara, This Bulletin, **30**, 199 (1957).
2) H. Adkins and H. R. Billica, *J. Am. Chem. Soc.*, **70**, 695 (1948).

comparatively small quantity of sodium hydroxide and contains a considerable amount of aluminum, or in a catalyst prepared from an alloy containing less nickel.

b) In the preparation of Urushibara nickel catalysts[3,4], which are obtained by treating finely divided nickel, precipitated from a nickel chloride solution by zinc dust, with aqueous caustic alkali or with acetic or propionic acid, it proved harmful to the activity of the catalysts to use a concentrated solution of the developing reagent and mild conditions are favorable so far as the time for the preparation is tolerable. It suggests that use of a strong alkali may be unfavorable also in the preparation of the Raney nickel catalyst.

From this point of view, the author attempted with success to prepare Raney nickel catalyst with a higher activity by adding a sodium hydroxide solution in portions to the suspension of a Raney alloy in water. In the course of this study, it was found that the Raney alloy, after being partly leached with a very dilute sodium hydroxide solution, reacts with, and is developed by, water, forming a large quantity of white aluminum hydroxide, which was confirmed to be bayerite by the X-ray diffraction analysis[5]. After the reaction with water has subsided and the alloy has been covered with grey films of bayerite, the product reacts only very mildly with a concentrated sodium hydroxide solution, which can be added at one time without arousing a violent reaction. Then the digestion is continued to remove the bayerite and to complete the development.

The Raney nickel catalyst prepared in this way (denoted as T-4 when prepared from an alloy containing 40% of nickel) is more active than the W-7 catalyst of Adkins and Billica. The catalyst prepared under the same conditions as W-7 except that a larger quantity of the sodium hydroxide solution of the same concentration was used (denoted as W-7′) was less active than W-7.

It suggests that the W-7′ catalyst was overdeveloped or partly deactivated with the strong alkali in the course of the development. Table I shows the activities of these three catalysts in the hydrogenation of various organic compounds under the ordinary pressure and at 25°C.

TABLE I

TIME (min.) FOR THE HYDROGENATION OF ORGANIC COMPOUNDS WITH RANEY NICKEL CATALYSTS UNDER THE ORDINARY PRESSURE AND AT 25°C

Compound	Amount (g.)	Hydrogen absorbed (mole/mole)	Catalyst		
			T-4	W-7	W-7′
Cyclohexanone	3.93	1	17	21	24
Acetophenone	4.81	1	34	40	50
Cyclohexene	3.29	1	7	9	9
Quinoline	2.58	2	83	84	
Benzonitrile	2.06	2	49	76	80
Cyclohexanone oxime	2.26	2	92	126	

a) The catalyst was prepared from 2 g. of a Raney alloy containing 40% of nickel each time just before the hydrogenation.
b) 20 cc. of 95% ethanol was used as the solvent.

From some apparently similar methods in the literature[6-9] the present method differs in the fact that the Raney alloy is developed mostly with water, but not with an alkali, forming a large quantity of bayerite, which prevents the catalyst from direct contact with a strong alkali and facilitates the later addition of the main portion of the sodium hydroxide solution. The procedure to prepare the T-4 catalyst is given in details in the experimental part.

Preparation of the Platinized Raney Nickel Catalysts. — In many hydrogenations it has been shown that the Raney nickel catalyst is greatly promoted by treatment with chloroplatinic acid. Delépine and Horeau[10,11] showed that a Raney nickel platinized with chloroplatinic acid was effective for the hydrogenation of carbonyl compounds with addition of a little aqueous sodium hydroxide. Lieber, Smith and their co-workers[12-17] showed

3) Y. Urushibara and S. Nishimura, This Bulletin, **27**, 480 (1954).
4) Y. Urushibara, S. Nishimura and H. Uehara, ibid., **28**, 466 (1955).
5) A small amount of bayerite is also formed in the preparation of the W-7 Raney nickel catalyst. cf. G. W. Watt and S. G. Parker, *J. Am. Chem. Soc.*, **74**, 1103 (1952).
6) F. Fischer and K. Meyer, *Ber.*, **67**, 253 (1934).
7) E. B. Maxted and R. A. Titt, *J. Soc. Chem. Ind.*, **57**, 197 (1938).
8) J. Yasumura, *Science and Ind.*, (*Kagaku to Kogyo*), **22**, 21 (1948).
9) R. Cornubert and J. Phélisse, *Bull. soc. chim. France*, [5], **19**, 399 (1952).
10) M. Delépine and A. Horeau, *Compt. rend.*, **201**, 1301 (1935); **202**, 995 (1936).
11) M. Delépine and A. Horeau, *Bull. soc. chim. France*, [5], **4**, 31 (1937).
12) E. Lieber and G. B. L. Smith, *J. Am. Chem. Soc.*, **58**, 1417 (1936).
13) J. R. Reasenberg, E. Lieber and G. B. L. Smith, ibid., **61**, 384 (1939).

that treatment with chloroplatinic acid or with chloroplatinic acid and triethylamine was also effective for many hydrogenations. These methods agree in the fact that the Raney nickel is treated with chloroplatinic acid, and may supposedly have the following disadvantages:

a) The activity of nickel itself may be partly lost on treatment with chloroplatinic acid and the nickel ion then formed may be a catalytic poison[12].

b) The chloride ion and/or the hydrogen ion may be also catalytic poisons[18] and it is not certain if they can be completely removed by mere addition of sodium hydroxide[19] or triethylamine.

Recently Blance and Gibson[20] prepared a platinized Raney nickel from a nickel-aluminum alloy containing 2% of platinum but such an alloy has to be made specially and may not always be readily available.

The present author improved the preparation of the platinized Raney nickel by platinizing and simultaneously leaching the Raney alloy: A chloroplatinic acid solution made alkaline with a little sodium hydroxide is added to the suspension of a Raney alloy in water. The partly leached and platinized Raney alloy reacts with water, forming a large quantity of bayerite, and then can be treated in the same way as in the preparation of the T-4 catalyst. The details of the procedure for the preparation are given in the experimental part.

The platinized T-4 catalyst prepared in this way is more active than the T-4 catalyst platinized by the method of Delépine and Horeau. Table II shows the activities of these two catalysts in the hydrogenation of some organic compounds, T-4-Pt denoting T-4 platinized by the present method and T-4-Pt (D. H.) T-4 platinized by the method of Delépine and Horeau.

TABLE II

TIME (min.) FOR THE HYDROGENATION OF ORGANIC COMPOUNDS WITH THE PLATINIZED RANEY NICKEL CATALYSTS UNDER THE ORDINARY PRESSURE AND AT 25°C

Compound	Amount (g.)	Hydrogen absorbed (mole/mole)	Catalyst	
			T-4-Pt	T-4-Pt (D.H.)
Cyclohexanone	3.93	1	10	13
Acetophenone	4.81	1	13	17
Quinoline	2.58	2	27	38
Benzonitrile	2.06	2	11	14
Cyclohexanone oxime	2.26	2	17	19

a) The catalyst was prepared from 2 g. of a Raney alloy containing 40% of nickel and 50 mg. of chloroplatinic acid, $H_2PtCl_6 \cdot 6H_2O$.

b) 20 cc. of 95% ethanol was used as the solvent.

Experimental

Preparation of T-4 Catalyst.—To a mixture of 2 g. of a Raney nickel-aluminum alloy containing 40% of nickel[21] and 10 cc. of water, contained in a 30 cc. Erlenmeyer flask with a stirrer and heated in a water bath of 50°C, 0.4 cc. of 20% aqueous sodium hydroxide is added with vigorous stirring, care being taken not to let the reaction become violent, and the mixture is stirred. In about one hour, the partly leached Raney alloy begins to react with water and turns grey in color, and the reaction almost subsides in one hour and a half. Then 6 cc. of 40% aqueous sodium hydroxide is added at one time with continued stirring.

The digestion is continued for one additional hour at 50°C with good stirring, until the upper layer becomes snow-white. The catalyst is washed by stirring and decanting four times with 15 cc. of water of 50°C and then three times with the same volume of ethanol. A specimen of the T-4 catalyst thus prepared contained 13.3% of aluminum and a little aluminum hydroxide.

Preparation of W-7 and W-7' Catalysts.—W-7 catalyst was prepared from 2 g. of the alloy and 12 cc. of a 20 per cent sodium hydroxide solution exactly as described by Adkins and Billica[2] except that the catalyst was washed as described above for the T-4 catalyst. W-7' catalyst was prepared from 2 g. of the alloy and 24 cc. of 20 per cent aqueous sodium hydroxide. The W-7 and W-7' catalysts thus prepared contained 13.3 per cent and 12.5 per cent of aluminum, respectively.

Preparation of Platinized T-4 Catalyst.—To a suspension of 2 g. of the Raney alloy in 10 cc. of water, 50 mg. of chloroplatinic acid, $H_2PtCl_6 \cdot 6H_2O$, dissolved in 2 cc. of water made alkaline with 0.4 cc. of 20 per cent aqueous sodium hydroxide, was added with vigorous stirring in a water bath of 50°C.

The procedure hereafter is exactly the same as described above for the T-4 catalyst. Incomplete digestion, which is indicated by the grey

14) S. S. Scholnik, J. R.Reasenberg, E. Lieber and G. B. L. Smith, ibid., **63**, 1192 (1941).
15) D. R. Levering and E. Lieber, ibid., **71**, 1515 (1949).
16) D. R. Levering, F. L. Morritz and E. Lieber, ibid., **72**, 1190 (1950).
17) G. S. Samuelsen, V. L. Garik and G. B. L. Smith, ibid., **72**, 3872 (1950).
18) J. N. Pattison and Ed. F. Degering, *J. Am. Chem. Soc.*, **73**, 611 (1951).
19) S. Watanabe, *Science and Ind.* (*Kagaku to Kogyo*), **31**, 195 (1957).
20) R. B. Blance and D. T. Gibson, *J. Chem. Soc.*, **1954**, 2487.

21) A 50-50% alloy can be used with a somewhat lower activity of the resulting catalyst.

color of the upper layer, does not develop the activating effect by platinum.

Platinization of the T-4 Catalyst by the Method of Delépine and Horeau.—To a suspension of the T-4 catalyst, prepared from 2 g. of the Raney alloy, in 10 cc. of water, 50 mg. of chloroplatinic acid, dissolved in 2 cc. of water, is added with vigorous stirring in a water bath of 50°C. In a few minutes, when the reaction is complete, a little sodium hydroxide solution is added with stirring, and then the catalyst is washed.

Hydrogenation. — After the catalyst, suspended in 15 cc. of ethanol, was saturated with hydrogen at 25°C, the substance dissolved in 5 cc. of ethanol was added and the mixture was shaken with hydrogen at 400—500 oscillations per minute.

Identification of Bayerite.—The snow-white precipitate in the upper layer formed during the digestion with alkali was collected by centrifuging and analyzed by means of the X-ray diffraction.

The diffraction pattern shown in Fig. 1 shows that the precipitate is bayerite, one form of aluminum trihydroxide. But the bayerite is different from that formed in the reaction of the alloy with water as shown in Fig. 2. According to Fricke[22], the former is bayerite a and the latter bayerite b.

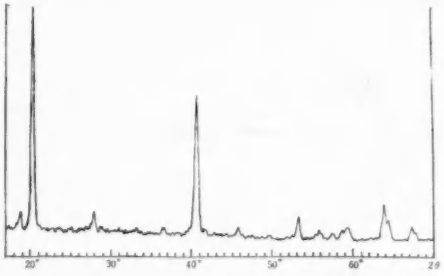

Fig. 1. Diffraction pattern of the precipitate formed during the digestion with alkali.

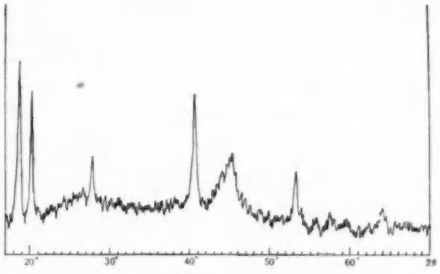

Fig. 2. Diffraction pattern of Raney alloy after the reaction with water.

The patterns were obtained by an X-ray diffractometer with Ni-filtered Cu-K_α radiation.

The author wishes to express his hearty thanks to Professor Yoshiyuki Urushibara for his kind guidance and valuable suggestion given throughout this work. The author is also indebted to Dr. Hiroshi Takahashi and Mr. Haruo Kuroda for their kind help in the measurement of the X-ray diffraction. This study has been supported by the Scientific Research Grant of the Ministry of Education.

Department of Chemistry
Faculty of Science
The University of Tokyo
Hongo, Tokyo

22) R. Fricke, *Z. anorg. allg. Chem.*, **175**, 249 (1928)

The Density of the Polycyclic Aromatic Compounds

By Hiroo INOKUCHI and Masayuki NAKAGAKI

(Received July 16, 1958)

It is already generally known that the physico-chemical properties of the polycyclic aromatic compounds are correlated closely to the number of carbon atoms comprised in the molecule. For instance, it has been found that the inner heat of sublimation of these hydrocarbons possesses a linear function of the number of carbon atoms with an average value of 1.5 kcal./mol. per carbon atom[1] and also that the increment of the number of benzene rings in the molecule of this series shows the increase of the electrical conductivity of these compounds[2].

These compounds belong to typical molecular crystal, in which molecules interact with each other by the van der Waals force. Lattice energies of crystals built up of homopolar molecules such as nitrogen or carbondioxide were first calculated by London[3]. The main object of this paper is to apply similar calculations of computing the density of the polycyclic aromatic compounds in comparison with the number of carbon atoms.

Experimental Procedures

The measurements of density for the polycyclic aromatic compounds were carried out at room temperature by means of the pycnometer as shown in Fig. 1. The total volume of this vessel, made of glass tubing of 15 mm. in diameter, was approximately 5 cc. The addition of the ground-on caps to cover the entrances of the vessel was helpful to prevent the evaporation of the pycnometer liquid.

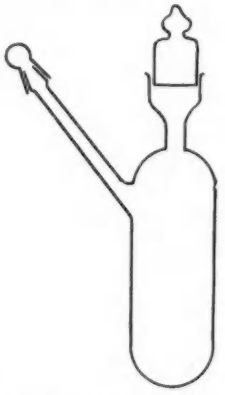

Fig. 1. The pycnometer

Since the solubility of violanthrene and *iso*-violanthrene in organic solvents is negligibly small at room temperature, ethanol can be used as the pycnometer liquid. The solubilities of anthanthrene and naphthacene were, however, fairly high in the alcohol. Therefore, distilled water mixed with a very small amount of a surface-active agent was employed as the pycnometer liquid for these compounds.

Through a preliminary experiment, it was recognized that the adherence of bubbles of air on a surface of an organic compound was a serious reason for the fluctuation of the observed density values. In order to remove as much of the air as possible, the vessel containing the specimen and liquid had to be attached to a water-pump and to be kept under a reduced pressure.

The polycyclic aromatic compounds used in this experiment were purified thoroughly by the methods already described in previous reports[2].

Results and Discussion

The potential energy of a molecule as

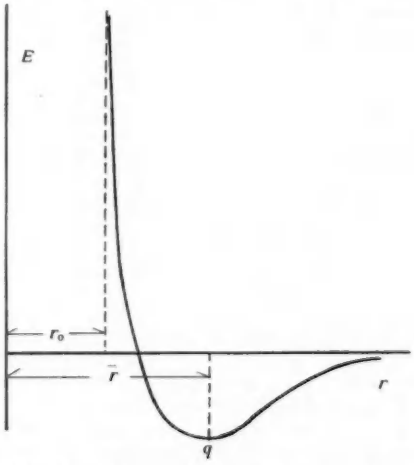

Fig. 2. The potential energy curve for intermolecular force.

1) H. Inokuchi, S. Shiba, T. Handa and H. Akamatu, This Bulletin, **25**, 299 (1952).
2) H. Akamatu and H. Inokuchi, *J. Chem. Phys.*, **18**, 810 (1950); **20**, 1481 (1952). H. Inokuchi, This Bulletin, **24**, 222 (1951); **25**, 28 (1952)
3) F. London, *Z. physik. Chem.*, **B11-12**, 222 (1930-1).

a function of an intermolecular distance, r, is generally expressed by a curve as shown in Fig. 2. This curve is made up of the sum of the dispersion and the repulsive force, the latter arising when the clouds of valence electrons of two molecules interpenetrate each other. These two forces are equal at the minimum point, q, of the potential energy curve. In addition, a strong repulsion due to the interpenetration of inner electron shells is assumed when the intermolecular distance is smaller than r_0. When the molecular weight of the hydrocarbon is very large, that is to say, the interaction between these molecules is very strong, it is reasonable to assume that the equilibrium distance between two molecules, $\bar{r}$, is nearly equal to r_0.

The molecule of the aromatic compound, a member of the series from benzene to graphite, has a plate-like shape, and is packed to make the molecules parallel to one another. Therefore, we can introduce the theory that r_0 corresponds to the interlayer spacing of graphite, 3.35Å, assuming that graphite is a kind of polycyclic aromatic compound having infinitely large molecular weight.

In calculating the sum of the dispersion forces and repulsive forces of atoms in the molecule, the contribution of hydrogen atoms may be neglected. Hence, the interation energy per one molecule $E(r)$ is expressed as,

$$E(r)=\frac{-AN^2}{(r-r_0)^6}+\frac{BN}{(r-r_0)^n} \tag{1}$$

in which N is the number of carbon atoms included in that molecule and A and B are constants.

At the equilibrium condition,

$$\left(\frac{\partial E(r)}{\partial r}\right)_{r=\bar{r}}=0=\frac{6AN^2}{(\bar{r}-r_0)^7}-\frac{nBN}{(\bar{r}-r_0)^{n+1}} \tag{2}$$

Therefore, $(\bar{r}-r_0)$ is represented as

$$(\bar{r}-r_0)^{n-6}=\frac{nB}{6A}\times\frac{1}{N} \tag{3}$$

The density of the aromatic compounds ρ is related to $\bar{r}$ by the equation

$$M/\rho=N_A S\bar{r} \tag{4}$$

in which M and S are the molecular weight and the area of one molecule of the aromatic hydrocarbon respectively, and N_A is Avogadro's number.

Since M and S may be proportional approximately to N, the number of carbon atoms in that molecule, Equation 4 can be rewritten in the form

$$\bar{r}=C/\rho$$
$$C=M/N_A S=\text{constant} \tag{5}$$

and also

$$r_0=C/\rho_\infty \tag{6}$$

Equation 3, therefore, becomes

$$\left(\frac{1}{\rho}-\frac{1}{\rho_\infty}\right)^{n-6}=\left(\frac{nB}{6AC^{n-6}}\right)\frac{1}{N} \tag{7}$$

This equation may be reduced to

$$\log\left(\frac{1}{\rho}-\frac{1}{\rho_\infty}\right)=-\frac{1}{n-6}\log N+\log Q \tag{8}$$

Here,

$$Q=nB/6AC^{n-6} \tag{9}$$

When we use the following numerical values

$\rho_\infty=2.26$ (density of graphite)

$n=8$

$B/AC^2=0.99$

in the above equation,

TABLE I

THE DENSITY OF POLYCYCLIC AROMATIC HYDROCARBONS

Compound	N	Density		Reference
		Observed	Calculated	
Benzene	6	1.04	1.02	
Naphthalene	10	1.15_2	1.16	4)
Anthracene	14	1.25	1.26	5)
Pyrene	16	1.27	1.29_5	6)
Naphthacene	18	1.33	1.33	
Tri-phenylene	18	1.3	1.33	7)
Perylene	20	1.35	1.36	
Benzperylene	22	1.35	1.38	8)
Anthanthrene	22	1.39	1.38	
Coronene	24	1.37_7	1.41	9)
Mesonaphthodianthrene	28	1.46	1.45	
Pyranthrene	30	1.47_5	1.46	
Ovalene	32	1.47_7	1.48	10)
Violanthrene	34	1.49	1.50	
Isoviolanthrene	34	1.50_5	1.50	
Circumanthracene	40	1.52	1.54	I1)
Graphite	∞	2.26	(2.26)	

4) J. M. Robertson, *Proc. Roy. Soc.*, **A142**, 674 (1933).
5) J. M. Robertson, ibid., **A140**, 79 (1932).
6) J. M. Robertson and J. G. White, *J. Chem. Soc.*, **1947**, 358.
7) A. Klug, *Acta Cryst.*, **3**, 165 (1950).
8) J. G. White, *J. Chem. Soc.*, **1948**, 1398.
9) J. W. Robertson et al., *Proc. Roy. Soc.*, **A220**, 311 (1953).
10) D. M. Donaldson and J. M. Robertson, ibid., **A207**, 101 (1951).
11) E. Clar, W. Kelly, J. M. Robertson and M. G. Rossman, *J Chem. Soc.*, **1956**, 3878.

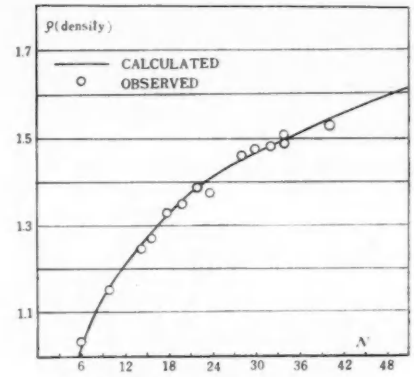

Fig. 3. The density of the polycyclic aromatic compounds.

$$\log\left(\frac{1}{\rho}-\frac{1}{2.26}\right)=-\frac{1}{2}\log N+0.120 \quad (10)$$

can be obtained.

The computed and also observed values of ρ are given in Table I and Fig. 3 for several polycyclic aromatic compounds. The agreement of these values in the table is satisfactory.

Table II
THE DENSITY OF CARBON BLACKS.

Specimen	L_a (Å)[12]	N	Density	
			observed	calculated
Royal Spectra	13.1	66	1.68	1.66
Philblack E	12.0	55	1.76	1.63
Peerless II-A	14.2	77	1.82	1.69
Tokyo Gas Carbon	13.4	69	1.68	1.67
Statex B	16.9	111	1.81	1.76
Philblack O	13.3	67	1.81	1.67

Applying Equation 10 to calculate the density of carbon blacks, we have the result in Table II. By means of the X-ray diffraction analysis, the dimension of a condensed polycyclic aromatic layer of the carbon, L_a, was calculated from the breadth of (10) reflection at half of the maximum intensity, applying Warren's formula for the random layer lattice. The area occupied by a carbon atom in the layer, may be assumed an equilateral triangle, for which b has the value of $a\sin 60°$, as illustrated in Fig. 4. Here, a possesses the distance of C−C bonding, 1.41Å. Thus, the number of carbon atoms in the layer is expressed

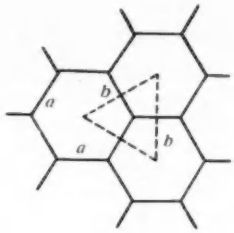

Fig. 4. The area occupied by a carbon atom in graphite layer.

$$N=4L_a^2/3\sqrt{3}\,a^2 \quad (11)$$

On the basis of this table the authors are inclined to think that they have derived a relation between the density and the molecular weight of carbon blacks.

Summary

The density (ρ) of the polycyclic aromatic hydrocarbons, from benzene (C_6H_6) to circumanthracene ($C_{10}H_{16}$), are correlated closely to the number of carbon atoms (N) included in the molecule. We may be expressed the relation as $\log(1/\rho-1/\rho_\infty)=-(1/2)\log N+0.120$, in which ρ_∞ is the density of graphite, 2.26. The agreement of the computed values with the observed results is satisfactory. A trial to apply the equation to calculate the density of carbons is made with some success.

The authors express hearty thanks to Professor H. Akamatu for his kind direction in this work. The cost of this research has been defrayed from the Scientific Research Encouragement Grant from the Ministry of Education to which the authors' thanks are due.

Department of Chemistry
Faculty of Science
The University of Tokyo
Hongo, Tokyo

12) H. Kuroda, *J. Colloid Sci.*, **12**, 496 (1957).

Formation and Aging of Precipitates. X. An Electron Micro-Diffraction Study on Crystal Habit of Barium Sulfate Precipitates*

By Kazuyoshi TAKIYAMA

(Received July 19, 1958)

The shapes of precipitated particles of sparingly soluble salts are usually classified into groups of perfect crystals having simple forms and dendrites having irregular forms. The author has previously reported the relationship between the condition of precipitation and the shape and size of precipitated particles of barium sulfate, by the direct mixing of reagents[1]. The rectangular perfect crystals were prepared from a solution below about 0.0005 M of initial concentration of barium sulfate, and the spindle-shaped dendrites having rugged edges were prepared in a range of initial concentration from about 0.001 to 0.2 M. Above 0.5 M, the precipitate was jelly-like at the beginning, but it changed gradually to the crystalline precipitate. Fischer[2] also studied the morphology of barium sulfate precipitates by electron microscopy and reported that the crystals formed as elevated temperature were somewhat more perfect than those formed at room temperature, and that the fairly perfect crystals were formed when very dilute solutions of reagents were mixed slowly by ionic diffusion through a thin membrane.

An attempt has been made in the present investigation to employ the electron micro-diffraction method for clarifying the crystal habit of barium sulfate.

Sample.—Solutions of 0.001 and 0.1 M barium chloride were placed in small beakers, which were kept at room temperature and at 80°C. Small thin films of Formvar were then floated on the surface of the solutions, and a drop of 0.001 M sulfuric acid was placed on each film. A few minutes were allowed for the reactant ions to diffuse slowly through the thin film and form the precipitates. Then the films with the drops were removed with the aid of a glass slide and refloated on the surface of water in another beaker. About ten minutes were allowed for diffusion of ions from the drop of mother liquid into the water below. Then the films with drops were scooped with specimen grids. After drying the specimen, the precipitates were observed with an electron microscope.

Rectangular perfect crystals were formed from 0.001 M solution independently of the reaction temperature. Dendrites were formed from 0.1 M solution. The growth direction of dendrite was dependent on the reaction temperature as mentioned later. The crystals formed by the diffusion mixing method are generally thin laminae, so they are suitable to study by the electron diffraction method. Crystals precipitated by the direct mixing of reagents have the same morphological characteristics as those precipitated by the diffusion mixing of ions, when the concentration and the reaction temperature are kept at the same condition.

Results

Morphology of Barium Sulfate Precipitates by Electron Microscopy.—A perfect crystal of barium sulfate is a rectangular platelet as shown in Fig. 1a. In a particular case of precipitation in dilute aqueous alcohol, octagonal or hexagonal platelet is formed as shown in Fig. 3a.

The dendrite prepared at room temperature is made of two main stems crossed perpendicularly to each other, which grow from the center of the crystal. Many primary and secondary branches are seen which grow from the main stems parallel to the stems (Fig. 4a). The dendrites prepared at elevated temperature are shown in Figs. 7a and 8a. The primary branches grow obliquely to the main stems crossed perpendicularly with each other (Fig. 7a). The main stems of the crystals shown in Fig. 8a has defects, and the large protuberances of these crystals correspond to the primary branches of the crystals shown in Fig. 7a. The secondary branchings are parallel to the primary branches, that is, they are oblique to the main stems (Figs. 7a and 8a). The relation of the main stems and the branches are shown in Figs. 9a and b.

* The nineth paper of this series, This Bulletin, **31**, 950 (1958).

1) E. Suito and K. Takiyama, ibid., **27**, 121, 123 (1954); **28**, 305 (1955).

2) R. B. Fischer, *Anal. Chem.*, **23**, 1667 (1951); R. B. Fischer and T. B. Rhinehammer, ibid., **25**, 1544 (1953).

The dendrite grows generally in two-dimension as shown by a replica of crystal in Fig. 10. The dendrite shown in Fig. 11 is sometimes observed. Here the platelet particle is set perpendicular to the supporting film. The crystal seems to be a twin, and twin planes estimated to be (110) were observed.

Analysis of N-Pattern Obtained by Electron Micro-Diffraction Method. — All electron diffraction patterns obtained from the crystals in the present study are N-patterns. The arrangement for orientation between the electron microscopic image and the electron diffraction pattern as well as the fixing of the index of each reflection spot were made as follows. The image of electron microscope is rotated at a certain angle with respect to the electron diffraction pattern owing to the difference of lens current. The method for an arrangement of these two images is described below, in Fig. 1 as an example. The electron diffraction pattern obtained from a selected crystal in Fig. 1a is shown in Fig. 1c. When the current of the intermediate lens is increased a little more than the value which gives the diffraction pattern, a pattern shown in Fig. 1b is obtained. In Fig. 1b the small bright field image appears at the center of the pattern and many small dark field images appear at the similar positions to the electron diffraction spots. The orientations of the bright and dark field images are the same, so the relative orientation of the electron microscopic image to the electron diffraction pattern can be known. All crystals are, of course, barium sulfate and belong to V_h^{16}. The reciprocal lattice of barium sulfate crystal and the intersection with Ewald sphere are obtained. Then N-pattern constructed is compared with that obtained by experiment (Fig. 1c), and the Miller's indices of reflection spots are fixed as shown in Fig. 2b.

Crystal Habit of Barium Sulfate Precipitates by Electron Micro-Diffraction Method. — All electron micrographs and diffraction patterns shown in this paper are arranged to the same orientation. Electron diffraction patterns obtained from most crystals are N-patterns same as that shown in Fig. 2b. From this, it has been revealed that the platelet crystals have grown along (100) plane. The laminae that give the N-pattern shown in Fig. 2b are perpendicular to the electron beam.

The short- and the long-axes of rectangular crystal shown in Fig. 1a are *b*- and *c*-axes respectively as shown in Fig. 2a. The normal to the platelet is *a*-axis. The normal to the octagonal lamina shown in Fig. 3a is also *a*-axis, and the side planes of that crystal are {010}, {011} and {001} groups.

The main stems of dendrite shown in Fig. 4a have grown to the direction along

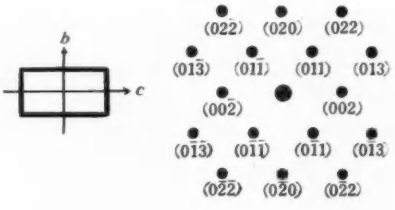

(a) (b)

Fig. 2. The direction of axes and the indices of electron diffraction pattern of perfect crystal of barium sulfate shown in Fig. 1.

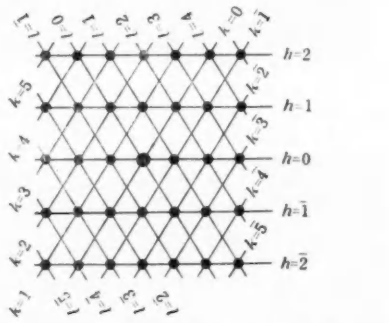

Fig. 6. The indices of electron diffraction pattern of dendrite of barium sulfate shown in Fig. 5.

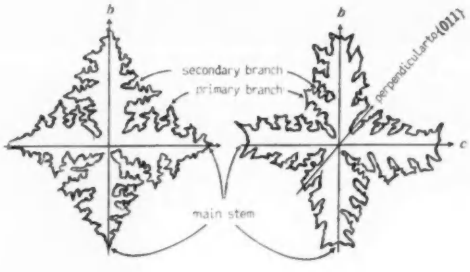

a b

Fig. 9. Schematic diagrams of two typical dendrites of barium sulfate crystals.
a: room temperature
b: 80°C

b- and *c*-axes. Small branchings also grow in parallel to these axes (Fig. 9a). The platelet of dendrite shown in Fig. 5a was placed inclined to the electron beam, and the angle between *a*-axis (normal to platelet) and the electron beam was proved 64° from the analysis of N-pattern as shown in Fig. 6. The main stems of the dendrite shown in Fig. 7a have grown along *b*- and *c*-axes, but the branches have grown to the direction perpendicular to the plane of {011} group (Fig. 9b). The dendrites shown in Fig. 8a have grown markedly to the direction perpendicular to the plane of {011} group.

Consideration

Generally speaking, when a crystal grows from a dilute reagent, the growth rate is so small that the perfect crystal is formed. The perfect crystal of barium sulfate is generally a rectangular platelet and the octagonal or hexagonal crystal is formed in a rare case.

Dendrite of barium sulfate crystal is formed in a range of initial concentration from about 0.001 M to 0.2 M. At the concentration above this range, the rate of nucleation is very rapid, so numerous nuclei appear but their growth immediately after mixing of reagents does not proceed. At the concentration below that range, the rate of nucleation is very slow and a small number of nuclei grows slowly to the perfect crystals. In the range of initial concentration mentioned above (0.001 to 0.2 M), both rates of nucleation and growth are a little more rapid than that in the case just mentioned above, and the edge or the corner of a crystal grows preferentially to form the dendrite.

Watson and Freemann[3] believed that the dendrite formed in an iron sol is composed of aggregated small cubic particles. However, the electron diffraction pattern of the dendrite of barium sulfate is N-pattern, which indicates a single crystal and that the crystal has grown from a single nucleus to the dendrite.

Summary

Barium sulfate precipitates in a form of rectangular perfect crystal from a solution of low initial concentration, and in a form of dendrite from a solution of higher initial concentration. They are platelets grown along (100) plane. The short- and long-axes of rectangular crystal are *b*- and *c*-axes respectively. The dendrite grows along *b*- and *c*-axes, or along the direction perpendicular to the plane of {011} group.

The author acknowledges his thanks to Professor Eiji Suito of Kyoto University for his guidance and discussion. He also wishes to express his hearty thanks particularly to Professor Masayoshi Ishibashi of Kyoto University for his continual advice and encouragement.

Institute for Chemical Research
Kyoto University
Takatsuki, Osaka

3) J. H. L. Watson and M. W. Freemann, *Kolloid-Z.*, **148**, 127 (1956).

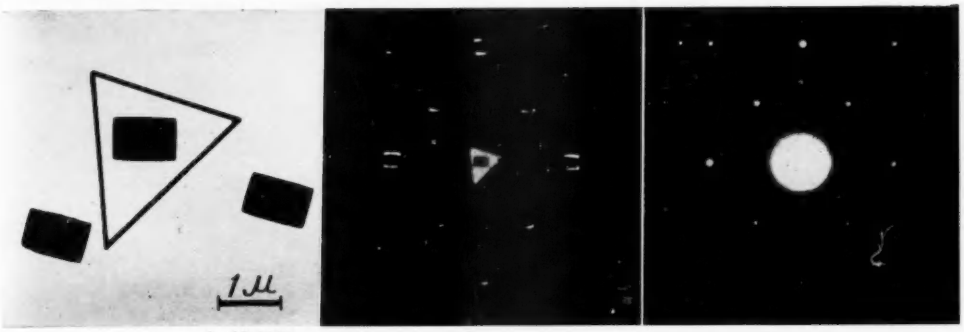

a (×10,000) b c

Fig. 1. Perfect crystal of barium sulfate prepared by diffusion mixing of 0.001 M H_2SO_4 and 0.001 M $BaCl_2$ at room temperature.

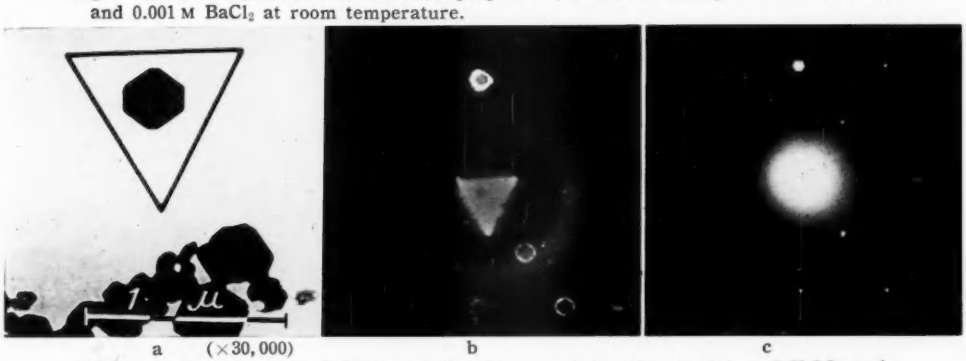

a (×30,000) b c

Fig. 3. Perfect crystal of barium sulfate prepared by direct mixing of H_2SO_4 and $Ba(OH)_2$ at the initial concentration of 0.05 M in 2.5% aqueous alcohol medium at room temperature.

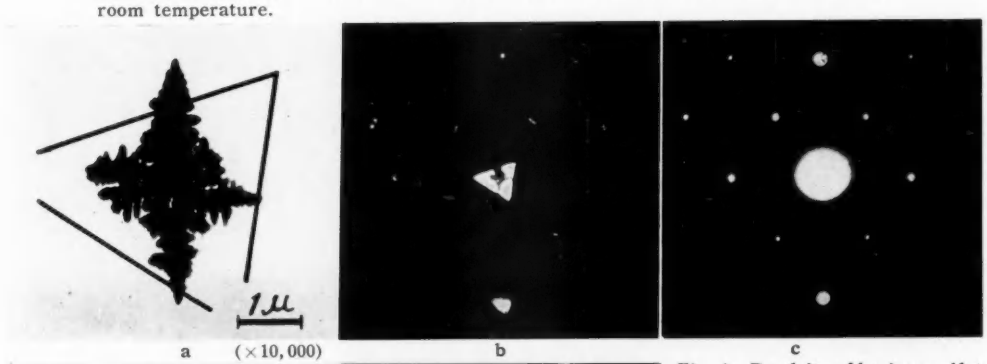

a (×10,000) b c

Fig. 4. Dendrite of barium sulfate prepared by diffusion mixing of 0.001 M H_2SO_4 and 0.1 M $BaCl_2$ at room temperature.

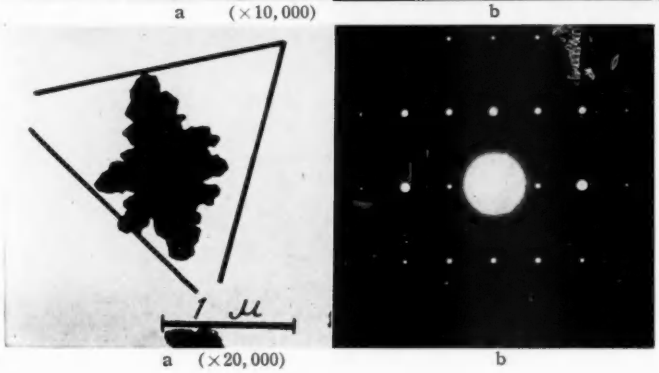

a (×20,000) b

Fig. 5. Dendrite of barium sulfate prepared by direct mixing of H_2SO_4 and $Ba(OH)_2$ at the initial concentration of 0.02 M at room temperature.

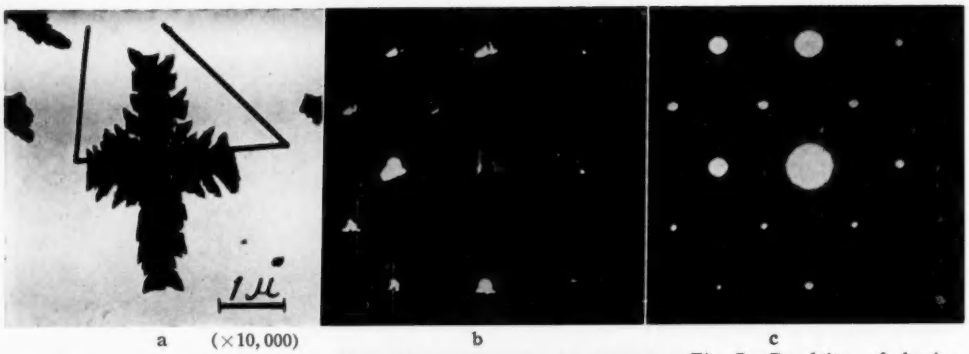

a (×10,000) b c

Fig. 7. Dendrite of barium sulfate prepared by diffusion mixing of 0.001 M H_2SO_4 and 0.1 M $BaCl_2$ at 80°C.

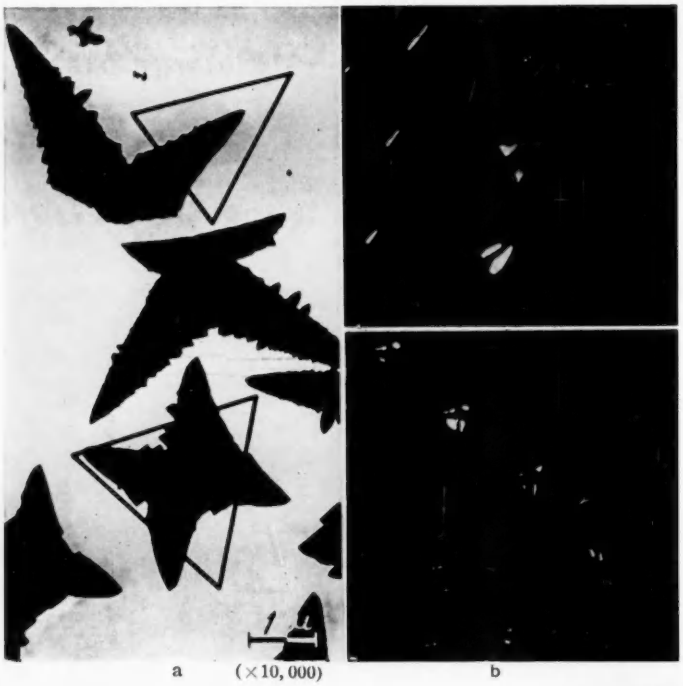

a (×10,000) b

Fig. 8. Dendrite of barium sulfate prepared by diffusion mixing of 0.001 M H_2SO_4 and 0.1 M $BaCl_2$ at 80°C.

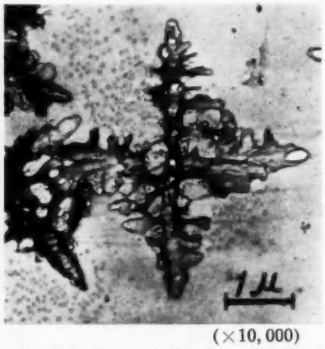

(×10,000)

Fig. 10. Replica of dendrite of barium sulfate prepared by direct mixing of 0.001 M H_2SO_4 and 0.1 M $BaCl_2$ at room temperature.

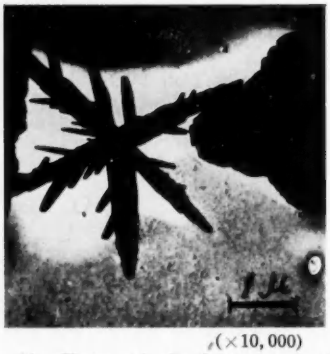

(×10,000)

Fig. 11. Twin of dendrite of barium sulfate prepared by direct mixing of H_2SO_4 and $Ba(OH)_2$ at the initial concentration of 0.01M at room temperature.

Untersuchungen über die Bildung der Proteinase aus einem Aspergillus awamori-Stamm. II. Charakterisierung des Proteinasebildungsvermögens des Mycels im Kultursverlauf durch seinen Stickstoffwechsel

Von Jiro HOSHINO

(Eingegagen am 23. Juli, 1958)

Aus dem ausgewaschenen ruhenden Mycel des Schimmelpilzes, ebenso wie Bakterie sind reichliche Mengen von Enzyme im reinen Zustand leicht zugänglich. Die Enzymbildung wird aber bei diesem experimentalen System durch verschiedene äussere Faktoren stark beeinflusst. Es ist bekannt, wie auch der Verfasser in der vorigen Mitteilung[1] über die Proteinasebildung bestätigt hat, dass sich das Vermögen der Zelle zur Enzymbildung, die eine der Mikroorganismus eigenen biochemischen Aktivitäten darstellt, mit der Züchtungsdauer ändert.

Nach der Angabe von O. Tanabe[2] wurde das Amylasebildungsvermögen des *Asp. oryzae*-Stammes in den früheren Stufen der Züchtung grösser erwiesen. Derselbe Tatbestand wurde von C. P. Hegarty bei der „*adaptiven*" Bildung von Enzyme aus *Streptococcus lactis* festgestellt[3]. Die Bakterien betreffend wurden noch von mehreren Forschern darüber mit den mannigfachen Ergebnisse verfolgt[4-8].

Es liegt nahe anzunehmen, dass verschiedene Stoffe innerhalb des Mycels für die Änderung dieser physiologischen oder biochemischen Aktivitäten verantwortlich sind, von denen die Nucleinsäuren als Spezifität-Donator und die Aminosäuren als Bausteine des Enzymproteins eine entschiedene Rolle spielen sollen.

Da die Ergebnisse über die Änderung des Proteinasebildungsvermögens mit der Züchtungsdauer, die der Verfasser in der vorigen Mitteilung kurz dargelegt hatte, eine sehr Wichtige zu bedeuten scheint, hat der Verfasser nun diese vorige Aufgabe wieder sich aufgestellt, um damit tiefere Übersicht auf die Beziehung des Proteinasebildungsvermögens mit dem Sammelbecken von Aminosäuren des Mycels und seinem Stickstoffwechsel gewinnen zu können.

1) J. Hoshino, Dieses Bulletin, **31**, 883 (1958).
2) O. Tanabe und K. Tonomura, *J. Agr. Chem. Soc., Japan* (*Nippon Nōgei-Kagaku Kaishi*), **30**, 596 (1956).
3) C. P. Hegarty, *J. Bact.*, **37**, 145 (1939).
4) E. F. Gale, "Chem. Act. of Bacteria" p. 51, Academic Press, Inc., New York, (1948).
5) D. Billen, *J. Bact.*, **61**, 515 (1951).
6) M. J. Pinsky, ebenda, **64**, 337 (1952).
7) M. Suda, *Symp. Enz. Chem.* (*Kōso Kagaku Symposium*), **4**, 18 (1950).
8) J. Fukumoto und T. Yamamoto, *J. Agr. Chem. Soc. Japan* (*Nippon Nōgei-Kagaku Kaishi*), **31**, 421 (1957).

Arbeitsmethode

Bestimmung des Proteinasebildungsvermögens des Mycels.—Zur Ermittelung des Proteinasebildungsvermögens des Mycels wurde die Aktivität der in die Kulturflüssigkeit sezernierten Proteinase nach dem zwanzigstündigen Schütteln des ausgewaschenen Schüttelmycels (1.0 g feuchtes: ungefähr 0.2 g trocknes), welches aus den verschiedenen Phasen einer Entwicklungskultur abgeerntet worden war, in der 1.0 prozentige Glucose haltigen M/5-Phosphatpufferlösung (pH=6.1) nach der Folinschen Methode bestimmt und mit derselben pro g trocknes Mycels angegeben. Diese Aktivität wird vom Verfasser provisorisch als „*potentiale Aktivität des Proteinasebildungssystems*" (PAPS) bezeichnet.

Züchtung des Pilzes und Gewinnung des ausgewaschenen Schüttelmycels wurden in der vorigen Mitteilung ausführlich dargelgt.

Bestimmung des organischen Stickstoffs des Mycels.—Zur Bestimmung des organischen Stickstoffs des Mycels wurde die semi-mikro Kjeldahlsche Methode nach A. O. A. C. verwendet. Den organischen Gesamtstickstoffgehalt hat der Verfasser experimentell in zwei Gruppen, d. h. Proteine- und non-Proteine-N, eingeteilt, wobei der erstere denjenigen Gesamtstickstoff bedeutet, der sich in der 5.0 prozentigen Trichloressigsäure löslichen Fraktion befindet. Den letztere kann man rechnerisch leicht erreichen. Bestimmung dessen ist wie folgt: Das üblicherweise gut ausgewaschene und abgepresste Mycel (ungefähr 0.2 g trocknes) wurde mit 40 ccm 5 prozentiger Trichloressigsäurelösung 20 Minuten am Rückfluss gekocht. Das Extrahieren wurde in analoger Weise noch zweimal wiederholt. Sodann wurde das rückstehende Mycel getrocknet und zur Ermittelung des Stickstoffs herangezogen.

Ergebnisse

Abhängigkeiten der PAPS und N-Konstitution des Mycels von seinen Entwicklungsphasen. — Das Proteinasebildungsvermögen (PAPS) des Mycels und seine Gehalte am Gesamt-(N_t), Proteine-(N_p) und non-Proteine-N(N_{np}) wurden in den verschiedenen Entwicklungsphasen ermittelt, um damit auf die Frage zu beantworten, welche Bestandteile an die Biosynthese von Proteinase teilnehmen. Die Resultate sind in der Abb. 1 illustriert.

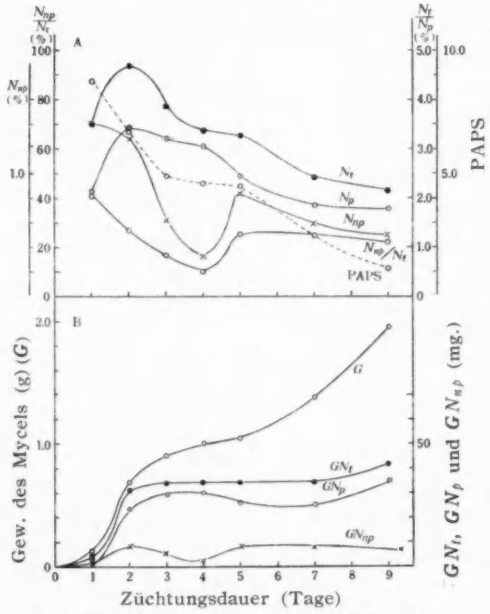

Abb. 1. Abhängigkeiten der PAPS und N-Konstitution des Mycels von seiner Züchtungsdauer.
N_t: totaler Stickstoffgehalt des Mycels
N_p: Proteinstickstoffgehalt des Mycels
N_{np}: non-Proteinstickstoffgehalt des Mycels

Die Sporen wurden in der vorliegenden Arbeit nicht behandelt, weil die Dauer kurz nach dem Impfen dieselbe der Keimung darstellt und der Stoffwechsel dabei von der Mycelentwicklung recht verschieden sein soll[9].

Vom ersten bis zum zweiten Tagen nach dem Impfen hat sich das Mycel sehr stark entwickelt, und solche Phase wurde 4~5 Tage danach wieder beobachtet. Dass das Mycel in dieser Entwicklungsphase allmählich reicher an N_t und N_p, und im Gegenteil armer an N_{np} geworden ist, ist es nun bedeutungsvoll. Daraus geht es klar hervor, dass in dieser Entwicklungsphase die Myceleiweisskörpern aus den Aminosäuren kräfting synthetisiert werden, wobei also der anabolische Stoffwechsel den Eiweissstoff betreffend eine dominierends Rolle spielt. Vom 4 Tage nach dem Impfen fängt der Amino-N Gehalt des Mycels plötzlich an zuzunehmen und dementsprechend fängt der N_p Gehalt an abzunehmen. In Anbetracht, dass der Gesamt-N inzwischen unveränderlich bleibt, (Abb. 1, B) müssen die Aminosäuren innerhalb des Mycels unter dem Verbrauch von Myceleiweisskörpern anhäufen. In dieser Phase scheint daher der catabolische Stoffwechsel den Eiweisskörper betreffend in analogem Sinne eine dominierende Rolle zu spielen.

Die in der Figur gegebenen Versuche zeigen weiter, dass sich das Proteinasebildungsvermögen (PAPS) in der anabolischen Phase allmählich erschwächt und es gerade mit dem Aminosäuregehalt des Mycels gleichläuft. Daraus folgt es, dass die Proteinasebildung von der Menge der inneren Aminosäuren beschränkt wird, und sich vermindert, wenn die Aminosäuren zur Myceleiweissstoffbildung verbraucht worden sind.

Den Züchtungsverlauf in der Figur kann man in zwei „Lebenskreise" einteilen, von denen das Erste einen typischen Entwicklungs- oder Stoffwechselsprozess bietet: die catabolische Phase entspricht der „*lag*" Phase und die anabolische Phase der „*log*" d.h. kräftig entwickelnden Phase. Das Mycel, das sich zwischen diesen beiden Phasen befindet und also die Aminosäuren am meisten enthält, hat das grösste Proteinasebildungsvermögen in jedem Kreis.

Beziehung der Änderung des Vermögens zur Mycelentwicklung mit der Proteinasebildung. — Da das Mycel, das ein erhebliches Vermögen zur Proteinasebildung besitzt, nicht dasjenige, das ein sich kräftig entwickelendes Mycel, sondern dasjenige ist, das sich in der Vorstufe der „*log*" Phase befindet und damit, wie aus der Abb. 1 ersichtlich ist, uns seine kommende kräftige Entwicklung erwarten liess, hat der Verfasser das potentiale Entwicklungsvermögen des Mycels in den jeden Phase in folgender Weise ermittelt: 1.0 g wie üblich dargestelltes Schüttelmycel wurde in die frische Nährlösung unter sterilen Bedingungen übergetragen und weiter bei

9) T. Yanagita, *Arch. für Mikrobiol.*, **26**, 329 (1957).

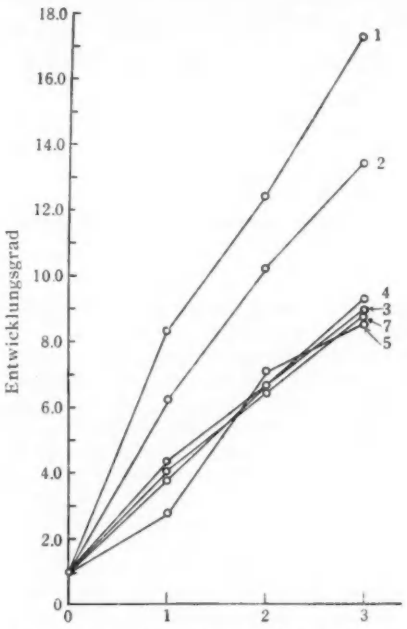

Abb. 2. Entwicklungsverläufe der in verschiedenen Entwicklungsphasen abgeernteten Mycel. Die Ziffern in der Figur zeigen die Züchtungsdauer an.

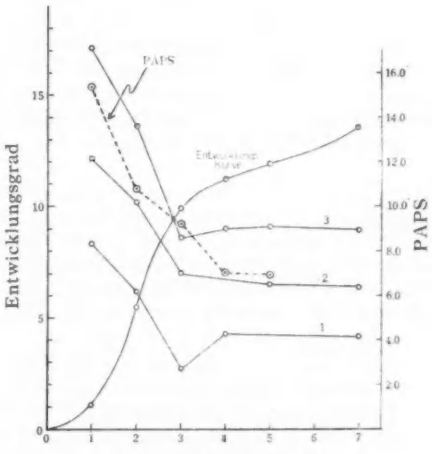

Abb. 3. Abhängigkeiten der PAPS und Entwicklungsvermögens des Mycels von seiner Züchtungsdauer. Die Ziffern in der Figur zeigen die Schüttelungsdauer bei der Entwicklungsprüfung an.

30°C fortgeschüttelt. Je nach 1, 2 und 3 Tagen wurde je ein Kolben abgebrochen und die sich entwickelte Mycel abgeerntet, ausgewaschen, sodann zur Wägung getrocknet.

Als Entwicklungsgrad wurde das Gewichtsverhältnis dieses Mycels zum unterworfenen Mycel ermittelt. In der Abb. 2 werden die Entwicklungsgrade der Mycel verschiedener Züchtungsphasen in Kurvenform gegeben. Dabei ergab es sich, dass das jüngere Mycel ein grösseres Entwicklungsvermögen besitzt, ohne „*lag*" Phase zu zeigen. Die Mycel in den Züchtungsphasen von 3, 4, 5 und 7 Tagen zeigten aber beinahe gleichartige Entwicklungsverläufe. Diese Umstände sind auf der Abb. 3 leicht begreiflich. Hierbei wurde es gezeigt, dass ein deutlicher Parallelismus zwischen dem Proteinasebildungs- und dem Entwicklungsvermögen des Mycels auch in diesem Falle besteht.

Der „*lag*" Phase des zweiten "Lebenskreises" entpricht also die Phase, wovon die Fläche der Kurven des Entwicklungsvermögens beginnt. Während der Prüfung über das Entwicklungsvermögen wurde keine massgebende Bildung der Proteinase beobachtet.

Unter Berücksichtigung dieser Tatsachen wurde es festgestellt, dass das erhebliche Proteinasebildungsvermögen einem Mycel gehört, welches ein kräftiges Entwicklungsvermögen besitzt und reichliche Mengen von Aminosäuren enthält. Diese Erscheinungen stellen daher vermutlich zwei Seiten eines Attributes dar, und sie antagonieren einander gegen ein Sammelbecken von Aminosäuren. Dieser Befund steht in voller Übereinstimmung mit den Untersuchungen von M. Nomura[10], in denen er eine antagonistische Biosynthese von Amylase durch *Bacillus subtilis* gegen dieselbe der Zelleiweissstoffen beobachtet und die Amylasebildung als „*abnorme*" Biosynthese bezeichnet hat.

Beziehung des Proteinasebildungsvermögens der in verschiedenen Bedingungen entwickelten Mycel mit seinem Amino-N Gehalt. — Aus den hierher geschilderten Ergebnisse schien der Aminosäuregehalt des Mycels bei der Proteinasebildung eine dominierende Rolle zu spielen. In Anbetracht dessen wurden die N-Bestandteile desjenigen Mycels in Bezug auf seine Proteinasebildungs- und Entwicklungsvermögen untersucht, das sich unter der

10) M. Nomura, J. Hosoda, B. Maruo und S. Akabori, *J. Biochem.*, **43**, 841 (1956).

TABELLE I

PAPS UND N-KONSTITUTION DES SICH UNTER VERSCHIEDENEN BEDINGUNGEN ENTWICKELTEN MYCELS

N-Quelle % C-Quelle %	Gew. des Mycels in mg	N_t (%)	N_p (%)	N_{np} (%)	N_{np}/N_t (%)	PGA*	PAPS**
NH_4NO_3 4 % Rohrzucker 4 %	312	5.7	3.5	2.2	38.3	4.6	5.1
NH_4NO_3 1.5% Rohrzucker 10 %	345	5.2	3.6	1.6	29.8	4.4	5.5
NH_4NO_3 0.2% Rohrzucker 20 %	427	4.0	3.2	0.8	20.8	4.7	6.2

* Entwicklungsvermögen: dies wurde mit dem Entwicklungsgrad der 24-stündigen Prüfung angegeben.

** Proteinasebildungsvermögen: dies steht im Text geschrieben.

variierenden N-Konzentration entwickelt hatte. Die Ergebnisse sind in der Tabelle I zusammengestellt.

Dabei hat es sich ergeben, dass kein wesentlicher Parallelismus zwischen dem Aminosäuregehalt und den beiden Vermögen des Mycels besteht, während es dem Verfasser gelungen ist, auf obige Weise den Aminosäuregehalt des Mycels zu verändern. Daraus darf festgestellt werden, dass der Gehalt des Mycels an Aminosäuren nicht immer für die Proteinasebildung ein entschiedener Faktor ist. Doch ist es so zu deuten, dass das Mycel, das erhebliche Proteinasebildungs- und Entwicklungsvermögen besitzt, stets reichliche Aminosäuren darin enthält.

Die Aufgabe, was für ein Substanz auf die Proteinasebildung in diesem experimentalen System eine dominierende Rolle spielt, bleibt auf Grund der oben dargelegten Resultaten noch unlöslich und bedarf noch weitere Untersuchungen.

In der vorliegenden Arbeit wurde am Schlusse das Proteinasebildungsvermögen des Mycels im Kultursverlauf in Bezug auf das Mycelentwicklung durch seinen Stickstoffwechsel charakterisiert.

Schlusswort

Die Proteinasebildungsvermögen des Pilzmycels wurde in Anbetracht seines Stickstoffwechsels verfolgt. Gleichungen wurden durch die Verfolgungen der Änderung der Stickstoffskonstitution und des Entwicklungsvermögens des Mycels im Kultursverlauf abgeleitet, um damit auf die Frage zu beantworten, ob ein Sammelbecken von Aminosäuren bei der Biosynthese von Proteinase eine dominierende Rolle spielt.

Es wurde gezeigt, dass ein „Lebenskreis" des Mycels in einige metabolische Phasen, d. h. catabolische und anabolische usw. eingeteilt wird und dass Mycel, das sich zwischen diesen beiden Phasen befindet, wo der Vorstufe der gebräuchlichen „*log*" Phase entspricht und Aminosäuren am meisten enthalten sind, das grösste Proteinasebildungsvermögen zeigt.

Das erhebliche Proteinasebildungsvermögen gehört zu einem Mycel, welches neben dem grossen Sammelbecken von Aminosäuren ein kräftiges Entwicklungsvermögen besitzt.

Aus dem Versuch mit dem Mycel, das sich unter der variierenden N-Konzentration entwickelt hatte, wurde es aber festgestellt, dass der Aminosäuregehalt des Mycels nicht immer für die Proteinasebildung ein dominanter Faktor ist.

In der vorliegenden Arbeit konnte der Verfasser zusammenfassend das Proteinasebildungsvermögen des Mycels im Kultursverlauf in Bezug auf das Mycelentwicklung durch seinen Stickstoffwechsel charakterisieren.

Zum Schlusse ist es mir eine angenehme Pflicht, Herrn Professor Dr. N. Taketomi, und Herrn ausserordentlichen Professor H. Suzuki für ihre vielfache Anregungen und Revisionen bei der Anfertigung dieser Arbeit meinen besten Dank auszusprechen.

Laboratorium der Gärungs- und Biochemie
Abteilung für Angewandte Chemie
Naturwissenschaftlich-Technische Fakultät
Universität Waseda, Shinjuku-ku, Tokyo

Dichroism of Dyes in the Stretched PVA Sheet. II[1]. *The Relation between the Optical Density Ratio and the Stretch Ratio, and an Attempt to Analyse Relative Directions of Absorption Bands**

By Yoshié TANIZAKI

(Received July 26, 1958)

Hitherto, dichroic properties have been mainly utilized to investigate dyeing mechanism[2] or the percentage orientation of fibres[3]. A conclusion derived from a number of experimental results shows that almost all dye molecules in dyed state should lie lengthwise along the cellulose chains[4]. In the previous paper[1], this conclusion was applied to presume the relative direction of transition moments of absorption bands of certain direct dyes in the stretched polyvinyl alcohol sheet from their dichroic properties. A similar attempt may not be applied to short molecules which show poor dichroism, and it is still more difficult, as it is not sure that such molecules are adsorbed on a fibre so as to orient parallel to the fibre axis. However, the fact that an observed optical density ratio (to be defined later) depends upon the stretch ratio of the sheet may give a key to analyse the direction of transition moment of the absorption band of the dye molecule. The purpose of this paper is to derive an expression for the density ratio as a function of the stretch ratio, to apply it to absorption bands of certain basic dyes, and to analyse their relative direction.

Experimental

Materials.—Polyvinyl alcohol (abbreviated to PVA) with the polymerization degree of about 1500 was used for preparing sheets by the method described in the previous paper[1].

Dyes used were crystal violet and auramine yellow which were recrystallized twice from ethanol, starting from the pure ones produced in the Laboratory of Hodogaya Kagaku Co., Ltd. The paper chromatography detected no colored impurities in these dyes.

PVA sheets, swollen fully in distilled water, were soaked in the aqueous dye solution at room temperature.

Measurements.—Measurements were carried out with a Shimadzu QB-50 spectrophotometer, in filter hole of which a sheet-polarizer of PVA-iodine[5] was set. To determine the correlation between the electric vector of polarized incident light and the stretching direction of the sample sheet, an apparatus shown in Fig. 1 was used. A colored and an uncolored PVA sheet were respectively pasted on a metal ring to be fixed in R_1 and R_2. The disk D graduated 0° to 360° on its circumference can be rotated at will in concentric with the toothed wheel G_1, and at the same time the rotation is transmitted through G_2, being used as a change gear, to R_1 and R_2. Gear ratios are all the same. This apparatus is set in the cell box of the spectrophotometer in place of

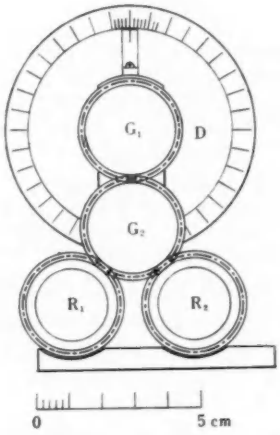

Fig. 1. Apparatus for rotating sample sheets.

1) Part I of this series, Y. Tanizaki and N. Ando. *J. Chem. Soc. Japan, Pure Chem. Sec.* (*Nippon Kagaku Zasshi*), **78**, 542 (1957).

* Presented at 11th Annual Meeting of the Chemical Society of Japan, April 1958.

2) T. H. Morton, *J. Soc. Dyers Col.*, **62**, 272 (1946); H. H. Summer, T. Vickerstaff and E. Waters, ibid., **69**, 181 (1953).

3) J. M. Preston, ibid., **47**, 312 (1931); D. R. Morey, *Tex. Research*, **4**, 491 (1934); **5**, 105 (1935); J. M. Preston and P. C. Tsien, *J. Soc. Dyers Col.*, **62**, 368 (1946); **66**, 361 (1950); J. M. Preston and Y. F. Su, ibid., **66**, 357 (1950); D. R. Morey and E. V. Martin, *Tex. Research J.*, **21**, 607 (1951).

4) T. Vickerstaff, "The Physical Chemistry of Dyeing", Second Edition, Oliver and Boyd, London (1954), p. 183.

5) Y. Tanizaki, This Bulletin, **30**, 935 (1957).

the cell holder. Thus the correlation mentioned above was determined by means of the Malus' law.

Notations.—A circle drawn on the sheet before stretching is deformed into an ellipse after stretching. The ratio of the long axis of the ellipse to the short one is defined as the *stretch ratio* R_s[6]. $D_{\parallel}$ and $D_{\perp}$ are optical densities for completely and linerly polarized lights whose electric vectors are respectively parallel and perpendicular to the stretching direction. An *optical density ratio* R_d is then defined as $D_{\parallel}/D_{\perp}$.

Theoretical

Let us suppose that an imaginary sphere in substrate of PVA sheet is deformed, being kept at a constant volume by stretching into a spheroid. If the optical property around the stretching direction were isotropic and any unit vector with an angle θ_0 against the stretching direction in the sphere were transformed into a unit vector with θ in the spheroid, the distribution of vectors after stretching, $f(\theta)$, would be determined in the following way,

$$f(\theta)=\int_0^{\pi/2} G(\theta,\theta_0)F(\theta_0)\mathrm{d}\theta_0 \qquad (1)$$

where $F(\theta_0)$ means a function of distribution before stretching, and $G(\theta,\theta_0)$ is a function of transformation which makes θ_0 transform to θ by stretching. Since it is natural to consider that the distribution of vectors before stretching is quite at random, then $F(\theta_0)$ may be expressed as follows,

$$F(\theta_0)=\sin\theta_0$$

or

$$=\frac{\tan\theta_0}{\sqrt{1+\tan^2\theta_0}} \qquad (2)$$

On the basis of the assumption that the deformation takes place under a constant volume, the relation between θ_0 and θ is expressed as follows,

$$\tan\theta_0=R_s\tan\theta$$

where R_s is the axial ratio of the ellipsoid and is equal to the stretch ratio mentioned above. Then the transformation function may be written as follows

$$G(\theta,\theta_0)=\delta(\tan^{-1}(R_s\tan\theta)-\theta_0)\rho(\theta_0) \qquad (3)$$

where δ is a delta-function and ρ is a surface element, namely

$$\rho(\theta_0)=R_s\frac{\sin\theta_0\cos^2\theta_0}{\sin\theta\cos^2\theta} \qquad (4)$$

By the combination of Eqs. 1, 2, 3 and 4,

$$f(\theta)=\int_0^{\pi/2}\delta(\tan^{-1}(R_s\tan\theta)-\theta_0)\times\frac{R_s}{\sin\theta\cos^2\theta}\frac{\tan^2\theta_0\,\mathrm{d}\theta_0}{(1+\tan^2\theta_0)^2}$$

The interval of this integration involves zero. So that, according to the nature of δ-function[7], this integration becomes equal to the integrand excluding δ-function, in which θ_0 is replaced by $\tan^{-1}(R_s\tan\theta)$, that is,

$$f(\theta)=\frac{R_s^3\tan^2\theta}{\sin\theta\cos^2\theta(1+R_s^2\tan^2\theta)^2}$$

or

$$f(\theta)=\frac{R_s^3\sin\theta}{\{1+(R_s^2-1)\sin^2\theta\}^2} \qquad (5)$$

where $R_s\geq 1$ and $0\leq\theta\leq\pi/2$. Determining $N(R_s)$ so as to make the integration with respect to θ unity, namely,

$$\int_0^{\pi/2}N(R_s)f(\theta)\mathrm{d}\theta=1$$

$N(R_s)f(\theta)$ for several values of R_s provides the curves shown in Fig. 2. This figure indicates that for large R_s values, that is, when the PVA sheet is stretched to a high degree, the greater part of vectors becomes able to meet the stretching direction. This

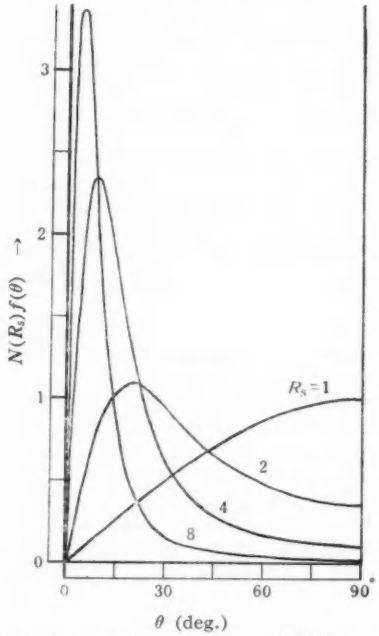

Fig. 2. Distribution curves, $N(R_s)f(\theta)$, for several values of the stretch ratio, R_s.

6) E. H. Land, *J. Opt. Soc. Am.*, **41**, 957 (1951).

7) P. A. M. Dirac, "Quantum Mechanics", Third Edition, Oxford (1947), p. 58.

will correspond to a distribution of a characteristic direction, which is regarded as a vector and is called hereafter an *orientation axis*, of the molecular species. So that, when the direction of the transition moment corresponding to an absorption band is on the orientation axis, the problem is rather easy to be dealt with. For the present purpose, however, it is necessary to consider a general case where transition-directions of dye molecules do not always coincide with orientation axes. Therefore, it will be convenient to introduce here an imaginary plane made of an orientation axis and a direction of transition moment. This plane does not necessarily coincide with the usual molecular plane, and is temporarily called a *light absorption-plane*. The transition moment μ of an absorption band can be decomposed into two components within the light absorption-plane, one of which is normal and the other parallel to the orientation axis, namely μ_b and μ_a respectively. Consequently, if the value of $|\mu_a/\mu_b| = r$ can be obtained, $\cot^{-1} r$ will give the angle of a direction of transition against the orientation axis of a molecule.

Now, if we imagine rectangular coordinates in the PVA substrate, so as to run the Z axis parallel with the stretching direction (see Fig. 3), and if the angle between Z and μ_a is θ, then three components of μ_a can be written as follows,

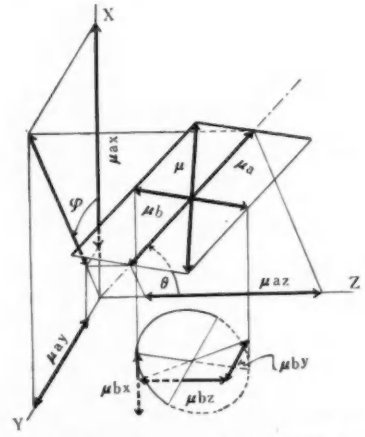

Fig. 3. Rectangular coordinates in the PVA substrate, of which the Z axis is taken parallel to the stretch direction of the PVA sheet. A transition moment μ of a dye molecule is decomposed to a parallel component μ_a and a normal μ_b to the orientation axis in the light absorption-plane.

$$\begin{aligned} \mu_{aX} &= \mu_a \sin\theta\cos\varphi \\ \mu_{aY} &= \mu_a \sin\theta\sin\varphi \\ \mu_{aZ} &= \mu_a \cos\theta \end{aligned} \tag{6}$$

where φ is the angle between X and the projection of μ_a on the XY-plane. Similarly, corresponding ones for μ_b can be represented by

$$\begin{aligned} \mu_{bX} &= \mu_b(\cos^2\theta + \sin^2\theta\sin^2\varphi)^{1/2}\cos\phi \\ \mu_{bY} &= \mu_b\left(\frac{\sin^4\theta\sin^2\varphi\cos^2\varphi\cos^2\phi + \cos^2\theta\sin^2\phi}{\cos^2\theta + \sin^2\theta\sin^2\varphi}\right)^{1/2} \\ \mu_{bZ} &= \\ &\mu_b\left(\frac{\sin^2\theta\cos^2\theta\cos^2\varphi\cos^2\phi + \sin^2\theta\sin^2\varphi\sin^2\phi}{\cos^2\theta + \sin^2\theta\sin^2\varphi}\right)^{1/2} \end{aligned} \tag{7}$$

where φ is the angle between the X axis-orientation axis-plane and the light absorption-plane. The angle θ takes values of zero to $\pi/2$, and φ and ϕ values of zero to 2π. Integration with respect to φ and ϕ must be averaged for the region. Thus the components of μ for the X, Y and Z directions should be of the form

$$\begin{aligned} \mu_X^2 &= \int_{\theta=0}^{\pi/2}\frac{1}{2\pi}\int_{\varphi=0}^{2\pi}\frac{1}{2\pi}\int_{\phi=0}^{2\pi} \\ &\quad \times(\mu_{aX}^2 + \mu_{bX}^2)N(R_s)f(\theta)\mathrm{d}\phi\mathrm{d}\varphi\mathrm{d}\theta \\ &\text{etc.} \end{aligned} \tag{8}$$

Substitution of Eqs. 6 and 7 for Eq. 8, and integrations with respect to φ and ϕ, give

$$\begin{aligned} \mu_X^2 = \mu_Y^2 &= \frac{1}{4}\int_0^{\pi/2}\{2\mu_a^2\sin^2\theta \\ &\quad + \mu_b^2(1+\cos^2\theta)\}N(R_s)f(\theta)\mathrm{d}\theta \\ \mu_Z^2 &= \frac{1}{2}\int_0^{\pi/2}(2\mu_a^2\cos^2\theta \\ &\quad + \mu_b^2\sin^2\theta)N(R_s)f(\theta)\mathrm{d}\theta \end{aligned} \tag{9}$$

Since the optical density D is proportional to μ^2, it may be possible to write

$$R_d \equiv \frac{D_\parallel}{D_\perp} = \frac{\mu_Z^2}{\frac{1}{2}(\mu_X^2 + \mu_Y^2)} = \frac{\mu_Z^2}{\mu_X^2} \tag{10}$$

For non-stretched state, i. e. $R_s = 1$, integration of Eq. 9 gives $\mu_X^2 = \mu_Y^2 = \mu_Z^2 = \mu^2/3$. Hence the following relation can be obtained by the aid of Eq. 10,

$$R_d = 1 \quad (R_s = 1)$$

For $R_s > 1$, combination of Eqs. 9 and 10, and integration with respect to θ give

$$R_d = \frac{2 + 2(2r^2-1)T(R_s)}{(2r^2+1) - (2r^2-1)T(R_s)} \tag{11}$$

where

$$T(R_s)=\frac{R_s^2}{R_s^2-1}\left\{1-\frac{N(R_s)}{\sqrt{R_s^2-1}}\log(R_s+\sqrt{R_s^2+1})\right\}$$

$$N(R_s)=2\left\{\frac{1}{\sqrt{R_s^2-1}}\log(R_s+\sqrt{R_s^2-1})+R_s\right\}^{-1}$$

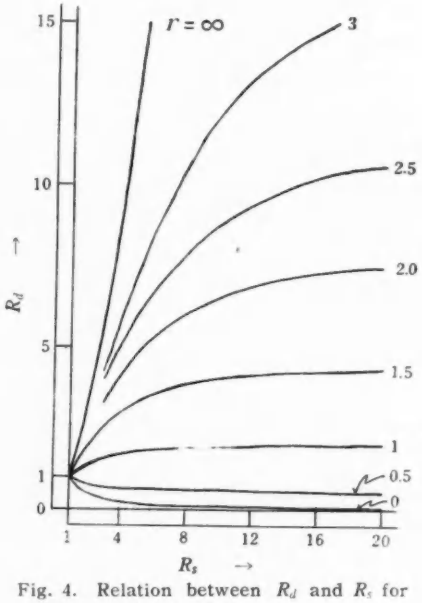

Fig. 4. Relation between R_d and R_s for various values of r.

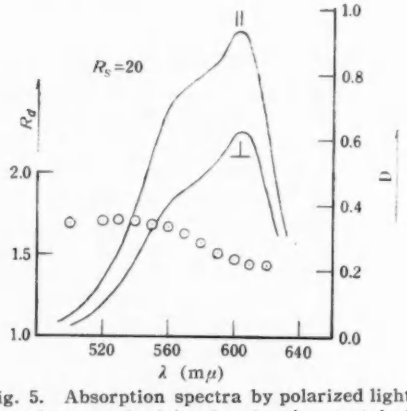

Fig. 5. Absorption spectra by polarized light of the crystal violet ion in the stretched PVA sheet. ∥ means the absorption curve when the electric vector of incident light is parallel and ⊥ means when the vector is normal to the stretch direction. Circles indicate the optical density ratio, R_d.

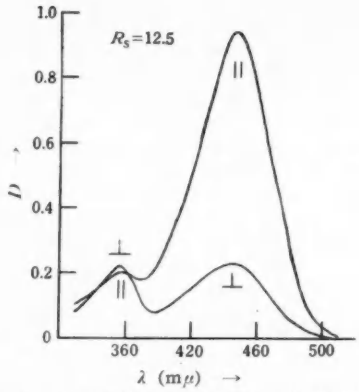

Fig. 6. Absorption spectra by polarized light of the auramine yellow ion in the stretched PVA sheet. The meaning of ∥ and is the same as in Fig. 5.

and $R_s>1$.

This is the final expression. Plotting R_d against R_s for various values of a parameter r curves representing Eq. 11 are obtained as shown in Fig. 4.

Results

Absorption spectra by polarized light of the crystal violet and the auramine yellow ion in stretched PVA sheets are shown in Figs. 5 and 6, respectively. Fig. 5 shows that the crystal violet ion has an absorption maximum at about 605 mμ and a shoulder at about 560 mμ, and that R_d values near the shoulder are larger than that at the absorption maximum. Fig. 6 shows that the auramine yellow ion has the first (445 mμ) and the second (~375 mμ) band whose dichroic properties are different from each other. This means that transition moments corresponding to these absorption bands have different directions.

Observed and calculated relations between R_d and R_s of each absorption band are shown in Figs. 7 and 8. Fig. 7 shows the case of the crystal violet ion; the observed values at 605 mμ are represented by the white circles and those of 560 mμ by the half solid circles, and the full lines are the curves obtained from Eq. 11 putting $r=0.86$ for the 605 mμ band and $r=0.90$ and 0.92 for the 560 mμ band. Similarly, Fig. 8 shows the result of the auramine yellow ion; the observed values for the first band are indicated by the white circles and for the second band (375 mμ)

by the half solid circles, and the corresponding full lines are calculated by Eq. 11 putting $r=1.55$ and 1.60 for the first band and $r=0.60$, 0.65 and 0.70 for the second band, respectively. In Fig. 8 it is noticed that, in the small region of R_s, the observed value of R_d are smaller for the first band and larger for the second band than the calculated ones represented by the full lines. This fact may be simply interpreted as the effect due to the overlap of both bands. That is to say, on account of the mutual superposition of the bands the first band with large R_d may apparently increase the small R_d value of the second band and the converse would hold good. For the large R_s value, however, the observed R_d values roughly run along the respective calculated lines. In the case of crystal violet (Fig. 7), the observed R_d values for small R_s values are smaller than the calculated ones, and these differences are larger at 560 mμ than at 605mμ.

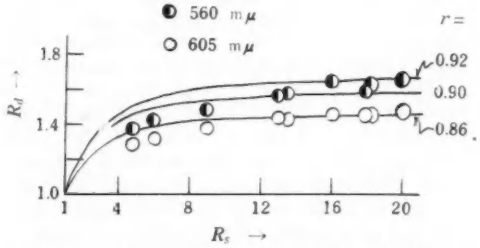

Fig. 7. Observed and calculated relations between R_d and R_s of the crystal violet ion in the stretched PVA sheet.

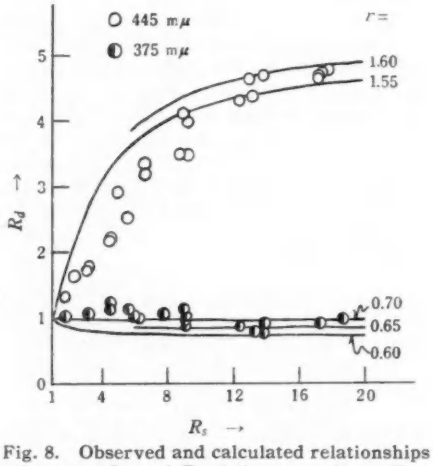

Fig. 8. Observed and calculated relationships between R_d and R_s of the auramine yellow ion in the stretched PVA sheet.

Thus, it can be said that Eq. 11 explains the experimental relation between R_d and R_s except for the smaller region of R_s and accordingly that Eq. 5 represents approximately well the nature of the distribution of such short molecules as the crystal violet ion in the stretched PVA substrate.

Discussion

The crystal violet ion. — Lewis and his coworkers[8] considered that the absorption band in the visible region of the crystal violet ion consists of those of isomers A and B. According to their consideration, the isomer A has a structure like a propeller with three blades (i. e. three benzene rings) and the isomer B has a similar form in which one blade is turned in the opposite direction from the others. As regards the absorption band here discussed, the main band belongs to the A isomer and the shoulder indicates the superposition of two bands A and B. In radially symmetrical molecules such as crystal violet, so-called x and y bands, which are both in the molecular plane[9], coincide with each other. In such a case, the transition moment is equal in all directions of the plane. This should be indeed the case of the A isomer. Furthermore, if we assume that the orientation axis is in the molecular plane, we should expect the value of r to be unity; that is, the angle of the direction of the transition moment against the orientation axis is expected to be 45°. According to our result, however, r equals to 0.86 and the corresponding orientation angle is $\cot^{-1} r = 49°$. On the other hand, though the B isomer has not the same symmetry as the A isomer, the apparent moment would be regarded to be still equal in all directions of the molecular plane of the B isomer in the statistical sense, because the spacial extent, which may be one principal factor to govern the orientation of the molecule, seems to be passably symmetrical considering its solid thickness. So that, also in the case of the B isomer the angle mentioned above would be expected again to be 45°. But the present result indicates that r equals 0.92~0.90, hence $\cot^{-1} r$ equals to 47.5°~48°.

Fig. 5 indicates that the R_d values near the absorption maximum are always

8) G. N. Lewis, T. T. Magel and D. Lipkin, *J. Am. Chem. Soc.*, **64**, 1774 (1942).
9) G. N. Lewis and J. Bigeleisen, ibid., **65**, 2102 (1943).

smaller than that of the shoulder. According to resolution of the observed band into those of isomers made by Lewis and his coworkers[8], the maximum corresponding to the isomer A is scarcely overlapped by the band of the isomer B, while the slope of the former almost covers the latter. This implies that the observed R_d value at the maximum wavelength gives the true R_d value for the A isomer, but the observed one at the shoulder, gives the smaller than the true value for the B isomer. Accordingly, it is considered that the absorption corresponding to the B isomer has the possibility of taking the r value of unity (i. e. the corresponding angle is 45°). From this fact we should be led to the conclusion that the orientation axis of the molecule deviates from its plane in the A isomer rather than in the B isomer. This seems indeed to be improbable from the point of view of their geometrical shapes. Therefore it seems wise to discard the abovementioned explanation and to adopt the alternative[10] that both bands originate from only one species. That is to say, the light absorption bands originate from two kinds of transition in one molecular species, one of which lies on the molecular plane and the other of which has two components parallel and normal to the plane. The former may correspond to the 560 mμ band and the latter to 605 mμ. Thus we can explain the experimental facts that the 560 mμ band has always the greater R_d value than that at 605 mμ, and the R_d value of the former has the possibility to take the r value of unity.

The auramine yellow ion.—For the first band of the auramine yellow ion, the corresponding r value is 1.55~1.60 (see Fig. 8). Accordingly the angle of the transition-direction against the orientation axis is 32.5°~32°. Similarly, since the most probable value of r for the second band is 0.65, the corresponding angle is obtained as 57°. Since the mutual correlation of the absorption planes of both bands is unfortunately unknown, the angle between two directions of the corresponding transition moments can not be decided directly. Nevertheless, when it is supposed that the absorption planes coincide with each other, namely when both transitions are on the same molecular plane, the angle just mentioned would be 57°+32°=89° or 57°−32°=25°. Here the former value approximates to a right angle. This fact is of interest, because, in such a molecule as the auramine yellow ion, there may exist the x and y bands which are on the molecular plane and at right angles to each other[9].

10) Y. Mori, Presented at the Symposium of Electronic State, Nagoya, Oct. 1956.

Summary

1) An expression for the optical density ratio was derived as a function of the stretch ratio.

2) Dichroism of the crystal violet and auramine yellow ion in stretched PVA sheets was observed, and the relation of the optical density ratio to the stretch ratio was plotted. It was shown that the theoretical expression derived here could explain rather well the experimental relation between these two quantities.

3) The analytical results were as follows. The main absorption band and the shoulder of the crystal violet ion did not orginate from the two isomers but were perhaps due to one species. For the auramine yellow ion the angle between the transition directions corresponding to the first and the second band might be approximately a right angle provided that the *absorption-planes* were in a same plane.

The author is indebted to Professor Noboru Ando and Dr. Ikuzo Tanaka for their encouragement to carry out this work and also to Dr. Hideo Yamazaki for his helpful suggestions on the theoretical part. Many thanks are due to Mr. Junzo Ito of Nippon Gosei Kagaku Co., Ltd. who gave polyvinyl alcohol, to Mr. Norio Ikari of Hodogaya Kagaku Co., Ltd. who gave the dye samples, and also to Mr. Toshiro Iijima who helped the author in chromatographical tests.

Laboratory of Physical Chemistry
Tokyo Institute of Technology
Meguro-ku, Tokyo

Studies on Antibiotics and Related Substances. VII. The Structure of Kanamycin

By Sumio UMEZAWA, Yukio ITŌ and Shunzō FUKATSU

(Received August 5, 1958)

Kanamycin has been described by H. Umezawa and coworkers[1] as an antibiotic produced by a strain of *Streptomyces kanamyceticus*. It is low toxic and very active against a variety of Gram-positive and Gram-negative bacteria including streptomycin-resistant strain. Kanamycin was isolated in a pure state as a crystalline monosulfate which was converted into a crystalline free base[2,3]. Analysis and electrometric titrations of the salt and the free base indicated that the antibiotic is a tetra-acidic base of the composition $C_{18}H_{36}O_{11}N_4$. Acetylation of kanamycin with acetic anhydride in methanol gave tetra-*N*-acetyl kanamycin[3,4]. On the other hand, when kanamycin was acetylated with acetic anhydride and pyridine, undeca-acetylkanamycin was obtained[4].

Information about the degradation products of kanamycin was obtained by studying the products formed by acid hydrolysis[3,4]. From the hydrolyzate of kanamycin by 6 N hydrochloric acid, Maeda, et al.[4], isolated two kinds of reducing aminohexoses and diamino-trihydroxycyclohexane which was identical with deoxystreptamine (I) isolated from the vigorous hydrolysis of neomycin[5]. Moreover, Ogawa and Itō[6] obtained deoxystreptamine and two kinds of methylaminohexosides by methanolysis of kanamycin. Recently, we received an information from Hooper and others[7] that they identified the two aminohexose-moieties of kanamycin to be D-6-amino-6-deoxyglucose (pyranose form) (II) and 3-amino-3-deoxyaldohexose (pyranose form) (III).

Therefore, the hydrolytic cleavage of kanamycin could be represented by the following equation:

$$C_{18}H_{36}O_{11}N_4 + 2H_2O \rightarrow C_6H_{14}O_3N_2 + 2C_6H_{13}O_5N$$
(I) (II) and (III)

The present authors[8] recently reported in a short communication that the acid-hydrolysis of exhaustively methylated *N*-acetylkanamycin resulted in the isolation of mono-*O*-methyldeoxystreptamine which presents evidence to show that both of the two aminohexose moieties are directly joined to deoxystreptamine. The situation is different from streptomycin in which streptidine is linked with streptobiosamine, or from neomycin in which deoxystreptamine is linked with neobiosamine.

The present paper deals with the sites of glucosidic linkages occurring between the above-mentioned three moieties in detail.

The tetra-*N*-acetylkanamycin prepared by the method of Cron and others[3] was methylated with dimethyl sulfate and sodium hydroxide by the method of West and Holden[9] to yield a crude methylated product, which was chromatographed through a cellulose powder column to yield a colorless gum. The acetyl determination showed that the methylated product is partially de-*N*-acetylated. When the methylated product was acetylated again to make sure, the tetra-*N*-acetyl-hepta-*O*-methylkanamycin was obtained. It was further ascertained by infrared spectrum that no free hydroxyl group is contained in the methylated product.

The methylated product was hydrolyzed with 6 N hydrochloric acid. Paper chromatography studies of the hydrolyzate showed three ninhydrin positive spots of

1) H. Umezawa, M. Ueda, K. Maeda, K. Yagishita, S. Kondo, Y. Okami, R. Utahara, Y. Osato, K. Nitta and T. Takeuchi, *J. Antibiotics, Series A*, **10**, (5), 181 (1957).
2) K. Maeda, M. Ueda, K. Yagishita, S. Kawaji, S. Kondo, M. Murase, T. Takeuchi, Y. Okami and H. Umezawa, ibid., 228 (1957)
3) M. J. Cron, D. L. Johnson, F. M. Palermiti, Y. Perron, H. D. Taylor, D. F. Whitehead and I. R. Hooper, *J. Am. Chem. Soc.*, **80**, 752 (1958).
4) K. Maeda, M. Murase, H. Mawatari and H. Umezawa, *J. Antibiotics, Series A*, **11**, (2), 73 (1958).
5) F. A. Kuehl, M. N. Bishop, K. Folkers, L. H. Sommer, N. S. Marans, G. M. Goldberg, J. Rockett and P. P. Pioch, *J. Am. Chem. Soc.*, **73**, 881 (1951).
6) H. Ogawa and T. Itō, *J. Antibiotics, Series A*, **10**, (6), 267 (1957); ibid., **11**, (2), 70, 72 (1958).
7) M. J. Cron, O. B. Farding, D. L. Johnson, H. Schmitz, D. F. Whitehead, I. R. Hooper and R. V. Lemieux, *J. Am. Chem. Soc.*, **80**, 2342, 4741 (1958).
8) S. Umezawa, Y. Itō and S. Fukatsu, *J. Antibiotics, Series A*, **11** (5), 120 (1958).
9) E. S. West and R. F. Holden, *J. Am. Chem. Soc.*, **56**, 930 (1934).

R_f 0.08, 0.32 and 0.41 with a *n*-butanol-ethanol-water mixture. The hydrolyzate was evaporated to dryness, taken up in methanol and treated with ether to yield an amorphous precipitate, which consisted of the product of R_f 0.08, containing a small amount of the product of R_f 0.32. The precipitate was chromatographed through a cellulose powder column to yield the colorless, crystalline hydrochloride of mono-*O*-methyldeoxystreptamine (IV), which was optically inactive and, upon oxidation with periodate, consumed two moles of periodate without the formation of formic acid.

The hydrochloride was acetylated with acetic anhydride in pyridine to yield the colorless prisms of the diacetate (V) of mono-*O*-methyl-di-*N*-acetyldeoxystreptamine.

Finally, the diacetate was subjected to de-*O*-acetylation with ammonia in absolute methanol solution at 0°C to yield the colorless prisms of mono-*O*-methyl-di-*N*-acetyldeoxystreptamine (VI). This consumed no periodate and was also optically inactive.

The compounds (IV, VI) with the *O*-methyl group in the 5-position should be optically inactive while the compounds with the *O*-methyl group in the 4- or 6-position should be optically active. The di-*N*-acetyl compound (VI) with the *O*-methyl group in the 5-position should consume no periodate while the corresponding compound with the *O*-methyl group in the 4- or 6-position should consume one mole of periodate. The compound IV with the *O*-methyl group in the 5-position should be oxidized with two moles of periodate without the formation of formic acid while the corresponding compound with the *O*-methyl group in the 4- or 6- position should consume two moles of periodate with the formation of one mole of formic acid.

Therefore, the experimental evidences presented above have led the authors to conclude that the mono-*O*-methyl-deoxystreptamine (IV) is 1,3-diamino-4,6-dihydroxy-5-methoxycyclohexane and, considered with the previous findings, permit the assignment of structure VII to kanamycin.

Experimental

Methylation of *N*-Acetylkanamycin.—To a vigorously stirred solution of tetra-*N*-acetylkanamycin (4.0 g.) in water (8 cc.) was added a solution of dimethyl sulfate (52 g.) in carbon tetrachloride (40 cc.). During this and the subsequent addition of alkali the temperature of the reaction was kept at 50~55°C. A solution of sodium hydroxide (108 g.) in water (100 cc.) was then added dropwise over a one-hour period, with vigorous stirring. The temperature was then raised slowly to 70~75°C and dimethyl sulfate (103 g.) was added dropwise over a 30-minute period. Again, a solution of sodium hydroxide (36 g.) in water (30 cc.) was added and then dimethyl sulfate (52 g.) was added gradually in a 15-minute period. After this addition the water-bath was heated to boiling and kept at this temperature for 30 min. The temperature was then lowered to about 50°C and the mixture was stirred vigorously with chloroform (150 cc.) for 15 min. The mixture was filtered and the sodium sulfate precipitate was washed with chloroform. The aqueous portion of the filtrate was re-extracted with chloroform as described above. The chloroform extracts were combined and dried with sodium sulfate. Evaporation of the solvent in vacuo left an amber

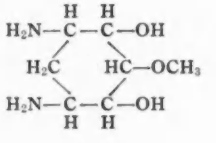

(IV)

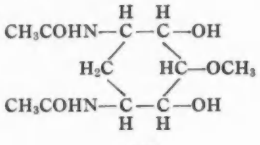

(VI)

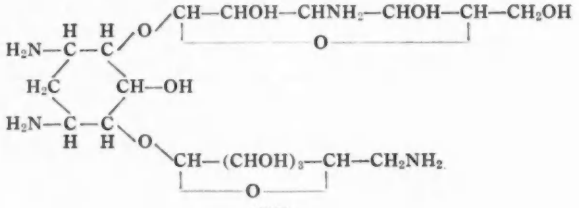

(VII)

Kanamycin

gum (3.22 g.) soluble in methanol, ethanol, chloroform and water. A sample was dried in vacuo at 60~70°C. The determination of methoxyl content gave 27.44% OCH_3.

The crude product (11.17 g.) was dissolved in a solution (30 cc.) of *n*-butanol-ligroin-water (38 : 60 : 2) and chromatographed on a column (2.5×40 cm.) of cellulose powder washed with the same solvent. Sixteen fractions of eluate with the same solvent were limited to 40 cc. each, evaporated in vacuo to dryness and weighed. Fractions 7-14 were combined to yield 7.0 g. of exhaustively methylated *N*-acetyl-kanamycin, m. p. 80°C (sintered at about 65°C). The determinations of methoxyl and acetyl content gave 28.35% OCH_3 and 12.25% $COCH_3$.

It was ascertained by infrared spectrum that no free hydroxyl group is contained in the methylated product.

A portion (2.5 g.) of the methylated product of tetra-*N*-acetylkanamycin was dissolved in absolute methanol (22.5 cc.) and to the solution acetic anhydride (4.3 cc.) was added. After being allowed to stand overnight, the acetylation mixture was filtered and evaporated to dryness. The residue was dissolved in water (20 cc.) and extracted thrice with chloroform (20 cc.). The chloroform extracts were combined and dried with sodium sulfate. Evaporation of the solvent left a colorless gum which resisted attempts to crystallize it (1.17 g.).

Anal. Found: OCH_3, 27.5; $COCH_3$, 21.6. Calcd. for $C_{15}H_{21}C_4(OCH_3)_7(NHCOCH_3)_4$: OCH_3, 28.9; $COCH_3$, 22.9. Calcd. for $C_{18}H_{22}O_5(OCH_3)_6(NHCOCH_3)_4$: OCH_3, 25.3; $COCH_3$, 23.4%.

Isolation of Mono-*O*-methyldeoxystreptamine Hydrochloride (IV) from Hydrolyzed Methylated *N*-acetylkanamycin.—Exhaustively methylated *N*-acetyl-kanamycin (7.0 g.) was refluxed with 6 N hydrochloric acid (100 cc.) for 1.5 hr. The reaction mixture was evaporated to dryness at 60°C in vacuo. The residue was dissolved in water (100 cc.) and evaporated again to dryness. The evaporation to remove hydrogen chloride was repeated thrice. The residue was dissolved in water (100 cc.) and the solution was decolorized with active charcoal (1.0 g.).

Paper chromatography of the hydrolyzate using the top-layer of *n*-butanol-ethanol-water (4 : 1 : 5) gave 3 zones with ninhydrin. The R_f values were 0.08 (brown), 0.32 (orange) and 0.41 (violet), respectively.

The decolorized solution was evaporated at 60°C in vacuo to dryness and dried in a desiccator overnight. The amber residue was dissolved in methanol (20 cc.) and the solution was diluted with ether (50 cc.) to yield a precipitate (1.90 g.). Paper chromatography of the precipitate using the above-mentioned solvent showed the main spot with R_f 0.08 (brown) and a trace with R_f 0.32 (orange).

The precipitate (1.90 g.) was dissolved in the top-layer (10 cc.) of *n*-butanol-ethanol-water (4 : 1 : 5) and chromatographed on a column (1.5×50 cm.) of cellulose powder (18 g.) washed with the same solvent. Twenty fractions of eluate with the same solvent were limited to 20 cc. each, evaporated to dryness in vacuo and weighed. Fractions 6—9 were combined to yield the crude hydrochloride of mono-*O*-methyldeoxystreptamine (1.65 g.).

Three recrystallizations from methanol-ethanol gave colorless needles (350 mg.) of the hydrochloride of 1, 3-diamino-4, 6-dihydroxy-5-methoxycyclohexane (IV), m. p. 207~209°C (decomp.), which was optically inactive.

Anal. Found: C, 34.03; H, 7.17; N, 10.94; OCH_3, 11.65. Calcd. for $C_6H_7(OH)_2(NH_2)_2(OCH_3)\cdot 2HCl$: C, 33.73; H, 7.23; N, 11.24; OCH_3, 12.45%.

Periodate Oxidation.—The accurately weighed sample (20.1 mg.) of 1, 3-diamino-4, 6-dihydroxy-5-methoxycyclohexane hydrochloride was dissolved in 0.023 N sodium periodate solution (20 cc.) and 2 cc. aliquots were titrated with 0.1 N sodium arsenite at the intervals listed in Table I, according to the procedure of Fleury and Lange[10]. Two moles of periodate was consumed without the formation of formic acid.

TABLE I
PERIODATE OXIDATION*

	Time (hr.)					
	0.5	1	2	3	4	6
1, 3-Diamino-4, 6-dihydroxy 5-methoxy-cyclohexane·2HCl	1.91	1.88	—	1.98	—	1.95
1, 3-Diacetamido-4, 6-dihydroxy-5-methoxy-cyclohexane	0.18	0.25	0.14	—	0.23	—

* Expressed in terms of moles of periodate consumed per mole of substance.

1, 3-Diacetamido-4, 6-diacetoxy-5-methoxycyclohexane (V).—The crude hydrochloride (1.2 g.) of 1, 3-diamino-4, 6-dihydroxy-5-methoxycyclohexane was acetylated with acetic anhydride-pyridine (18 cc. : 36 cc.) at 27°C for 24 hr. The acetylation mixture was concentrated to dryness at 40°C in vacuo; the residue was dissolved in water (20 cc.) and decolorized with active charcoal (0.5 g.). The filtrate was again evaporated to dryness in vacuo and dried in a desiccator overnight. The residue was washed with ether (30 cc.), and taken up in chloroform (20 cc.); a small quantity of insoluble part was filtered off and the filtrate was dried with sodium sulfate. Evaporation of the solvent was followed by extraction with hot ethyl acetate. Crystallization from the extract yielded colorless prisms (215 mg.), m. p. 220°C (decomp. sintered at about 170°C).

Anal. Found: C, 52.35; H, 6.65; N, 8.18; OCH_3, 9.22. Calcd. for $C_6H_7(OCH_3)(OCOCH_3)_2\cdot(NHCOCH_3)_2$: C, 52.32; H, 6.98; N, 8.14; OCH_3, 9.01%.

10) P. F. Fleury and J. Lange, *J. pharm. chim.*, [8] **17**, 107, 196 (1933).

The mother liquor was concentrated and allowed to stand at room temperature to yield the second crop of crystals (350 mg.).

1,3-Diacetamido-4,6-dihydroxy-5-methoxycyclohexane (VI). — A solution of 1,3-diacetamido-4,6-diacetoxy-5-methoxycyclohexane (460 mg.) in absolute methanol (130 cc.) was treated with a stream of dry ammonia gas for 1 hr. After being allowed to stand 3 hr. at room temperature, the mixture was evaporated at about 50°C in vacuo to dryness. The residue was dissolved in absolute methanol (50 cc.) and evaporated again to dryness in vacuo. The residue was taken up in absolute ethanol (30 cc.) and the solution was filtered to remove a small quantity of insoluble part. When the filtrate was concentrated and cooled, colorless needles crystallized out. Recrystallization from absolute ethanol yielded 130 mg. of 1,3-diacetamido-4,6-dihydroxy-5-methoxycyclohexane. The product was optically inactive.

Anal. Found: C, 50.94; H, 7.47; N, 10.64; OCH_3, 11.32; *N*-acetyl, 32.99, 33.87. Calcd. for $C_6H_7(OH)_2(OCH_3)(NHCOCH_3)_2$: C, 50.77; H, 7.69; N, 10.77; OCH_3, 11.9. *N*-acetyl, 33.08%.

Periodate Oxidation. — An accurately weighed sample (25.3 mg.) of 1,3-diacetamido-4,6-dihydroxy-5-methoxycyclohexane was dissolved in 0.0287 N sodium periodate (20 cc.) and 2 cc. aliquots were titrated with 0.1 N sodium arsenite at the intervals listed in Table I.

Summary

Evidence is presented to show that both the two aminohexose moieties in kanamycin are directly joined to deoxystreptamine through hydroxyl groups by glucosidic linkages. Proof for the sites of attachment of the two aminohexose moieties rests on the periodate oxidation of the optically inactive 1,3-diamino-4,6-dihydroxy-5-methoxycyclohexane and its *N*-acetyl derivative which were obtained by the degradation of exhaustively methylated *N*-acetylkanamycin by acid hydrolysis followed by acetylation. Kanamycin is therefore represented by formula VII.

The authors wish to express their appreciation to Professor H. Umezawa of National Institute of Health, Dr. I. R. Hooper of Bristol Laboratories and Dr. H. Ogawa of Research Laboratories of Meiji Seika Co. for helpful advice and to Meiji Seika Co. for the generous gift of kanamycin samples.

Department of Applied Chemistry
Engineering Faculty of Keio University
Koganei, Tokyo

Vapor Pressure of Molecular Crystals. XIII. Vapor Pressure of α-Glycine Crystal. The Energy of Proton Transfer

By Sadao TAKAGI*, Hideaki CHIHARA and Syûzô SEKI

(Received August 7, 1958)

Glycine is the simplest amino acid, having the zwitterion configuration within the crystal lattice[1]. Three modifications have been reported[2] and the α-form is probably the most stable one at room temperature. The molecular structure of glycine in the vapor phase is not known probably owing to low vapor pressure of the crystal. If glycine sublimes with the molecular configuration (and not the zwitterion configuration), a proton must be transferred from an NH_3^+ group of a zwitterion to a COO^- group of the neighboring zwitterion in the crystalline state. Or, in an alternative way, the proton transfer must occur in the vapor state after the zwitterion has sublimed, and this transfer undoubtedly accompanies greater energy change than it would in the crystalline state[3]. On the other hand, if the sublimation does not accompany the proton transfer, the heat of sublimation would be as great as that of an ionic crystal. The present study aims at the energetics of sublimation, with a hope of obtaining some information about such

* Present address, The Institute of Polytechnics, Osaka City University, Kita-ku, Osaka.

1) G. Albrecht and R. Corey, *J. Am. Chem. Soc.*, **61**, 1087 (1939); H. Baba, et al., *J. Chem. Soc. Japan, Pure Chem. Sec.* (*Nippon Kagaku Zasshi*), **70**, 333 (1949); K. Kuratani, ibid., **70**, 453 (1949).

2) Y. Iitaka, *Proc. Japan Acad.*, **30**, 109 (1954); J. Bernal, *Z. Krist.*, **78**, 363 (1931).

3) R. W. Gurney, "Ionic Processes in Solution", McGraw-Hill, N. Y., 1953.

proton transfer. The determination of the relative stability of the modifications of glycine crystals by measurements of vapor pressures presents another interesting problem but will not be considered here.

Experimental

Material.—Glycine (Organic Synthetic Chemicals Co., special grade) was recrystallized from aqueous solution repeatedly and dried over phosphorus pentoxide. The more satisfactory method of drying crystals by vacuum sublimation was not applied because it was found that sublimation gave a mixture of α and γ form of glycine. The modifications were identified by use of the X-ray powder diffraction patterns. Occlusion of water within the crystal lattice may cause a serious error in the measurement of vapor pressure[4] and it is highly probable particularly when we deal with crystals of polar molecules. Pieces of glycine crystals, of the same batch as that used for the pressure measurements, were heated in vacuo to see if the occluded water was present, with the result that no water evolution was detected up to the decomposition temperature, ca. 230°C. The constancy of the vapor pressure at a fixed temperature during a fixed length of time, a few hours, was considered to provide another assurance.

Measurements of Vapor Pressures.—The sublimation pressure was measured between 138 and 153°C with an apparatus, the same as the one reported elsewhere[5], based on the Knudsen effusion method.

Results.—The vapor pressures are listed in Table I. These data well fit the vapor pressure equation

$$\log P(\text{mmHg}) = 13.666 - (6816.8/T)$$

obtained by the method of least squares. The heat, entropy and free energy of sublimation derived from the equation are given in Table II.

TABLE I

VAPOR PRESSURE OF α-GLYCINE

t°C	P(mmHg) $\times 10^3$	t°C	P(mmHg) $\times 10^3$
138.9_8	1.344	145.9_7	2.459
140.6_6	1.557	147.3_3	2.877
142.0_9	1.789	149.2_6	3.289
143.4_9	1.978	150.6_6	3.899
144.7_9	2.360	152.6_8	4.362

TABLE II

HEAT, ENTROPY AND FREE ENERGY OF SUBLIMATION

Heat	Entropy	Free Energy at 298.16°K
31.18±0.49 kcal./mole	49.33±1.17 cal./deg.mole	16.47±0.60 kcal./mole

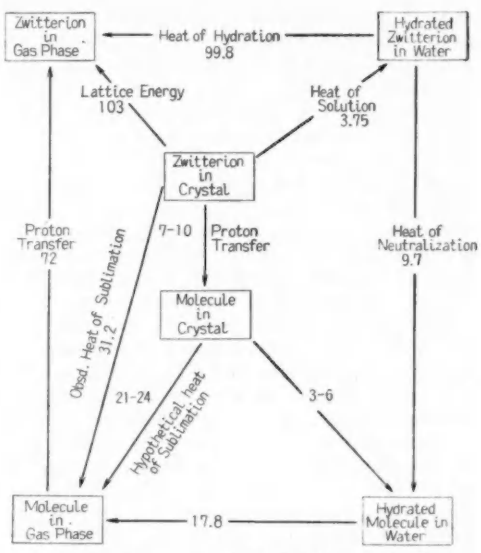

Fig. 1. Energy cycle of glycine (in kcal./mole). Arrows indicate the direction of endothermic changes.

Discussion of the Results

Fig. 1 illustrates an energy-cycle for glycine constructed by use of available thermochemical values. Arrows in Fig. 1 indicate the directions of endothermic changes. This is the final set-up of the energy diagram and we examined other possibilities also, because it was not a priori apparent that the measured heat of sublimation 31.2 kcal./mole corresponds to the change from 'zwitterion in crystal' to 'molecule in gas phase'.

It was first assumed that the observed 31.2 kcal. is the change in heat content in going from the crystal to zwitterions in vapor; in other words this value represents the lattice energy of the crystal if allowance is made for the average kinetic energy of dipolar-ions in vapor. An independent estimate of the lattice energy of glycine has been reported by Shimura from the measured partial molal volume of glycine in aqueous solution by help of Kirkwood's theory on the free energy of hydration[6]. This estimate gives the lattice energy a value as great as 103 kcal./mole. The dipole moment of glycine determined by Buckingham[7] (13.3D) shows

4) S. Seki, H. Chihara and K. Suzuki, "Hydrogen Bond", Iwanami Co. (1956), p. 40.

5) I. Nitta, S. Seki, M. Momotani and K. Sato, *J. Chem. Soc. Japan, Pure Chem. Sec.* (*Nippon Kagaku Zasshi*), **71**, 378 (1950).

6) K. Shimura, *J. Agr. Chem. Soc. Japan* (*Nippon Nōgei-Kagaku Kaishi*), **24**, 412 (1951).

7) A. D. Buckingham, *Australian J. Chem.*, **6**, 323 (1953).

that it is reasonable to assume that unit point charges rest on N and O atoms in a zwitterion so that the electrostatic interaction energy alone in the crystal would amount to about 60 kcal./mole. The total lattice energy including the van der Waals and the hydrogen bond energy will be at least 80 kcal./mole. Therefore our first assumption was wrong and the observed heat of sublimation must correspond not to the lattice energy but to the change in heat content in going from the crystal to molecules in vapor state.

Estimation of the heat of sublimation of a hypothetical crystal composed of glycine molecules, NH_2CH_2COOH.*—The van der Waals energy will contribute about 7.7 kcal. to this hypothetical lattice energy, which is the heat of sublimation[8] of 2-methyl-1-butene, a molecule which is isoelectronic with glycine. The following energy values are assigned to the three hydrogen bonds: 5~6 kcal. for the NH···O 2.76Å long (in diformylhydrazine[9] 2.80Å), 2.5~3.5 kcal. for the bifurcated bonds 2.93 and 3.05Å long (in urea[9] 2.99 and 3.04Å) and 3~4 kcal. for the bond of intermediate length 2.88Å. The sum of all these energy values 20.7~24.7 kcal./mole will be taken as the hypothetical heat of sublimation of molecular crystal of glycine**.

The energies of proton transfer.—By combining the hypothetical heat of sublimation with the observed heat of sublimation 31.2 kcal./mole, we see that the zwitterion crystal is more stable than the molecular crystal by about 7~10 kcal./mole, or in other words a proton transfer in the crystal (a change from $N^+H\cdots O^-$ to $OH\cdots N$) would accompany a heat absorption of 7~10 kcal./mole. If the proton transfer occurred in vapor state, the change

$$NH_2CH_2COOH \rightarrow NH_3^+CH_2COO^-$$

would accompany as much energy absorption as 72 kcal./mole and the "molecular" configuration would be extremely stable in vapor phase in contrast to the situation in the crystalline state. The result that the energy of proton transfer in vapor is about ten times as great as that in a crystal shows that the proton transfer can occur non-adiabatically in the crystal lattice: i.e. as a proton moves along the N···O bond by absorbing the necessary energy, the potential energy curve changes its shape as illustrated schematically in Fig. 2. The strong crystal field may be participating in such a change in the potential

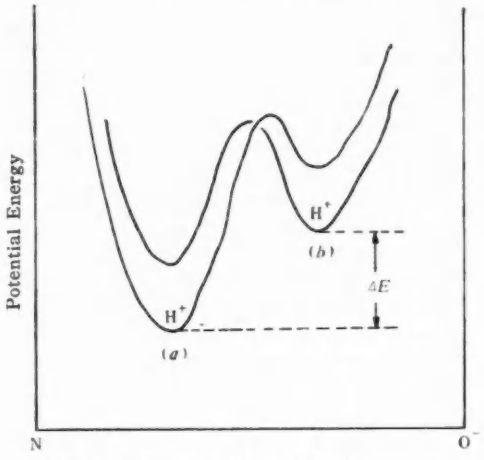

Fig. 2. Change of the potential energy curve in the course of proton transfer. ΔE is the energy of proton transfer (from *a* to *b*) in crystal.

energy diagram. Thus the energy of proton transfer in crystal here obtained does not represent the energy for a single proton to move within a fixed "double minimum" potential field, but the energy required for the overall rearrangement of electronic charges in the entire volume of a crystal is included.

This is a piece of information which we consider to be important in connection with energetics of hydrogen bonding. Participation of hydrogen bonding has often been assumed in various chemical reactions such as in simple hydrogen-deuterium exchange reactions and keto-enol isomerization reactions. Nuclear resonance studies in solution has come to attention of many investigators[10] in relation to the acid-base interaction and they will be one of significant methods of attack against proton transfer in solution.

Glycine is the simplest amino acid constituting complex protein molecules. In

* By hypothetical it is meant that the crystal structure is the same as that of the zwitterion-crystal except for the position of a hydrogen atom; actually the OH···O bonds would be formed if the molecular crystal were more stable.

8) S. S. Todd, G. D. Oilver and P. M. Huffman, *J. Am. Chem. Soc.*, **69**, 1519 (1947); D. W. Scott, G. Waddington, J. C. Smith and H. M. Huffman, ibid., **71**, 2767 (1949).

9) K. Suzuki, S. Onishi, T. Koide and S. Seki, This Bulletin, **29**, 127 (1956).

** The range of uncertainty was taken wide enough in order to cover the limit of validity of discussions.

10) J. N. Shoolery and B. J. Alder, *J. Chem. Phys.*, **23**, 805 (1955); E. Grunwald, A. Loenstein and S. Meiboom, ibid., **27**, 630, 641 (1957).

view of relatively small amount of energy required for a proton jump in a strong crystalline field, it may be reasonably supposed that such proton jumps can frequently occur in many protein systems with or without bound water molecules. Thus a diminishingly small degree of stimulation, given one end of a fibrous nerve protein coiled in a helical arrangement through NH···O hydrogen bonds, may easily be conveyed to the other end of that nerve protein by synchronous proton transfer. Such a mechanism, in fact, has been proposed by several authors[11] and we believe that we could here present some grounds for such speculative discussions.

The energy of proton transfer in vapor state may be very roughly evaluated by the sequence of changes:

$$NH_2CH_2COOH \underset{D}{\rightarrow} NH_2CH_2COO + H \underset{A}{\rightarrow}$$

$$NH_2CH_2COO^- + H \underset{I}{\rightarrow} NH_2CH_2COO^- + H^+$$

$$\underset{P}{\rightarrow} NH_3^+CH_2COO^-$$

D, A, I and P may be replaced by the bond dissociation energy of an O—H bond (110.2 kcal./mole), the electron affinity of an O atom (−87.7 kcal./mole), the ionization energy of a hydrogen atom (312.1 kcal./mole) and the proton affinity of an NH_3 molecule (−219 kcal./mole[12]), respectively. The overall change in energy will be 116 kcal./mole in comparison with 72 kcal./mole given in Fig. 1.

Estimation of the heat of self-neutralization in solution and other heats derived therefrom.—The process of self-neutralization in solution may be divided into two steps;

$$H_3N^+CH_2COO^- + H^+ = H_3N^+CH_2COOH - \Delta H_a$$

and

$$H_3N^+CH_2COOH = H_2NCH_2COOH + H^+ + \Delta H_b.$$

ΔH_a can be evaluated from the temperature variation of pK_a, giving 1.16 kcal./mole[13]. ΔH_b may be approximated by the heat (10.8 kcal./mole) associated with the change

$$H_3N^+CH_2COO^- = H_2NCH_2COO^- + H^+.$$

It is believed that this approximation will not cause a significant error since the reaction takes place in aqueous solution having the static dielectric constant larger than 80. The heat of self-neutralization will then be 9.7 kcal./mole (Fig. 1). This value was used to obtain the heat of solution of hypothetical crystals of molecular glycine 3~6 kcal./mole and the heat of solution of glycine vapor (heat of hydration) 17.8 kcal./mole, both giving a hypothetical solution of molecular glycine*. This is reasonable for a heat of hydration if we assume the hydrogen bond formation scheme like the following one:

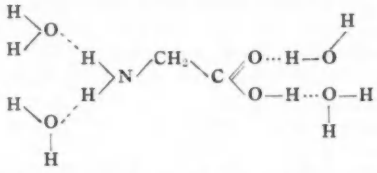

The difference 82 kcal./mole between the heat of hydration of zwitterion in vapor and the heat of hydration of molecules in vapor (giving ionic and molecular solutions, respectively) is a rough indication of the effect of ionic charge on N and O atoms when placed in aqueous solution.

Concluding remarks. — The molecular-dipolar ion (zwitterion) relationship now demonstrated for glycine is by no means an exceptional case but may be found in other more familiar systems such as ammonium chloride decomposing into ammonia and hydrogen chloride in the vapor state. Here are apparently the proton jumps occurring in sublimation process, to which a formal analogy of the present treatment may be applicable. It will be interesting to examine the movement of protons or the rôle of hydrogen bonding in more complex amino acids or polypeptides by more-or-less direct means.

Summary

Sublimation pressures of crystalline α-glycine were measured between 138 and 153°C by the effusion method. The pressure equation

$$\log P(\text{mmHg}) = 13.666 - (6816.8/T)$$

11) I. Oshida, Y. Oshika and R. Miyasaka, *J. Phys. Soc. Japan*, **10**, 849 (1955); M. L. Huggins, *Am. Scientist*, **31**, 338 (1943); N. Riel, *Naturwissenshaften*, **43**, 145 (1956).

12) H. Tsubomura, private communication.

13) E. J. Cohn and J. T. Edsall, "Proteins, Amino Acids and Peptides as Ions and Dipolar Ions", Reinhold, New York (1943), p. 80.

* This heat of hydration may be compared with the heat of hydration (7.8 kcal.) of propionic acid corrected for the difference in the interaction energy of a methyl group (3.4 kcal.) and that of an amino group (5.6 kcal.) with water, where it has been assumed that three water molecules accommodate to each of methyl and amino groups (cf. J. A. V. Butler, *General Discussion of the Faraday Soc. on the Structure and Molecular Forces in Pure Liquid and Solution*, 229 (1936));
$7.8+(3\times5.6)-(3\times3.4)=14.4$ kcal./mole.

fits well the experimental data. The heat, entropy and free energy (at 25°C) of sublimation were 31.18±0.49 kcal./mole, 49.33 ± 1.17 cal./deg. mole and 16.47 ± 0.60 kcal./mole, respectively. An energy cycle was constructed which correlates zwitterion and molecule in crystal and vapor states, and hydrated zwitterion and molecule in solutions. The observed heat of sublimation corresponds to the change in heat content in going from the zwitterion-crystal to gaseous molecules. The molecular configuration is more stable in vapor state. By using the experimental values of the heat of sublimation, the heat of solution of crystals into water and the temperature dependence of pK_a in solution, with the help of the theoretical values of the lattice energy of the crystal, the following heat values were determined; the heat of proton jump in vapor, $NH_3^+CH_2COO^- \rightarrow NH_2CH_2COOH$, −72 kcal./mole, the heat of proton jump in the crystal 7∼10 kcal./mole, hypothetical heat of sublimation of crystals composed of molecules 21∼24 kcal./mole, the heats of hydration of a zwitterion and a molecule −99.8 and −17.8 kcal./mole, respectively, the heat of solution of the hypothetical crystal to give a solution of molecular glycine 3∼6 kcal./mole, and the heat of self-neutralization in aqueous solution 9.7 kcal./mole. The negative quantities show that the processes are exothermic. It was shown that the proton transfer in a medium of large dielectric constant or in a strong crystalline field requires only a small amount of energy and its significance in chemical reactions and biochemical activities was suggested. Each of the derived heat values was examined by independent checks from different sources, except for the energies of proton transfer.

The authors wish to express their sincere gratitude to Professor I. Nitta for his interest in this research. They are also indebted to the Ministry of Education for the financial support.

Department of Chemistry
Faculty of Science
Osaka University
Kita-ku, Osaka

---

*Photometric Study on the Change of Basic Rhodochromium Ion to Basic Erythrochromium Ion in Aqueous Solution**

By Masayasu MORI, Shigeru UESHIBA and Hideo YAMATERA**

(Received August 7, 1958)

The so-called rhodochromium salt has attracted the attention of some investigators in coordination chemistry because of the peculiar reaction of its aqueous solution toward aqueous alkalis. This reaction may be represented by the scheme in Table I.

When Jörgensen discovered these salts, he thought that I and IV were isomers, while II was isomeric to III. Wilmarth, Graff and Gustin[1] investigated this problem using various methods. By careful analyses they denied this isomerism and found the correct formulae of the basic erythro salt and the erythro salt to be as given in Table I.

The reaction II → III may, therefore, be considered as a kind of replacement reaction of the coordinated ammonia molecule. Wilmarth and others called attention to the ease with which this reaction occurs and attributed it to the peculiar structure of the basic rhodo salt with a possible π-bonding as demonstrated by their magnetic measurements. They also found by visual observation that the reaction velocity is not affected by the hydroxide ion concentration ranging from 10^{-4} to 6.0 N in alkali.

It seemed to the present authors that the quantitative study of the kinetics of this reaction II → III would be of value in knowing the energy relation and the

* Presented at the Symposium on Coordination Chemistry, held in Nagoya on Nov. 16∼17, 1957.

** Present Address: Faculty of Science, Rikkyo University, Toshima-ku, Tokyo.

1) W. K. Wilmarth, H. Graff and S. T. Gustin, *J. Am. Chem. Soc.*, **78**, 2683 (1956).

TABLE I

THE RELATION BETWEEN THE RHODOCHROMIUM SALT AND ITS DERIVATIVES

Rhodochromium Salt		Erythrochromium Salt
$[Cr(NH_3)_5OHCr(NH_3)_5]X_5$		$[Cr(NH_3)_5OHCr(NH_3)_4OH_2]X_5$
(I)		(IV)
red		red
$\overset{Alkali}{\rightleftarrows}$		$\overset{Alkali}{\rightleftarrows}$
Basic Rhodochromium Salt		Basic Erythrochromium Salt
$[Cr(NH_3)_5OCr(NH_3)_5]X_4$	$\xrightarrow{Time}$	$[Cr(NH_3)_5OHCr(NH_3)_4OH]X_4$
(II)		(III)
blue		red

TABLE II

THE RESULT OF ANALYSIS OF DECAMMINE-μ-OL-DICHROMIUM(III) CHLORIDE PERCHLORATE

$[Cr(NH_3)_5OHCr(NH_3)_5]_2Cl_3(ClO_4)_7 \cdot xH_2O$

	Cr	N	Cl	Cl in ClO_4	H_2O
Calcd. $x=0$	15.02	20.22	7.68	17.91	0
Calcd. $x=2$	14.64	19.71	7.49	17.46	2.54
Found in Sample I	15.10	19.56	7.40	16.45	1.74
Found in Sample II	15.22	18.78	7.18	16.78	{2.8, 3.4
Found in Sample III	15.07	19.60	6.90	17.15	2.58
Found in Sample IV	15.27	19.82	7.53	17.02	1.57

The poor agreement of the analytical data with the calculated values in some samples is possibly due to the incomplete removal of perchloric acid owing to the fineness of crystals. Special attention has been paid in sample IV to avoid this. It seemed difficult to determine the content of water molecules on account of the slow decomposition of the complex at 100°C.

structure of the related compounds. These salts have characteristic absorption spectra in the visible and ultraviolet region and, therefore, the reaction velocities can be readily pursued by the aid of a spectrophotometer.

Experimental

Materials.—Decammine-μ-ol-dichromium(III) chloride perchlorate, $[Cr(NH_3)_5OHCr(NH_3)_5]_2Cl_3(ClO_4)_7 \cdot xH_2O$ has been used in most of the present research. The chloride prepared as described by Jörgensen was converted into this salt by dissolution in water and addition of perchloric acid. Even recrystallization with perchloric acid did not alter the composition. The preparation of the perchlorate was the first aim, but it was found fairly difficult owing to the high solubility and ready decomposition of the salt. The results of analyses of some chloride perchlorate preparations are given in Table II.

Absorption Measurements.—The absorption mearsurement was carried out with a Beckman DU spectrophotometer. In the kinetic study a solution of rhodo salt (about 0.004 g. ion/l. in 0.1 N perchloric acid) and an equal volume of aqueous ammonia (about 4 N) were first mixed. At the moment of mixing ($t=0$) the whole complex salt should be of the form of basic rhodo salt (II), which will be changed to basic erythro salt (III) as the reaction proceeds. Then at proper intervals the absorbance (A_t) at 392 mμ and the time (t) of the measurement were recorded. Finally the absorbance was measured after the lapse of sufficient time, when the reaction was virtually complete. This absorbance A_∞ should correspond to that of the basic erythro salt (III). It is readily seen that $A_t - A_\infty$ is proportional to the amount of the rhodo salt remaining at time t.

Results and Discussion

When $\log(A_t - A_\infty)$ is plotted against time, the resulting curves are nearly straight lines as shown in Figs. 1a~1d. The slight bending of the curve at the end of each experiment is possibly due to further decomposition of the basic erythro salt produced. A very slow change of absorbance is actually observed in a solution of purified basic erythro salt. However, its velosity is quite low compared with that of the main reaction and its effect seems negligible in the present discussion.

The reaction is, therefore, of the first order and represented by the equation:

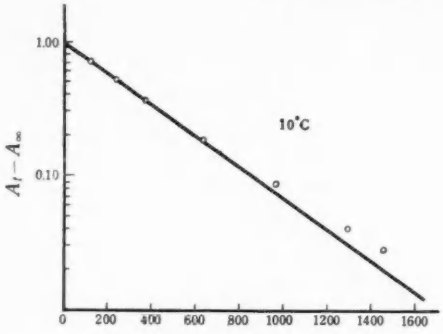

Fig. 1a.

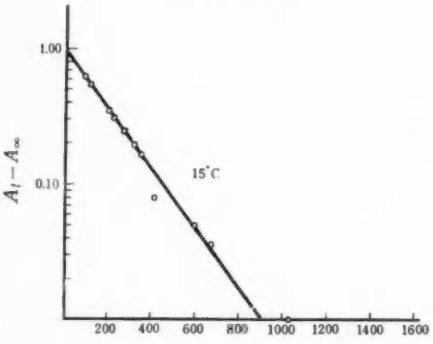

Fig. 1b.

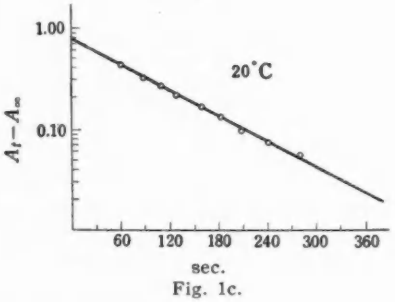

Fig. 1c.

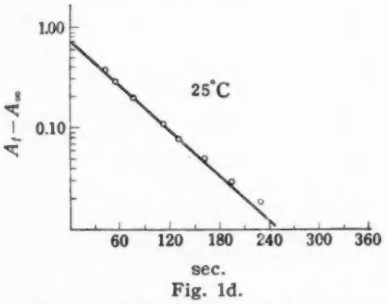

Fig. 1d.

Fig. 1. Change of A_t-A_∞ with time (in a semilog scale).

$$kt=\ln(A_0-A_\infty)-\ln(A_t-A_\infty)$$

where k is the velocity constant and A_0 is absorbance at $t=0$ and corresponds to the absorbance of the basic rhodo salt initially present. These values are readily estimated from the plot in Fig. 1. In Table III are given the velocity constant k and the half-value period $\tau=0.693/k$ obtained in this way.

TABLE III
THE VELOCITY CONSTANT AND HALF-VALUE PERIOD OF THE REACTION

T°C	10	15	20	25
$k\times10^3$	2.64	5.08	9.66	17.3
τ	258	136	72	40

The k values at different temperatures give us the energy of activation E, the frequency factor A and the entropy of activation ΔS^* according to the relations:

$$\ln k = \ln A - E/RT$$

$$\ln A = \ln(kT/h) + \Delta S^*/R - 1$$

The numerical data thus obtained are as follows: $E=21$ kcal/mole, $A=4.5\times10^{13}$ l./mole sec., $\Delta S^*=2$ kcal/deg. mole.

The effect of the hydroxide ion concentration on the reaction velocity was examined by the use of different species and concentration of alkalis. The result, given in Table IV, shows that the increase in

TABLE IV
THE EFFECT OF THE HYDROXIDE ION CONCENTRATION ON THE VELOCITY CONSTANT AT 10°C

Concentration of the complex (In the reacting system)	Concentration of the alkali (In the reacting system)	k
0.00215 g. ion/l.	2.25 N in NH_3	0.00264
0.00107 〃	〃 3.37 N in NH_3	0.00259
0.00107 〃	〃 0.0735 N in NaOH	0.00237
0.00215 〃	〃 0.490 N in NaOH	0.00223
0.00107 〃	〃 0.735 N in NaOH	0.00214

the hydroxide ion concentration caused the decrease in the observed velocity constant. This decrease in the reaction velocity may be due to the increase in the viscosity of the solution; but there is also a possibility that some side reactions or slow deposition of hydrous chromium oxide increased the apparent absorption, and consequently decreased the calculated velocity constant. However, the fact that the reaction is not accelerated by the hydroxide ion excludes the possibility of the S_{N2} mechanism involving a direct attack of the complex by the hydroxide ion.

The addition of sodium perchlorate to the reacting system at 20°C showed that the ionic strength over 0.08 to 1.32 has little effect on the velocity constant. When the concentration of sodium perchlorate exceeded 2.5F, the reaction velocity seemed to decrease, but the fluctuation of the data was significant. This fluctuation may be due to the formation of a fine precipitate of basic rhodo perchlorate even though not visually perceptible.

As seen from the preceeding argument, the aqueous solution of basic rhodo salt is unstable, so that it is difficult to obtain its absorption spectrum directly. When the kinetic data are available, however, the absorbance of the basic rhodo salt (A_0) can be derived from A_t and A_∞ by calculation or on the graph. The curve of the absorption spectrum drawn in this way is shown in Fig. 2. The very characteristic feature of the absorption spectrum probably demonstrates the different electronic structures of the basic rhodo salt from those of other chromium ammines, but the assignment of any electronic transition to each observed absorption band possibly requires a further investigation.

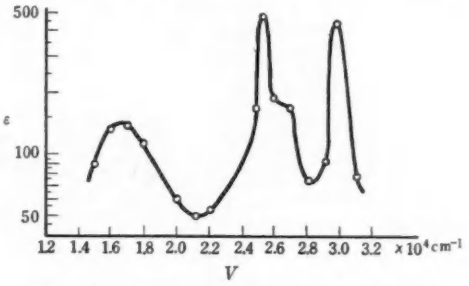

Fig. 2. Absorption spectrum of basic rhodo salt obtained from kinetic data.

Summary

The conversion reaction of the basic rhodo ion to the basic erythro ion in an alkaline solution was found to be of the first order. The velocity constants at 10°, 15°, 20° and 25°C were measured, and the energy of activation, the frequency factor and the entropy of activation calculated. The reaction velocity appeared to be somewhat diminished by higher concentration of sodium hydroxide. The absorption spectrum of unstable basic rhodo salt was derived from the kinetic data.

The authors wish to express their debt of gratitude to Assistant Professor Yukio Kondo of the Rikkyo University for sending them a reprint of his paper concerning the absorption spectra of binuclear ammine complexes.

Institute of Polytechnics
Osaka City University
Kita-ku, Osaka

The Dissociation Constants of Carboxytropone and Carboxytropolones

By Nobuyuki TANAKA, I. T. OIWA*, Toshiko KUROSAWA** and Tetsuo NOZOE

(Received August 4, 1958)

Although tropolones possess the properties characteristic of enols and phenols, they may be regarded, in respect of acidity, as vinylogs of carboxylic acids. Their dissociation constants are closer to the latter than to those of phenols[1-4]. This is attributed to the resonance of the ions A and B. However, the acidity is not so enhanced as would be expected

A B C D

from the stabilization of the ion species A and B. This fact has been explained by considering the "aromatic" resonance of the species C and D, the former being less favored than the latter[2].

In this study, the dissociation constants of 2-carboxytropone, 3-carboxytropolone and its derivatives have been determined by potentiometric titrations with a glass electrode. From the results obtained, the chelation between the substituted carboxyl group and the hydroxyl group of tropolones is discussed.

Experimental

Materials.—Eight compounds that were investigated in the present study were prepared in this laboratory and had the properties given in Table I. Ten milligrams of each compound was weighed accurately and dissolved in redistilled water ($\kappa < 10^{-6}$ mho/cm.) to prepare a solution of approximately 10^{-3} mole/l. in concentration (Table I). A 0.01 M carbonate-free sodium hydroxide solution was prepared by the usual method[16], and its concentration was standardized against recrystallized oxalic acid. The solution was kept in a bottle with a buret which had an arrangement for protection against carbon dioxide.

Three buffer solutions recommended by the National Bureau of Standards (U. S. A.)[17] were employed for the standard for the pH measurement. They are 0.05 M potassium hydrogen phthalate of pH 4.008 at 25°C, 0.025 M potassium

TABLE I

CARBOXYTROPONE AND CARBOXYTROPOLONES INVESTIGATED

No.	Compound	Molecular weight	M. p., °C	Conc. of soln., mM	Reference
1	2-Carboxytropone	150.13	148 (decomp.)	0.574	5
2	3-Carboxytropolone	166.13	218 (decomp.)	1.004	6, 7
3	4-Carboxytropolone	166.13	218	1.194	8, 9, 10
4	5-Carboxytropolone	166.13	290 (decomp.)	0.461	9, 11
5	3-Carboxy-4-methyltropolone	180.15	196 (decomp.)	1.001	12, 13
6	3-Carboxymethyltropolone	180.15	174 (decomp.)	1.001	14
7	Anhydride of 3,4-dicarboxytropolone[a]	192.12	254	0.825	12, 15
8	3-Carboxy-4-carboxymethyltropolone	244.16	183 (decomp.)	1.018	10, 12

a) This substance gives 3,4-dicarboxytropolone when dissolved in water.

* Present address, Research Laboratories, Shin-etsu Chemical Industry, Iriarai, Ohta-ku, Tokyo.
** Present address, 2217, 5-Chome, Matsumoto-cho, Mito.

1) W. von E. Doering and L. H. Knox, *J. Am. Chem. Soc.*, **73**, 828 (1951).
2) P. L. Pauson, *Chem. Revs.*, **55**, 9 (1955).
3) N. Yui and T. Nozoe, *Sci. Repts. Tôhoku Univ. First Ser.*, **35**, 83 (1951).
4) N. Yui, ibid., **40**, 102, 114 (1956).
5) T. Nozoe, K. Takase, et al., to be published.
6) T. Nozoe, Y. Kitahara and S. Masamune, *Proc. Japan Acad.*, **29**, 17 (1953).
7) J. W. Cook, L. D. Loudon and D. K. V. Steel, *J. Chem. Soc.*, **1954**, 530.
8) T. Nozoe and Y. Kitahara, *Proc. Japan Acad.*, **30**, 204 (1954).
9) Y. Kitahara, *Sci. Repts. Tôhoku Univ. First Ser.*, **40**, 74 (1956).
10) R. D. Haworth and J. D. Hobson, *J. Chem. Soc.*, **1951**, 561.
11) J. W. Cook, R. A. Raphael and A. I. Scott, ibid., **1952**, 4416.
12) T. Nozoe, Y. Kitahara, K. Doi, S. Masamune, M. Endo, M. Ishii and Je-Gyun, *Sci. Repts. Tôhoku Univ. First Ser.*, **38**, 257 (1954),
13) R. D. Haworth, B. P. Moore and P. L. Pauson, *J. Chem. Soc.*, **1948**, 1045.
14) T. Nozoe, Y. Kitahara, et al., to be published.
15) D. W. Crow, R. D. Haworth and P. R. Jefferies, *J. Chem. Soc.*, **1952**, 3705.
16) I. M. Kolthoff and E. B. Sandell, "Textbook of Quantitative Inorganic Analysis," MacMillan Co., New York, p. 526 (1952).
17) R. G. Bates, "Electrometric pH meaurements," John Wiley & Sons, Inc., New York, p. 118 (1954).

dihydrogen phosphate and 0.025 M disodium hydrogen phosphate of pH 6.857 at 25°C and 0.05 M borax of pH 9.180 at 25°C.

Apparatus and Procedure.—The cell

Ag-AgCl	0.1 M HCl (inner)	glass membrane	
sample solution +NaOH (outer)	saturated KCl	Hg_2Cl_2-Hg	

was constructed for the pH measurement. The glass electrode which was designed by one of the authors (I. T. O.) had the shape of a small flask of approximately 30 ml. capacity. A standardized 0.1 M hydrochloric acid was placed inside. A titration cell used is shown in Fig. 1.

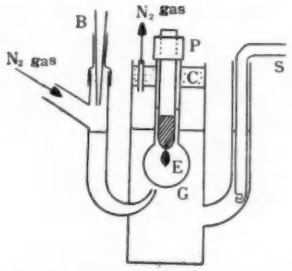

Fig. 1. Schematic diagram of the titration cell: G, glass membrane; E, silver-silver chloride electrode: P, polyethylene seal; C, cork; S, salt bridge; B, buret.

The pH of the solution was determined by the measurement of the electromotive force (e. m. f.) of the above cell. The measurement of e. m. f. was made by means of an instrument which consisted of a potentiometer and the combination of a UX-54 type vacuum tube (corresponding to the FP-54 type vacuum tube in the United States) and a galvanometer[18].

In order to remove the dissolved carbon dioxide and to stir the solution, purified nitrogen gas was passed through the solution before the titration and also after every addition of sodium hydroxide solution during the titration. The e. m. f. was measured with an accuracy of 0.0001 volt; therefore the pH was determined with an accuracy of 0.005 pH-unit. All measurements were carried out in a thermostat of 25.00±0.01°C.

Results

Titration Curves. — Typical titration curves obtained are reproduced in Fig. 2.

Calculation of Dissociation Constants.— (a) *Monobasic acid (HA).*—The dissociation constant of a monobasic acid, K_1, was calculated with the equation

$$K_1 = \frac{a_{H^+} \times a_{A^-}}{a_{HA}} = \frac{a_{H^+}\left(b + \frac{a_{H^+}}{f_{H^+}}\right) f_{A^-}}{c - \left(b + \frac{a_{H^+}}{f_{H^+}}\right)} \qquad (1)$$

where c means the total concentration of an acid titrated, b the concentration of sodium hydroxide added, a_{H^+}, a_{HA} and a_{A^-} mean the activities of the hydrogen ion, the undissociated acid and the dissociated acid anion, respectively, and f_{H^+} and f_{A^-} the activity coefficients of the hydrogen ion and the dissociated acid anion, respectively. The activity coefficient of the undissociated acid HA was assumed to be unity, while those of the dissociated acid anion A^- and the hydrogen ion were calculated with the equation

$$\log f_i = -\frac{0.358 Z_i^2 \sqrt{I}}{1 + 0.2325 a_i \times 10^8 \sqrt{I}} \qquad (2)$$

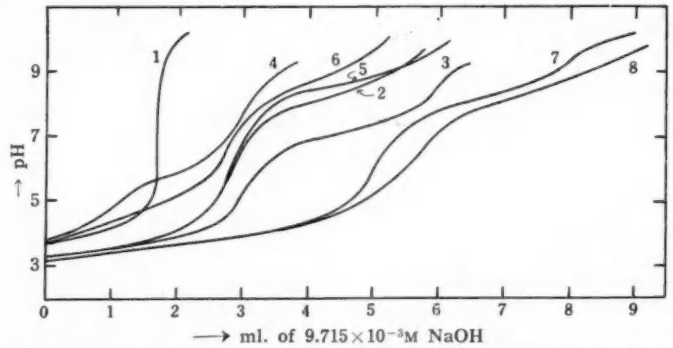

Fig. 2. Titration curves of carboxytropone and carboxytropolones. The curves are given the same number as in Table I.

18) N. Tanaka, I. T. Oiwa and M. Kodama, *Anal. Chem.*, **28**, 1555 (1956).

where Z_i represents the ionic charge, Γ the total ionic concentration, and a_i the ion-size parameter[19]. Because 2-carboxytropone was considered to have a molecular volume similar to that of benzoic acid, its ion-size parameter was assumed to be 6 Å according to Kielland's[19] tables.

(b) *Dibasic acids* (H_2A).—When $K_1/K_2 \geq 10^3$, the first dissociation constant, K_1, was calculated with eq. 1 in which f_{A^-} was replaced by f_{HA^-}, the effect of the second dissociation being neglected. In this calculation, the part of the titration curve before the equivalence point for the first dissociation was used. The second dissociation constant, K_2, was calculated with the equation

$$K_2 = \frac{a_{H^+} \times a_{A^{2-}}}{a_{HA^-}} = \frac{a_{H^+}\left(b + \frac{a_{H^+}}{f_{H^+}} - [OH^-]\right) f_{A^{2-}}}{\left(2c + [OH^-] - \frac{a_{H^+}}{f_{H^+}} - b\right) f_{HA^-}} \qquad (3)$$

from the observed values which were obtained between the equivalence points for the first and the second dissociations on the titration curve.

(c) *Tribasic acids* (H_3A).—From the titration curves given in Fig. 2 it was seen that K_1/K_2 is not greater than 10^3, so that K_1 and K_2 were not able to be calculated by the procedure given in (b). In this case they were calculated with the equations

$$K_1K_2 = \frac{a_{H^+}^2 \times a_{HA^{2-}}}{a_{H_3A}} = a_{H^+}^2 \left(\frac{b + \frac{a_{H^+}}{f_{H^+}} - [OH^-]}{2c - b - \frac{a_{H^+}}{f_{H^+}} + [OH^-]} \right) \times \left\{ 1 + \frac{K_1 f_{H^+}}{a_{H^+}} \left(\frac{b - c + \frac{a_{H^+}}{f_{H^+}} - [OH^-]}{b + \frac{a_{H^+}}{f_{H^+}} - [OH^-]} \right) \right\} f_{HA^{2-}} \qquad (4)$$

$$K_1 = a_{H^+} \left(\frac{b + \frac{a_{H^+}}{f_{H^+}} - [OH^-]}{c - b - \frac{a_{H^+}}{f_{H^+}} - [OH^-]} \right) \times \left\{ 1 - K_1K_2 \left(\frac{f_{H^+}}{a_{H^+}} \right)^2 \left(\frac{2c - b - \frac{a_{H^+}}{f_{H^+}} + [OH^-]}{b + \frac{a_{H^+}}{f_{H^+}} - [OH^-]} \right) \right\} f_{H_2A^-} \qquad (5)$$

from the values obtained before the equivalence point for the second dissociation on the titration curve.

The third dissociation constant, K_3, was calculated with the equation,

$$K_3 = \frac{a_{H^+} \times a_{A^{3-}}}{a_{HA^{2-}}} = \frac{a_{H^+}\left(b + \frac{a_{H^+}}{f_{H^+}} - [OH^-]\right) f_{A^{3-}}}{\left(3c - b - \frac{a_{H^+}}{f_{H^+}} + [OH^-]\right) f_{HA^{2-}}} \qquad (6)$$

from the values obtained between the equivalence points for the second and third dissociations on the titration curve.

In Table II are given the typical examples of calculation for the mono- and di-basic acid, and in Table III, the dissociation constants obtained for the compounds investigated. For comparison, the dissociation constants of several substances which have structures similar to the compounds investigated in this study are also given in Table III.

Discussion

2-Carboxytropone (E_1).—This acid is stronger than benzoic acid. This is attributed to the fact that the inductive (electron withdrawal) effect of a tropone ring is stronger than that of a benzene ring.

3-Carboxytropolone (E_2) and 3-carboxy-4-methyltropolone (E_5).—The values of pK_1 are smaller than those of benzoic acid and 2-carboxytropone. This shows the stronger inductive effect of the tropolone ring as well as the existence of chelation

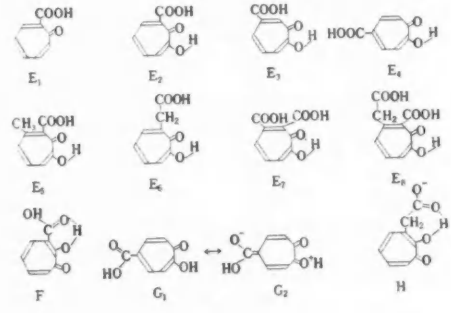

19) J. Kielland, *J. Am. Chem. Soc.*, **59**, 1675 (1937).

TABLE II
RESULTS OF TITRATION

2-Carboxytropone with 9.715×10^{-3}M NaOH

NaOH, ml.	pH	$a_{H^+}\times10^4$	f_{H^+}	$b\times10^4$	$[A^-]\times10^4$	f_{A^-}	$K_1\times10^4$
0.14	3.66	2.18_3	0.982	0.448	2.592	0.982	1.88
0.31	3.73	1.86_2	.981	0.993	2.890	.981	1.89
0.57	3.85	1.39_0	.980	1.811	3.229	.980	1.82
0.75	3.95	1.12_2	.979	2.369	3.515	.979	1.85
0.91	4.04	0.91_2	.978	2.860	3.791	.978	1.89
1.10	4.18	0.65_4	.977	3.436	4.105	.977	1.82
						mean	1.86
						$pK_1=3.73\pm0.01$	

3-Carboxytropolone with 9.715×10^{-3}M NaOH

NaOH, ml.	pH	$a_{H^+}\times10^4$	f_{H^+}	$b\times10^4$	$[HA^-]\times10^4$	f_{HA^-}	$K_1\times10^4$
0.15	3.30	5.01_2	0.973	0.483	5.623	0.973	6.28
0.42	3.35	4.41_6	.973	1.341	5.877	.973	6.26
0.61	3.39	3.99_9	.973	1.951	6.060	.973	6.22
0.88	3.46	3.46_8	.973	2.768	6.326	.973	6.23
1.12	3.52	3.02_0	.972	3.496	6.601	.972	6.28
						mean	6.25
						$pK_1=3.20\pm0.01$	

NaOH, ml.	pH	$a_{H^+}\times10^9$	f_{H^+}	$b\times10^4$	$[HA^-]\times10^4$	f_{HA^-}	$[A^{2-}]\times10^4$	$f_{A^{2-}}$	$[OH^-]\times10^6$	$K_2\times10^8$
4.46	8.29	5.12	0.944	12.57	4.939	0.941	12.55	0.787	1.79_7	1.08
4.64	8.38	4.16	.943	13.01	4.417	.941	12.98	.785	2.66_7	1.02
4.93	8.65	2.23	.942	13.71	3.591	.940	13.66	.782	4.22_1	1.02
									mean	1.04
									$pK_2=7.98\pm0.01$	

TABLE III
DISSOCIATION CONSTANTS OF CARBOXYTROPONE, CARBOXYTROPOLONES AND THE RELATED COMPOUNDS

Compound	pK_1	pK_2	pK_3
2-Carboxytropone	3.73 ± 0.01		
3-Carboxytropolone	3.20 ± 0.01	7.98 ± 0.01	
4-Carboxytropolone	3.42 ± 0.005	7.03 ± 0.01	
5-Carboxytropolone	4.05 ± 0.01	6.41 ± 0.02	
3-Carboxy-4-methyltropolone	3.15 ± 0.01	8.29 ± 0.01	
3-Carboxymethyltropolone	4.52 ± 0.02	8.77 ± 0.05	
3,4-Dicarboxytropolone	3.24 ± 0.03	6.26 ± 0.03	8.57 ± 0.01
3-Carboxy-4-carboxymethyltropolone	3.75 ± 0.03	5.90 ± 0.05	8.08 ± 0.02
Acetic acid	4.756[20]		
Benzoic acid	4.201[20]		
Tropolone	6.92[3]		
4-Methyltropolone	7.26[3]		

such as given in structure F. The larger values of pK_2 also show the existence of stable chelation.

4-Carboxytropolone (E_3) and 5-carboxytropolone (E_4). — In these substances the carboxyl group will not be able to form the chelation of type F, which 3-carboxytropolone forms. The magnitudes of pK_1 of these acids, therefore, are expected to be larger than those of 3-carboxytropolone and 3-carboxy-4-methyltropolone, and the magnitudes of pK_2 of the former, smaller than those of the latter. The experimental results agree with this expectation; The pK_1 of 5-carboxytropolone is much greater than that of 4-carboxytropolone, this may be attributed to the contribution of structure G_2. It is also interesting to notice that the difference between pK_1

20) R. A. Robinson and R. H. Stokes, "Electrolytic Solutions," Butterworths Scientific Publications, London, p. 436 (1955).

and pK_2 of 5-carboxytropolone is much smaller than the differences of other monocarboxytropolones (See Table III).

3-Carboxymethyltropolone (E_6). — The methylene group shields the inductive effect of a tropolone ring upon the carboxyl group, and, consequently, the pK_1 value is close to that of acetic acid. The large pK_2 value indicates the existence of the stable chelation (structure H).

3, 4-Dicarboxytropolone (E_7) and 3-carboxy-4-carboxymethyltropolone (E_8). — 3, 4-Dicarboxytropolone gives a pK_1 value which is nealy equal to that of 3-carboxytropolone (E_2), while 3-carboxy-4-carboxymethyltropolone gives a somewhat larger pK_1. This seems to be due to the greater steric interference of a carboxymethyl group in the 4-position.

Summary

The thermodynamic dissociation constants of 2-carboxytropone, 3-carboxytropolone, 4-carboxytropolone, 5-carboxytropolone, 3-carboxy-4-methyltropolone, 3-carboxymethyltropolone, 3, 4-dicarboxytropolone and 3-carboxy-4-carboxymethyltropolone have been determined by means of the pH titration with a glass electrode.

The relationships between the magnitudes of the dissociation constants and the structures of these compounds have been discussed.

The authors thank the Ministry of Education for the financial support granted for this research.

Department of Chemintry,
Faculty of Science,
Tohoku University
Katahira-cho, Sendai

SHORT COMMUNICATIONS

Absolute Estimation of the Ionic Entropies of Transfer

By Toshio IKEDA

(Received September 9, 1958)

The earlier attempts[1,2] of estimating the absolute ionic entropies of transfer are all based on an artificial assumption. Recently, the first absolute estimation has been carried out successfully by Agar and Breck[3]. The present report would give the second way of estimating these values exclusively from the observed data concerning the "Soret effect" and thermocells without making any assumption except the additivity of the ionic entropies of transfer, which was originally proposed by Eastman[1] and lately has been confirmed by Alexander[4] at low concentrations. For a thermocell of the system, $Ag|AgCl_s, MCl_{aq}, AgCl_s|Ag$, we can write, when the Soret effect is hindered, as follows:

$$\boldsymbol{F}\frac{d\varphi}{dT} = -t_+S_+^* + t_-S_-^* - S_{el}^* + S_{Ag} - S_{AgCl} + t_+S_{MCl} \qquad (1)$$

where $\boldsymbol{F}$ is Faraday's constant, $d\varphi$ is the thermopotential difference due to the temperature gradient dT, t_+ and t_- are the transference numbers of positive and negative ions of the salt MCl (here uni-univalent) respectively, S_+^*, S_-^* and S_{el}^* are the entropies of transfer of hydrated positive and negative ions in solution phase and that of electron in metallic phase respectively, S_{Ag} and S_{AgCl} are the molar entropies of metallic silver and solid silver chloride respectively, and S_{MCl} is the molar

1) E. D. Eastman, *J. Am. Chem. Soc.*, **50**, 283, 292 (1928).
2) J. C. Goodrich, F. M. Goyan, E. E. Morse, R. G. Preston and M. B. Young, ibid., **72**, 4411 (1950).
3) J. N. Agar, and W. G. Breck, *Trans. Faraday Soc.*, **53**, 167, 179 (1957).
4) K. F. Alexander, *Z. physik. Chem.*, **203**, 213 (1954).
5) H. B. Callen. *Phys. Rev.*, **73**, 1349 (1948); S. R. de Groot, "Thermodynamics of Irreversible processes", North Holland Publ. Co., Amsterdam and Intersc. Publ., New York., (1951).

TABLE I

IONIC ENTROPIES OF TRANSFER (cal./deg./mole) IN AQUEOUS m-MOLAL SOLUTION OF MCl AT 25°C. σ(deg.$^{-1}$), dφ/dT(μV/deg.), S_{Ag}=10.1, S_{AgCl}=23.0, S_{Hg}=18.3, S_{HgCl}=23.4 cal./deg./mole.

System MCl	Ag/AgCl, MCl(m=0.05)					Ag/AgCl, MCl(m=1.0)					Hg/HgCl,MCl(m=1.0)		
	t_+[g]	$\sigma\times10^3$	dφ/dT[b]	S_+*	S_-*	t_+[g]	$\sigma\times10^3$	dφ/dT[b]	S_+*	S_-*	dφ/dT[b]	S_+*	S_-*
HCl	0.829	−1.76[c]	145	10.4	18.4[f]	0.845	−7.3[a]	− 83	4.1	18.$_2$	330	3.5	19.$_9$
LiCl	0.321	+0.31[a]	511	6.5	24.$_5$	0.26	0. [d]	289	0.2	19.$_6$	630	0.2	19.$_6$
NaCl	0.388	−1.91[a]	482	18.1	24.9	0.363	−1.56[d]	228	13.1	18.8	560	13.2	18.7
KCl	0.490	−1.20[a]	493	27.4	24.9	0.485	−0.93[d]	261	22.$_6$	19.$_4$	610	22.$_3$	19.$_7$
NH_4Cl	0.491	0.0 [e]	498	29.$_0$	24.$_4$	—	—	—	—	—	—	—	—

a, K. F. Alexander, *Z. physik. Chem.*, **203**, 213 (1954); b, H. A. Bernhardt and H. D. Crockford, *J. Phys. Chem.*, **46**, 473 (1942); c, J. Chipman, *J. Am. Chem. Soc.*, **48**, 2577 (1926); d, C. C. Tanner, *Trans. Faraday Soc.*, **23**, 75 (1927); e, Th. W. Richards, *Z. physik. Chem.*, **24**, 39 (1897); f, This anomalous value might be due to the fact that Chipman's value of σ here used is incorrect, probably too low; g, I. C. T; B. E. Conway "Electrochemical Data", Elsevier Publ. Co., Amsterdam, (1952).

entropy of MCl in solution phase. Here $S_{MCl}=S_+ + S_-$, S_+ and S_- being the partial molar entropies of hydrated positive and negative ions produced from one molecule of the salt MCl in solution phase.

Coupling the relations[5], $S_+^*=Q_+^*/T+S_+$ and $S_-^*=Q_-^*/T+S_-$, with the approximation formula[6] $\sigma=-(Q_+^*+Q_-^*)/2RT^2$ for the Soret coefficient σ, one may yield the molecular entropy of transfer of the salt MCl as

$$S_+^*+S_-^*=-2RT\sigma+S_{MCl} \qquad (2)$$

where Q_+^* and Q_-^* are the heat of transfer of hydrated positive and negative lons of MCl in solution phase, and R is the gas constant.

Upon solving Eqs. 1 and 2 with respect to S_+^* and S_-^* by the aid of the relation of $t_+ + t_- = 1$, one may yield

$$\left.\begin{aligned} S_-^* &= F\mathrm{d}\varphi/\mathrm{d}T - S_{Ag} + S_{AgCl} \\ &\quad -2t_+RT\sigma + S_{el}^* \\ S_+^* &= -F\mathrm{d}\varphi/\mathrm{d}T + S_{Ag} - S_{AgCl} \\ &\quad -2t_-RT\sigma - S_{el}^* + S_{MCl} \end{aligned}\right\} \qquad (3)$$

Since S_{el}^* is very small as compared with the other terms in Eq. 3, sufficiently correct values of the ionic entropies of transfer may be obtained even by omitting term of S_{el}^* from Eq. 3. Some of the values of S_+^* and S_-^* thus estimated for the 0.05 and 1 molal aqueous solutions of some electrolytes at 25°C are tabulated in Table I. There can be seen some remarkable facts: (1) the values of S_+^* and S_-^* persist their proper values, independent of what system they are originated from; (2) the value of S_-^* is consistently the same, entirely independent of the nature of its conjugate cations present in the chloride solutions; (3) S_i^* is a function of the concentration.

Finally it is very interesting to have a possibility of determing the heats of transfer for positive and negative ions separately, if only the individual ionic activity coefficients are known.

Department of Chemistry, Faculty of Liberal Arts and Science, Shizuoka University, Oiwa-cho, Shizuoka

6) S. R. de Groot, *J. Phys. Radium*, **8**, 129, 193 (1947).

*Studies of the Structure of Bergenin**

By Shin-ichiro FUJISE, Morio SUZUKI, Yasuhiko WATANABE and Sumu MATSUEDA

(Received October 21, 1958)

Two reports on the structure of bergenin were published recently by J. Evelyn Hay et al.[1] and by Posternak et al.[2]. We also wish to report here our results on the structure of bergenin (I) from the bark of *Corylopsis Spicata*[3].

The periodate oxidation of di-*O*-methylbergenin (II) gave 5, 6, 7-trimethoxyisocoumarin-3-aldehyde (III). By careful catalytic hydrogenation of III, 3-hydroxymethyl-5, 6, 7-trimethoxyisocoumarin (IV)

* The paper was read at Annual Meeting of Chemical Society of Japan, April 5, 1958.

1) J. E. Evelyn Hay et al., *J. Chem. Soc.*, **1958**, 2231.

2) Posternak et al., *Helv. Chim. Acta*, **41**, 1159 (1958).

3) Hattori, *Acta Phytochim., (Japan)*, **4**, 327 (1929).

(its 3-acetoxymethyl derivative (V)), 3-methyl-5, 6, 7-trimethoxyisocoumarin (VI) and 3-methyl-5, 6, 7-trimethoxy-3, 4-dihydroisocoumarin (VII) were isolated through three steps.

The alkaline treatment of III gave 5, 6, 7-trimethoxy-3, 4-dihydroisocoumarin-3-carboxylic acid (VIII), i. e., an intermolecular Cannizzaro reaction was observed. The values of U. V. spectrum of these compound are given in Tables I and II.

TABLE I

U. V. ABSORPTION OF BERGENIN AND ITS DERIVATIVES

(λ_{max} in mμ)

Group 1			Group 2		
Compound	λ_{max}	log ε	Compound	λ_{max}	log ε
I	275	3.903	III	335	3.856
	220	4.426		245	4.600
II	268	3.914	IV	338	3.726
	220	4.482		247	4.680
VII	305	3.485	V	335	3.705
	265	3.962		247	4.684
	220	4.415			
VIII	303	3.397	VI	340	3.658
	265	3.874		245	4.655
	220	4.388			

TABLE II

CARBONYL STRETCHING FREQUENCIES IN I. R. SPECTRA OF BERGENIN AND ITS DERIVATIVES

Compound	ν(cm^{-1})
I	1703
II	1721, 1711
Penta-*O*-acetylbergenin	1775, 1733

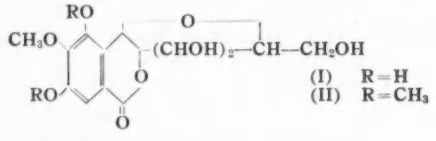

(I) R=H
(II) R=CH_3

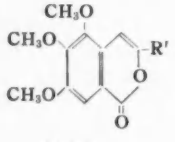

(III) R'=CHO
(IV) R'=CH_2OH
(V) R'=CH_2OCOCH_3
(VI) R'=CH_3

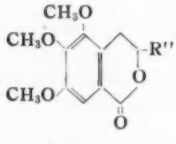

(VII) R''=CH_3
(VIII) R''=COOH

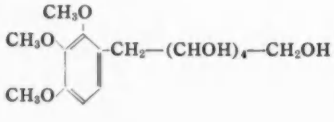

(IX)

From the results shown in Table I, we conclude that bergenin and di-*O*-methylbergenin have dihydroisocoumarin-ring, but not isocoumarin-ring (the absence of 330 mμ absorption). The results also agreed with those in Table II, i. e., I. R. spectrum of 3-methyl-3, 4-dihydroisocoumarin (1716 cm^{-1}) indicated the identical structure with that of bergenin and of di-*O*-methylbergenin.

The catalytic reduction of II, by using Raney catalyst (at 200°, 100 atm.) resulted in obtaining 6-(2, 3, 4-trimethoxyphenyl)-1, 2, 3, 4, 5-heptahydroxyhexane IX, being accompanied by both decarboxylation and hydrogenation. The products was stable to Fehling's solution. The constitution of IX was also confirmed by the oxidation with sodium metaperiodate. In the case that 4 moles of this reagent were consumed, oxidation product was isolated to be prove as 2, 3, 4-trimethoxy phenylacetaldehyde 2, 4-dinitrophenyl hydrazone.

The alkaline hydrogen peroxide oxidation of I gave arabinose (as 2, 4-dinitrophenylhydrazone). II was found to be also stable to Fehling's solution. Deducing from the above-mentioned experimental results, bergenin is concluded to be represented by the formula I.

TABLE III

ANALYSES

No.	Formula, m. p.	Found. C%	Found. H%	Calcd. C%	Calcd. H%
III	$C_{13}H_{12}O_6$ m. p. 160~161°	58.85	4.53	59.09	4.58
IV	$C_{13}H_{14}O_6$ m. p. 141~142°	58.88	5.51	58.64	5.30
V	$C_{15}H_{16}O_7$ m. p. 93~94°	58.42	5.06	58.44	5.23
VI	$C_{13}H_{14}O_5$ m. p. 84~86°	62.57	5.71	62.39	5.64
VII	$C_{13}H_{16}O_5$ m. p. 67~69°	61.60	6.10	61.89	6.39
VIII	$C_{13}H_{14}O_7$ m. p. 157~158°	55.33	5.08	55.32	5.00
IX	$C_{15}H_{24}O_8$ m. p. 182~183°	54.87	6.51	54.21	7.28

Department of Chemistry, Faculty of Science, Tohoku University
Katahira-cho, Sendai

4) J. Blair et al., *J. Chem. Soc.*, **1955**, 2871.

Remarks on the Composition Potential

By V. S. VAIDHYANATHAN

(Received November 1, 1958)

Suryanarayana and Venkatesan[1] have defined a quantity, which they call the composition potential, viz., the ratio of the mole fraction of a solute (electrolyte) in a solution at an arbitrary concentration to the mole fraction at the saturation point. The authors have stated that this ratio, denoted by C_p, to be a truly thermodynamic potential. This is not in accordance with the accepted definition of thermodynamic potentials. The thermodynamic potentials have and must have the following fundamental property[2]. "If we know one of the thermodynamic potentials as a function of its variables, to which it corresponds, we can express all the other thermodynamic variables as a function of this potential and its derivatives". The potentials that can be defined as "thermodynamic potentials" and which conform to this statement are the Gibbs and Helmholtz functions, energy, enthalpy, entropy and the chemical potential and they alone. From a more general point of view, the potential can be defined as one whose gradient yields the force in a direction. To neither of these definitions does the definition of the composition potential agree.

The number of moles is an extensive variable and the ratio of two extensive variables yields an intensive variable[3]. The mole-fractions are intensive. We know that the ratio of two intensive quantities to be intensive, and that any combinations of them to be still intensive. The derivative of an extensive variable with respect to another extensive is intensive. The composition potential defined by the said authors, is an intensive variable and is dimensionless. Apart from this, no other thermodynamic significance can be attributed to 'C_p'. It is a property of the solution and a variable in the thermodynamic sense. The mere fact that a particular property (e. g. the sum of the mole fractions) has a constant specified value does not merit being called thermodynamic potential.

Department of Chemistry, Illinois Institute of Technology
Chicago 16, U. S. A.

1) C. V. Suryanarayana and V. K. Venkatesan, This Bulletin, **31**, 442 (1958).
2) I. Prigogine, "The Molecular Theories of Solutions", North Holland Publ. Co., Amsterdam (1957).
3) E. A. Guggenheim, "Thermodynamics", North Holland Publ. Co., Amsterdam (1952).

---

*Paramagnetic Resonance Absorption in Solution of the Sodium Adducts of Styrene and 1, 1-Diphenylethylene**

By Kozo HIROTA, Keiji KUWATA and Kazuo MORIGAKI

(Received November 21, 1958)

As reported already[1], paramagnetic resonance absorption with hyperfine structure could be observed on the red adduct of styrene with sodium in tetrahydrofuran (THF) solution. Such absorption has been observed by Weissman and his collaborators[2] in caces of polynuclear condensed aromatic hydrocarbons, e. g., naphthalene, anthracene, and naphthacene. Moreover, it is interesting that the adduct of styrene polymerizes easily, turning into a so-called "living polymer". The research, therefore, was continued with an apparatus of higher sensitivity, thus obtaining more interesting and confirmative results. It is the object of the present communication to report them and also a similar research on 1,1-diphenylethylene (DPE), which also forms a living polymer[3].

As shown in Figs. 1a and 1b, two kinds of spectrum were observed in the adduct of styrene, and it was found that they could be observed in the solutions when the adduct of high degree of polymerization was depolymerized with metallic sodium, and after repeated experiment it

1) K. Hirota, K. Kuwata and K. Morigaki, This Bulletin, **31**, 538 (1958).
2) D. Lipkin, D. E. Paul, J. Townsend and S. I. Weissman, *Science*, **117**, 534 (1953); T. L. Chu, G. E. Pake, D. E. Paul, J. Townsend and S. I. Weissman, *J. Phys. Chem.*, **57**, 504 (1953); S. I. Weissman, J. Townsend, D. E. Paul and G. E. Pake, *J. Chem. Phys.* **21**, 2227 (1953); T. R. Tattle, Jr. and S. I. Weissman, ibid., **25**, 189 (1956).
* Part of this communication was already spoken at the meetings of the Phys. Soc. of Japan (March 1958, Tokyo), and of the Chem. Soc. of Japan (April 1958, Tokyo).
3) K. Kuwata, S. Ishida and K. Hirota, *J. Chem. Soc. Japan. Pure Chem. Sec.* (*Nippon Kagaku Zasshi*), to be published.

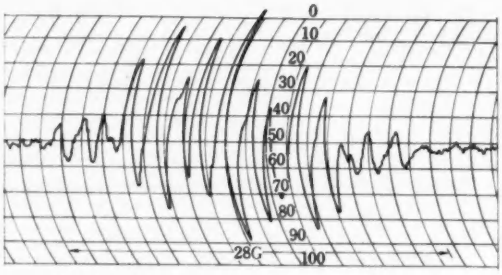

Fig. 1a. Resonance spectrum of styrene radical.

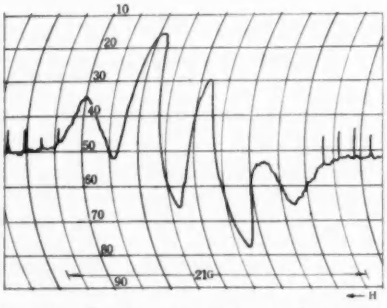

Fig. 1b. Resonance spectrum of styrene radical.

was confirmed that, according as the depolymerization is performed to much extent or not, the spectra observed were composed of about 23 lines or of four lines, as shown in Figs. 1a and 1b, but the reproducibility of the former was not confirmed. It is noteworthy that the spectrum of four lines did not separate into more lines when the measurment was done at such low temperature as about −100°C and when dioxane was used as the solvent, or potassium was substituted for sodium to prepare the adduct.

Similar situation was found on the adduct of DPE whose spectra are shown in Figs. 2a and 2b. The spectrum composed of 32~33 lines (Fig. 2a) could be obtained on the adduct freshly prepared from DPE monomer and sodium in THF. The spectrum, changed into the one composed of nine lines (Fig. 2b), when the sample was kept at 110°C for two days. Now it is clear that solutions of the sodium adducts of styrene and DPE contain some free radicals. Taking such fact into consideration, some discussions on the nature of these adducts were attempted.

These radicals in the adduct of styrene are considered to have the following

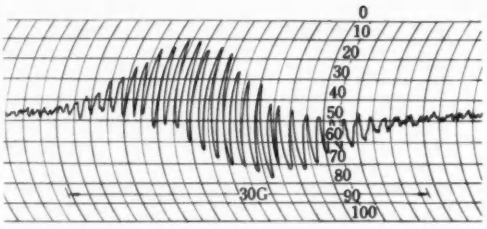

Fig. 2a. Resonance spectrum of DPE radical.

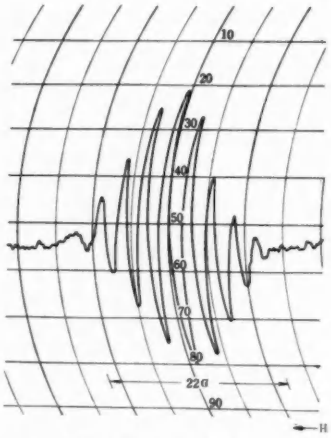

Fig. 2b. Resonance spectrum of DPE radical.

structures on the view of the polymerization reaction, it is believed that these two radicals are the origin of such two resonance spectra*:

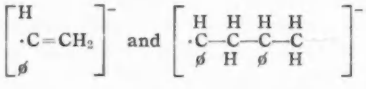

In case of DPE the situation is similar, but is more confirmative by the analysis of the spectra. The structures of the radicals corresponding to the spectra shown by Fig. 2a and Fig. 2b are as follows, respectively:

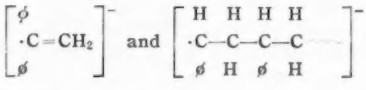

The detailed result and discussion will be published in near future.

* By these formulae all resonace formulae are represented for both adducts.

The writers express sincere thanks to Professor Junkichi Itoh of Osaka University who made the measurement of the paramagnetic resonance absorption possible.

Faculty of Science, Osaka University
Kita-ku, Osaka

2ξ, 3-(3'-Oxocyclohex-4'-eno)-cholest-4-ene and 2ξ, 3-(3'-Oxocyclohex-4'-eno)-5α-cholestane (Preliminary Note)

By Yoshiyuki URUSHIBARA and Jihei INOMATA

(Received December 10, 1958)

Chololest-4-en-3-one (I) was condensed with ethyl formate by the action of sodium methoxide to give 2-hydroxymethylene-cholest-4-en-3-one (II), m. p. 110°C[1]. The substance II was then condensed with freshly distilled methyl vinyl ketone in ethyl acetate in the presence of trimethylamine[2], and chromatography of the product on alumina and recrystallization from ethanol-methanol yielded 2ξ-(3'-oxobutyl)-cholest-4-en-3-one (III), m. p. 86~88°, λ_{max} 242 mμ(ethanol) (ε=14500), infrared absorptions 5.813, 5.970, and 6.160 μ (Found: C, 82.11; H, 11.19. Calc. for $C_{31}H_{50}O_2$: C,81.88; H, 11.08%). The diketone (III) gave a dioxime melting at 84°C (Found: N, 5.83. Calcd. for $C_{31}H_{52}O_2N_2$: N, 5.78%).

Treatment of the diketone (III) with alcoholic potash in the stream of nitrogen, chromatography of the product on alumina and recrystallization from ethanol, gave 2ξ,3-(3'-oxocyclohex-4'-eno)-cholest-4-ene (IV), m. p. 149—150° (Found: C, 85.08; H, 11.17. Calcd. for $C_{31}H_{48}O$: C, 85.26; H, 11.08%). The substance IV dissolved in ethanol showed an absorption maximum at 296 mμ (ε=30000) and in Nujol gave infrared absorptions at 6.000, 6.143 and 6.301 μ, which are proofs of the dienone structure IV.

Reaction of 2-hydroxymethylene-cholest-4-en-3-one (II), methanolic sodium methoxide and freshly prepared 4-(diethylamino)-2-butanone methiodide[3], followed by chromatography of the product on alumina and recrystallization from ethanol, gave directly the same dienone (IV), m. p. 141°C, which could be purified with difficulty.

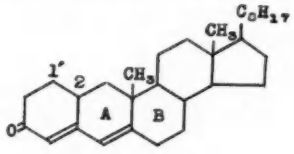

(IV)

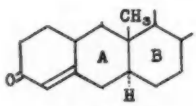

(IX)

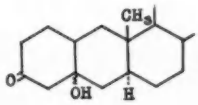

(VIII)

5α-Cholestan-3-one (V) was transformed into a monohydroxymethylene derivative, m. p. 180~185°C, in the same way as mentioned above(Found: C, 81.14; H, 11.31. Calcd. for $C_{28}H_{46}O_2$: C, 81.13; H, 11.11%). The structure of the product was proved to be 2-hydroxymethylene-5α-cholestan-3-one (VI)[4] by the formation of 2,3-seco-5α-cholestane-2,3-dioic acid, m. p. 193~194°C, on oxidizing the substance with hydrogen peroxide and caustic soda[5]. The dicarboxylic acid was identified with the specimen prepared from 5α-cholestan-3β-ol by the method of Windaus et al.[6]

Reaction of 2-hydroxymethylene-5α-cholestan-3-one (VI), 4-(diethylamino)-2-butanone methiodide and ethanolic potash, followed by chromatography of the product on alumina and recrystallization, gave 2ξ-(3'-oxobutyl)-5α-cholestan-3-one (VII), m. p. 113~114°C, infrared absorption 5.808~5.840μ (Found: C, 81.63; H, 11.52. Calc. for $C_{31}H_{52}O_2$: C, 81.52; H, 11.48%), and 2ξ,3-(3'-oxocyclohexano)-5α-cholestan-3ξ-ol (VIII), m. p. 230~231°C, infrared absorptions 2.826 and 5.790 μ (Found: C, 81.80; H, 11.70. Calcd. for $C_{31}H_{52}O_2$: C, 81.52; H, 11.48%).

1) J. G. Burr, Jr., W. F. Holton and C. N. Webb., *J. Am. Chem. Soc.*, **72**, 4903 (1950); R. B. Woodward., A. A. Patchett, D. H. R. Barton, D. A. J. Ives and R. B. Kelly, *J. Chem. Soc.*, **1957**, 1131.

2) G. I. Poos, G. E. Arth, R. E. Beyler and L. H. Sarett, *J. Am. Chem. Soc.*, **75**, 422 (1953).

3) Cf. E. C. Du Feu, F. J. McQuillin and R. Robinson, *J. Chem. Soc.*, **1937**, 53.

4) Cf. L. Ruzicka, U. S. Patent, 2,281,622; *Chem. Abstr.*, **36**, 5958 (1942).

5) Cf. D. Arigoni, H. Bosshard, H. Bruderer, G. Büchi, O. Jeger and L. J. Krebbaum, *Helv. Chim. Acta*, **40**, 1733 (1957); D. H. R. Barton et al., *J. Chem. Soc.*, **1954**, 4660.

6) A. Windaus and Cl. Uibrig, *Ber.*, **47**, 2384 (1914).

Compounds VII and VIII yielded the same 2ξ, 3-(3′-oxocyclohex-4′-eno)-5α-cholestane (IX), m. p. 153°C, on treatment with sodium hydroxide in the stream of nitrogen, followed by chromatography of the product on alumina and recrystallization from ethyl acetate (Found: C, 84.75; H, 11.57. Calcd. for $C_{31}H_{50}O$: C, 84.86; H, 11.49%). The substance IX dissolved in ethanol showed an absorption maximum at 243 mμ(ε=15000) and in Nujol infrared absorptions at 5.970 and 6.160μ, which prove the structure IX.

2-Hydroxymethylene-5α-cholestan-3-one (VI) reacted with methyl vinyl ketone on addition of a few drops of 10% ethanolic potash in the heat, and treatment of the product, m. p. 134~135°C, probably the 2-formyl intermediate, with ethanolic potash in the stream of nitrogen gave the same 2ξ-(3′-oxobutyl)-5α-cholestan-3-one (VII).

The 2ξ, 3-(3′-oxocyclohexano)-5α-cholestan-3ξ-ol (VIII), m. p. 231~232°C, and its 3-stereoisomeride, m. p. 217~219°C (Found: C, 81.16; H, 11.42. Calcd. for $C_{31}H_{52}O_2$: C, 81.52; H, 11.48%), were obtained by the action of *N*-ethylanilinomagnesium bromide on 2ξ-(3′-oxobutyl)-5α-cholestan-3-one (VII) followed by hydrolysis of the intermediate product with dilute hydrochloric acid[7].

No experimental evidence has yet been obtained concerning the configuration around the carbon atom 2 in compounds III, IV, VII, VIII and IX[8], but it seems almost certain for these deformylated compounds that carbon atom 1′ is situated at the more stable α-configuration and consequently the hydrogen in position 2 is attached there with the β-bond, axial to both ring A and the added ring.

Details will follow.

Department of Chemistry
Faculty of Science
The University of Tokyo
Hongo, Tokyo

7) Cf. J. Colonge, *Bull. soc. chim. France*, (5), **1**, 1101 (1934).
8) Cf. S. A. Szpilfogel, W. J. van Der Burg, C. M. Siegmann and D. A. van Dorp, *Rec. trav. chim.*, **75**, 1043 (1956) and A. Wettstein, K. Heusler, H. Ueberwasser and P. Wieland, *Helv. Chim. Acta*, **40**, 323 (1957).

High Resolution Proton Magnetic Resonance in Fluorobenzene

By Shizuo Fujiwara, Mikio Katayama and Hiroshi Shimizu

(Received November 11, 1958)

Gutowsky et al. resolved the proton nuclear magnetic resonance spectrum of fluorobenzene into a doublet and interpreted that it would refer to the case where the fluorine was equally coupled through electrons with the ortho-, meta- and paraprotons[1]. Baker also presented the same conclusion[2]. But this conclusion is a quite perplexing one to the chemists, and we continued the efforts to resolve the spectrum further and observed that the components of the doublet were different in the intensity from each other, consistent with the observation by Gutowsky et al.[1], each having the structure as shown in Fig. 1.

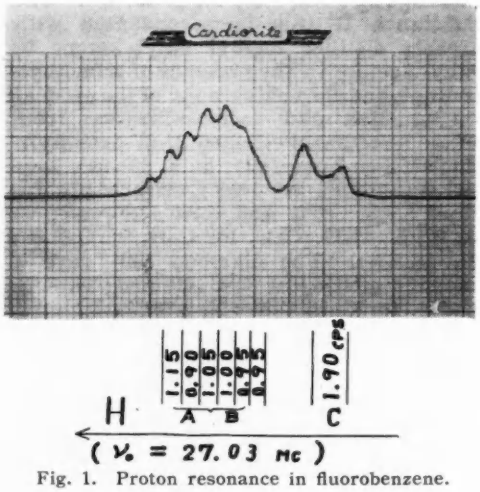

Fig. 1. Proton resonance in fluorobenzene.

The separation between each component of the multiplets is shown in Figure 1. In spite of the argument given by Baker[2] for the fluorine spectrum of this compound, we assume that the proton resonance spectrum of Fig. 1 would refer to the case where the effect of the non-equivalent distribution of electrons participates in

1) H. S. Gutowsky, L. H. Meyer and D. W. McCall, *J. Chem. Phys.*, **23**, 982 (1955).
2) E. B. Baker, ibid., **13**, 984 (1955).

the resonance phenomena. A possible assignment of the line components may be done with the help of the molecular theory[3] by taking the peaks of A, B and C (A is the highest in the resonant field) as referring to meta-, para- and ortho-protons, respectively.

During this experiment, we could know that Bak, Shoolery and Williams[4] reached the same conclusion as ours of unequal H-F couplings, but, in their article, the spectrum of the proton resonance is not shown. Further efforts to make the assignments of each component line and to make measurements at higher field are now being on.

Our thanks are due to Dr. G. A. Williams of Stanford University who sent us the preprint. Thanks are also due to Professor O. Simamura of the University of Tokyo who supplied us the sample.

University of Electro-Communications
Chôfu, Tokyo

3) For example C. A. Coulson: "Valence," Oxford University Press, (1953).
4) B. Bak, J. N. Shoolery and G. A. Williams, III, to be published in *J. Molecular Spectroscopy*.

Hydrogenolysis and Hydrogenation of Some 2, 3-Unsaturated Alcohols with Platinum Oxide and with Platinized Raney Nickel

By Shigeo Nishimura and Kazuko Mori

(Received December 10, 1958)

The hydrogenation of cholest-4-ene-3β, 6β-diol (I) in neutral ethanolic solution with platinum oxide as a catalyst gives 5β-cholestane-3β,6β-diol (II)[1]. The present authors carried out the same reaction in the presence of a trace of hydrochloric acid, when a little less than three moles of hydrogen were absorbed and 5α-cholestane (III) was obtained as the main product[2] (Table I). Shoppee et al.[3] obtained similar results in the hydrogenation of cholest-4-en-3-ols and related compounds, but they gave no account on the course of the hydrogenation.

Since it has been found that neither 5α-cholestane-3β, 6β-diol nor 5β-cholestane-3β, 6β-diol can be hydrogenolyzed with platinum oxide and hydrochloric acid, it can be assumed that the cholestenediol (I) underwent for the most part the hydrogenolysis before the saturation of the double bond, giving 5α-cholestane as the main product as illustrated below:

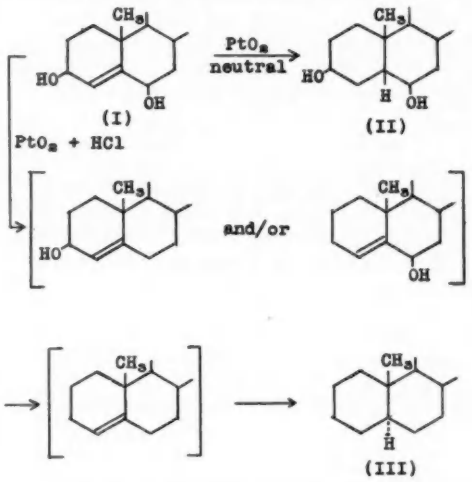

The above assumption is further supported by the fact that the product obtained by an incomplete hydrogenation of the cholestenediol (I) gave coloration with tetranitromethane in chloroform, while the cholestenediol (I) is entirely indifferent to the reagent.

The formation of 5β-cholestane from 3α-acetoxycholest-4-ene[3] can not be explained in a similar way, because, if cholest-4-ene were an intermediate product, then 5α-cholestane should be the main product as in the hydrogenation of the cholestenediol (I).

Similar results have been obtained in the hydrogenation of other 2,3-unsaturated alcohols and phenol, as summarized in Table I.

In the presence of platinum oxide and hydrochloric acid the substances absorbed more hydrogen than is necessary to transform them into the corresponding saturated alcohols. Since none of 3-phenyl-1-propanol, tetrahydrofurfuryl alcohol and

1) V. Prelog and E. Tagmann, *Helv. Chim. Acta*, **27**, 1880 (1944).
2) In ether-acetic acid solution, two moles of hydrogen are absorbed by the diacetate of the diol, and 5α-cholestane-3β,6β-diol, 5α-cholestan-3β-ol and 5α-cholestane are obtained: O. Rosenheim and W. W. Starling, *J. Chem. Soc.*, **1937**, 383.
3) C. W. Shoppee, B. D. Agashe and G. H. R. Summers, ibid., **1957**, 3107.

TABLE I
MOLES OF HYDROGEN ABSORBED IN 95% ETHANOL AT THE ORDINARY TEMPERATURE AND PRESSURE

Compound	Catalyst		
	PtO_2	PtO_2 +HCl	Platinized Raney Ni[5]
Cholest-4-ene-3β,6β-diol	1.0	2.7	1.1
Cinnamyl alcohol	1.0	1.5	0.98
Furfuryl alcohol[4]		3.1	2.1
Phenol		3.4	3.0

cyclohexanol could be hydrogenolyzed under the same conditions, it is concluded that the hydrogenolysis took place prior to the saturation of the double bond. On the other hand, in neutral ethanolic solution cinnamyl alcohol absorbed only 1 mole of hydrogen in the presence of either platinum oxide or platinized Raney nickel prepared in alkaline solution[5], while furfuryl alcohol gave a quantitative yield of tetrahydrofurfuryl alcohol with the latter catalyst.

It has been reported that cinnamyl alcohol gives about equal moles of 3-phenyl-1-propanol and propylbenzene with palladium-charcoal and hydrogen[6]. It is very probable that the catalyst contained a trace of hydrochloric acid.

The authors wish to express their hearty thanks to Professor Yoshiyuki Urushibara for his kind guidance.

Department of Chemistry, Faculty of Science, The University of Tokyo
Hongo, Tokyo

4) Furfuryl alcohol absorbs about 2.5 moles of hydrogen in the hydrogenation with platinum oxide either in the presence or in the absence of ferrous chloride or sulfate giving tetrahydrofurfuryl alcohol along with other products: W. E. Kaufmann and R. Adams, *J. Am. Chem. Soc.*, **45**, 3029 (1923); J. S. Pierce and C. Parks, ibid., **51**, 3384 (1929).

5) S. Nishimura, This Bulletin **32**, 61, (1959).

6) R. Baltzly and J. S. Buck, *J. Am. Chem. Soc.*, **65**, 1984 (1943). Cf. W. H. Hartung and R. Simonoff, "Org. Reactions", Vol. VII, p. 267, John Wiley & Sons (1953).